DISSERTATION

submitted to the
Combined Faculties for the Natural Sciences and for Mathematics
of the Ruperto-Carola University of Heidelberg, Germany
for the degree of
Doctor of Natural Sciences

presented by
Corinna Schaffroth, M. Sc.
born in Heilbronn
Oral-examination: 18.05.2015

Tryparedoxin peroxidases protect African trypanosomes from iron-induced damages of distinct cellular membranes

---

Referees

PD Dr. Tobias P. Dick

Prof. Dr. R. Luise Krauth-Siegel

Ich widme diese Arbeit meinem Ehemann Manuel Schaffroth,

der mich bei allem immer unterstützt hat.

Ohne ihn wäre die Arbeit nicht möglich gewesen.

... und alles wegen der Flauschigkeit der roten Königin

Acknowledgements

A PhD thesis is not only the work of a single person, thus I want to thank the people who made all this happen. First of all, I would like to cordially thank Prof. Luise Krauth-Siegel for giving me the great possibility to perform my PhD thesis in her welcoming group and to work on this exciting and challenging project. Providing not only the laboratory equipment but also the intellectual guidance, she made my work successful. She was open for discussions and constructive comments all time. You promoted my personal and scientific development.

Dr. Tobias Dick and Prof. Christine Clayton are committed TAC members. Their new suggestions and ideas supported my research. I would like to show my gratitude to Petra Krapp-Meiser for ordering all my materials and arranging all the job-related bureaucracy and to Prof. Heiner Schirmer for the beautiful flowers.

Besides, I thank Dr. Alejandro “the Postdoc” Leroux who supported me in any respect and listened to my experimental issues. He was always a detailed reviewer and answered all my questions, especially when they were weird and unusual. Blessing Musunda and Marta Bogacz contributed both to a nice atmosphere in this lab. Thank you for having a great time. I also want to thank Kathrin Diederich for scientific brain storming and new ideas. With her warm character, she encouraged me in stressful moments. Natalie Dirdjaja introduced me into all methods and guided me throughout my thesis, being a real friend of mine and Lillypuh. She also helped me a lot by correcting half of my thesis. I will miss you all so much!

It was also an honour to be part of HBIGS. The international atmosphere and the scientific career courses further advanced my professional and personal PhD life. I also thank the DFG for financial support.

Ich danke auch meiner Familie und meinen Freunden, besonders meinen lieben Eltern, Martina Muth und Siegfried Hiller, die mich von Kind auf ermutigt haben mehr zu erreichen. Das Ende meiner Doktorarbeit läutet auch das Ende meiner Ausbildung ein, bei der sie mich immer finanziell unterstützt haben und so vieles für mich selbstverständlich sein durfte. Die nähsten Menschen haben immer am meisten auszuhalten und deshalb danke ich Manuel für all seine Unterstützung und Liebe. Nur die hat mich alles erreichen lassen.

Publications

C. Hiller, A. Nissen, D. Benítez, M. A. Comini, R. L. Krauth-Siegel (2014). Cytosolic Peroxidases Protect the Lysosome of Bloodstream African Trypanosomes from Iron-Mediated Membrane Damage. PLoS Pathogen 10(4): e1004075. doi:10.1371/journal.ppat.1004075

C. Schaffroth, N. Dirdjaja, A. Nißen, R. L. Krauth-Siegel (2015). Either Cytosolic or Mitochondrial Tryparedoxin Peroxidase Is Required for the Protection of Procyclic African Trypanosomes towards Iron-Mediated Damage. (in preparation)

Summary

In African trypanosomes, detoxification of lipid hydroperoxides is achieved by three virtually identical non-selenium glutathione peroxidase (Px)-type enzymes which obtain their reducing equivalents from the unique trypanothione/tryparedoxin system. Previous knockout studies in bloodstream *Trypanosoma brucei* revealed that the two cytosolic Px I and II are essential in contrast to the mitochondrial Px III. Parasites lacking Px I and II are fully viable in the presence of Trolox, but show severe lipid peroxidation and lysis when the vitamin E analog is removed from the medium. Here, I showed that the underlying mechanism is an iron-induced damage of the lysosome. Live cell imaging and immunofluorescence analysis of *px I-II* knockout cells displayed the progressive loss of different lysosomal signals upon withdrawal of Trolox. In addition, staining of the lysosomal membrane protein p67 was lost prior to the MitoTracker Red signal in accordance with lysosomal disintegration preceding damage of the mitochondrion. Lysis of the *px I-II* knockout cells was accelerated by supplementing the medium with iron and transferrin whereas it was slowed down in the presence of apo-transferrin and the iron chelator deferoxamine. These data demonstrated that the lethal phenotype was linked to the high-efficiency endocytic iron acquisition of bloodstream trypanosomes. In contrast, generation and phenotypic analyses of procyclic cells lacking either the cytosolic, the mitochondrial or all three enzymes revealed that in the insect form, the cytosolic or the mitochondrial peroxidase is sufficient for cell viability and proliferation whereas the knockout of the whole *px* locus resulted in cells that require the presence of Trolox. The phenotype was also linked to the iron metabolism of the parasite. Deferoxamine in the medium protected the cells from lysis but starch-coupled deferoxamine − residing in the endosomal/lysosomal compartments − displayed almost no protection. Immunofluorescence microscopy with MitoTracker and antibodies against the glycosomal aldolase and the lysosomal p67 revealed that mitochondrial damage precedes that of the other organelles. Indeed, in procyclic parasites, the mitochondrion seems to be the primary site of intracellular oxidative injury. The distinct mechanisms for the acquisition and metabolism of iron can explain the different phenotypes observed upon deletion of the Px-type enzymes in the infective and insect stage of *T. brucei*.

Zusammenfassung

In afrikanischen Trypanosomen erfolgt die Entgiftung von Lipidhydroperoxiden durch drei nahezu identische nicht-selenhaltige Glutathionperoxidasen (Px), welche ihre Reduktionsäquivalente von dem einzigartigen Trypanothion/Tryparedoxin-System erhalten. Aus vorherigen Knockout-Studien an *Trypanosoma brucei* Blutstromformen ist bekannt, dass die zytosolischen Px I und II, nicht aber die mitochondriale Px III, essentiell sind. Px I-II-defiziente Parasiten sind in Gegenwart von Trolox lebensfähig, zeigen aber starke Lipidperoxidation und Lyse, wenn das Vitamin E-Analogon aus dem Medium entfernt wird. Ich konnte nachweisen, dass der zugrunde liegende Mechanismus auf einem Eisen-induzierten Schaden des Lysosoms beruht. Lebendzell- und Immunfluorezenz-Analysen der Px I-II-defizienten Zellen offenbarten den zunehmenden Verlust verschiedener lysosomaler Signale nach Entfernen von Trolox. Außerdem verschwand die Anfärbung des lysosomalen Membranproteins p67 vor dem MitoTracker Red-Signal, das heißt, die Auflösung des Lysosoms geht der mitochondrialen Schädigung voraus. Die Lyse der Px I-II-defizienten Zellen wurde durch exogene Zugabe von Eisen oder Transferrin beschleunigt, wohingegen sie in Gegenwart von Apotransferrin oder dem Eisenchelator Deferoxamin verlangsamt wurde. Diese Ergebnisse zeigten, dass der lethale Phänotyp mit der hoch-effizienten endozytotischen Eisenaufnahme der Blutstrom-Trypanosomen verknüft ist. Im Gegensatz dazu ergab die Erschaffung und phänotypische Analyse prozyklischer Zelllinien, in denen entweder die zytosolischen, das mitochondriale oder alle drei Enzyme deletiert waren, dass in der Insektenform die zytosolische oder die mitochondriale Peroxidase für die Lebensfähigkeit und Proliferation ausreichend ist, wohingehend der Knockout des kompletten *px*-Lokus zu Zellen führte, die Trolox benötigen. Der Phänotyp war auch hier mit dem parasitären Eisenmetabolismus verknüpft. Deferoxamin im Medium schützte die Px I-II-defizienten Zellen vor Lyse, wogegen Stärke-gekoppeltes Deferoxamin, welches in endosomalen bzw. lysosomalen Kompartimenten verbleibt, kaum Schutz bot. Die Immunfluoreszenz mit MitoTracker und Antikörpern gegen die glykosomale Aldolase und das lysosomale p67 machte deutlich, dass die mitochondriale Veränderung anderen Organellschäden vorausgeht. In der Tat scheint in prozyklischen Parasiten das Mitochondrium der primäre Ort von intrazellulärem oxidativem Schaden zu sein. Die unterschiedlichen Mechanismen der Aufnahme und des Stoffwechsels von Eisen erklären die verschiedenen Phänotypen bei Deletion der individuellen Peroxidasen in der infektiösen Blutstrom- bzw. der Insektenform von *T. brucei*.

Content

List of Abbreviations

AL	Aldolase
amp	Ampicillin resistance cassette
apoLI	Apolipoprotein LI
APS	Ammonium persulfate
ASCT	Acetate:succinate CoA-transferase
ATP	Adenosine triphosphate
BiP	Immunoglobulin binding protein
bla	Blasticidin resistance cassette
bp	Base pairs
BS	Bloodstream form of *T. brucei*
°C	Degree Celsius
CQ	Chloroquine
CSF	Cerebrospinal fluid
C-terminus/terminal	Carboxyl terminus/terminal
Da	Dalton
DAPI	4',6-diamidino-2-phenylindole
dATP	2'-deoxyadenosine 5'-triphosphate
dfx	Deferoxamine
DIDS	4,4′-Diisothiocyanatostilbene-2,2′-disulfonic acid disodium salt hydrate
DMSO	Dimethyl sulfoxide
DMT1	Divalent metal transporter 1
DNA	Deoxyribonucleic acid
dNTP	Deoxyribonucleoside triphosphate
dox	Doxycycline
DTNB	5,5'-dithiobis-(2-nitrobenzoic acid)
DTT	Dithiothreitol
E. coli	*Escherichia coli*
EDTA	Ethylenediaminetetraacetic acid
e.g.	For example
EP	Protein with tandem repeats of glutamate (E) and proline (P)
ER	Endoplasmatic reticulum
ESAG	Expression-site associated genes
EtOH	Ethanol
FACS	Fluorescence activated cell sorting
FCS	Fetal calf serum

Fe/S	Iron/sulfur
FPLC	Fast protein liquid chromatography
g	Gram
GB	GB domain of protein G
GPEET	Protein with internal pentapeptide repeats
GPI	Glycosylphosphatidylinositol
GPx	Glutathione peroxidases
GSH	Reduced glutathione
GSH1	γ-glutamylcysteine synthetase
GSH2	Glutathione synthetase
GSSG	Glutathione disulfide
GR	Glutathione reductase
GRAVY	Grand average of hydropathy
Grx	Glutaredoxin
h	Hours
HAT	Human African trypanosomiasis
H_2O_{MilliQ}	Water, which has been deionized and purified
15-(S)-HpETE	15S-hydroperoxy-5Z,8Z,11Z,13E-eicosatetraenoic acid
13-(S)-HpODE	13S-hydroperoxy-9Z,11E-octadecadienoic acid
HRP	Horseradish peroxidase
IAM	Iodoacetamide
IF	Immunofluorescence microscopy
IgG	Immunglobuline G
IgM	Immunglobuline M
IPTG	Isopropyl-β-D-thiogalacto-pyranoside
IU	International unit
k	Kilo
kan	Kanamycin resistance cassette
KO	Knockout
l	Liter
LAA	Linoleamide alkyne
LB	Luria Bertani
LCI	Life cell imaging
LipDH	Lipoamide dehydrogenase
M	Molar
m	Meter or milli
MALDI-TOF-MS	Matrix-assisted laser-desorption ionization-time-of-flight MS
MBP	Maltose-binding protein
MCP	Mitochondrial carrier protein

MCU	Mitochondrial calcium uniporter
MEM-Pros	Minimal essential medium used for procyclic trypanosomes
min	Minute
mRNA	Messenger ribonucleic acid
MS	Mass spectroscopy
MTS	Mitochondrial targeting sequence
n	Nano
N-terminus/terminal	Amino terminus/terminal
NADPH	Nicotinamide adenine dinucleotide phosphate
NaOAc	Sodium acetate
NEM	*N*-ethylmaleimide
neo	Neomycin (G418) resistance cassette
NusA	N utilization substance protein A
OD	Optical density
ODC	Ornithine decarboxylase
p67	Lysosomal LAMP-like membrane protein type I
pac	puromycin resistance cassette
PAGE	Polyacrylamide gel electrophoresis
PBS	Phosphate buffered saline
PC	Procyclic form of *T. brucei*
PCR	Polymerase chain reaction
PFA	Paraformaldehyde
pH	Pondus hydrogenii
PMSF	Phenylmethanesulfonyl fluoride
puro	Puromycin
PVDF	Polyvinylidene fluoride
Prx	2-Cys-peroxiredoxin
Px	Non-selenium glutathione peroxidase-like enzymes
RNA	Ribonucleic acid
RNAi	RNA interference
ROOH	Hydroperoxides
ROS	Reactive oxygen species
rpm	Revolutions per minute
RT	Room temperature
SDS	Sodium dodecyl sulfate
sec	Second
SOC	Super Optimal Broth
SpdS	Spermidine synthase
SRA	Serum resistance protein

st-dfx	Starch-deferoxamine
T	Tetracycline
T_m	Melting temperature
TAE	Tris-acetate-EDTA
TB	Terrific Broth
T. b. brucei	*Trypanosoma brucei brucei*
TBS	Tris buffered saline
TCA	Tricarboxylic acid
T. cruzi	*Trypanosoma cruzi*
TEMED	N, N, N', N'-tetramethylethylenediamine
TEV	Tobacco etch virus
TF	Transferrin
TFA	Trifluoroacetic acid
TLF	Trypanolytic factor
TPP	Triphenylphosphonium
Tpx	Tryparedoxin of *T. brucei*
TR	Trypanothione reductase of *T. brucei*
Trolox	(±)-6-Hydroxy-2,5,7,8-tetramethylchromane-2-carboxylic acid
Trx	Thioredoxin
TryS	Trypanothione synthetase
TS_2	Trypanothione disulfide
$T(SH)_2$	Reduced trypanothione
µ	Micro
U	Unit
Ubi	Ubiquinone
UTR	Untranslated region
UV	Ultraviolet
V	Volt
VSG	Variant surface glycoprotein
WB	Western blot
WHO	World Health Organization
WT	Wild type
ZIP14	ZRT/IRT-like protein 14
ZZ	Synthetic Z-domain of protein A

List of Tables and Figures

1 Introduction

1.1 Trypanosomes

1.1.1 Trypanosomiasis

Human African trypanosomiasis (HAT), also called sleeping sickness, is a vector-borne parasitic disease occurring in 36 sub-Saharan countries [WHO, 2014]. It is transmitted during a blood-sucking meal of an infected tsetse fly belonging to the genus *Glossina*. The subsequent infection is caused by the protozoan parasite *Trypanosoma brucei* which proliferates extracellularly in the blood and tissue fluids of the host [Steverding, 2008]. Two subspecies are involved in HAT progression (Figure 1.1): *T. b. gambiense* mostly found in western and central Africa accounts for over 98% of diagnostic cases [WHO, 2014]. The incubation period without symptoms can vary between months or even years and the parasite causes a chronic infection often affecting the central nervous system. In contrast, *T. b. rhodesiense* is most common in eastern and southern Africa and causes a fast and acute infection. In Uganda, both parasite species exist bearing the risk of co-infections and treatment failures [Kennedy, 2013].

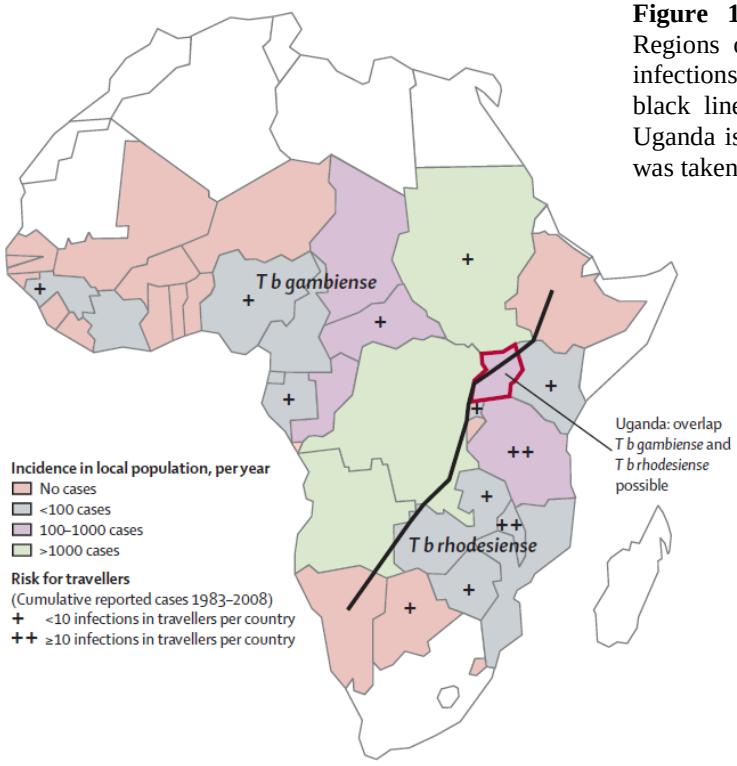

Figure 1.1: Distribution of HAT in Africa. Regions of *T. b. gambiense* and *T. b. rhodesiense* infections with incidences and traveler risk. The black line separates the areas of the subspecies. Uganda is highlighted by a red frame. The picture was taken from Brun *et al.* 2010.

Other diseases caused by trypanosomatids comprise Chagas' disease and the various forms of leishmaniasis. Chagas' disease mostly found in Latin America is caused by *T. cruzi* whereas the widely-distributed leishmaniasis is transmitted by Phebotomine sandflies infected with different species of *Leishmania* [Stuart *et al.*, 2008].

Animal trypanosomiasis is wide-spread in wild as well as domestic animals, the best known example being Nagana cattle disease. The main causative agents are *T. b. brucei*, *T. congolense*, and *T. vivax* [Steverding, 2008]. These infections are detrimental for the economic and cultural development of endemic regions. Animals can also be an important reservoir for both human pathogens aggravating the situation [Hamill *et al.*, 2013; Njiokou *et al.*, 2006].

In Africa, three major epidemics of sleeping sickness have been reported starting in 1896, 1920, and 1970 [Steverding, 2008]. In certain regions of South Sudan or the Democratic Republic of Congo, prevalence reached 50% which caused mortality rates higher than that of HIV [WHO, 2014]. The most recent epidemic was caused by neglected surveillance combined with socioeconomic instability and did not ameliorated before eflornithine was introduced in 1990 [Steverding, 2008]. After continued control efforts, annual case reports between 2000 and 2012 reveal a promising reduction of 73% of the number of newly infected individuals [WHO, 2014]. Although the number of new infections steadily declines, statistical analysis estimates a number of actual cases of 20000 and 70 million people at risk [WHO, 2014]. Transmission is still facilitated by poverty, limited access to health services, and the lack of human and material resources for exhaustive screenings. Efforts by e.g. the World Health Organization (WHO) and the Bill and Melinda Gates Foundation are directed to provide technical assistance for national control programs, free of charge medicines through a partnership with Bayer AG and Sanofi-Aventis, and to support operational research [WHO, 2014].

The treatment of HAT depends of the disease progression and staging. The first stage (haemolympathic phase) implies the proliferation of the parasites in the blood, lymph, and subcutaneous tissues resulting in classical infection symptoms like fever, headaches, and joint pains developing to cardiac failures and lymphadenopathy [Kennedy, 2013; Steverding, 2008]. In the second stage (neurological phase), trypanosomes reach the central nervous system by crossing the blood brain barrier or the blood cerebrospinal border [Mogk *et al.*,

2014; Wolburg *et al.*, 2012]. Typical symptoms are disturbance of the sleep cycle, confusion, extreme lethargy or motor system disturbances [Kennedy, 2013]. Sleeping sickness is virtually lethal if left untreated or insufficiently treated [Jamonneau *et al.*, 2012; Steverding, 2008]. Unfortunately, current treatment is not adequate as all main drugs are not orally available, often unacceptably toxic, show resistance developments, and are poorly effective [Fairlamb, 2003]. Drugs used in the first stage exhibit lower toxicity and better tolerance. These are pentamidine and suramin for *T. b. gambiense* and *T. b. rhodesiense* infections, respectively [Kennedy, 2013]. The diagnosis of the early stage of HAT is based on a smear of periphery blood (Figure 1.2) and the long-established card agglutination trypanosomiasis test [Kennedy, 2006]. The second stage is diagnosed by the examination of cerebrospinal fluid (CSF) through lumbar puncture and treated with melarsoprol and eflornithine (only effective against *T. b. gambiense*) and more recently with a combination of nifurtimox and eflornithine. Especially melarsoprol as an arsenic drug shows severe side effects that can culminate in reactive encephalopathy [Pépin *et al.*, 1995].

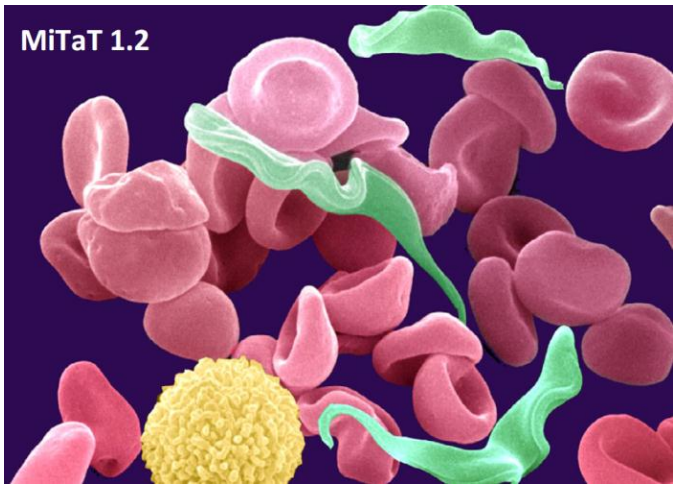

Figure 1.2: Bloodstream *T. b. brucei* among erythrocytes and immune cells. Blood smear from rats infected with the monomorphic strain MiTat 1.2. It was taken three days post intraperitoneal infection. The figure was taken from Mogk *et al.* 2014.

1.1.2 The life cycle of T. brucei

Tsetse flies are found in sub-Saharan Africa, mostly in rural areas inhabited by populations which depend on fishing, agriculture, and stock farming [WHO, 2014]. Both, female and male flies are blood-suckers and thus, transmit the disease [Brun *et al.*, 2010]. Alternative infection routes are a mother-to-child transmission as the parasite can cross the placenta or, accidently, by a contaminated needle during laboratory work. In general, *Glossina* subspecies are poor vectors since only 2 - 20% of the flies are infected [Dyer *et al.*, 2013].

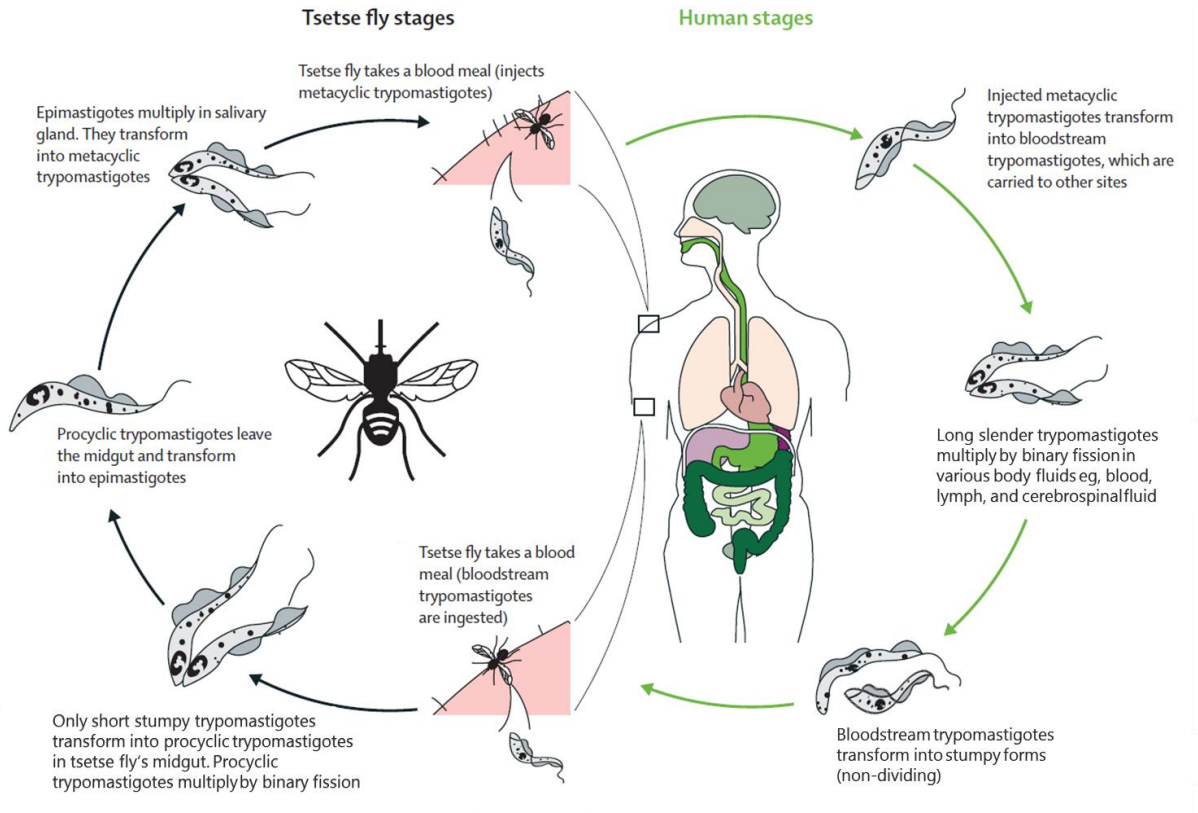

Figure 1.3: Life cycle of *T. brucei*. During a blood meal, an infected tsetse fly injects metacyclic parasites into the mammalian host which multiply in the body fluids as bloodstream forms. Trypanosomes ingested by a fly transform into procyclic parasites moving from the midgut to the salivary glands for the transmission into a new host. For details see text. The picture was taken from Kennedy *et al.* 2013 and modified.

During the blood meal of an infected tsetse fly, metacyclic trypomastigotes located in the salivary glands are transferred into the mammalian host (Figure 1.3). The parasites differentiate into long slender bloodstream (BS) trypomastigotes and enter the blood through the lymphatic system. They multiply by binary fission and some of them transform by a quorum-sensing signal into non-dividing, stumpy forms [Pays *et al.*, 2006; Reuner *et al.*, 1997]. After the next blood meal of a fly, the ingested stumpy parasites differentiate into proliferative procyclic (PC) trypomastigotes in the lumen of the midgut while the slender forms lyse [Dyer *et al.*, 2013]. After migrating anteriorly to the proventriculus, the PCs transform into long and short epimastigotes and migrate through the foregut to the salivary glands [Van Den Abbeele *et al.*, 1999]. The differentiation into infective metacyclic cells closes the life cycle. The incubation period in the tsetse fly takes three to five weeks and the fly persists infected for life [Brun *et al.*, 2010; Kennedy, 2013]. In the laboratory, we work with culture-adapted long slender BS and PC trypomastigotes.

1.1.3 The peculiarities of trypanosomes

Compared to higher eukaryotes, trypanosomes display a variety of morphological, biochemical as well as genetic peculiarities. The long slender BS form of *T. brucei* escapes the immune system by periodic switching of its variant surface glycoprotein (VSG) [Horn, 2014]. This homodimeric protein is linked to the plasma membrane by a glycosylphosphatidylinositol (GPI) anchor and provides a dense surface coat of 10^7 VSG molecules per cell [Ferguson *et al.*, 1988]. Only one VSG variant is expressed at a specific time uniquely transcribed by RNA polymerase I [Günzl *et al.*, 2003]. In addition, VSG genes are transcribed from ~20 expression sites situated on telomeres. It is proposed that around 30% of the genome encode 2000 VSG and pseudo genes [Horn, 2014]. In PC cells, the VSG is exchanged by a coat made of GPEET and EP procyclins [Acosta-Serrano *et al.*, 2001].

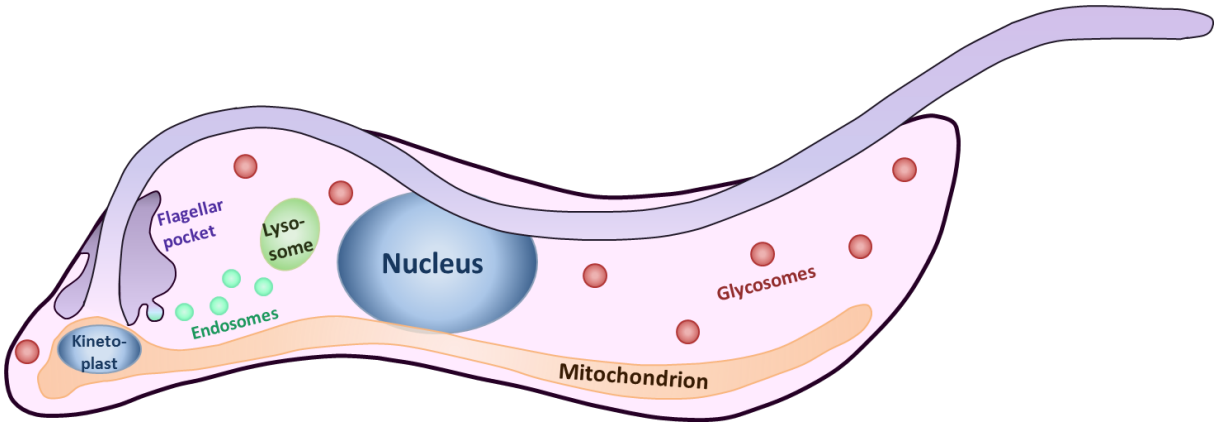

Figure 1.4: A schematic cell structure of BS *T. brucei*. Trypanosomes are 15 - 30 µm long with an attached flagellum. The single, tubular mitochondrion devoid of cristae (orange) contains the kinetoplast (blue). The flagellar pocket (dark violet) presents the site of endo- and exocytosis from which endosomes (light green) are formed. The terminal lysosome is present as a single copy (dark green). Glycosomes are peroxisome-like organelles (red) harboring the glycolytic pathway. The picture was modified from Engstler 2000.

In *T. brucei*, some organelles are single copies like the lysosome and the mitochondrion highlighting the parasite as an excellent model organism for organellar analysis (see Figure 1.4) [Matthews, 2005]. Trypanosomes belong to the order of Kinetoplastida defined by the presence of an unusual disk-shaped mitochondrial DNA. This so-called kinetoplast is composed of maxi- and minicircles which encode mitochondrial proteins and guide RNAs, respectively [Liu *et al.*, 2005]. For functional mRNAs, maxicircle transcripts have to be post-transcriptionally edited relying on the guide RNAs [Liu *et al.*, 2005]. This extensive editing process incorporates or deletes uridylate residues. In BS cells, the kinetoplast is located at the posterior end while it exhibits a sub-terminal cell position in PC parasites [Matthews, 2005]. The nuclear genome of *T. brucei* comprises eleven megabase chromosomes and >100

minichromosomes. The genes are transcribed polycistronically and mRNAs are formed by subsequent trans-splicing and polyadenylation [Liang *et al.*, 2003]. Gene expression is mainly regulated post-transcriptionally by mRNA stability and the translation rate [Clayton and Shapira, 2007].

In other organisms, glycolysis takes place in the cytosol while trypanosomatids evolved specific organelles for compartmentalization named glycosomes [Michels *et al.*, 2006]. One cell contains about 230 glycosomes sequestering the first seven enzymes of glycolysis [Opperdoes *et al.*, 1984; Opperdoes and Michels, 1993]. Trypanosomes have a single mitochondrion [Tomás and Castro, 2013]. In PC cells, the organelle is a large and highly branched network while in BS parasites it is small and rudimentary. The morphology is linked to the function and consequently to the bioenergetics metabolism. BS *T. brucei* rely on glycolysis for ATP production reflecting their glucose-rich environment [van Hellemond *et al.*, 2005]. Although BS cells do not have a fully functional oxidative chain, the mitochondrion is required for NAD^+ regeneration by the glycerol-3 phosphate shuttle and the alternative oxidase. In contrast, the insect stage displays an active respiratory chain with an unusual tricarboxylic acid (TCA) cycle [Tielens and van Hellemond, 2009; van Hellemond *et al.*, 2005]. This fully functional organelle is also largely involved in the biogenesis of Fe/S cluster and heme-containing proteins mainly present in PC cells [Lukeš and Basu, 2014; Tripodi *et al.*, 2011].

The animal pathogen *T. brucei brucei* is highly sensitive to the trypanolytic factors (TLFs) present in the blood of humans and some primates such as baboons [Pays *et al.*, 2006; Vanhollebeke and Pays, 2010]. TLF-1 is a high-density lipoprotein containing the haptoglobin-related protein and can be taken up by the parasite haptoglobin/hemoglobin receptor whereas TLF-2 is an IgM-rich complex which uptake mechanism is not fully characterized [Uzureau *et al.*, 2013; Vanhollebeke *et al.*, 2008; Vanhollebeke and Pays, 2010]. *T. brucei* species that are infective for humans are resistant to the lytic component apolipoprotein LI (apoLI) of both TLFs [Pérez-Morga *et al.*, 2005; Vanhamme *et al.*, 2003]. *T. b. rhodesiense* evolved a VSG-like gene encoding the serum resistance protein (SRA) which binds apoLI in the lysosome and prevents the pore-forming activity of apoLI and the subsequent cell lysis of the parasite [De Greef and Hamers, 1994; Pérez-Morga *et al.*, 2005; Xong *et al.*, 1998]. *T. b. gambiense* is resistant by other mechanisms comprising the reduced expression of the haptoglobin/hemoglobin receptor [Kieft *et al.*, 2010] or the expression of a

low affinity receptor [DeJesus *et al.*, 2013]. Stiffening of endosomal membranes by the VSG-like TgsGP may also confer TLF-resistance of *T. b. gambiense* [Capewell et al., 2013; Uzureau et al., 2013] as well as an increased activity of the lysosomal protease cathepsin-L [Alsford *et al.*, 2014].

1.1.4 The trypanothione metabolism of trypanosomatids

In virtually all organisms including humans, the intracellular thiol redox homeostasis relies on the glutathione (GSH) / glutathione reductase (GR) and thioredoxin/thioredoxin reductase system [Deponte, 2013]. Trypanosomatids lack GR and thioredoxin reductase [Berriman *et al.*, 2005] and their redox cycle is based on the low molecular weight dithiol, trypanothione [N^1, N^8-bis(glutathionyl)spermidine] which consists of two glutathione molecules linked by a spermidine bridge [Fairlamb *et al.*, 1985]. Trypanothione reductase (TR), a flavoenzyme, catalyzes the reduction of trypanothione disulfide (TS_2) to the dithiol trypanothione ($T(SH)_2$) (Figure 1.5) [Krauth-Siegel and Comini, 2008; Krauth-Siegel *et al.*, 1987].

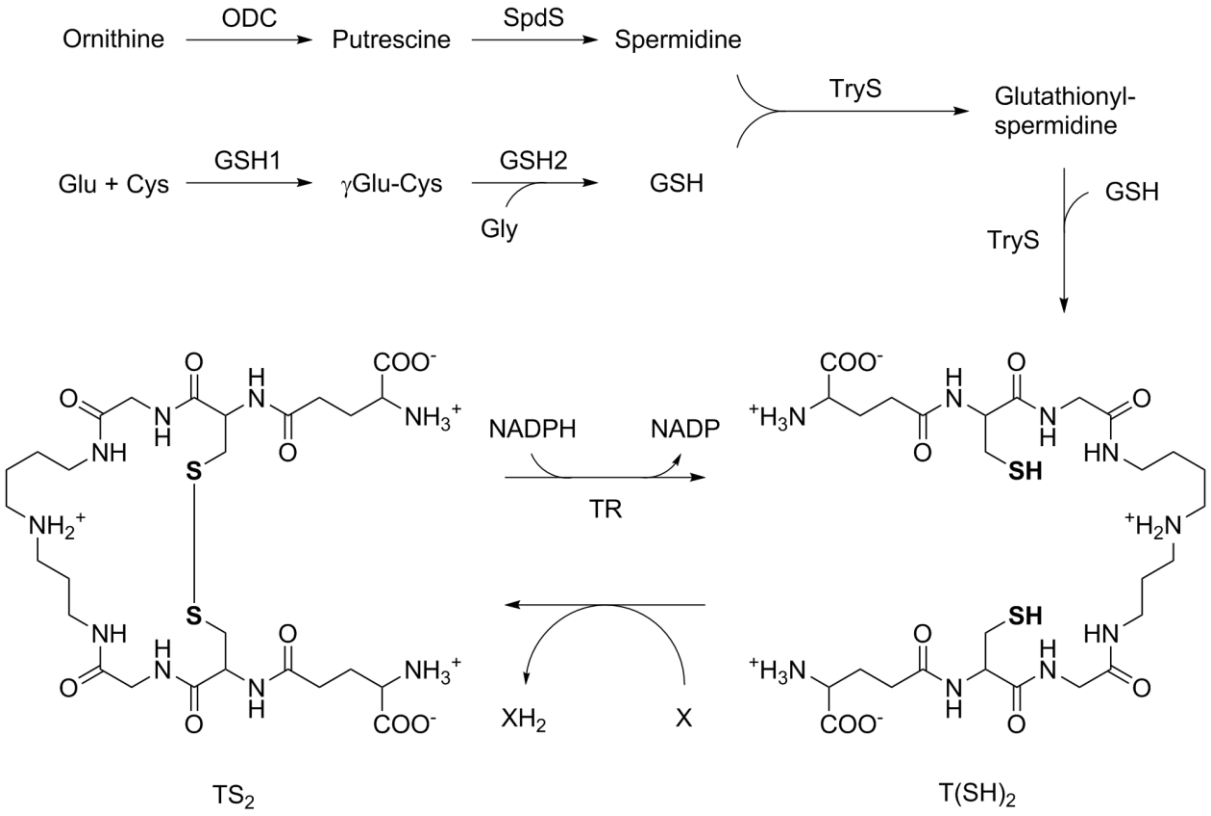

Figure 1.5: Synthesis and reduction of $T(SH)_2$ in *T. brucei*. Ornithine decarboxylase (ODC) generates putrescine which then reacts with decarboxylated S-adenosyl-L-methionine to spermidine catalyzed by the spermidine synthase (SpdS). In a two-step catalysis, GSH is produced from glutamate, cysteine, and glycine by γ-glutamylcysteine synthetase (GSH1) and glutathione synthetase (GSH2). $T(SH)_2$ is synthesized out of GSH and spermidine by trypanothione synthetase (TryS). $T(SH)_2$ is oxidized in different reactions (X) to TS_2 and reduced back by the NADPH-dependent trypanothione reductase (TR). For review see Krauth-Siegel and Leroux, 2012.

$T(SH)_2$ synthesis comprises three major pathways (for details see Figure 1.5). In a two-step catalysis, GSH is produced and spermidine is obtained through the polyamine pathway in African trypanosomes [Krauth-Siegel and Leroux, 2012]. Two molecules of GSH and one molecule of spermidine are then conjugated by the ATP-dependent trypanothione synthetase to finally yield $T(SH)_2$ [Krauth-Siegel and Comini, 2008].

$T(SH)_2$ is a more powerful reducing agent compared to GSH. One reason is its pK value of 7.4 which is similar to the physiological pH in the cytosol of BS and PC *T. brucei* [Moutiez *et al.*, 1994]. In addition, the dithiol character of $T(SH)_2$ kinetically favors disulfide bond formation compared to the intermolecular disulfide in the case of glutathione disulfide (GSSG) [Gilbert, 1990]. $T(SH)_2$ spontaneously reduces the disulfide forms of the parasite thioredoxin (Trx), glutaredoxins (Grx), tryparedoxin (Tpx), as well as GSSG [Krauth-Siegel and Comini, 2008]. The $T(SH)_2$/TR system is involved in crucial cellular pathways such as the reduction of ribonucleotides [Dormeyer *et al.*, 2001], protein repair [Arias *et al.*, 2011] as well as the detoxification of hydroperoxides [Castro and Tomás, 2008] which is the subject of this thesis.

1.2 Peroxidases

1.2.1 Glutathione-dependent peroxidases

Glutathione peroxidases (GPx) catalyze the reduction of hydrogen peroxide and organic hydroperoxides to water or the corresponding alcohol [Brigelius-Flohé and Maiorino, 2013]. Most of the human GPxs are selenoproteins - containing a selenocysteine in their catalytic site - but extended to all domains of life, the majority of these proteins possesses an active site cysteine instead of Sec. This catalytic tetrad comprises Sec or Cys, Gln, Trp, and Asn [Tosatto *et al.*, 2008]. Following a ping-pong mechanism, the selenolate/thiolate reacts with the hydroperoxide to selenenic/sulfenic acid. In the case of the selenoproteins, the selenic acid is reduced back by two GSH molecules in two steps via a glutathionylated enzyme intermediate [Mauri *et al.*, 2003; Toppo *et al.*, 2009]. In the cysteine homologues, the sulfenic acid formed at the peroxidatic cysteine builds an intramolecular disulfide with a so-called resolving cysteine which is subsequently reduced by a "redoxin", mostly Trx or in trypanosomes, Tpx [Castro and Tomás, 2008; Toppo *et al.*, 2009].

In mammals, eight GPxs have been identified so far [Brigelius-Flohé and Maiorino, 2013]. As the trypanosomal peroxidases (Px I-III) are closest related to GPx4, this human peroxidase is described in more detail. GPx4 can be seen as a moonlighting protein that is involved not only in antioxidant defense and 12,15-lipoxygenase-mediated apoptosis but it is also implicated as structural protein during spermatogenesis [Brigelius-Flohé and Maiorino, 2013; Schneider *et al.*, 2009; Seiler *et al.*, 2008]. The monomeric GPx4 is also known as phospholipid GPx as it reduces hydroperoxides of complex lipids or cholesterol even within biomembranes [Imai and Nakagawa, 2003; Thomas *et al.*, 1990; Ursini *et al.*, 1982]. Short and long versions of GPx4 are formed by alternative transcription and the use of different translation start sites [Pushpa-Rekha *et al.*, 1995]. The short form is found in the nucleus, endoplasmatic reticulum (ER), and the cytosol whereas the longer protein is translocated to the mitochondrion where it is truncated to the same size as the short GPx4 [Brigelius-Flohé and Maiorino, 2013]. The cytosolic GPx4 is the only isoform which is not dispensable in embryogenesis [Yant *et al.*, 2003]. Studies on inducible GPx4 depletion in primary mouse embryonic fibroblasts showed that α-tocopherol rescued the lethal phenotype supporting its role in membrane protection [Seiler *et al.*, 2008].

1.2.2 Peroxidases in T. brucei

Trypanosomes lack catalase and selenocysteine-containing GPxs. Two types of thiol peroxidases namely the 2-Cys-peroxiredoxins (Prx) and the non-selenium containing glutathione peroxidase-type enzymes (Px) catalyze the detoxification of hydroperoxides and are linked to the $T(SH)_2$/TR system via Tpx [Castro and Tomás, 2008; Krauth-Siegel and Comini, 2008]. Tpx is a dithiol protein and distant relative to the superfamily of Trx-type proteins [Lüdemann *et al.*, 1998]. Using NADPH as primary electron donor, the reducing equivalents were carried via TR, $T(SH)_2$, and Tpx onto the peroxidases which then catalyze the reduction of hydroperoxides as shown in Figure 1.6 for the Px-type enzymes [Budde *et al.*, 2003; Hillebrand *et al.*, 2003; Tetaud *et al.*, 2001; Wilkinson *et al.*, 2002a]. While the Prx-type peroxidases present a high substrate preference for hydrogen peroxide, the Px-type enzymes specifically detoxify fatty acid-derived hydroperoxides [Diechtierow and Krauth-Siegel, 2011]. In the *T. brucei* genome, three Prx genes have been identified encoding two identical cytosolic proteins and another mitochondrial one [Tetaud *et al.*, 2001]. Previous RNA interference (RNAi) studies reveal that only the cytosolic peroxidases are essential [Wilkinson *et al.*, 2003]. These cytosolic enzymes efficiently reduce hydrogen peroxide as well as hydroperoxides derived from cumene, thymine, or tert-butanol and are rapidly

inactivated by lipid hydroperoxides [Budde *et al.*, 2003; Diechtierow and Krauth-Siegel, 2011; Tetaud *et al.*, 2001].

Figure 1.6: Detoxification of lipid hydroperoxides by the Px-type enzymes. Hydroperoxides (ROOH) are reduced to the respective alcohols by the Px-type enzymes which in turn are oxidized. The reducing equivalents are derived from a cascade of Tpx, $T(SH)_2$, and TR consuming NADPH as final electron source. The picture was taken from Diechtierow, PhD thesis 2011 and Krauth-Siegel and Comini, 2008.

The second type of Tpx peroxidases, namely the Pxs, presents pronounced similarities to the human GPx4. Although the Pxs contain a cysteine in the active site, the physiological function as phospholipid peroxidase, which protects membranes against lipid peroxidation, is conserved. Px-type enzymes are also monomers and occur in the cytosol and mitochondrion. The three virtually identical genes are tandemly arranged on chromosome 7 of *T. brucei* (Figure 1.7) [TriTrypDB, 2015]. Previous RNAi and knockout (KO) studies showed that the cytosolic Px I-II are essential whereas the mitochondrial Px III is dispensable in BS *T. brucei* [Wilkinson *et al*., 2003; Schlecker *et al*. 2005; Diechtierow and Krauth-Siegel, 2011]. As in the case of the human GPx4, parasites depleted of Px I-II are fully viable in the presence of the antioxidant Trolox. After removal of this vitamin E analogue, the KO cells display a rapid cell lysis [Diechtierow and Krauth-Siegel, 2011]. The main part of my thesis focused on this unusual phenotype in *T. brucei*.

Figure 1.7: The *px* locus of *T. brucei*. The three *px* genes encoding Px I-III are tandemly arranged on chromosome 7. They are virtually identical except for the N-terminal mitochondrial targeting sequence (green) and C-terminal glycosomal targeting sequence of *px III*. The intergenic regions between *px I* and *px II* as well as *px II* and *px III* (light brown) are identical except that the *px I*/*px II* UTR is 25 bp longer. The picture was taken from Diechtierow, PhD thesis 2011.

1.2.3 A novel glutathione-dependent peroxidase in T. cruzi

Studies in *T. cruzi* revealed an additional glutathione peroxidase-type enzyme, named here Px IV [Wilkinson *et al.*, 2002b]. Using immunofluorescence microscopy with antibodies against the recombinant protein, Px IV is proposed to be an ER-resident protein. In kinetic analyses with different hydroperoxides, the protein presents highest activity against the hydroperoxides of lineloic acid in the presence of a GSH-based redox system. However, the apparent K_m of

GSH is rather high (5 mM). From these data, Px IV is described as a peroxidase involved in the protection of newly synthesized phospholipids in the ER of *T. cruzi*. An orthologue is encoded in the *T. brucei* Lister strain 427 on chromosome 11 [TriTrypDB, 2015]. As a distant relative of Px I-III, the protein was studied in this thesis as well.

1.3 Iron metabolism

1.3.1 Human iron metabolism

Cellular iron is essential for cell survival and stored in the multimeric protein ferritin [Arosio and Levi, 2010]. In humans, most iron is found in erythrocytes sequestered in hemoglobin [Lane *et al.*, 2015]. From the blood, iron bound to transferrin is taken up via receptor-mediated endocytosis by the transferrin receptor [Hentze *et al.*, 2010]. In late endosomes, ferric iron is released due to the low pH and reduced by an endosomal ferric reductase or ascorbate [Escobar *et al.*, 1992; Lane and Richardson, 2014; Ohgami *et al.*, 2005]. The apo-transferrin/receptor complex is recycled back to the plasma membrane where apo-transferrin is released [Taylor and Kelly, 2010]. Ferrous iron is delivered from the endosome/lysosome to the cytosol by the divalent metal transporter 1 (DMT1) [Gunshin *et al.*, 1997] or the ZIP14 transporter [Jenkitkasemwong *et al.*, 2012; Zhao *et al.*, 2010] and used for metabolism (incorporating into proteins) or for storage in ferritin.

As mitochondria are involved in heme synthesis and Fe/S cluster biogenesis, these organelles are linked to iron metabolism [Lill, 2009; Sheftel and Lill, 2009]. Three important mechanisms of mitochondrial iron uptake have been proposed: (a) a direct interaction of the mitochondrion and the endosomes (kiss-and-run hypothesis) [Sheftel *et al.*, 2007], (b) direct iron uptake from the cytosol forced by the negative membrane potential, and (c) uptake from the cytosolic non-labile iron pool by an unknown cytosolic-mitochondrial transfer system [Lane *et al.*, 2015; Shvartsman *et al.*, 2007]. The iron transport through the outer mitochondrial membrane is not fully characterized whereas iron import through the inner mitochondrial membrane is mediated by the specific ferrous iron transporters, mitoferrin 1 and 2 [Paradkar *et al.*, 2009] and possibly by the mitochondrial calcium uniporter (MCU) [Uchiyama *et al.*, 2008]. Imported iron can be used for heme or Fe/S cluster biosynthesis [Lane *et al.*, 2015]. The last step of heme biosynthesis involves the Fe/S-containing ferrochelatase which inserts ferrous iron into the protoporphyrin IX [Sheftel and Lill, 2009]. Fe/S clusters occur mostly as 4Fe-4S and 2Fe-2S and are coordinated via cysteine or histidine

residues to the proteins [Lill, 2009]. Fe/S proteins are involved in a variety of cellular functions like electron transfer (complex I-III of the respiratory chain), metabolic sensors (cytosolic aconitase), and DNA replication (DNA polymerases) and repair (DNA helicases of nucleotide excision repair) [Netz *et al.*, 2012; Sheftel *et al.*, 2010].

1.3.2 Iron metabolism in trypanosomes

In BS parasites, the major iron source is host transferrin that is taken up by clathrin-dependent receptor-mediated endocytosis [Morgan *et al.*, 2001; Schell *et al.*, 1991]. The trypanosomal transferrin receptor is a heterodimer encoded by the two expression-site associated genes (ESAGs) 6 and 7 and linked to the plasma membrane by one GPI anchor [Chaudhri *et al.*, 1994; Ligtenberg *et al.*, 1994; Steverding *et al.*, 1994]. These ESAGs are rather diverse due to a hypervariable region in the different expression sites [Taylor and Kelly, 2010]. It is proposed that this diversity presents adaption of the receptor to transferrin from different mammalian hosts [Bitter *et al.*, 1998; van Luenen *et al.*, 2005]. Estimation of the iron uptake revealed that the BS parasite takes up 85000 iron ions per generation time but requires only 40000 [Steverding, 1998]. In contrast to the mammalian TF-receptor, the parasite receptor binds both holo- and apo-transferrin with similar dissociation constants in the low nM-range (only 5-fold difference) [Steverding, 1998]. After delivery into the lysosome, the receptor releases transferrin which is degraded by cathepsin B-like proteases [O'Brien *et al.*, 2008] while the receptor is recycled to the cell surface. The enzyme catalyzing the reduction of ferric to ferrous iron has not yet been identified [Taylor and Kelly, 2010]. A mucolipin-type 1 protein has been presented as a putative iron transporter in the lysosomal membrane [Taylor *et al.*, 2013]. In the infective form of the parasite, iron is incorporated into the ribonucleotide reductase (DNA synthesis) [Dormeyer *et al.*, 2001; Hofer *et al.*, 1997], superoxide dismutase (antioxidant defense) [Le Trant *et al.*, 1983], aconitase [Overath *et al.*, 1986], and alternative oxidase (energy metabolism) [Clarkson *et al.*, 1989]. BS cells have a low demand of mitochondrial Fe/S cluster proteins but the cytosolic Fe/S cluster assembly machinery is essential in both life stages as it may be needed for cytosolic and nuclear Fe/S cluster proteins [Basu *et al.*, 2014]. How iron is transported into the parasite mitochondrion is not yet known. However, the putative mitochondrial carrier protein (MCP) 17 displays high similarities to human and yeast iron carriers [Colasante *et al.*, 2009].

In PC trypanosomes, the iron uptake mechanism is not well studied although they have a higher iron demand compared to BS cells [Taylor and Kelly, 2010]. The recent hypothesis is

that PC *T. brucei* reduce ferric iron by a ferrireductase located in the plasma membrane and then take up ferrous iron by a divalent metal transporter [Mach *et al.*, 2013]. Iron is especially needed in the insect stage for the biogenesis of Fe/S clusters and cytochrome-containing complexes required for oxidative phosphorylation [Taylor and Kelly, 2010]. Iron could be also generated from heme by a heme oxygenase, however no respective gene has been identified yet in *T. brucei* [Korený *et al.*, 2013]. Heme-iron may be however also released non-enzymatically in the presence of GSH [Atamna and Ginsburg, 1995] or hydrogen peroxide [Gutteridge, 1986; Nagababu and Rifkind, 2000]. For *L. infantum*, heme has been shown as an iron source [Carvalho *et al.*, 2009]. No Kinetoplastida possess the complete heme biosynthesis pathway, particularly *T. brucei* is heme auxotroph. [Korený *et al.*, 2010]. Heme is required as a co-factor for various mitochondrial and non-mitochondrial proteins especially in PC parasites. But also in BS cells, heme is needed e.g. for the putative cytochromes b5 and P450 involved in the desaturation of fatty acids and biosynthesis of sterols, respectively [Tripodi *et al.*, 2011].

1.3.3 Iron-induced ROS production in eukaryotes

The cellular iron metabolism is closely linked to that of the so-called reactive oxygen species (ROS) like superoxide anion, hydrogen peroxide, and hydroxyl radical [Koskenkorva-Frank *et al.*, 2013]. Iron is not only involved in the formation of ROS but also in their scavenging. The removal of these species is mediated by antioxidant enzymes including superoxide dismutase, catalase, and GPxs or directly by antioxidants like ascorbate, GSH, and α-tocopherol [Koskenkorva-Frank *et al.*, 2013]. In trypanosomes, four superoxide dismutase isoforms have been identified. They are located in the glycosomes and the mitochondrion and contain an iron ion instead of manganese or zinc/copper described for the mammalian enzymes [Wilkinson *et al.*, 2006].

In many cell types, mitochondria are the main site of endogenous oxidative damages caused by ROS which are formed as side products of oxidative phosphorylation [Koskenkorva-Frank *et al.*, 2013; Turrens, 2003]. About 1 - 3% of the electrons leak out of the transduction cascade and result in the one electron reduction of molecular oxygen to superoxide performed by complex I and III of the respiratory chain [Valko *et al.*, 2007]. The mitochondrial superoxide dismutase converts superoxide anions into hydrogen peroxide. As mitochondria in human cells are the major organelles of iron utilization and contain a labile iron pool, hydrogen peroxide can react with ferrous iron via Fenton chemistry [Petrat *et al.*, 2001;

Sheftel and Lill, 2009]. Iron may be also released by superoxide from iron-containing proteins as shown for Fe/S-containing enzymes especially aconitase [Liochev and Fridovich, 1994; Vasquez-Vivar *et al.*, 2000]. In particular, hydroxyl radicals produced by the Fenton reaction are highly reactive and interact with all biomolecules in their vicinity [Koskenkorva-Frank *et al.*, 2013]. This can cause damages to proteins, lipids, and DNA of mitochondria and destroy mitochondrial function [Murphy and Smith, 2007]. The hydroxyl radicals can also take one electron from polyunsaturated fatty acids which result in lipid radicals (Figure 1.8). These radicals can react with molecular oxygen to produce lipid peroxyl radicals initiating lipid peroxidation and finally producing unsaturated aldehydes such as malondialdehyde and 4-hydroxy-2-nonenal [Valko *et al.*, 2007].

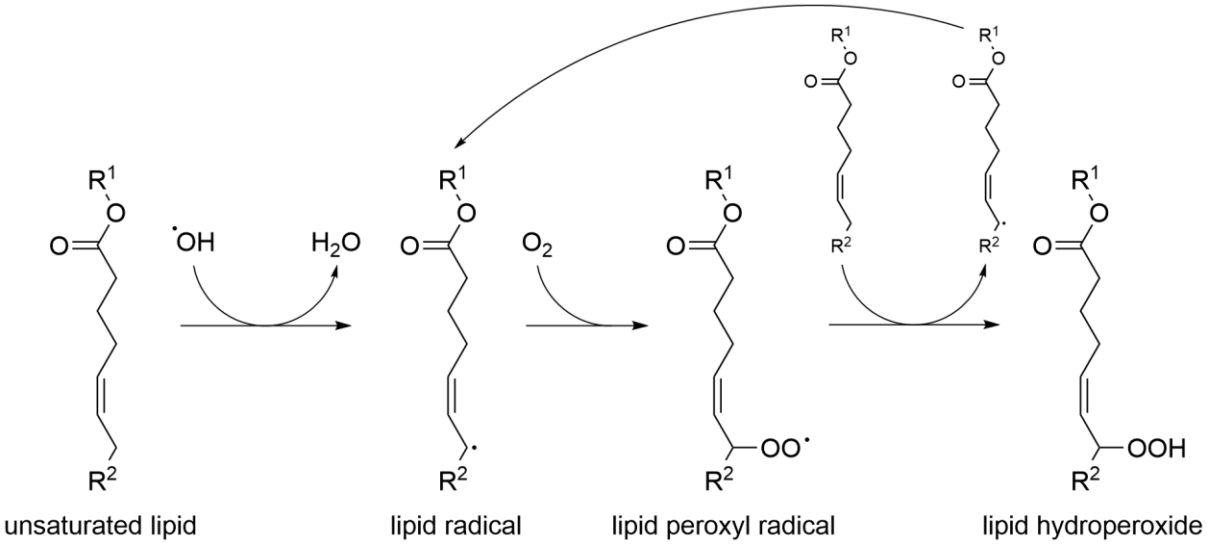

Figure 1.8: Lipid peroxidation. An unsaturated fatty acid can react with a hydroxyl radical ($OH^{\cdot}$) to a fatty acid radical. In the presence of molecular oxygen, these unstable radicals form lipid peroxyl radicals which can react with a second unsaturated fatty acid to another lipid radical and a lipid hydroperoxide. This process initiates lipid peroxidation which can be terminated by e.g. vitamin E.

Iron can be also found in large amount in the lysosome of human cells [Koskenkorva-Frank *et al.*, 2013]. In trypanosomes, the organelle has been proposed as iron storage [Lu *et al.*, 2007]. Through the endocytosis of transferrin and hemoglobin in *T. brucei*, iron and heme are present in the lysosome and can react with hydrogen peroxide to initiate lipid peroxidation as outlined above for mitochondria [Higdon *et al.*, 2012]. As iron-containing proteins are degraded, redox-active iron should be present in high concentrations and subjects lysosomes to oxidative damage [Kurz *et al.*, 2011]. As a consequence of lipid peroxidation and subsequently membrane rupture, lysosomal enzymes are released and trigger apoptosis or

necrosis as shown for human cells [Kirkegaard and Jäättelä, 2009]. Lysosomal iron has been suggested to be present in the ferrous state due to the acidic pH and the presence of reductants including ascorbate and cysteine [Escobar *et al.*, 1992; Pisoni *et al.*, 1990]. Hydrogen peroxide originated from the mitochondrion can easily cross membranes and thus, may also diffuse into the lysosome [Terman and Kurz, 2013]. As the cytosol contains a whole battery of H_2O_2-consuming enzymes like Prxs and catalase, the significance of the latter reaction is not clear [Winterbourn, 2008]. Another source of lysosomal ROS production is linked to the redox cycle of ubiquinone [Nohl and Gille, 2005]. Ubiquinones are not evenly distributed between all cellular membranes but high levels of reduced ubiquinones are found in lysosomes [Gille and Nohl, 2000; Kalén *et al.*, 1987]. Hydroxyl radicals have been detected in native lysosomal fractions, possibly obtained by the univalent reduction of ubiquinone [Gille and Nohl, 2000]. Ubiquinone is also found in relative high amounts in *T. brucei* [Ellis, 1994].

1.4 Aim of the PhD thesis

The aim of this work was to elucidate the physiological role(s) of the distinct glutathione Px-type enzymes in African trypanosomes. The following approaches were addressed:

1. Physiological role of the cytosolic Px I-II and the mitochondrial Px III in the BS as well as PC form of *T. brucei*.

   1.1 Life cell imaging of intracellular damage in BS parasites lacking the cytosolic peroxidases (*px I-II*$^{-/-}$).

   1.2 Generation of KO cell lines in PC parasites that lack all three peroxidases (*px I-III*$^{-/-}$) and only the mitochondrial Px III, respectively.

   1.3 Effect of iron and iron chelators on the mutant BS and PC cell lines.

   1.4 Immunofluorescence analysis of BS *px I-II*$^{-/-}$ and PC *px I-III*$^{-/-}$ cell lines in order to identity the damaged organelle after Trolox removal.

   1.5 Analyzing the protective effect of ubiquinone antioxidants on KO BS and PC cell lines.

2. Partial characterization of another distantly related *T. brucei* Px IV.

   2.1 Cloning and analysis of the recombinant protein.

   2.2 Generation of KO cell lines of Px IV in BS parasites.

2 Materials and Methods

2.1 Materials

2.1.1 Chemicals

Chemicals [catalog number]	Provider
Acetic acid [20104.334]	VWR AnalaR Normapur
Acetonitrile [34998]	Sigma-Aldrich
Agar, Select [30391-023]	Invitrogen
Agarose (standard) low electroendosmosis [50402]	Biomol
Ammonium acetate ($CH_3CO_2NH_4$) [09690]	Fluka
Ammonium bicarbonate (NH_4HCO_3) [1066-33-7]	J. T. Baker
Ammonium chloride (NH_4Cl) [12125-02-9]	J. T. Baker
Ammonium iron (III) citrate, ~18% Fe, DAC [CN77.1]	Carl Roth
Ammonium persulfate (APS) [10316]	Grüssing
Anti-Digoxigenin-AP [1093274]	Roche
Basic Minimal Essential Medium (MEM) [T9021-10]	Biochrom
Bathocuproine disulfonic acid disodium [B1125]	Sigma-Aldrich
Biotin [B4501]	Sigma-Aldrich
Blasticidin S hydrochloride [CP14]	Carl Roth
Boric acid (H_3BO_3) [100165]	Merck Millipore
Bromophenol blue [108122]	Merck Millipore
Calcium chloride ($CaCl_2$ x 2 H_2O) [172570]	Merck Millipore
Carbenicillin [69101/15875]	Novagen / SERVA Electrophoresis
CDP star [1685627]	Roche
Chloramphenicol [16785]	SERVA Electrophoresis
Cobalt chloride ($CoCl_2$ x 6 H_2O) [102539]	Merck
Coenzyme Q10 [C9538]	Sigma-Aldrich
Coomassie blue R250 [12553]	Merck Millipore
Copper chloride ($CuCl_2$ x 2 H_2O) [102733]	Merck
Cyanogen bromide-activated sepharose 4B [17-0430-01]	GE Healthcare
Cystatin [C8917]	Sigma-Aldrich
D(+) Glucose [108342]	Merck

4',6-Diamidino-2-phenylindole (DAPI) [D8417]	Sigma-Aldrich
Decyltriphenylphosphonium bromide (Decyl-TPP)	Mike Murphy, Cambridge, UK
Decylubiquinone [D7911]	Sigma-Aldrich
Deferoxamine mesylate salt [D9533]	Sigma-Aldrich
Dextran-Alexa Fluor 488 (10,000 MW) [D-22910]	Life Technologies
DIG Easy Hyb Granules [11796895001]	Roche
DIG labeled DNA ladder IV [11669940910]	Roche
Dimethyl sulfoxide (DMSO) [102950]	Merck Millipore
4,4′-Diisothiocyanatostilbene-2,2′-disulfonic acid disodium salt hydrate (DIDS) [D3514]	Sigma-Aldrich
Di-potassium hydrogen phosphate trihydrate (K_2HPO_4 x 3 H_2O) [A4001]	AppliChem
Di-sodium hydrogen phosphate dihydrate (Na_2HPO_4 x 2 H_2O) [A3567]	AppliChem
5,5'-Dithiobis-(2-nitrobenzoic acid) (DTNB) [20735]	SERVA Electrophoresis
Dithiothreitol (DTT) [04010]	Biomol
Ethylenediaminetetraacetic acid (EDTA) [A3553]	AppliChem
Ethanol, absolute (EtOH) [32205]	Sigma-Aldrich
Ethanolamine [398136]	Sigma-Aldrich
Ethidium bromide [HP46]	Carl Roth
Fetal calf serum (FCS) [50613/50615]	Biochrom
G418 sulfate [345810]	Merck Millipore
Gelatine [A1693]	AppliChem
GeneRuler 100 bp Plus DNA Ladder [SM0321]	Thermo Scientific
GeneRuler 1 kb Plus DNA Ladder [SM1331]	Thermo Scientific
Glycerol anhydrous [A3552/33226]	AppliChem/Sigma-Aldrich
Glycine [A1377]	AppliChem
H_2O_2, 30% [07209]	Merck Millipore
Hemin [51280]	Fluka/Sigma-Aldrich
Hemoglobin from bovine blood [51290]	Sigma-Aldrich
15S-Hydroperoxy-5Z,8Z,11Z,13E-eicosatetraenoic acid (15(S)-HpETE) [44720]	Cayman Chemical
13S-Hydroperoxy-9Z,11E-octadecadienoic acid (13-(S)-HpODE) [48610]	Cayman Chemical
Hydrochloric acid (HCl), 37 % [100317]	Merck Millipore
Hygromycin [CP13]	Carl Roth

Hypoxanthine [H9377]	Sigma-Aldrich
Iodoacetamide (IAM) [16125]	Sigma-Aldrich
Imidazole [104716]	Merck Millipore
Iron (III) chloride x 6 H_2O [31232]	Sigma-Aldrich
Iron (III) nitrate x 9 H_2O [254223]	Sigma-Aldrich
Iron (II) sulfate x 7 H_2O [31236]	Sigma-Aldrich
Iscove's Modified Dulbecco's Medium [42200-030]	Life Technologies
Isopropanol [20880.290]	VWR International
Isopropyl-β-D-thiogalacto-pyranoside (IPTG) [37-2020]	Peqlab
Kanamycin [26899]	SERVA Electrophoresis
L-Cysteine [C7352]	Sigma-Aldrich
L-Glutathione, reduced [G4251]	Sigma-Aldrich
Loading dye (6x) [R0611]	Thermo Scientific
LysoTracker Green DND-26 [L-7526]	Life Technologies
Lysozyme, chicken egg white [4403]	Merck Millipore
MALDI matrix (α-cyano-4-hydroxycinnamic acid) [201344]	Bruker
Maleic acid [800380]	Merck
Magnesium chloride ($MgCl_2$ x 6 H_2O [A3618]	AppliChem
Magnesium sulfate ($MgSO_4$ x 7 H_2O) [10034-99-8]	J. T. Baker
MEM non-essential amino acid solution 100x [M7145]	Sigma-Aldrich
MEM vitamin solution 100x [M6895]	Sigma-Aldrich
2-Mercaptoethanol [63689]	Sigma-Aldrich
Methanol [32213-2]	Sigma-Aldrich
Milk powder [T145]	Carl Roth
MitoQ (Mitoquinone)	Mike Murphy, Cambridge, UK
MitoTracker Red CMXRos [M-7512]	Life Technologies
N, N, N', N'-Tetramethylethylenediamine (TEMED) [2367]	Carl Roth
N-Ethylmaleimide (NEM) [1271]	Sigma-Aldrich
Nicotinamide adenine dinucleotide phosphate (NADPH) [16156]	Biomol
Ni-NTA Superflow [30430]	Qiagen
Penicillin/Streptomycin (5,000 U/ml/5,000 µg/ml) [P4458]	Sigma-Aldrich
PageRuler Plus Prestained Protein Ladder [26619, SM1811]	Thermo Scientific
Paraformaldehyde (PFA) [16005]	Riedel-de-Haën
Pepstatin [P5318]	Sigma-Aldrich

Peptide Calibration Standard [206195]	Bruker
Phenol red [7241]	Merck
Phleomycin from *S. verticillus* [P9564]	Sigma-Aldrich
Phenylmethanesulfonyl fluoride (PMSF) [P7626]	Sigma-Aldrich
Poly-L-lysine solution [P8920]	Sigma-Aldrich
Potassium chloride (KCl) [A3582]	AppliChem
Potassium dihydrogen phosphate (KH_2PO_4) [A3620]	AppliChem
Puromycin dihydrochloride from *S. alboniger* [P8833]	Sigma-Aldrich
RNase A solution (1 mg/ml)	Christine Clayton
Rotiphorese gel 30 (37.5:1): 30% acrylamide/bisacrylamide [3029]	Carl Roth
Sodium acetate (NaOAc) [32319]	Sigma-Aldrich
Sodium azide (NaN_3) [11112]	Ferak
Sodium bicarbonate ($NaHCO_3$) [31437]	Sigma-Aldrich
Sodium chloride (NaCl) [31434]	Sigma-Aldrich
Sodium dodecyl sulfate (SDS) [20765]	SERVA Electrophoresis
Sodium hydroxide (NaOH) [1310-73-3]	Grüssing
Sodium pyruvate [P4562]	Sigma-Aldrich
Starch-deferoxamine	John Lemasters, Charleston, USA
Super Optimal Broth (SOC) outgrowth medium [B9020S]	New England BioLabs
Tetracycline hydrochloride [T7660]	Sigma-Aldrich
Thiamine hydrochloride [04573]	Fluka
Thymidine [T1895]	Sigma-Aldrich
Transferrin, apo bovine [T1428]	Sigma-Aldrich
Transferrin, holo bovine [11107-018]	Life Technologies
Trifluoroacetic acid (TFA) [14264]	Sigma-Aldrich
Tris [4855]	Carl Roth
Trisodium citrate [A2403]	AppliChem
Triton X-100 reduced [X100RPC]	Sigma-Aldrich
Trolox (±6-hydroxy-2,5,7,8-tetramethylchromane-2-carboxylic acid) [238813]	Sigma-Aldrich
Trypsin [V5111]	Promega
Tryptone/peptone ex casein [8952]	Carl Roth
Tween 20 (Polysorbat 20) [817072]	Merck Millipore

Urea [1244]	Gerbu Biotech
Yeast extract [2363]	Carl Roth
Zinc chloride ($ZnCl_2$) [14424]	Riedel-de-Haën

2.1.2 Consumables

Consumables	Provider
Amicon Ultra centrifugal filters 15 & 2 ml with molecular weight cut-offs	Merck Millipore
Antifect N liquid	Schülke
Chromatography paper 3MM Chr	Whatman
Centrifuge tube 15 and 50 ml, CELLSTAR	Greiner Bio-One
Chromatography column (14 cm high, empty), Econo-Pac	Bio-Rad
Cover slip	Knittel Glass/ Carl Roth
Cryogenic sterile 1 ml storage vial with screw cap, Cyro.s	Greiner Bio-One
Filter tip Gilson 1000, 100, & 10 µl	Greiner Bio-One
Gel-loader pipette tip	Greiner Bio-One
Glass micropipette	Brand
Glass slide 76 x 26 mm	Menzel-Gläser
Gloves, XCEED nitrile powder-free	Mircoflex
Hyperfilm ECL	Amersham Biosciences
Membrane filter 0.22 µm	Merck Millipore
Parafilm	Sigma-Aldrich
Pasteur capillary pipettes 230 mm	Wu Mainz
PCR tube 0.2 ml	Kisker Biotech
Petri dish	Greiner Bio-One
Pipette tips 1000, 100, & 10 µl, type Gilson	Greiner Bio-One
Pipette with tip 25, 10, & 5 ml, sterile	Greiner Bio-One
Polystyrole cuvette	Sarstedt
Polyvinylidene fluoride (PVDF) membrane 0.45 µm, Hybond P	Amersham Biosciences
PVDF membrane 0.45 µm, Westran S	Whatman
Reaction tube 0.5, 1.5, & 2 ml, SafeSeal	Sarstedt
Scalpel	Braun
Southern blot membrane, Hybond-N^+	Amersham Biosciences
SuperSignal West Pico solutions	Pierce

Syringe 5 & 10 ml	BD
Syringe filter 22 µm, Millex-GS	Merck Millipore
Tip for kinetics 1000 & 100 µl, epT.I.P.S standard unsterile	Eppendorf
Tissue culture flask 50 ml + vented cap	Falcon & Greiner Bio-One
Tissue culture flask 50 ml + plug seal cap	Falcon & Greiner Bio-One
Tissue culture flask 250 ml + vented cap, CELLSTAR	Greiner Bio-One
Tissue culture flask 250 ml + plug seal cap, CELLSTAR	Greiner Bio-One
Tissue culture plate 24-well	Greiner Bio-One
Vacuum filter system 0.22 µm, Stericup & Steritop	Merck Millipore
Zip Tip pipette tips (µC18)	Merck Millipore

2.1.3 Laboratory equipment

Laboratory Equipment	Type	Provider
Agarose gel systems; mini, midi & maxi	PerfectBlue	Peqlab
Analytical balance	CP4235-OCE	Sartorius
		Mettler
Autoclave	Vx-150	Systec
Bag sealer	Vacupack Plus F 380 70	Krups
Bunsen burner	Labogaz	campingaz
Centrifuge	Heraeus Biofuge fresco	DJB labcare
	MicroV	Fisher Scientific
	miniSpin	Eppendorf
	Centrifuge 5810 R	
	Universal 320R	Hettich
Centrifuge, large	Sorvall RC 6 Plus	Thermo Scientific
	Sorvall LYNX 4000	
Centrifuge rotors	Super-Lite	Thermo Scientific
	Fiberlite	
Digital camera	Powershot G12	Canon
Documentation set of agarose gels	Camera, visualization	Peqlab
	Printer P93D	Mitsubishi
Electrophoresis chamber	Mighty Small SE250	GE Healthcare
Electrophoresis glass and ceramic plates		GE Healthcare

Film processor (Developing/Fixing)	SRX-101A	Konica and Minolta
Flow cytometer	Canto II	BD
FPLC + fraction collector		GE Healthcare
FPLC fridge (4°C)	Unichromat 700	uniequip
Heating block	ThermoStat plus	Eppendorf
	neoBlock-HeizerDuo	neoLab
Ice machine		Ziegra
Incubator (37 °C): *Escherichia coli* (*E. coli)*	Steri-Cult 200	Thermo Scientific
Incubator (37 °C, 5% CO_2)	B-5060-EK-CO2	Heraeus
Incubator (27 °C)	B-series	Binder
Lab shaker	Duomax 1030	Heidolph
Laminar flow hood	Herasafe	Heareus
		Thermo Scientific
Magnetic stirrer	IKAMAG REO	IKA
	MR Hei-Tec/MR Hei-Mix 2	Heidolph
Mass spectrometer	Ultraflex	Bruker
Microscopes	DM1000 LED	Leica
	M40	Wild Heerbrugg
	Dialux 22EB	Leitz
	Axiovert 200	Zeiss
	LSM 510 META	
Microwave	M9235	Samsung
NanoDrop	ND-1000	Peqlab
Neubauer cell counting chamber	Improved	Hecht-Assistent
		Brand
		Marienfeld-Superior
Nucleofector device	Amaxa Biosystems Nucleofector II	Lonza
PCR machine	Mastercycler gradient	Eppendorf
pH meter	PB-11	Sartorius
Pipette-boy	Accu-jet pro	Brand
Pipette	Research 2-20, 100-1000, Research plus 20-200, Reference 100-1000	Eppendorf

Pipette	Pipetman P10, P2	Gilson
Power supply		H. Holzel
	EPS 601	GE Healthcare
Shaker	MaxQ 6000	Thermo Scientific
	Unitron	Infors HT
Spectrophotometer	V-650	Jasco
Vacuum pump	Pump system MZ 2C	Vacuubrand
Vortexer	MS1 Minishaker	IKA
Water bath (cell culture)	1083	GFL
Water installation for H_2O_{MilliQ}		SG

2.1.4 Enzymes and substrates

Enzyme/components	Provider
*Acc*65I (10 U/µl)	Thermo Scientific
*Bam*HI (10 U/µl)	Thermo Scientific
*Bcl*I (10 U/µl)	Thermo Scientific
10x Buffer R, G, O, Tango, *Eco*RI, *Bam*HI	Thermo Scientific
dATP (2 mM)	Thermo Scientific
dNTP mix (2 mM each)	Thermo Scientific
*Dpn*I (10 U/µl)	Thermo Scientific
*Eco*RI (10 U/µl)	Thermo Scientific
FastDigest buffer (10x)	Thermo Scientific
GR, human, recombinant	Uschi Göbel, Heiner Schirmer
GPx4, bovine erythrocytes	Regina Brigelius-Flohé
*Hind*III (10 U/µl)	Thermo Scientific
*Hpa*I FastDigest	Thermo Scientific
*Kpn*I (10 U/µl)	Thermo Scientific
Magnesium chloride ($MgCl_2$; 25 mM)	Thermo Scientific
*Mlu*I (10 U/µl)	Thermo Scientific
*Nco*I (10 U/µl)	Thermo Scientific
*Not*I (10 U/µl)	Thermo Scientific
*Not*I FastDigest	Thermo Scientific
Pfu buffer with $MgSO_4$ (10x)	Thermo Scientific
Pfu DNA polymerase (2.5 U/µl)	Thermo Scientific

*Pfu*Ultra HS DNA polymerase	Agilent Technologies
*Pfu*Ultra reaction buffer (10x)	Agilent Technologies
Prx, *T. brucei* , recombinant	Michael Diechtierow
*Pst*I (10 U/µl)	Thermo Scientific
*Pst*I FastDigest	Thermo Scientific
Px III, *T. brucei*, recombinant	Michael Diechtierow
Px IV, *T. brucei*, recombinant, untagged	This work
Px IV, *T. brucei*, recombinant, His-tagged	This work
Q5 High-Fidelity DNA polymerase	New England BioLabs Inc.
Q5 reaction buffer (5x)	New England BioLabs Inc.
*Sca*I FastDigest (10 U/µl)	Thermo Scientific
T4 DNA ligase (5 Weiss U/µl)	Thermo Scientific
T4 DNA ligase buffer (10x)	Thermo Scientific
Taq DNA polymerase (1 U/µl)	Thermo Scientific
Taq buffer + $(NH_4)_2SO_4$ - $MgCl_2$ (10x)	Thermo Scientific
Tpx, *T. brucei*, recombinant	Natalie Dirdjaja
TR, *T. cruzi*, recombinant	Natalie Dirdjaja
Trypanothione, reduced ($T(SH)_2$)	Natalie Dirdjaja
*Xba*I (10 U/µl)	Thermo Scientific
*Xho*I (10 U/µl)	Thermo Scientific
*Xho*I FastDigest	Thermo Scientific

2.1.5 Kits

Kits [catalog number]	Provider
Amaxa Human T Cell Nucleofector Kit [VPA-1002]	Lonza
Click-iT Lipid Peroxidation Imaging Kit - Alexa Fluor 488 [C10446]	Life Technologies
DNA Clean & Concentrator-5 [D4003]	Zymo Research
DNeasy Blood & Tissue [69506]	Qiagen
NucleoBond Xtra Midi [740410]	Macherey-Nagel
NucleoSpin Plasmid [740588]	Macherey-Nagel
pGEM-T Easy Vector System I [A1360]	Promega
Zymoclean Gel DNA Recovery [D4001]	Zymo Research

2.1.6 T. brucei brucei strains

Eukaryotic cell line	Information	Provider
Wild type (WT) 449 Lister strain 427 (PC and BS)	Culture-adapted *T. brucei* strains transfected with the pHD449 vector to stably express the tetracycline repressor	Cunningham and Vickerman, 1962; Biebinger *et al.*, 1997
PC 449 *px I-II*$^{-/-}$ clone ½ 4C4 and 4C2	The *px I* and *px II* have been deleted in the PC WT 449 strain using pHD1747 and pHD1748	Nißen, MD thesis 2014
BS 449 *px I-II*$^{-/-}$ clone J1	KO of *px I* and *px II* in BS WT 449 cells by the transfection with pHD1747 and pHD1748	Diechtierow and Krauth-Siegel, 2011
BS 449 *px III*$^{-/-}$ clone Z11	BS WT 449 parasites deleted of *px III*	
BS 2T1 *px IV*$^{+/-}$ + c-myc-Px IV clone 2A1	Single allele KO of *px IV* by *pac* in the BS 2T1 cells encoding a tetracycline-inducible c-myc-tagged Px IV	Liu, MD thesis 2015
BS 449 *px IV*$^{+/-}$ clone 2D3	Deletion of one allele of *px IV* by *pac* in the BS WT 449 cells	
BS 449 *px IV*$^{+/-}$ (clone 1D2, 2C4, and 2C5)	Deletion of one allele of *px IV* by *neo* in the BS WT 449 cells	this work (with Ebersoll)
BS 449 *px IV*$^{+/-}$ clone 1C1	Knockout of *px IV* in BS WT 449 transfected with pHD1747/pHD1747-Neo	this work (with Ebersoll)
PC 449 *px I-III*$^{-/-}$	The whole *px* locus had been deleted in PC WT 449 cells by pHD1747 and pHD1748	this work
PC 449 *px I/III*$^{-/-}$	Insertion of *px II* + 3'untranslated region (UTR) of *px II* in the *px* locus of the PC 449 *px I-III*$^{-/-}$ parasites	this work

2.1.7 E. coli cell lines

E. coli cell line	Information	Provider
BL21 (DE3) *E. coli*	Contain a T7 RNA polymerase gene inducible by IPTG (*lacUV5* promoter)	Merck Millipore
BL21 (DE3) pLysS *E. coli*	Express T7 lysozyme preventing basal T7 RNA polymerase expression, for tight induction	Merck Millipore
NEB 5-alpha Competent *E. coli*	Competent *E. coli* strain for plasmid transformation	New England BioLabs Inc.
NovaBlue *E. coli*		Merck Millipore

Origami 2 (DE3) *E.coli*	Contain mutations in the GR and thioredoxin reductase genes to enhance disulfide bond formation in the cytoplasm	Merck Millipore
Rosetta (DE3) pLysS *E. coli*	Strain that supplies rare tRNAs to improve the codon usage of *E. coli*	Merck Millipore
SHuffle T7 Express Competent *E. coli*	Are engineered to improve disulfide bond formation in the cytoplasm by the expression of the isomerase DsbC	New England BioLabs Inc.
Tuner (DE3) *E. coli*	Deletion mutants of *lacZY* from the BL21 strain, enable homogenous, adjustable induction in culture	Merck Millipore

2.1.8 Primary antibodies and other cell staining reagents

Antibody / Staining	Host / Color	Description	Application / Dilution	Provider
Px, *T. brucei*	rabbit	Polyclonal anti-Px antibody	WB 1:2000	Diechtierow and Krauth-Siegel, 2011
TR, *T. brucei*	rabbit	Polyclonal antiserum	WB 1:1000	Schlecker *et al*., 2005
Transferrin, bovine	sheep	Affinity purified polyclonal antiserum	WB 1:1000	Biomol, Bethyl Laboratories Inc. [A10-122A]
p67, *T. brucei*	mouse	Monoclonal antibody, lysosomal marker	IF 1:500	Bangs/Russell, Alexander *et al.* 2002
Aldolase, *T. brucei*	rabbit	Polyclonal antiserum, glycosomal marker	IF 1:500	Clayton 1987
Lipoamide dehydrogenase (LipDH), *T. brucei*	rabbit	Polyclonal antiserum, mitochondrial marker	IF 1:1000	Roldán *et al.* 2011
Acetyl: succinate CoA-transferase (ASCT)	rabbit	Polyclonal antiserum, mitochondrial matrix marker	IF 1:1000	Rivière *et al.* 2004
Myc	mouse	Monoclonal anti-c-myc antibody	WB 1:400	Roche
Px IV, *T. brucei*	rabbit	Polyclonal antiserum	WB 1:500	this work
MitoTracker Red CMXRos	red	Stains mitochondria in living cells with intact membrane potential	IF 0.12 µM	Life Technologies

Dextran	green	Dextran coupled to Alexa Fluor 488, delivered to the endocytic system	LCI 2.5 mg/ml in medium	Life Technologies
LysoTracker Green DND-26	green	Staining of acidic organelles	LCI 5 µM	Life Technologies
DAPI	blue	DNA staining	IF 500 ng/µl	Sigma-Aldrich

WB =Western Blot, IF = Immunofluorescence, LCI = Life cell imaging

2.1.9 Secondary antibodies

Antibody	Host	Conjugate	Application / Dilution	Provider
Anti-mouse IgG	goat	Alexa Fluor 488 (green)	IF 1:1000	Life Technologies
		Alexa Fluor 594 (red)		
Anti-rabbit IgG	goat	Alexa Fluor 488 (green)	IF 1:1000	Life Technologies
		Alexa Fluor 594 (red)		
Anti-rabbit IgG-HRP	goat	Horseradish peroxidase	WB 1:10000	Santa Cruz Biotechnology
Anti-sheep IgG-HRP	rabbit	Horseradish peroxidase	WB 1:10000	Santa Cruz Biotechnology

WB =Western Blot, IF = Immunofluorescence

2.1.10 Primer

All primers were obtained from Eurofins MWG Genomics, Ebersberg. The melting temperature (T_m) and GC content was calculated by the provider. Some primers were evaluated on the basis of single primer cross-reactions: good, ok or unspecific. The restriction sites and mutated bases are highlighted in bold.

Name	Information	Sequence (5' - 3')	GC [%]	T_m [°C]	Producer
b-tub-s	Probe for detection of tubulin genes in the Southern blot analysis	GACCGTATCATGAT GACTTTC	60	56	Schmidt
b-tub-as		CTTCATTACCTACT GCTAATG	58	54	Schmidt

KO_PxI-III_3'F	Amplification of the 3'UTR of *px III* from pHD1747_KO*pxIII* with 5'*Pst*I and 3'*Not*I sites for gene deletion	TAA**CTGCAG**AAGAAGAATACGTCTCTGG	43	63.7	Diechtierow, PhD thesis 2011
KO_PxI-III_3'R		AT**GCGGCCGC**CCAAAGGAATGAAGCAAAC	55	69.5	
Bla-F	Forward *bla* primer used for sequencing (good)	AGCTGCTGGCCAAGCCTTTGTCTCAAG	56	68	Diechtierow, PhD thesis 2011
Bla_R_MD	Reverse *bla* primer for sequencing (good)	GAGCTGCGCTGGCGA	73	56	Diechtierow, PhD thesis 2011
P1	Used as an sequencing forward primer for *px III*	GCGC**AAGCTT**ATGCTGCGTTCATCTCGG	57	69.5	Diechtierow, PhD thesis 2011
P7	Forward primer binding in the 5'UTR of *px I*	GCA**GGATCC**GGAGGAGGCGCCTAC	71	71.3	Diechtierow, PhD thesis 2011
P18	Reverse primer binding in the 3' region *px I* and *II* for analysis	AGACGCGCTCTGCGTGCT	67	60.5	Diechtierow, PhD thesis 2011
P22	Forward primer of *px III* binding to the mitochondrial targeting sequence (MTS)	ATGCTGCGTTCATCTCGG	56	56	Diechtierow, PhD thesis 2011
P24	Used as an sequencing reverse primer for *px III*	GCAT**GGATCC**AAGTCGCGCACTCCC	64	69.5	Diechtierow, PhD thesis 2011
P26	Forward primer of *px II* (start) for PCR analysis	ATGTCAGCTGCTTCGTCAATC	48	57.9	Diechtierow, PhD thesis 2011
NeoF_BM	Internal primers (reverse and forward) located in *neo* (ok)	GAAAGTATCCATCATGGCTGATG	43.5	58.9	Musunda
NeoR_BM		CATCAGCCATGATGGATACTTTC	43.5	58.9	
Puro_CC_Rv	*Pac* sequencing primers from Clayton (reverse and forward) (ok)	CGGCTAAGCTCAGGCACCGGGCTTGCGGG	72.4	>75	Clayton
Puro_CC_Fw		GA**GCGGCCGC**ATGACCGAGTACAAGCCCAC	66.7	75	

P22r_CH	Sequencing reverse primer binding to the MTS of *px III*	CGAGATGAACGCAGCATG	55.6	56	this work
P31_MD	Reverse primer binding in the 3'UTR of *px III* (inside the cloning region), re-ordered	TTCAACCTCAACTCCACTG	47.4	54.5	Diechtierow, PhD thesis 2011
3UTR_PxIII_R1	Sequencing reverse primers bind in the 3'UTR of *px III* (outside the cloning region) (good)	CACGCATACAAACATGGACG	50	57.3	this work
3UTR_PxIII_R2		GAGGCCATCATAATGTGAGCAC		60.3	
PuroF_CH2	Sequencing forward primer binding in the coding region of *pac* (good)	CGCAGCAACAGATGGAAGG	57.9	58.8	this work
BlaR_CH	Sequencing reverse primer of *bla* (good)	GGCGACGCTGTAGTCTTCAG	60	61.4	this work
PuroR_CH2	Sequencing reverse primer of *pac* (unspecific)	GCCTTCCATCTGTTGCTGCG		61.4	this work
P7_CH	Similar to Diechtierow's P7 primer located in the 5'UTR of *px I* (without restriction site)	GTTGGAGGAGGCGCCTAC	66.7	60.5	this work
PxI-IISonde CH F	Probe for detection of *px I* and *px II* in the Southern blot analysis	CTTTGACTTTGAGGTGCTTGAC	45.5	58.4	this work
PxI-IISonde CH R		ACAGTGAAGCCCTGTGACTTG	52.4	59.8	
PxIIIKOmtFw2	Primers for the insertion of 3'UTR of *px II* + MTS of *px III* from genomic DNA into the pGEM-T Easy vector with 5'*Hind*III and 3'*Xho*I	GGTG**CTCGAG**GTAATTAAGTCAGAAGGGAAGTGG	50	70.7	this work
PxIIIKOmtRe2		GTAG**AAGCTT**CTTTTTCCGAGATGAACGCAGCAGG	48.6	70.6	
Mut4'HindIII F	Mutation of a *Hind*III site in the 3'UTR of *px II* in the pGEM-T Easy vector	GGAAGTGGTTAAGGGGCAAG**A**TTCTGTTTTTGTGAACGAGG	46	72.4	Diechtierow, PhD thesis 2011
Mut4'HindIII R		CCTCGTTCACAAAAACAGAA**T**CTTGCCCCTTAACCACTTCC	46	72.4	

PxIIImtATG Fw	Primers for the mutagenesis of the ATG from MTS of *px III* in pGEM-T Easy	CAAGACTACCAACTC**G**TGCTGCGTTCATCTCGG	54.5	72	this work
PxIIImtATG Rv		CCGAGATGAACGCAGCA**C**GAGTTGGTAGTCTTG	54.5	72	
BlaF_CH	Forward primer binding in *bla* for PCR analysis (unspecific)	CGTCGCCAGCGCAGCTC	76.5	62.4	this work
PuroR_CCCH	*Pac* reverse primer "similar" to Puro_CC_Rv from the Clayton Lab (ok)	AGGCACCGGGCTTGC	73.3	56	this work
PxII_CH_Fw	"Specific" forward primer binding in the middle of *px II*	GGCGTTCCCGTGTAACC	64.7	57.6	this work
PuroR_opt_CH	*Pac* reverse primer (unspecific)	CACCGGGCTTGCGGGTCA	72.2	62.8	this work
3'UTR PxIII_CH	Reverse primer binding in 3'UTR of *px III* (ok)	GATTGCCTCAAGCCAGTGCT	55	59.4	this work
5'UTR PxI_CH	Forward primer binding in 5'UTR of *px I* (ok)	TGGACCGCTCATTTGACGAA	50	57.3	this work
NeoSeqRS_rv	Sequencing reverse primer for pHD1748-Neo aligned to *neo* and its restriction site (5'*Xba*I)	CTTGTTCCACCAT**TCTAGA**	42.1	52.4	this work
Px1SeqRS_fw	Sequencing forward primer for pHD1748-Neo located in the *px I* gene plus restriction sites (5'*Hind*III/*Mlu*I)	**AAGCTTACGCGT**ATGTCTAC	45	55.3	this work
Px I-II in NeFw	Cloning of the *px I*-UTR-*px II*-UTR locus from genomic DNA into pHD1748-Neo using 5'*Mlu*I and 3'*Xba*I	GATA**ACGCGT**ATGTCTACAATCTTTGACTTTG	37.5	64.4	this work
Px I-II in NeRv		GAGC**TCTAGA**GAGTTGGTAGTCTTG	48	63.0	
PxIIIKONeo Fw	Cloning primers for the generation of a 5'multiple cloning site (5'*Hind*III/*Mlu*I/*Xba*I) and *neo* into the pHD1748_KO*pxI-III* vector	GATC**AAGCTTACGCGT**TA**TCTAGA**ATGGTGGAACAAGATG	42.5	70.5	this work
PxIIIKONeo Rv		GGTC**GAATTC**TCAGAAGAACTCGTCAAGAAGGC	48.5	69.5	this work

PuroPxIII_Fw	Primers for the amplification of *pac* with 5'*Xba*I and 3'*Eco*RI sites	GAGC**TCTAGA**ATG ACCGAGTACAAG	48	63	this work
PuroPxIII_Rv		TATC**GAATTC**TCAG GCACCGGGC	56.5	64.2	
T7	T7 forward primer for sequencing of plasmids	TAATACGACTCACT ATAGGG	40	53.2	this work
MTS_R	Cloning reverse primer with *Xba*I located in the MTS of *px III*	GATT**TCTAGA**GATG AACGCAGCACGAG	48.1	65	this work
P26RS_Fw	Forward primer of *px II* with *Mlu*I	GATA**ACGCGT**ATGT CAGCTGCTTCG	52	64.6	this work
4UTR_Fw_CH	Amplification of UTR-*px III* without glycosomal targeting sequence from genomic DNA using 5'*Xba*I and 3'*Eco*RI sites	GATC**TCTAGA**TGGA TTTGTCGCTGAAAC GG	46.7	66.8	this work
PxIII-ARL_Rv_CH		GATC**GAATTC**TCAA CTCCCGAGCAGC	53.8	66.4	
NeoClon_Fw_CH	Amplification of *neo* into the pHD1748_re-insert*pxIII*-ARL vector with 5'*Mlu*I and 3'*Xba*I sites	GATC**ACGCGT**ATG GTGGAACAAGATG	50	64.8	this work
NeoClon_Rv_CH		GAGC**TCTAGA**TCAG AAGAACTCGTCAAG	46.4	65.1	
Px4 pHD1700 Fw	Cloning primers for the generation of pHD1700_untagged-PxIV (over-expression of untagged Px IV) using 5'*Mlu*I and 3'*Bam*HI sites	GATT**ACGCGT**ATGA ATGGCGGCGC	58.3	66.1	this work
Px4 pHD1700 Rv		GATT**GGATCC**TCAC TCATCGCACAACTG	50	66.6	
PxIV_3'UTR_Ext	Reverse primer located outside the cloning region of *px IV*	CGGAAGTGGTGGAA TGCTGAAG	54.5	62.1	Liu, MD thesis 2015
Px4 Internal Fw	Internal primers of *px IV* (marked base should be C, typing mistake during order procedure) (ok)	TCTCACTCGGTTCT AATGGACGG	52.2	62.4	this work
Px4 Internal Rv		CCAGCGAGTTTCCT GGCTG	63.2	61	
pRPa_NmycPxIV_F	Primers for the cloning of the pRPa plasmids for expressing N- or C-myc tagged Px IV in *T. brucei* (created for the MD thesis of Liu)	GATT**CCTAGG**AATG GCGGCGCC	63.6	65.8	this work
pRPa_NmycPxIV_R		GAGC**GGATCC**TCA CTCATCGCAC	60.9	66	this work
pRPa_CmycPxIV_F		GAGC**TTAATTAA**TG AATGGCGGCGCC	50	64.8	this work
pRPa_CmycPxIV_R		GAGC**TCTAGA**CTCA TCGCACAACTG	52	64.6	this work

6R_PxIVpQE	Cloning primer with 5'*Pst*I and 3'*Bam*HI sites to create the pQE-30 vector expressing recombinant His-tagged Px IV	GAAC**CTGCAG**TCA CTCATCGCACAACT G	53.6	68	this work
5F_PxIVpQE		GATT**GGATCC**ATGA ATGGCGGCGCCATT	53.6	68	this work
3F_tPxIV	Forward primer with *Nco*I site to create truncated (Δ1-18) Px IV	GACT**CCATGG**GCCT GTCCAAGTATGCTG	57.1	69.5	this work
1F_PxIV	Amplification of *px IV* from genomic DNA for insertion into the pETtrx_1b vector with 5'*Nco*I and 3'*Acc*65I sites	GATT**CCATGG**GCA ATGGCGGCGCCATT	59.3	69.5	this work
2R_PxIV		GCTC**GGTACC**TCAC TCATCGCACAACTG	57.1	69.5	this work

2.1.11 Plasmids

All pHD plasmids were kindly provided by Prof. Dr. Christine Clayton. The pET vectors were obtained from Dr. Gunter Stier and the pQE-30 and pGEM-T Easy vectors were commercially available.

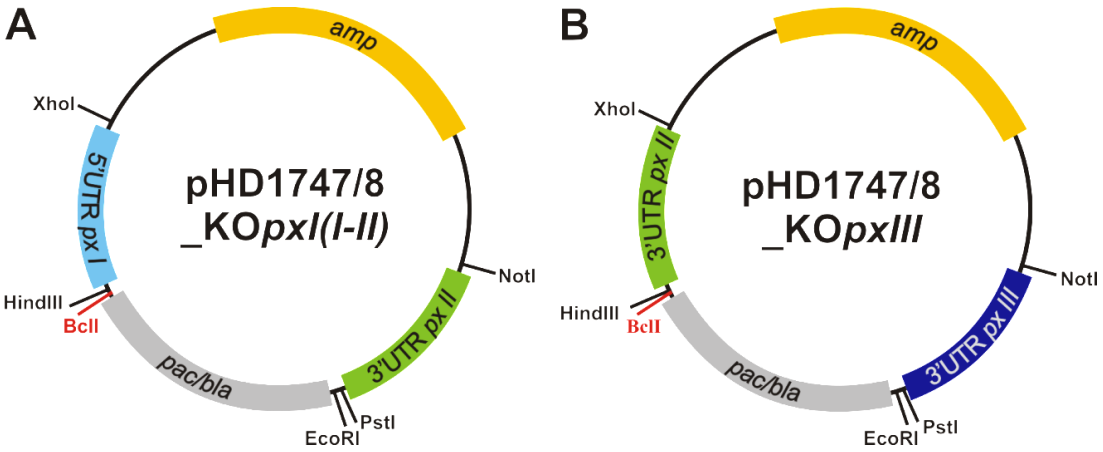

Figure 2.1: Vectors generated by Diechtierow. These pHD-vectors for gene KO were published in Diechtierow and Krauth-Siegel, 2011. They were used for cloning of the pHD1747_KO*pxI-III* and pHD1748_KO*pxI-III* vectors (see Figure 2.2 and 2.4). The *Bcl*I (red) site is only present in the pHD1748 plasmid.

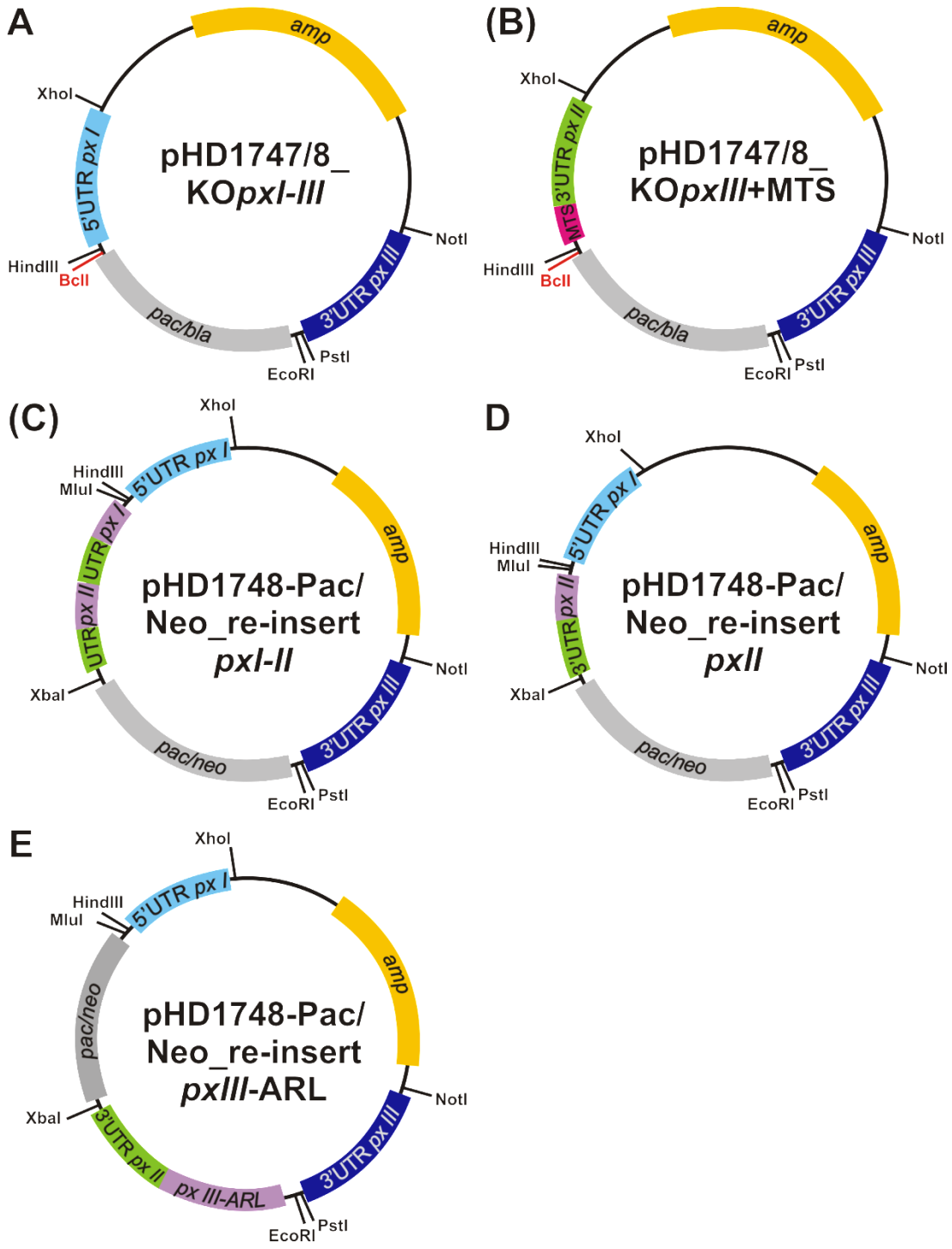

Figure 2.2: Plasmids for the Px I-III project (KO and insert vectors). These pHD-vectors were used for the generation of various procyclic KO parasites and for the insertion of altered genes or locus fragments (insert). They encode an ampicillin resistance gene (*amp*, yellow) for bacterial selection. All plasmids are available with a puromycin resistance cassette (pHD1747: *pac*, grey), plasmids **A** and **B** also with a blasticidin resistance gene (pHD1748: *bla* grey) and vectors **C**, **D**, and **E**. with a neomycin resistance gene (pHD1748-Neo: *neo*, grey) for *T. brucei* selection. The *Bcl*I restriction site (red) exists only in the pHD1748 vectors, all other important restriction sites present in both pHD1747 and pHD1748 are displayed in black. The 5'UTR of *px I* is shown in light blue, the 3'UTR of *px III* in dark blue, and the 3'UTRs of *px II* and *III* in green. The MTS (pink) was included in the vectors **B** for homologous recombination. The coding regions of the *px* genes are presented in purple. Plasmids **C** were used to re-insert the *px I* + UTR + *px II* + UTR locus in PC *px I-III*$^{-/-}$ parasites. Transfections with plasmid **B** and **C** did not yield a *px III*$^{-/-}$ cell line. **D** and **E** contain the *px II* + UTR and UTR + *px III* + UTR without glycosomal targeting sequence (ARL), respectively, for re-introduction into the PC *px I-III*$^{-/-}$ cells.

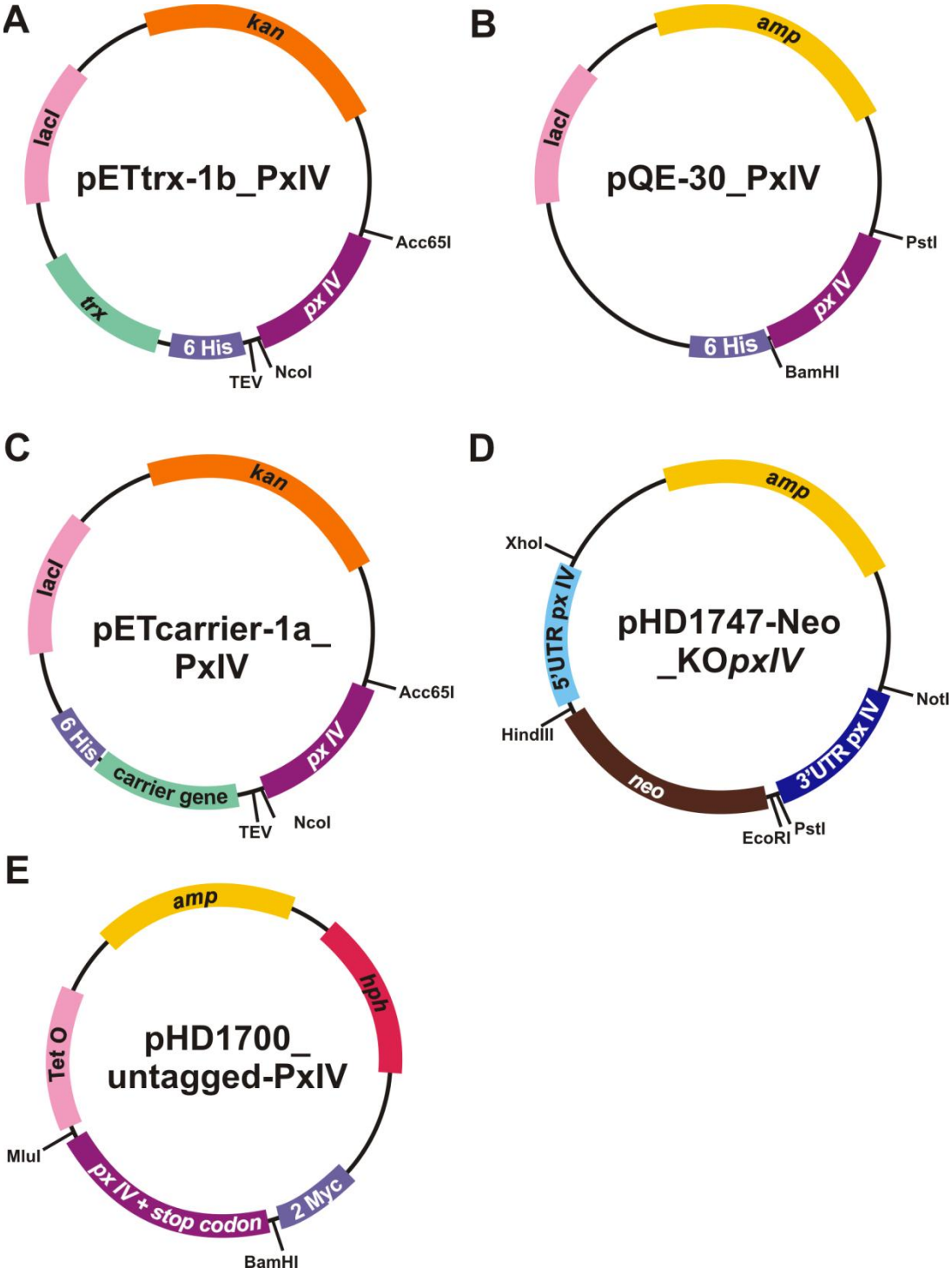

Figure 2.3: Plasmids for the Px IV project. The vectors **A**-**C** were used for expression of the recombinant Px IV protein in *E. coli*. The vectors **D** and **E** were generated for the KO and over-expression, respectively of *px IV* in BS parasites, respectively. For bacterial selection, the plasmids encode a kanamycin (**A** and **C**; *kan*; orange) or ampicillin resistance gene (**B**, **D**, and **E**; *amp*; yellow). Vectors **A**-**C** contain a *lac* repressor (lacI) and **E** a tetracycline-operator (TetO) system (pink). The pHD1747-Neo_KO*pxIV* vector (**D**) encodes a neomycin resistance gene flanked by the 5' and 3'UTRs of *px IV* (*neo*; brown). PHD1700_untagged-PxIV (**E**) a hygromycin resistance gene as selection marker in the parasite (*hph*; red). Tags are marked in purple: 6x His-tag in plasmid **A**-**C** and 2x Myc-tag in **E**. Restriction sites used for cloning the constructs are included. The pETcarrier-1a_PxIV vector (**C**) was created with different carrier proteins; synthetic Z-domain of protein A (ZZ), maltose-binding protein (MBP), GB domain of protein G (GB), and N utilization substance protein A (NusA). The *px IV* gene is marked in mulberry.

2.2 Methods

Some methods were already described in Hiller *et al.*, 2014 and will be described in Schaffroth *et al.*, 2015. Thus, parts of this thesis were taken from these papers. I supervised the practical work of two students, Samantha Ebersoll and Philippa Lantwin. Part of this work is included in this thesis. The MD thesis by Ilon Liu under my supervision is only mentioned shortly in the result and discussion part.

2.2.1 Cloning of px KO vectors to create stable cell lines and of bacterial expression vectors to produce recombinant Px IV protein.

The pHD1747 and pHD1748 vectors containing a puromycin and blasticidin resistance cassette, respectively, were used for the KO of the *px I-III* and *px IV* genes in *T. brucei* 449 cells. The pHD1747_KO*pxIV* and the pHD1748_KO*pxI-III* plasmid served as a template to replace the puromycin and blasticidin, respectively, by a neomycin resistance cassette referred to as pHD1747-Neo_KO*pxIV* and pHD1748-Neo, respectively. These KO vectors could be used in BS as well as in PC parasites. A schematic cloning strategy of the *px I-III* KO plasmid including puromycin resistance cassette is displayed in Figure 2.4.

The pQE-30 and different pET plasmids were used for the expression of Px IV proteins in *E. coli*. The cloning strategy is presented for the pETtrx_1b plasmid in Figure 2.5.

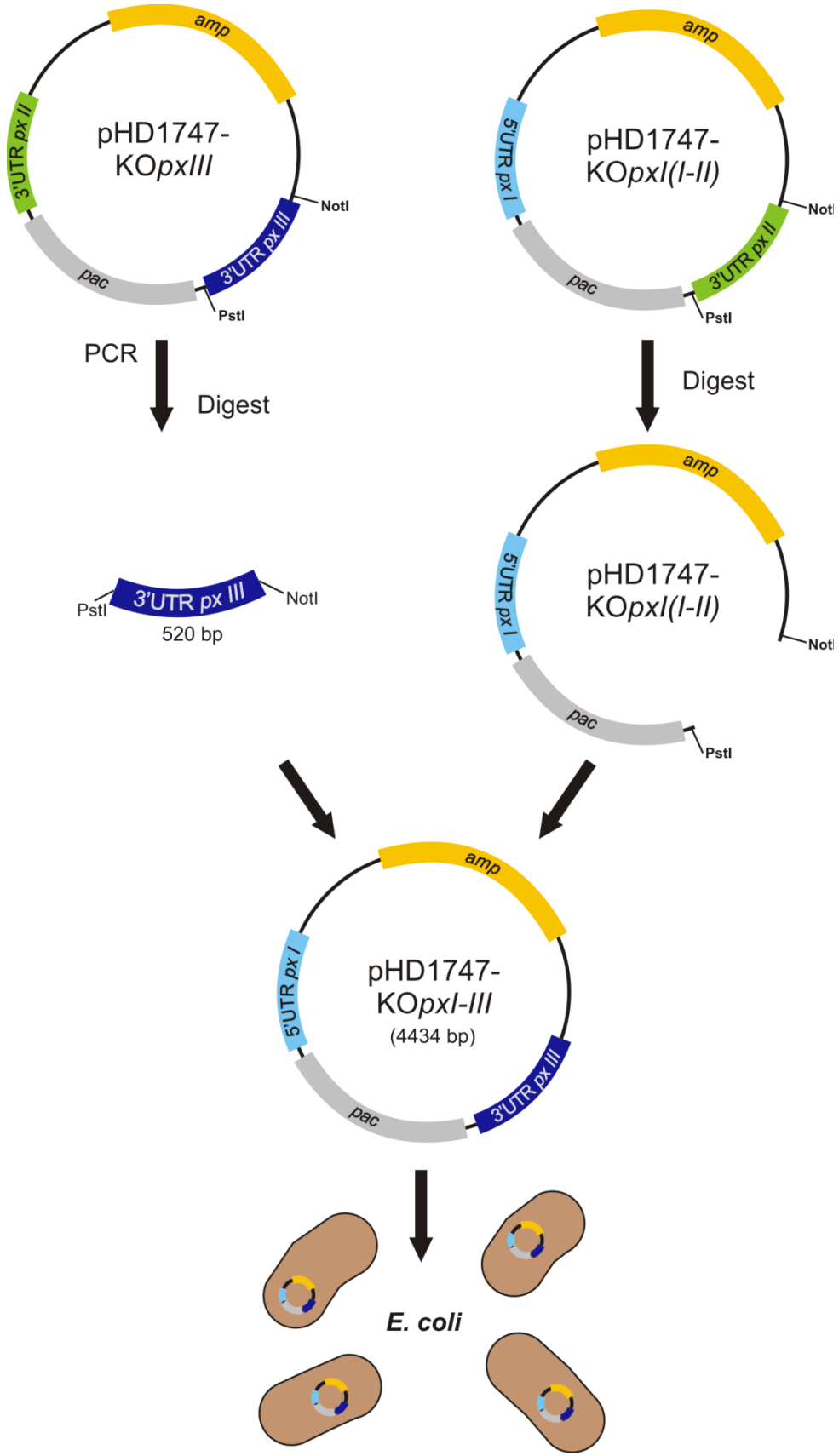

Figure 2.4: Cloning procedure for the *px I-III* KO pHD1747 transfection plasmid. A 520 bp stretch of the 3'UTR of *px III* (dark blue) was amplified from the pHD1747_KO*pxIII* vector by PCR. The primers added 5'*Pst*I and 3'*Not*I restriction sites which are also found in the pHD1747_KO*pxI*(*I-II*) plasmid. PCR product and target plasmid were digested, purified, and ligated. Competent NovaBlue *E. coli* were transformed with the plasmid and selected for carbenicillin (*amp*, yellow) resistance.

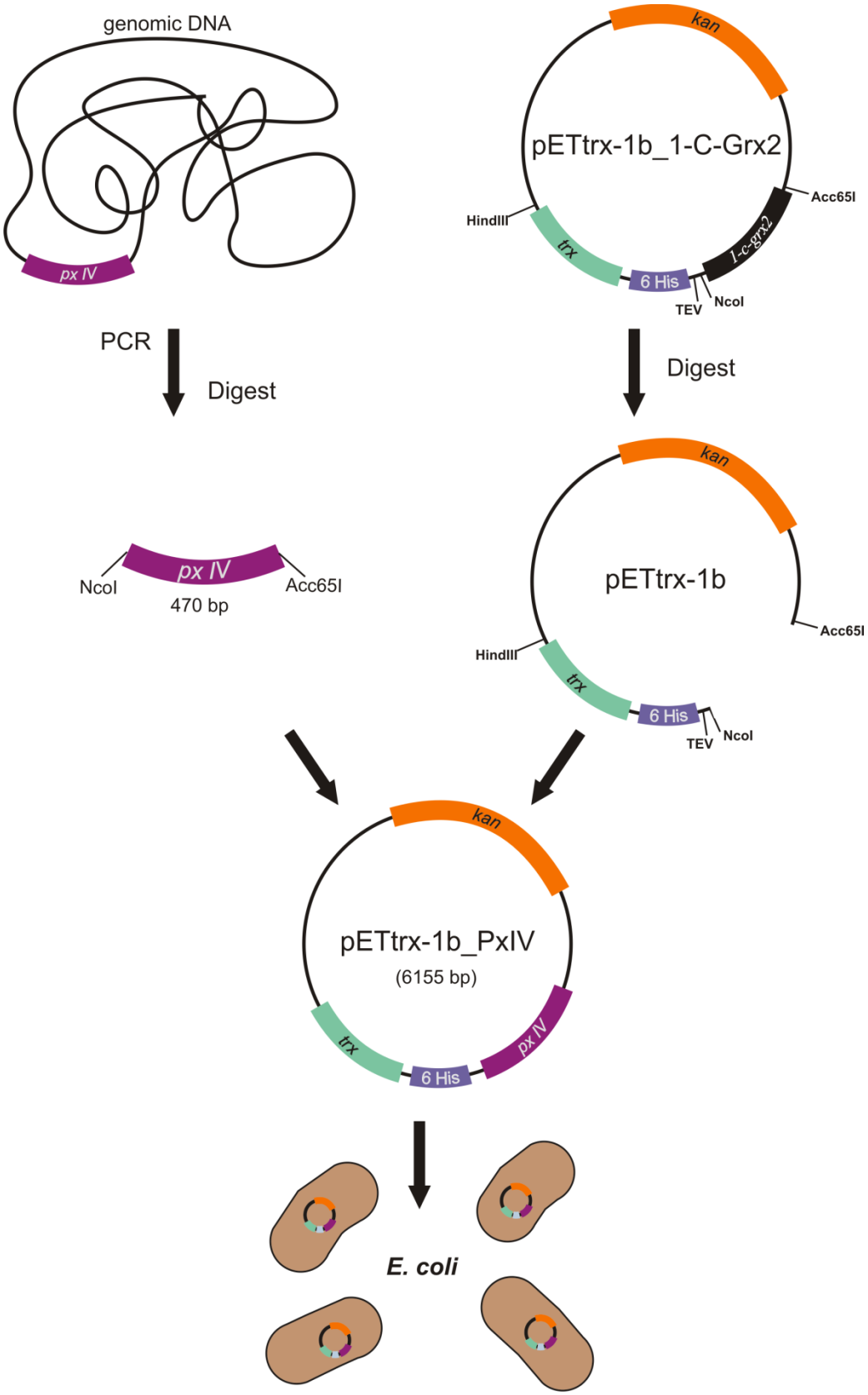

Figure 2.5: Cloning scheme for the bacterial Px IV expression plasmid. The coding region of *px IV* (mulberry) was amplified from genomic DNA by PCR using primers with 5'*Nco*I and 3'*Acc*65I restriction sites corresponding to sites in the pETtrx_1b vector. The *1-c-grx2* gene (black) from the starting pETtrx-1b vector was cut out. The digested plasmid and insert were purified, ligated and NovaBlue *E. coli* were transformed and selected by kanamycin (*kan*, orange).

2.2.1.1 Polymerase chain reaction (PCR)

Master mix

- Deoxyribonucleoside triphosphate (dNTPs) 200 µM each
- Primer forward 0.5 - 1 µM
- Primer reverse 0.5 - 1 µM
- DNA template ~ 0.1 ng/µl
- Reaction buffer 1x
- optional, depending on buffer: $MgCl_2$ 1.25 - 2.5 mM
- DNA polymerase 1 µl
- H_2O_{MilliQ} ad 50 µl

Thermal setup

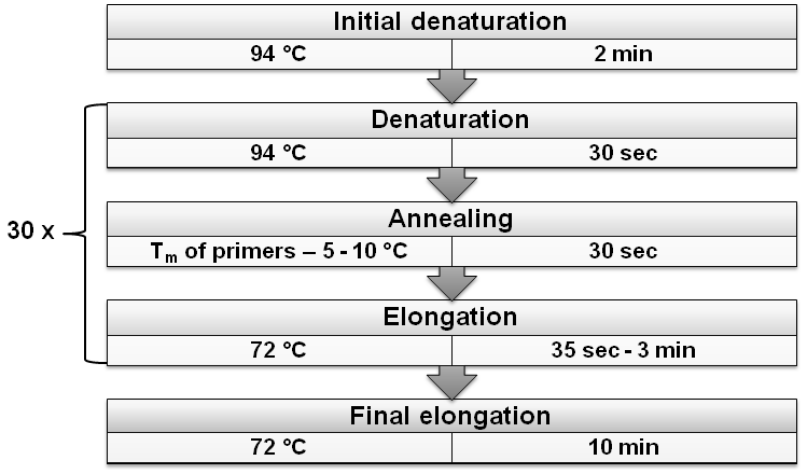

Annealing temperature and elongation time were adjusted to the primer pair and product length, respectively.

2.2.1.2 Mutagenesis PCR for a point mutation

Master mix

- dNTPs 200 µM each
- Primer forward 2.5 ng/µl
- Primer reverse 2.5 ng/µl
- Plasmid DNA (template) 0.4 ng/µl
- *Pfu* Ultra buffer 1x

- *Pfu* Ultra HS polymerase 1 µl
- H_2O_{MilliQ} ad 50 µl

The primer length should be between 25 - 45 bp and their T_m 78 - 85 °C. Elongation time is adjusted to vector length (1 min/1 kb). Calculation of T_m for mutagenesis primer: T_m= 81.5 °C + 0.41 (% GC content) - (675/primer length) - % mismatch

Thermal setup

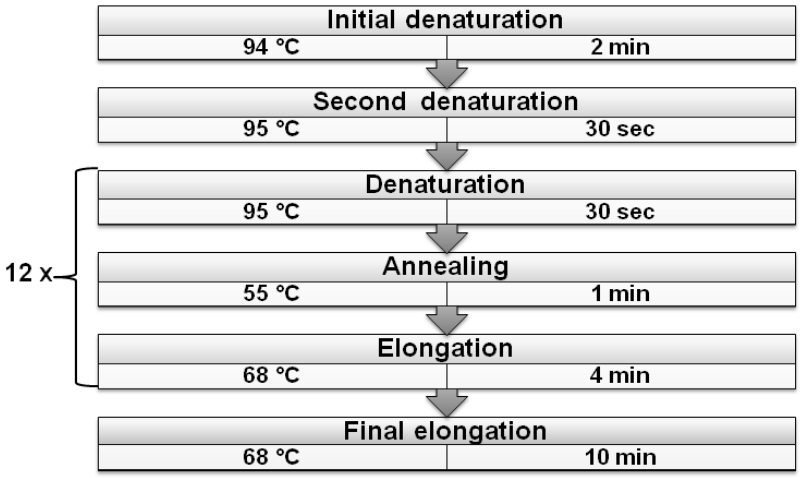

2.2.1.3 Agarose gel electrophoresis

In this thesis, 0.8 - 2% agarose gels were used. The prepared gel solution was heated in a microwave until the agarose powder was completely dissolved. The solution was poured into a gel caster sealed with tapes and equipped with a comb. After the gel was fixed, the gel caster was placed into an electrophoresis chamber filled with 1x Tris-acetate-EDTA (TAE) buffer till the gel was submerged. DNA samples were mixed with 6x loading dye and loaded into the wells. A DNA ladder mix was used for size determination. Depending on the product and chamber size, the gel ran at 100 - 130 V for 45 - 80 min at room temperature (RT). For visualization, gels were kept for up to 20 min in an ethidium bromide bath. The DNA bands were visualized by UV light on a UV table for purification or in a gel documentation system for analysis.

50x TAE buffer	**amount (for 1 l)**	**concentration**
• Tris	242.3 g	2 M
• 99% Acetic acid	57.2 ml	1 M

• EDTA x 2 H_2O	37.2 g	0.1 M
• adjust to ~ pH 8 (in general not needed)		
• in H_2O_{MilliQ}		

1% Agarose gel	**amount (for 0.1 l)**	**concentration**
• Agarose	1 g	0.01 g/ml
• in 1x TAE buffer		

2.2.1.4 DNA restriction

PCR products and vectors were digested by the listed restriction enzymes using the respective buffers (Thermo Scientific). DNA purified from bacterial colonies (test digests) were treated in a total volume of 10 µl at 37 °C for at least 1 h.

***a)* For cloning of *px IV* and truncated *px IV* into pET vectors**

*Nco*I:	5'-C^CATG G-3'	*Acc*65I:	5'-G^GTAC C-3'
	3'-G GTAC^C-5'		3'-C CATG^G-5'

The *px IV* coding region amplified from genomic DNA was gel purified and about 20 µl of the eluted sample was mixed with 2x Tango buffer, 10 or 3 U of *Nco*I, 20 or 6 U of *Acc*65I, and H_2O_{MilliQ} digested at 37 °C for 1 h and overnight, respectively, in a total volume of 50 µl. The pETtrx-1b_1-c-grx2-MTS vector (5 µg) was digested accordingly.

***b)* For cloning *px IV* into the pQE-30 vector**

*Bam*HI:	5'-G^GATC C-3'	*Pst*I:	5'-C TGCA^G-3'
	3'-C CTAG^G-5'		3'-G^ACGT C-5'

After amplification from genomic DNA, the *px IV* coding sequence was purified by gel electrophoresis and 20 µl of the eluted DNA and 4 µg of the vector pQE-30_GrxII-MTS 2/1 were mixed with 1x Tango buffer, 3 U of *Bam*HI, 3 U of *Pst*I, and H_2O_{MilliQ} digested at 37 °C overnight in a total volume of 50 and 30 µl, respectively.

***c)* For inserting *neo* into pHD1747_KO*pxIV* vector (performed by Ebersoll)**

*Hind*III:	5'-A^AGCT T-3'	*Eco*RI:	5'-G^AATT C-3'
	3'-T TCGA^A-5'		3'-C TTAA^G-5'

The gel-purified PCR product of the neomycin resistance cassette (obtained from Dirdjaja) and the pHD1747_KO*pxIV* were digested in buffer R by 5 U of *Hind*III and 5 U of *Eco*RI at 37 °C for 2 h in a total volume of 30 µl.

***d)* For cloning *px IV* (+ stop codon) into pHD1700 vector (performed by Lantwin)**

*Mlu*I:	5'-A^CGCG T-3'	*Bam*HI
	3'-T GCGC^A-5'	

The *px IV* PCR product from genomic DNA and the pHD1700 was digested in buffer *Bam*HI, H_2O_{MilliQ} with 20 U of *Mlu*I and 10 U of *Bam*HI in a total volume of 60 µl.

e)* For cloning the 3'UTR of *px III* into pHD1747/48_KO*pxI(I-II)

*Pst*I	*Not*I:	5'-GC^GGCC GC-3'
		3'-CG CCGG^CG-5'

For the *px I-III* KO vectors, 20 µl of gel purified 3'UTR of *px III* amplified by PCR from pHD1747_KO*pxIII* was mixed with 1x buffer O, 10 U of *Pst*I, 10 U of *Not*I, and H_2O_{MilliQ} and incubated at 37 °C for 2 h in a total volume of 30 µl. The digestion of the pHD1748_KO*pxI(I-II)* (4.5 µg) and pHD1747_KO*pxI(I-II)* (4 µg) vector were conducted accordingly.

***f)* For cloning the 3'UTR of *px II* + MTS into pHD1747/48 vectors**

*Xho*I:	5'-C^TCGA G-3'	*Hind*III
	3'-G AGCT^C-5'	

To obtain the mutated insert (3'UTR of *px II* + MTS), the pGEM-T Easy vector + insert (10 µg) was digested by 5 U of *Xho*I and 5 U of *Hind*III in 1x buffer R at 37 °C for 1.5 h in a total volume of 10 µl. The pHD1747 and pHD1748 vectors were digested accordingly.

***g)* For cloning the coding region of *neo* into pHD1748 vector**

The digest was performed as outlined in *c)* using 10 U of each enzyme and incubated at 37 °C for 1 h.

***h)* For inserting the *px I*-UTR-*px II*-UTR locus into pHD1748-Neo vector**

*Mlu*I *Xba*I: 5'-T^CTAG A-3'
3'-A GATC^T-5'

The PCR-purified product (13 µl) amplified from genomic DNA and the pHD1748-Neo vector were digested by 15 U of *Mlu*I and 15 U of *Xba*I in 2x Tango buffer at 37 °C for 1 h in a total volume of 20 µl.

***i)* For cloning *pac* into pHD1748-Neo_re-insert*pxI-II* and pHD1748-Neo_re-insert*pxII* vector**

Restriction digest was performed as described in *g)*.

***j)* For inserting *px II* + 3'UTR of *px II* into pHD1748-Neo vector**

For the *px III* KO cloning strategy, the digest was performed as described in *h)* with 10 U of each enzyme. The digested vector was used from the digest of *h)*.

***k)* For inserting the 3'UTR of *px II* + *px III*-ARL in pHD1748-Neo vector**

*Xba*I *Eco*RI

The PCR product (14.5 µl) amplified from genomic DNA of the PC *px I-II*$^{-/-}$ cells and the pHD1748-Neo vector (5.4 µg) were digested in 2x Tango buffer using, 10 U of *Xba*I, and 5 U of *Eco*RI at 37 °C for 1 h in a total volume of 20 µl.

***l)* For cloning *neo* into pHD1748_re-insert*pxIII*-ARL vector**

Performed as described in *h)* using 10 U of the enzymes.

***m) Dpn*I digest after mutagenesis PCR**

*Dpn*I: 5'-…Gm6A^ TC…-3'
3'-…C T^m6AG…-5'

*Dpn*I cleaves adenomethylated *dam* sites. PCR sample was mixed with 1x Tango buffer and 10 U of *Dpn*I and incubated at 37 °C for 2 h in a total volume of 50 µl.

2.2.1.5 Purification of the PCR and digestion products

The DNA Clean & Concentrator-5 kit and the Zymoclean Gel DNA Recovery kit from Zymo Research were used for the purification of the PCR products and plasmids according to the manufacturer's protocol.

2.2.1.6 Ligation

Digested plasmid (1 µl) and PCR product (2.5 µl) were mixed with 0.5 µl of 10x ligation buffer and 5 U of T4 DNA ligase in a total volume of 5 µl and the solution was kept at RT for at least 2 h.

2.2.1.7 Transformation of competent E. coli cells

Plasmid uptake into bacterial cells was performed by a heat shock transformation. For the cloning into NovaBlue or NEB 5-alpha *E. coli*, 2.5 µl of the ligation solution was gently mixed with 25 µl of cell suspension and stored on ice for 15 min. After 30 s at 42 °C, the cells were incubated again on ice for 5 min. Up to 125 µl pre-warmed SOC medium were added and the suspension was kept at 37 °C and 190 rpm for 1 h. The bacterial cells (10 µl and the complete remaining suspension, respectively) were distributed on antibiotic LB agar plates and incubated at 37 °C overnight or at RT for three days. In the case of re-transformations, 0.5 - 1 µl of plasmid solution was used.

Luria-Bertani (LB) medium:	**amount (for 1 l)**
• Tryptone/peptone	10 g
• Yeast extract	5 g
• NaCl	5 g
• adjust to pH 7.5 (NaOH)	
• in H_2O_{MilliQ}	

LB agar	**amount (for 1 l)**
• Agar	15 g
• in LB medium (pH 7.5)	

2.2.1.8 Plasmid DNA extraction and purification (mini and midi)

Plasmids were purified following the instructions in the NucleoSpin Plasmid and NucleoBond Xtra Midi kit obtained from Macherey-Nagel.

2.2.1.9 DNA sequencing

The plasmids were sequenced by GATC, Konstanz, or Eurofins Genomics, Ebersberg.

2.2.2 Cell culture

The cell culture work was performed in sterile laminar flow hoods. The solution bottles, laboratory equipment, and other materials were treated with disinfectant or autoclaved before use.

2.2.2.1 Media preparation

Phleomycin solution	**amount (for 2 ml)**	**concentration**
• Phleomycin	5 mg	2.5 mg/ml
• in H_2O_{MilliQ}		

HMI-9 basic medium	**amount (for 10 l)**	**concentration**
• Iscove's modified Dulbecco's medium	176.6 g	17.66 g/l
• Hypoxanthine	1.36 g	1 mM
• $NaHCO_3$	30.24 g	36 mM
• Sodium pyruvate	1.1 g	1 mM
• Thymidine	0.39 g	161 µM
• Bathocuprone disulfonic acid disodium	0.28 g	49 µM
• adjust to pH 7.0 - 7.5 (NaOH)		
• in H_2O_{MilliQ}		

The medium was stored in 450 and 900 ml aliquots at -20 °C.

HMI-9 complete medium	**amount (for 0.5 l)**	**concentration**
• HMI-9 basic medium	450 ml	90% (v/v)
• FCS (heat-inactivated at 60°C for 1 h)	50 ml	10% (v/v)
• Penicillin (5,000 U/ml)	5 ml	50 U/ml
• Streptomycin (5,000 µg/ml)		50 µg/ml
• L-Cysteine	93 mg/5 ml H_2O_{MilliQ}	150 mM
• 2-Mercaptoethanol (14.27 M)	7 µl/5 ml H_2O_{MilliQ}	200 µM
• Phleomycin (2.5 mg/ml)	40 µl	0.2 µg/ml

L-cysteine (93 mg) and 2-mercaptoethanol (7 µl) was mixed with 5 ml H_2O_{MilliQ} before use. The medium was sterile filtrated and stored at 4 °C for 1 month.

Hemin solution	**amount (for 0.25 l)**	**concentration**
• Hemin	625 mg	2.5 g/l (~3.8 mM)
• in 0.1 M NaOH		

Basic MEM (recipe from Biochrome)	**amount (for 1 l)**
• HEPES	7.14 g
• NaCl	6.8 g
• NaH_2PO_4 x H_2O	0.14 mg
• $MgSO_4$ x 7 H_2O	0.2 mg
• KCl	0.4 mg
• $CaCl_2$ x 2 H_2O	265 mg
• Adenosine	12 mg
• Ornithine	10 mg
• Arginine x HCl	126 mg
• Glutamine	292 mg
• Cystine	24 mg
• Isoleucine	52 mg
• Histidine x HCl xH_2O	42 mg
• Leucine	52 mg
• Methionine	15 mg
• Lysine	73 mg
• Phenylalanine	100 mg
• Proline	600 mg
• Threonine	48 mg
• Tryptophan	10 mg
• Tyrosine	100 mg
• Valine	46 mg

Powder was dissolved in 900 ml of H_2O_{MilliQ} and adjusted to pH 7.4 (NaOH).

MEM-Pros complete medium	**amount (for 0.5 l)**	**concentration**
• Basic MEM	450 ml	90% (v/v)
• FCS (heat-inactivated at 60 °C for 1 h)	50 ml	10% (v/v)
• Penicillin (5,000 U/ml)	5 ml	50 U/ml
• Streptomycin (5,000 µg/ml)		50 µg/ml
• 10x MEM vitamins	5 ml	1x
• 10x MEM non-essential amino acids	5 ml	1x
• Hemin (2.5 mg/ml in 0.1 M NaOH)	1.4 ml	7 µg/ml (~11 µM)
• Phenolic red	5 mg	10 mg/l
• Phleomycin (2.5 mg/ml)	100 µl	0.5 µg/ml

The medium was sterile filtrated and stored at 4 °C for ≤ 2 - 3 months.

1x Phosphate buffered saline (PBS) (pH 7.4)	**amount (for 1 l)**	**concentration**
• NaCl	8 g	136.9 mM
• Na_2HPO_4 x 2 H_2O	1.42 g	8 mM
• KCl	0.2 g	2.7 mM
• KH_2PO_4	0.23 g	1.7 mM
• adjust to pH 7.4 (in general not needed)		
• in H_2O_{MilliQ}		

Sterile filtrated and stored at 4 °C

2.2.2.2 Cultivation of T. brucei

BS parasites from Lister strain 427 were cultivated in HMI-9 complete medium at 37 °C and 5% CO_2 in 50 ml tissue culture flasks with vented cap. PC cells were grown in MEM-Pros complete medium at 27 °C in 50 ml tissue culture flasks with plug seal cap. BS and PC parasites were passaged when they were grown to a density of 1 - 4 x 10^6 cells/ml and 1 - 4 x 10^7 cells/ml, respectively.

The antibiotics used for transfection and induction experiments are listed in Table 2.1. The puromycin resistance gene *pac* encodes the puromycin N-acetyl-transferase, the blasticidin resistance cassette a blasticidin-S deaminase, *neo* the aminoglycoside 3‘-phosphotransferase, and hygromycin resistance cassette the hygromycin B phosphotransferase.

Table 2.1: Antibiotics used for parasite culture.

Antibiotic	Transfected vector	Experiment	Concentration [µg/ml]	
			BS	PC
Puromycin	pHD1747	KO in 449 cells	0.2	2
Blasticidin	pHD1748		5	10
G418	pHD1747/8-Neo		2.5	30
Tetracycline	pRPa^{ix6Mx}_*pxIV*_c-myc	Over-expression in 2T1 cells	0.1-1	-
Doxycycline			1	-
Hygromycin			2.5	-

For further analysis and experiments, parasites were harvested by centrifugation at 2000 g and 4 °C for 5 - 10 min. Generally, they were washed once with 1x PBS. Phenotypic analyses were performed with the compounds listed in Table 2.2.

Table 2.2: Compounds studied in phenotypic analyses.

Compound	Stock concentration	Solvent	Final concentration
Ammonium chloride	500 mM	H_2O	5 mM
Chloroquine	5 mM	H_2O	10, 50 µM
Coenzyme Q10	300 µM	warm ethanol	10, 1, 0.1 µM
Decylubiquinone	10 mM	ethanol	0.01 - 10 µM
Deferoxamine	6.5 mM	PBS	6.25, 25, 100, 400 µM
DIDS	100 mM	PBS	0.1, 0.5, 1 mM
G418	50 mg/ml	H_2O	15, 30, 50, 100 µg/ml
Hemin	2.5 mg/ml	0.1 M NaOH	7, 28, 35, 70, 105 µg/ml
Hemoglobin	10 mg in 10 ml medium	HMI-9 medium	1 mg/ml (16 µM)
Iron chloride	10, 100 mM	H_2O	100, 200 µM
Iron nitrate	100 mM	H_2O	100, 500 µM
Iron sulfate	10, 100 mM	H_2O + 2% HCl	10, 50, 100, 200, 500 µM
MitoQ	11 mM	ethanol	0.001 - 10 µM
Starch-deferoxamine	40 mM	0.9% NaCl	100 µM
Transferrin, holo	500 µM	PBS	5, 20, 25 µM
Transferrin, apo	25 mg in 1 ml medium	HMI-9 medium	25 mg/ml (320 µM)
Trolox	100 mM	ethanol	0.1, 1, 10, 100 µM

2.2.2.3 Freezing and thawing of glycerol stocks

Up to 3 x 10^7 parasites were harvested and resuspended in 3 ml of freezing medium. The cell suspension was transferred into cryogenic storage vials (1 ml/vial). The vials were labeled, wrapped in several layers of tissues for slow freezing, and stored at -80 °C.

Freezing medium	**amount (for 25 ml)**	**concentration**
• Glycerol	2.5 ml	10%
• in HMI-9/MEM-Pros medium		

The medium was sterile filtrated.

Parasites were quickly thawed in a 37 °C water bath, diluted in 5 ml of the respective pre-warmed medium, and centrifuged at 2000 g and 4 °C for 5 min. The supernatant was discarded and the cells were washed with 1x PBS. After centrifugation, the cells were resuspended in 5 ml of fresh, warm medium in a new 50 ml tissue culture flask.

2.2.2.4 Isolation of genomic DNA from parasites

About 5×10^7 cells were harvested. Genomic DNA was extracted. Further steps were performed as described in the DNeasy Blood & Tissue manual from Qiagen. The DNA was eluted with 100 - 200 µl of the provided elution buffer.

2.2.2.5 Transfection of parasites

About 10 µg of the plasmid (pHD1747 or pHD1748) in a total volume of 20 µl was digested with *Xho*I and *Not*I in buffer O or in the case of the FastDigest enzymes, in FastDigest buffer at 37 °C for at least 2 h. The digest was mixed with 100 µl of 4 M ammonium acetate and 500 µl of absolute ethanol and incubated on ice for at least 2 h. After centrifugation at 13000 rpm and 4 °C for 10 min, the supernatant was discarded and 100 µl of 70% ethanol was added as washing step. The suspension was centrifuged at 13000 rpm and 4 °C for 15 min, the supernatant was carefully removed, and the pellet was dried in a sterile fume hood for several hours or overnight. The dried plasmid was carefully mixed with 100 µl of human T cell nucleofactor solution and added to 4×10^7 harvested parasites in a final volume of up to 300 µl medium. The mixture was transferred without bubbles into a transfection cuvette and applied to the Amaxa nucleofactor system using the pre-installed program X-001. The transfected cells were mixed with 18 ml of conditioned medium (medium for 1 day at 37 °C) containing antibiotics or Trolox and cultivated in the respective incubator overnight. The cells were seeded in 1.5 - 2 ml of conditioned medium supplemented with the selecting antibiotics in 24-well tissue culture plates accordingly to the serial dilution scheme (see Figure 2.6). Clones obtained after 5 - 10 days were transferred to 50 ml culture flasks.

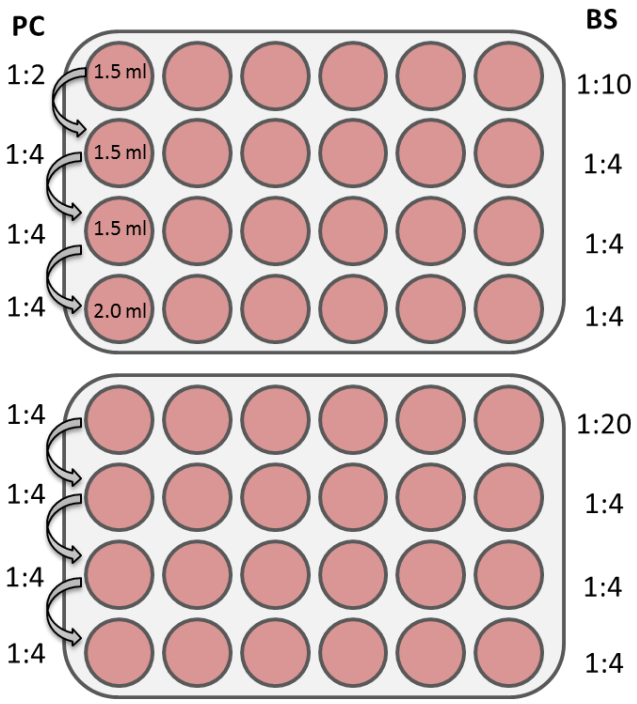

Figure 2.6: Seeding scheme for the transfection of *T. brucei*. Two 24-well culture plates were used with different dilution series for PC and BS parasites. Each well had a total volume of 1.5 - 2 ml of medium containing the respective antibiotics.

2.2.2.6 Sample preparation for WB

Between 2 x 10^6 and 2 x 10^7 parasites were harvested, washed once with 1x PBS, and mixed with 2x sample buffer (see chapter 2.2.4.1). Samples were boiled for 10 min and centrifuged at 13000 rpm and 4 °C for 5 min. The supernatant was directly subjected to SDS polyacrylamide gel electrophoresis (SDS-PAGE) or the whole sample was stored at -20 °C.

2.2.2.7 Genomic DNA isolation for Southern blot

Up to 2 x 10^9 parasites were harvested, resuspended in 1 ml of DNA extraction buffer, and incubated with 24 µl of RNase A solution at 37 °C for 1 h. The suspension was transferred to ice and mixed with 500 µl of ice-cold 4 M ammonium acetate for 1 min. After centrifugation at 8000 rpm and 4 °C for 5 min, the supernatant was transferred into a new reaction tube, 0.7x volume of cold isopropanol was added, and the tube was inverted several times to precipitate the DNA (white strand). After centrifugation at 13000 rpm and 4 °C for 15 min, the supernatant was discarded and the pellet washed with 500 µl of 70% ethanol. The tube was centrifuged at 13000 rpm and 4 °C for 1 min and washed again with 300 µl of absolute ethanol. After the same centrifugation step, the supernatant was carefully discarded. The open tube was kept for several hours under a hood. The dried pellet was dissolved in 200 µl of AE

buffer (from Zymo Research kits) and kept at 37 °C for 1 h or at 60 °C for 10 min. The DNA concentration was measured using the NanoDrop, Sinnig Group, BZH.

Buffer for DNA extraction:	**amount (for 0.5 l)**	**concentration**
• Tris	0.61 g	10 mM
• NaCl	0.29 g	10 mM
• EDTA	1.86 g	10 mM
• SDS	2.5 g	0.5% (w/v)
• adjust to pH 8.0 (HCl)		
• in H_2O_{MilliQ}		

2.2.2.8 Coating of IF slides with poly-L-lysine

The poly-L-lysine solution was diluted 1:10 in H_2O_{MilliQ} and 300 µl were added to each well of the 8-well slide. After 10 min incubation at RT, the slide was washed with H_2O_{MilliQ} three times and dried. Coating of the slides was done at the same day of the experiment.

2.2.2.9 Coupling of antibodies against bovine transferrin to CNBr-sepharose

Up to 12 ml of the antiserum containing 1 mg/ml IgG against bovine transferrin was concentrated to 2 ml by an Amicon centrifugal filter tube (size 50 kDa). The serum was transferred into a 20 ml chromatography column and 11 ml of coupling buffer was added. The CNBr-sepharose (1.7 g) was suspended in 50 ml of ice-cold 1 mM HCl and washed several times with 1 mM HCl (in total 200 ml) on a sintered glass filter with porosity G3. The material was transferred into the column using 4 ml of coupling buffer. The column was sealed and rotated at 25 °C for 2 h. The excess of antibodies was removed by washing with 10 ml of coupling buffer, the column was rotated end-overend with blocking buffer at RT for 1 h, and kept upright for 1 h. The column was washed with three cycles of 10 ml of washing and coupling buffer until the $\Delta A_{280\,nm}$ of the flow-through was zero. The column was equilibrated with 1x PBS or subjected to storage at 4 °C, in 1x PBS + 0.05% NaN_3.

Coupling buffer (freshly prepared)	**amount (for 0.5 l)**	**concentration**
• $NaHCO_3$	8.4 g	200 mM
• NaCl	14.61 g	500 mM
• adjust to pH 8.5 (NaOH)		
• in H_2O_{MilliQ}		

Column blocking solution (freshly prepared)	**amount (for 0.2 l)**	**concentration**
• Ethanolamine	12.1 ml	1 M
• adjust to pH 8.0 (HCl)		
• in H_2O_{MilliQ}		

Column washing buffer	**amount (for 0.5 l)**	**concentration**
• NaOAc	4.10 g	100 mM
• NaCl	14.61 g	500 mM
• adjust to pH 4.0 (HCl)		
• in H_2O_{MilliQ}		

Transferrin-depleted medium

The 8 ml anti-transferrin column was equilibrated with 30 ml of FCS-free HMI-9 medium at a flow rate of 0.5 ml/min at RT. Up to 30 ml of HMI-9 medium (+ FCS) was applied at a flow rate of 0.2 ml/min. For the first fraction, a volume of 7 ml was collected and for the following ones, 5 ml. The column was washed with 15 - 20 ml of 1x PBS followed by 45 ml of 8 M urea in 1x PBS until $\Delta A_{280\,nm}$ was zero, and finally with 20 ml of 1x PBS. Before the next run, the column was equilibrated again with FCS-free medium or stored as described above. The elution fractions were sterile filtrated and stored at 4 °C. After Western blot analysis, transferrin-free fractions were pooled and used for phenotypic analysis of the parasites.

2.2.3 Protein expression and purification

2.2.3.1 Test expression of Px IV

Bacterial cells suitable for recombinant protein expression were transformed with the desired Px IV expression plasmid (see chapter 2.2.1.7). After overnight incubation of the plate at 37 °C, a 50 ml Falcon tube was filled with 20 ml LB medium containing the respective antibiotics (see Table 2.3) and the medium was inoculated with bacterial colonies. The tube was kept not fully closed at 37 °C and 180 rpm overnight. On the next day, 200 µl of the culture was transferred into 20 ml fresh LB medium + antibiotic and incubated at 37 °C and 180 rpm. At an OD at 600 nm of 0.4 - 0.6, expression was induced with 1 mM or 0.2 mM IPTG. A sample of the culture (1 - 2 ml) prior to induction (uninduced) was taken, centrifuged at 4000 rpm and 4 °C for 5 min, and the cell pellet was stored at -20 °C. The bacterial culture

was incubated at the desired conditions and optional, a second sample was taken at the end of the day (evening sample). The final sample was taken on the next day and all samples were resuspended in 100 - 200 µl test lysis buffer. The uninduced and evening sample were analyzed as total lysates whereas the final samples were sonicated twice on ice for 5 sec and centrifuged at 4000 rpm and 4 °C for 5 min. The supernatant was transferred into a new reaction tube and the pellet was resuspended in 100 µl test lysis buffer. All samples were mixed with the respective volume of 4x SDS reducing sample buffer (see chapter 2.2.4.1), boiled in a water bath for 15 min, and subjected to SDS-PAGE or stored at -20 °C.

Test lysis buffer	**amount (for 10 ml)**
• Buffer A (chapter 2.2.3.2)	10 ml
• PMSF (chapter 2.2.3.2)	10 µl
• Lysozyme	~ 5 mg

Table 2.3: Antibiotics used for bacterial cultures.

Antibiotic	Concentration [µg/ml]	Resistance gene encodes the
Kanamycin	50	kanamycin phosphotransferase
Carbenicillin	100	carbenicillin β-lactamase
Chloramphenicol	34	chloramphenicol acetyltransferase
Tetracycline	10	tetracycline efflux pump

100x Trace elements for minimal medium	**amount (for 1 l)**	**concentration**
• EDTA x 2 H_2O	5 g	13.4 mM
• $FeCl_3$ x 6 H_2O	0.83 g	3.1 mM
• $ZnCl_2$	84 mg	616.3 µM
• $CuCl_2$ x 2 H_2O	13 mg	76.3 µM
• $CoCl_2$ x 6 H_2O	10 mg	42 µM
• H_3BO_3	10 mg	162 µM
• $MnCl_2$ x 4 H_2O	1.6 mg	8.1 µM
• in H_2O_{MilliQ}		

First, dissolve EDTA in 800 ml of H_2O_{MilliQ} and adjust pH to 7.5 (NaOH). Add all other components and fill up to 1 l with H_2O_{MilliQ} followed by sterile filtration.

10x M9 medium for minimal medium	**amount (for 1 l)**	**concentration**
• Na_2HPO_4 x 2 H_2O	75.2 g	423 mM
• KH_2PO_4	30 g	220 mM
• NaCl	5 g	86 mM
• NH_4Cl	5 g	94 mM
• in H_2O_{MilliQ}		

Sterile filtrated

Minimal medium	**amount (for 105 ml)**	**concentration**
• 10x M9 medium	10.5 ml	1x
• 100x Trace elements	1.05 ml	1x
• 20% Glucose	2.1 ml	0.4%
• $MgSO_4$ x 7 H_2O (1 M)	105 µl	1 mM
• Biotin (1 mg/ml)	105 µl	1 µg/ml
• Thiamine (1 mg/ml)	105 µl	1 µg/ml
• $CaCl_2$ x 2 H_2O (1 M)	32 µl	0.3 mM
• in sterile H_2O_{MilliQ}		

Add $CaCl_2$ at the end and prepare it sterile next to the flame.

Phosphate solution for Terrific Broth medium	**amount (for 0.1 l)**	**concentration**
• KH_2PO_4	2.31 g	170 mM
• K_2HPO_4	12.54 g	720 mM
• in H_2O_{MilliQ}		

Sterile filtrated

Terrific Broth (TB) medium	**amount (for 1 l)**
• Tryptone/peptone	12 g
• Yeast extract	24 g
• Glycerol	4 ml
• in H_2O_{MilliQ} and autoclaved	900 ml
• Phosphate solution	100 ml

2-YT medium	**amount (for 1 l)**
• Tryptone/peptone	20 g
• Yeast extract	10 g
• NaCl	10 g
• adjust to pH 7.5 (NaOH)	
• in H_2O_{MilliQ}	

2.2.3.2 Preparative expression of Px IV

Up to 40 ml LB medium containing kanamycin and chloramphenicol was inoculated with *E. coli* BL21 (DE3) pLysS cells transformed with the pETtrx-1b_PxIV_1A plasmid and kept at 37 °C and 180 rpm overnight. This pre-culture was then diluted 1:100 in 4 l of LB medium and further incubated at 37 °C and 180 rpm. Protein expression was induced at an $OD_{600\,nm}$ of about 0.54 by adding 0.2 mM IPTG. The bacteria were grown at 15 °C and 180 rpm overnight, harvested, and resuspended in 80 ml of lysis buffer. The tube was inverted several times at 4 °C for 15 min and the cells further lysed on ice by sonification, six times for 45 sec including 45 sec breaks. After centrifugation at 18000 rpm and 4 °C for 30 min, the combined supernatant was applied onto an 8 ml Ni-NTA column pre-equilibrated with H_2O_{MilliQ} followed by buffer A at 4 °C. The column was washed with 10 mM and 20 mM imidazole corresponding to 4% and 8% of buffer B, respectively. The protein was eluted in fractions of 3 ml at 80% buffer B and all protein-containing fractions were pooled. The column was washed with 100% buffer B followed by buffer A. The elution fraction was concentrated using a 10 kDa Amicon filter tube and buffer B was exchanged to buffer A. 0.5 ml Tobacco etch virus (TEV) protease solution was added to ≤3 ml of the elution corresponding to a final concentration of 0.3 mg/ml TEV protease. The protein solution was incubated for 30 min at RT and then stored at 4 °C overnight. The solution was loaded onto the second 1 ml Ni-NTA column and the flow-through was collected in 2 ml fractions. The column was finally washed with 80% and 100% buffer B, 4 column volumes of buffer A, 4 column volumes of H_2O_{MilliQ}, and 2 - 3 column volumes of 20% EtOH. Samples from various washing steps, flow-through, and elutions were collected and subjected to SDS-PAGE. The pellet sample was dissolved in each 100 µl of lysis buffer, 6 M of urea, and sample buffer. For the His_6-Px IV purification of a 2 l bacterial culture, the procedure was performed as described above. In addition, a third washing step with 50 mM imidazole was included on the 8 ml Ni^{2+}-NTA column.

Cystatin solution	**amount (for 962 µl)**	**concentration**
• Cystatin	0.5 mg	40 µM
• in buffer A (pH 7.5)		

Pepstatin solution	**amount (for 4.86 ml)**	**concentration**
• Pepstatin	5 mg	1.5 mM
• in DMSO		

PMSF solution	**amount (for 57.4 ml)**	**concentration**
• PMSF	1 g	100 mM
• in isopropanol		

Buffer A	**amount (for 1 l)**	**concentration**
• NaCl	17.5 g	300 mM
• NaH_2PO_4	6.9 g	50 mM
• adjust to pH 7.5 (NaOH)		
• in H_2O_{MilliQ}		
• Filtrated and degased		

Buffer B	**amount (for 0.5 l)**	**concentration**
• NaCl	8.76 g	300 mM
• NaH_2PO_4	3.44 g	50 mM
• Imidazole	8.51 g	250 mM
• adjust to pH 7.5 (HCl)		
• in H_2O_{MilliQ}		
• Filtrated and degased		

Lysis buffer	**amount (for 30 ml)**	**concentration**
• Lysozyme	10 mg	1 mg/1 g wet pellet
• DNase	spatula tip	spatula tip/30 ml
• PMSF	30 µl	100 µM
• Cystatin	3 µl	4 nM
• Pepstatin	3 µl	0.15 µM

- in buffer A

3 ml lysis buffer was used for 1 g wet cell pellet

2.2.3.3 Preparation of Px IV for antibody production

Partially purified recombinant, untagged Px IV obtained from pETtrx-1b_PxIV_1A plasmid expression (see chapter 2.2.3.2) was mixed with 4x SDS sample buffer and subjected to a preparative SDS-PAGE. One big (10 x 10.5 cm) and thick (1.5 mm) 14% gel was poured and 100 - 150 µg total protein was loaded into each of the four wells. The gel run at 25 mA for 2 - 3 h and the proteins stained with Coomassie at RT. Afterwards, the gel was extensively destained and washed with H_2O_{MilliQ}. The four protein bands were cut out and stored in a 1.5 ml reaction tube. The gel slices were sent for immunization of a rabbit by Eurogentec, Belgium.

2.2.4 Biochemical and cell biological analysis methods

2.2.4.1 SDS-PAGE

SDS gels were prepared according to their recipe (see below) in a gel caster. Up to 35 µl of protein samples were loaded per pocket of the gel in electrophoresis chambers filled with 1x SDS running buffer. The PageRuler Plus pre-stained protein marker was used for standardization. After the protein had been run through the stacking gel at 15 - 20 mA for ~20 min, the current was increased to 20 - 25 mA till the end of the run. The gel was stained with Coomassie solution (chapter 2.2.4.2) or used for Western blot analysis (chapter 2.2.4.3).

10% APS solution (freshly prepared)	**amount (for 3 ml)**
• APS	0.3 g
• in H_2O_{MilliQ}	

4x Resolving buffer (pH 8.8)	**amount (for 0.5 l)**	**concentration**
• SDS	2 g	0.4% (w/v)
• Tris/HCl, pH 8.8	90.86 g	1.5 M
• in H_2O_{MilliQ}		

Resolving gel solution	**(10%)**	**(12%)**	**(14%)**	**(16%)**
• 4x Resolving buffer	15 ml	15 ml	15 ml	15 ml
• 30% Acrylamide/bisacrlyamide	20 ml	24 ml	28 ml	32 ml
• TEMED	54 µl	54 µl	54 µl	54 µl
• 10% APS solution	900 µl	900 µl	900 µl	900 µl
• H_2O_{MilliQ}	23.56 ml	19.5 ml	15.5 ml	11.5 ml

2x Stacking buffer (pH 6.8)	**amount (for 0.5 l)**	**concentration**
• SDS	1 g	0.2% (w/v)
• Tris/HCl, pH 6.8	15.14 g	0.25 M
• in H_2O_{MilliQ}		

Stacking gel solution	**(6%)**
• 2x Stacking buffer	20 ml
• 30% Acrylamide/bisacrylamide	5 ml
• TEMED	48 µl
• 10% APS solution	1.2 ml
• H_2O_{MilliQ}	13 ml

4x Sample buffer	**amount (for 0.1 l)**	**concentration**
• Tris/HCl, pH 6.8	30.285 g	200 mM
• SDS	8 g	8% (w/v)
• Glycerol	40 ml	40% (v/v)
• Bromophenol blue	0.04 mg/ml	0.004%
• 2-Mercaptoethanol (fresh)	4 ml	0.57 M

10x SDS running buffer	**amount (for 1 l)**	**concentration**
• SDS	10 g	34.7 mM
• Tris	30.3 g	250 mM
• Glycine	144 g	1.9 M
• in H_2O_{MilliQ}		

2.2.4.2 Coomassie staining of SDS gels

SDS gels were kept in a box with 50 ml of Coomassie staining solution for 4 h or overnight at RT. Staining solution was removed and stored for further usage. Coomassie destaining solution was applied to the gel and changed every 1 h till the background of the gel was completely destained. For long-term storage, the gels were kept for several days in 20% EtOH and subjected to gel drying frames.

Coomassie staining solution	**amount (for 1.1 l)**
• Coomassie blue R250	0.5 g
• Acetic acid	100 ml
• EtOH	400 ml
• H_2O_{MilliQ}	600 ml
• filtrated	

Coomassie destaining solution	**amount (for 1.1 l)**
• EtOH	250 ml
• Acetic acid	80 ml
• in H_2O_{MilliQ}	

2.2.4.3 Western blot

After SDS-PAGE, 2x four Whatman paper, two sponges, and the SDS gel were equilibrated in the Western blot transfer buffer for 5 min. The PVDF membrane was activated by methanol incubation for 5 sec. One sponge, four wet Whatman papers, and the gel (on the top) were placed on a blotting cassette (black side). The membrane was placed on the gel with four Whatman papers and the second sponge. Air bubbles between the membrane and the gel were avoided. The blotting cassette was placed in the chamber, the black side orientated towards the negative electrode. The transfer was performed at 150 mA for 2 h. Non-specific binding was prevented by incubating the membrane in blocking buffer at RT for 1 h or overnight at 4 °C. The solution of the primary antibody (diluted in blocking buffer) was added to the membrane which was shaken at RT for 1 h or at 4 °C overnight. The membrane was washed three times with washing buffer for 5 - 30 min and treated with the secondary antibody solution (diluted in blocking buffer) at RT for 1 h. After washing three times with washing buffer for 5 - 30 min, the membrane was incubated in 5 ml ECL solution in the dark

at RT for 5 min. The remaining liquid was removed and the membrane was sealed in a plastic bag inside a developing cassette. The membrane was exposed for different times to ECL films which were developed in an X-ray film developing and fixation machine.

Blotting buffer	**amount (for 1 l)**	**concentration**
• Tris	3 g	24.8 mM
• Glycine	14 g	186.5 mM
• H_2O_{MilliQ}	800 ml	
• Methanol	200 ml	20% (v/v)

10x Tris buffered saline (TBS)	**amount (for 1 l)**	**concentration**
• NaCl	90 g	1.54 M
• Tris	121 g	1 M
• HCl	63 ml	760 mM
• should be ~ pH 7.5		

1x TBS-T	**amount (for 1 l)**
• 10x TBS	100 ml
• Tween 20	500 µl
• in H_2O_{MilliQ}	

Blocking buffer	**amount (for 50 ml)**	**concentration**
• Milk powder	2.5 g	5% (w/v)
• in 1x TBS-T		

2.2.4.4 Southern blot

All boxes, plates, and other materials was cleaned rigorously with autoclaved H_2O_{MilliQ} and ethanol and stored under a sterile hood. The hybridization probes were obtained by PCR from genomic DNA using *Taq* polymerase and the PCR DIG labeling mix. Up to 12 µg of genomic DNA from 2×10^9 cells was isolated and digested with 50 U of FastDigest restriction enzymes (for expected DNA fragments, see Table 2.4) in a total volume of 65 µl at 37 °C for 2 h. The samples and DIG-labeled DNA ladder were loaded onto a large, 1 cm thick 0.8% agarose gel and the gel was run at 60 - 70 V for 4 - 6 h at RT. The gel parts without samples

were cut off and the gel was placed into a box with 200 ml of DNA denaturing solution. After gently shaking for 20 min, the step was repeated, the gel was rinsed with autoclaved H_2O_{MilliQ}, and the gel was washed twice with 200 ml of neutralization solution for 20 min. An N^+ nylon membrane and two Whatman papers were cut 3 - 4 mm larger than the gel, and three Whatman papers were cut in 33 x 13 cm for the buffer transfer. The transfer system was assembled as shown in Figure 2.7. The two glass bowls were filled with 500 ml of 20x SSC buffer, the three large Whatman paper were placed on the glass plate and dipped into the bowls. The gel was assembled on the papers without bubbles and parafilm was placed around the gel. The membrane was rinsed with autoclaved H_2O_{MilliQ} and put onto the gel without bubbles. Two Whatman papers, two packages of grey tissue, glass plate, and more weight (e.g. thermal packs, ~2 kg) were set. The glass bowls were also covered with parafilm to prevent evaporation. After overnight blotting at RT, the pockets from the gel were marked on the membrane with a pencil, the membrane was rinsed with 2x SSC buffer, and put into a plastic bag. After cross-linking at 254 nm for 3 min, 10 ml of pre-heated DIG Easy Hyb Granules solution was poured into the bag and incubated at 42 °C for 2 - 5 h in a shaking water bath. For the hybridization, the PCR probe was boiled for 5 min and diluted to 20 - 50 ng/ml in 10 ml of pre-heated DIG Easy Hyb Granules solution. The solution in the bag was discarded and the hybridization solution was added at hybridization temperature (here: 42 °C) for 48 - 72 h. The membrane was placed in a box and washed twice with 200 ml of 2x SSC + 0.1% SDS buffer at RT for 15 min each. Then it was washed twice with 200 ml of 0.1x SSC + 0.1% SDS buffer for 15 min each and finally with hybridization buffer 1 for 5 min at RT. The membrane was blocked with hybridization buffer 2 at RT for 1 - 2 h in a plastic bag. For the antibody labeling, Anti-Digoxigenin-AP was diluted 1:10000 in 10 ml of hybridization buffer 2 and incubated with the membrane for 1 h at RT. The membrane was washed twice with hybridization buffer 1 for 20 - 30 min and then with hybridization buffer 3 for 5 min at RT. The detection was performed with CDP star diluted 1:100 in 1 ml of hybridization buffer 3. The CDP star solution (1 ml) was distributed on the DNA site of the membrane in a plastic bag and kept for 1 - 2 min shaking at RT. The membrane was transferred into a new plastic bag and developed by Hyperfilms in an X-ray film developer and fixer machine.

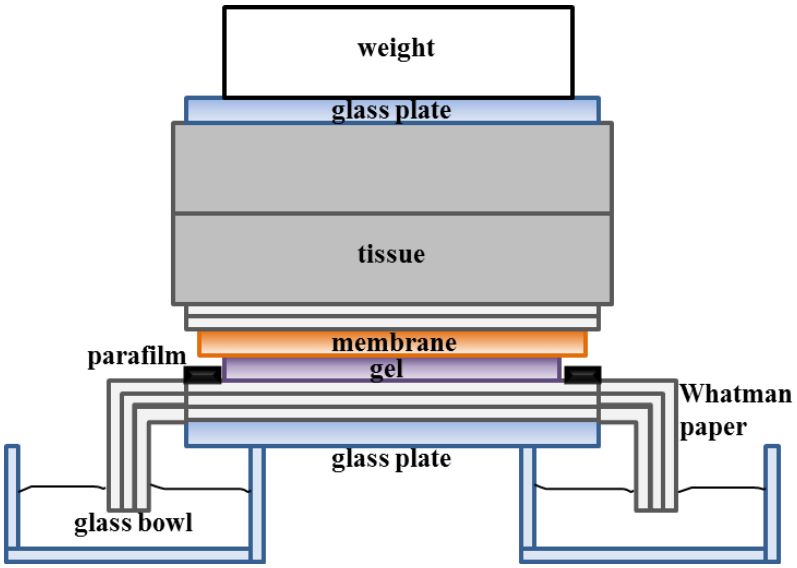

Figure 2.7: Blotting system for Southern blot analysis.

Table 2.4: Expected DNA fragments from Southern blot analysis. Genomic DNA of listed cell lines was digested with either *Hpa*I/*Pst*I or *Hpa*I/*Sca*I.

Cell lines	*Hpa* I/*Pst* I		*Hpa* I/*Sca* I	
	px I-II probe			
WT	X		2779 b	
	pac	*bla*	*pac*	*bla*
PC *px III* $^{-/-}$	2723 b	2549 b	2127 b	2676 b
PC *px II/III* $^{-/-}$	1787 b	1613 b	1944 b	1740 b
β-*tubulin* probe				
all	775 and 2859 b		3944 b	

DNA denaturing solution	**amount (for 0.5 l)**	**concentration**
• NaCl	43.83 g	1.5 M
• NaOH	8 g	0.4 M
• in H_2O_{MilliQ}		

Neutralization solution	**amount (for 0.5 l)**	**concentration**
• Tris	30.29 g	0.5 M
• NaCl	43.83 g	1.5 M
• adjust to pH ~7.5 (HCl)	~40 ml HCl	
• in H_2O_{MilliQ}		

20x SSC buffer	**amount (for 1 l)**	**concentration**
• NaCl	175.32 g	3 M
• Trisodium citrate	88.23 g	0.3 M
• adjust to ~pH 7.0 (NaOH)		
• in H_2O_{MilliQ}		
• autoclaved		

1% SDS solution	**amount (for 0.5 l)**	**concentration**
• SDS	5 g	1%
• in autoclaved H_2O_{MilliQ}		

2x SSC buffer + 0.1% SDS	**amount (for 0.5 l)**
• 20x SSC buffer	50 ml
• 1% SDS solution	50 ml
• in autoclaved H_2O_{MilliQ}	

0.1x SSC buffer + 0.1% SDS	**amount (for 0.5 l)**
• 2x SSC buffer + 0.1% SDS	25 ml
• 1% SDS solution	50 ml
• in autoclaved H_2O_{MilliQ}	

Hybridization buffer 1	**amount (for 0.5 l)**	**concentration**
• Maleic acid	5.80 g	0.1 M
• NaCl	4.38 g	0.15 M
• Adjust to ~pH 7.0 (NaOH)	~50 ml NaOH	
• in H_2O_{MilliQ}		
• autoclaved		
• Tween-20	1.5 ml	0.3% (v/v)

10x Blocking solution	**concentration**
• Blocking powder	10% (w/v)
• in hybridization buffer 1	

Boiled at 90 °C until it is dissolved and stored in aliquots at -20 °C

Hybridization buffer 2	**amount (20 ml)**	**concentration**
• 10x Blocking solution	2 ml	1x
• in hybridization buffer 1		

Hybridization buffer 3	**amount (for 0.5 l)**	**concentration**
• Tris	6.06 g	0.1 M
• NaCl	2.92 g	0.1 M
• adjust to pH 9.5 (HCl)		
• in H_2O_{MilliQ}		
• Autoclaved		

2.2.4.5 Phenotypic analysis

Parasites were harvested in the logarithmic growth phase, washed with 1x PBS, and resuspended in the respective medium ± Trolox and ± compound of interest. The phenotypic analyses were performed at a cell density of 3 - 9 x 10^5 cells/ml and viable cells were counted using a Neubauer chamber. To minimize the error, a specific flask was always counted in the same chamber. All four squares were counted and the mean was calculated. Data was normalized to the initial cell density at time point zero (100%). In general, the mean and the standard deviation of three individual experiments were presented. The p-value was calculated using the paired, two-tailored Student's t-test by the program Microsoft Excel.

2.2.4.6 Life cell imaging with fluorescent dextran and LysoTracker

For the dextran treatment, 2.5 x 10^6 BS parasites were incubated in medium ± Trolox at 37 °C and 5% CO_2 for 30 min. After harvesting, cells were resuspended in 50 µl of HMI-9 medium containing 2.5 mg/ml of fluorescent dextran and kept at 37 °C for 10 min. Parasites were washed twice with 1 ml of medium and 20 µl of the remaining supernatant was transferred to a glass slide. Boiled 1% agarose (5 µl) was mixed with the cells on the slide which was then sealed by a coverslip and nail polish. The slides were examined using a LSM 510 confocal microscope from Zeiss.

For LysoTracker staining, 2 x 10^6 cells were kept for different times in medium ± Trolox at 37 °C and 5% CO_2. Thirty min prior to harvesting, 5 µM of LysoTracker was added to the parasites. Afterwards the cells were washed twice with 1 ml of HMI-9 medium and examined as described for the dextran treatment.

2.2.4.7 Immunofluorescence microscopy

About 1 - 2 x 10^6 cells, which were grown in the logarithmic phase, were harvested and once washed with 1x PBS. Incubation for different times in medium ± Trolox was performed for BS parasites at 37 °C (5% CO_2) and for PC cells at 27 °C in a closed reaction tube. For MitoTracker staining, BS and PC parasites were kept in medium + Trolox and 0.12 µM of MitoTracker Red CMXRos solution for 15 min at 37 °C (5% CO_2) and 27 °C (closed), respectively. Cells were washed once with 1 ml of 1x PBS and incubated in medium + Trolox for 30 min at 37 °C (5% CO_2) or 27 °C (closed). When MitoTracker staining was performed, cells were always kept in the dark. After centrifugation, the supernatant was discarded and the cells were fixed in 500 µl of 4% PFA solution for 20 min at RT. The cells were washed twice with 1 ml of 1x PBS and transferred to 8-well slides. The slides were either pre-treated with poly-L-lysine and the cells allowed to settle down for at least 1 hour at RT or untreated slides were used and the cells settled down overnight at 4 °C. All further incubation steps were performed at RT. Cells were treated with 350 µl of permeabilization buffer for 20 min and washed twice with 500 µl of 1x PBS for 5 min. Up to 350 µl of blocking buffer was added for 20 min and the cells were kept in 350 µl of the primary antibody solution (dilution is antibody-dependent, see chapter 2.1.8) for 1 - 2 h. After washing four times with 500 µl of 1x PBS for 2 min, cells were incubated in 350 µl of the secondary antibody solution (see chapter 2.1.9) in the dark for 1 - 2 h and washed twice with 500 µl of 1x PBS for 5 min. For DNA staining, DAPI solution was diluted 1:100 in 1x PBS, slides were treated with 250 µl of DAPI solution in PBS for 15 min, and washed twice with 500 µl of 1x PBS for 5 min. The slide chamber was removed and the microscope slides were completely dried. About 5 µl of mounting solution was added in a plus-like shape on each well. Two cover slips were carefully pressed on four wells each of the slide and sealed by nail polish. Fluorescence microscopy was performed at the same day using a Carl Zeiss Axiovert 200 M microscope with an AxioCam MRm digital camera.

4% PFA solution	**amount (for 0.1 l)**	**concentration**
• PFA	4 g	4%
• in 1x PBS (pH 7.4)		

PFA was dissolved in 1x PBS at ~65 °C and stirred. Aliquots were stored at -20 °C.

MitoTracker solution	**amount (for 94 µl)**	**concentration**
• MitoTracker	50 µg	1 mM

- DMSO 94 µl

Permeabilization buffer	**amount (for 5 ml)**	**concentration**
• Triton X-100	10 µl	0.2% (v/v)
• in 1x PBS		

Blocking buffer	**amount (for 25 ml)**	**concentration**
• Gelatine	0.125 g	0.5% (w/v)
• in 1x PBS		

Heated in the microwave to be dissolved in warm PBS.

Antibody solution

- Antibodies diluted in blocking buffer (see chapter 2.1.8 and 2.1.9)

DAPI solution	**concentration**
• DAPI	50 µg/ml
• in H_2O_{MilliQ}	

Stored at -20 °C in aliquots in the dark.

Mounting solution	**amount (for 10 ml)**	**concentration**
• Glycerol	9 ml	90% (v/v)
• 1x PBS	1 ml	

2.2.4.8 Lipid peroxidation analysis by IF (performed by S. Ebersoll)

To detect lipid peroxidation, the Click-iT Lipid Peroxidation Imaging kit purchased from Life Technologies was used and we followed the instructions from the manufacturer. In order to improve the results, varying linoleamide alkyne (LAA) incubation times (30 min, 1 h, and 2 h) and LAA concentrations (10, 20, 50, and 200 µM) were used. Further procedure was adapted to normal immunofluorescence microscopy with parasites (see chapter 2.2.4.7).

2.2.4.9 Image analysis

Pictures from fluorescence microscopy were taken with a magnification of 6300x using an oil objective and processed by the AxioVision or the LSM 510 program of Zeiss. The exposure

time for each channel were kept the same for each slide. For the quantitative analysis, only cells which had a single signal for nucleus and kinetoplast DAPI staining were counted. The scale bar was added by the AxioVision/LSM 51 program. ImageJ, an image analysis and processing tool, was used for the adjustment of brightness and contrast and the generation of overlay fluorescent images. The figures were created by CorelDRAW Graphics Suite X3.

2.2.4.10 Flow cytometry

Flow cytometry is a quantitative method for the measurement of fluorescence intensity per cell. The signal of the forward scatter is directly proportional to the cell size and the side scatter signal displays the granularity of the cell in order to separate different cell populations, types, and apoptotic cells.

BS *px I-II*$^{-/-}$ and WT parasites were analyzed by flow cytometry. Between 3.5 - 5 x 10^6 cells were harvested at 2000 g and 4 °C for 5 min and washed with 1x PBS. After a second centrifugation step, the cells were transferred into 1.5 ml reaction tubes and mixed with 100 µl of the fluorescent dextran and kept at 37 °C for 10 min. After lysosomal staining, parasites were centrifuged at 8000 rpm at 4 °C for 2 min, washed with 1x PBS, and incubated with DAPI staining solution at RT for 10 min. Cells were washed three times with 1x PBS under the same conditions as before and transferred into flow cytometry tubes in a total volume of 0.5 ml in PBS ± Trolox and FCS. Unlabeled and cells stained only with DAPI or dextran were used as controls for the calibration. All cells were analyzed by the Canto II flow cytometer of BD, ZMBH, and FACSDiva software.

Dextran solution	**amount (for 0.1 ml)**	**concentration**
• Alexa Fluor 488-dextran (5 mg/ml) • in HMI-9 medium	50 µl	2.5 mg/ml

DAPI staining solution	**amount (for 0.25 ml)**	**concentration**
• DAPI solution (50 µg/ml) • in 1x PBS	25 µl	5 µg/ml

2.2.4.11 Thiol measurement by Ellman

In a 1 ml plastic semi-micro cuvette, 978 µl Ellman buffer was mixed with 20 µl of Ellman's reagent and 2 µl of sample yielding in a concentration of 20 - 40 µM of thiols. The increase in

absorption was measured at 412 nm in a spectrophotometer. The thiol content was calculated by the extinction coefficient of DTNB (13.6 $mM^{-1}cm^{-1}$) and the dilution factor (1/500).

Ellman buffer	**amount (for 0.5 l)**	**concentration**
• KH_2PO_4	3.4 g	50 mM
• adjust to pH 8.0 (KOH)		
• in H_2O_{MilliQ}		
Stored at 4 °C		

Ellman's reagent	**amount (for 0.1 l)**	**concentration**
• DTNB	0.4 g	10 mM
• in Ellman buffer		
Stored at 4 °C in the dark		

2.2.4.12 Peroxidase assay

The standard peroxidase assay contained Px buffer, 150 mU *T. cruzi* TR, 10 µM *T. brucei* Tpx, 100 µM $T(SH)_2$, 145 µM NADPH, and varying concentrations of recombinant Px IV (3.3 µM, 6.6 µM) in a total volume of 150 µl. The reaction was started by adding 50 µM H_2O_2 or HpETE and the NADPH consumption was followed by at 340 nm and 25 °C in a spectrophotometer.

Px buffer	**amount (for 0.2 l)**	**concentration**
• Tris	2.42 g	0.1 M
• EDTA x H_2O	0.37 g	5 mM
• adjust to pH 7.6 (HCl)		
• in H_2O_{MilliQ}		
• Triton X-100 (fresh)	200 µl	0.1% (v/v)

2.2.4.13 In-gel tryptic protein digestion and MALDI-TOF-MS

Purified recombinant His-tagged Px IV (18 µg in 20 - 25 µl) was treated with SDS sample buffer supplemented with or without 2-mercaptoethanol to differentiate between non-reduced and reduced form. Optional: samples were treated in sample buffer with 3 mM DTT at RT for

20 min prior to NEM-labeling. For blocking free cysteines, samples were incubated with 20 mM NEM in sample buffer at RT for 10 min.

Samples were subjected to SDS-PAGE and stained by Coomassie staining solution. The gel was destained several times, washed with H_2O_{MilliQ} five times for 30 min, and put on a clean glass plate. The Px IV band was cut out using a sharp and sterile scalpel. As blank control served a small piece of the gel without protein sample. The gel bands were chopped into several little pieces and transferred into a 1.5 ml reaction tube. About 100 µl of equilibration solution was added and the gel pieces were incubated for 10 min at RT. The supernatant was discarded and the procedure was repeated twice. 10 mM DTT solution (25 µl) was added and the tube was kept at 57 °C for 1 h. The supernatant was removed and 20 µl of 55 mM IAM-solution was added to alkylate all free cysteine residues. After incubation for 45 min at RT in the dark, the supernatant was discarded, and the gel pieces were washed with 100 ml of washing solution for 10 min. The supernatant was again removed, and the gel pieces were treated with 100 µl of equilibration solution for 10 min. To shrink the gel, the solution was taken off and the gel pieces were kept in 100 µl of 100% acetonitrile for 10 min. Acetonitrile was completely removed and 50 µl of 20 µg/ml trypsin solution was mixed with 75 µl of washing solution. About 30 µl of the ready-to-use trypsin solution was added to cover the gel pieces. After incubation on ice for 1 - 2 h, the suspension was kept at 37 °C overnight. To stop the proteolytic digest, 1.5 µl of 99% acetic acid was added (5%) and the pH of the prepared sample was measured (should be 2 - 3). The peptide-containing supernatant can be stored at -20 °C or directly be used for MALDI-TOF-MS analysis.

To prepare the thin saturated matrix layer, a spatula tip full of MALDI matrix (α-cyano-4-hydroxycinnamic acid) was mixed with 40 µl of acetone and vortexed for 1 min. After ultrasonic treatment for 1 - 2 min, the saturated matrix solution was spun down and the MALDI target plate was cleaned with methanol. About 15 µl of the thin layer matrix was applied to 3 - 4 spots on the target plate. For the sample preparation, a spatula tip full of MALDI matrix was transferred into a 1.5 ml reaction tube and mixed with 140 µl of 50% acetonitrile. The saturated matrix solution was again vortexed, sonificated, and spun down. A µC18 ZipTip was applied to a 20 µl pipette and equilibrated twice with 20 µl of acetonitrile by pipetting up and down. The ZipTip was aspirated twice with 20 µl of 0.1% TFA and 20 µl of the sample was loaded on the C18 column material of the ZipTip by pipetting up and down eight times. After washing with 0.1% TFA, 2 µl of the matrix solution was applied by a gel-

loader tip from the back on the C18 column material of the ZipTip. The ZipTip was placed on a 2 µl pipette and the matrix containing the peptide sample was pushed through the tip on a target plate spot. For the calibration of the instrument, 0.7 µl of the Peptide Calibration Standard was applied on a spot of the target plate and directly mixed with 0.7 µl matrix solution. All spots were dried at RT for 15 min to obtain white peptide crystals which could be measured in a Bruker Ultraflex mass spectrometer, AG Dr. T. Ruppert, ZMBH, Heidelberg. The machine was equipped with a 337 nm nitrogen laser and with the program Flex Control and Flex Analysis. The ion acceleration voltage was set to 20 kV. The detection range was selected from 500 - 4000 and the spectra from 400 laser shots were averaged. The calculated mass of the peptide peaks was compared with the theoretical masses by the MASCOT software. Possible cysteine modifications by NEM and IAM were considered.

Equilibration solution	**amount (for 5 ml)**	**concentration**
• NH_4HCO_3	10 mg	25 mM
• in 50% acetonitrile		

Washing solution	**amount (for 25 ml)**	**concentration**
• NH_4HCO_3	50 mg	25 mM
• in H_2O_{MilliQ}		

IAM solution	**amount (for 1 ml)**	**concentration**
• IAM	10 mg	55 mM
• in washing solution		

DTT solution	**amount (for 1 ml)**	**concentration**
• DTT	1.5 mg	10 mM
• in washing solution		

Trypsin solution	**amount (for 1 ml)**	**concentration**
• Trypsin	20 µg	20 µg/ml
• in 0.01% TFA		
Stored at -20 °C/80 °C		

3 Results

3.1 The physiological role of the cytosolic peroxidases in BS parasites

The text, figures, and figure legends of the following chapter 3.1 have been taken from Hiller *et. al.* (2014) and have been originally written by myself (marked by “”).

3.1.1 Withdrawal of Trolox results in a temperature-dependent lysis of px I-II$^{-/-}$ T. brucei

The peroxidase-type enzymes Px I-III specifically detoxify lipid hydroperoxides [Diechtierow and Krauth-Siegel, 2011]. BS *px I-II*$^{-/-}$ parasites, lacking the cytosolic peroxidases, show severe lipid peroxidation and lyse within 1 - 2 h after Trolox removal [Diechtierow and Krauth-Siegel, 2011]. However, the underlying mechanism of this rapid lysis was not known and thus, the subject of this thesis. “As a first step to elucidate the cellular processes responsible for the lethal phenotype of the *px I-II*$^{-/-}$ cells in the absence of Trolox, we followed the viability of the cells at different temperatures. After 90 min incubation at 37 °C, the mutant parasites were completely lysed, whereas 60% and >90% of the cells were still viable when the parasites were kept at 21 °C and 9 °C, respectively (Figure 3.1).“ [Hiller *et al.*, 2014]

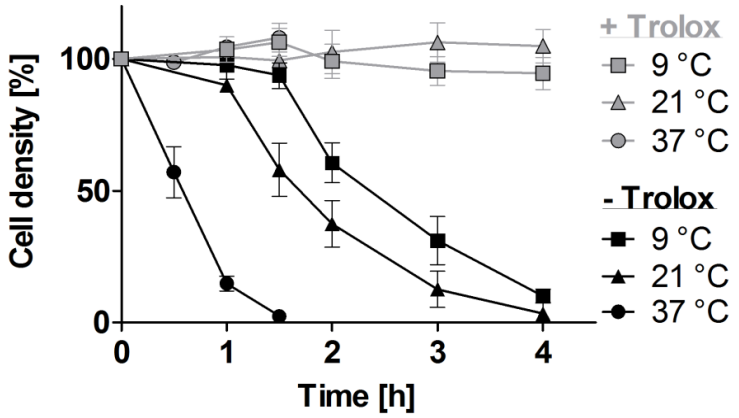

Figure 3.1: Lysis of the *px I-II*$^{-/-}$ BS cells is temperature-dependent. The *px I-II*$^{-/-}$ parasites were seeded at a density of 5 - 9 x 10^5 cells/ml in standard HMI-9 medium (which contains 10% FCS) supplemented ± 100 µM Trolox. The cells were incubated at 37 °C, 21 °C, and 9 °C, respectively. At the indicated time points, living cells were counted. The values represent the mean ± SD of three independent experiments. The figure and legend were taken from Figure 1 in Hiller *et al.* 2014 doi:10.1371/journal.ppat.1004075.g001

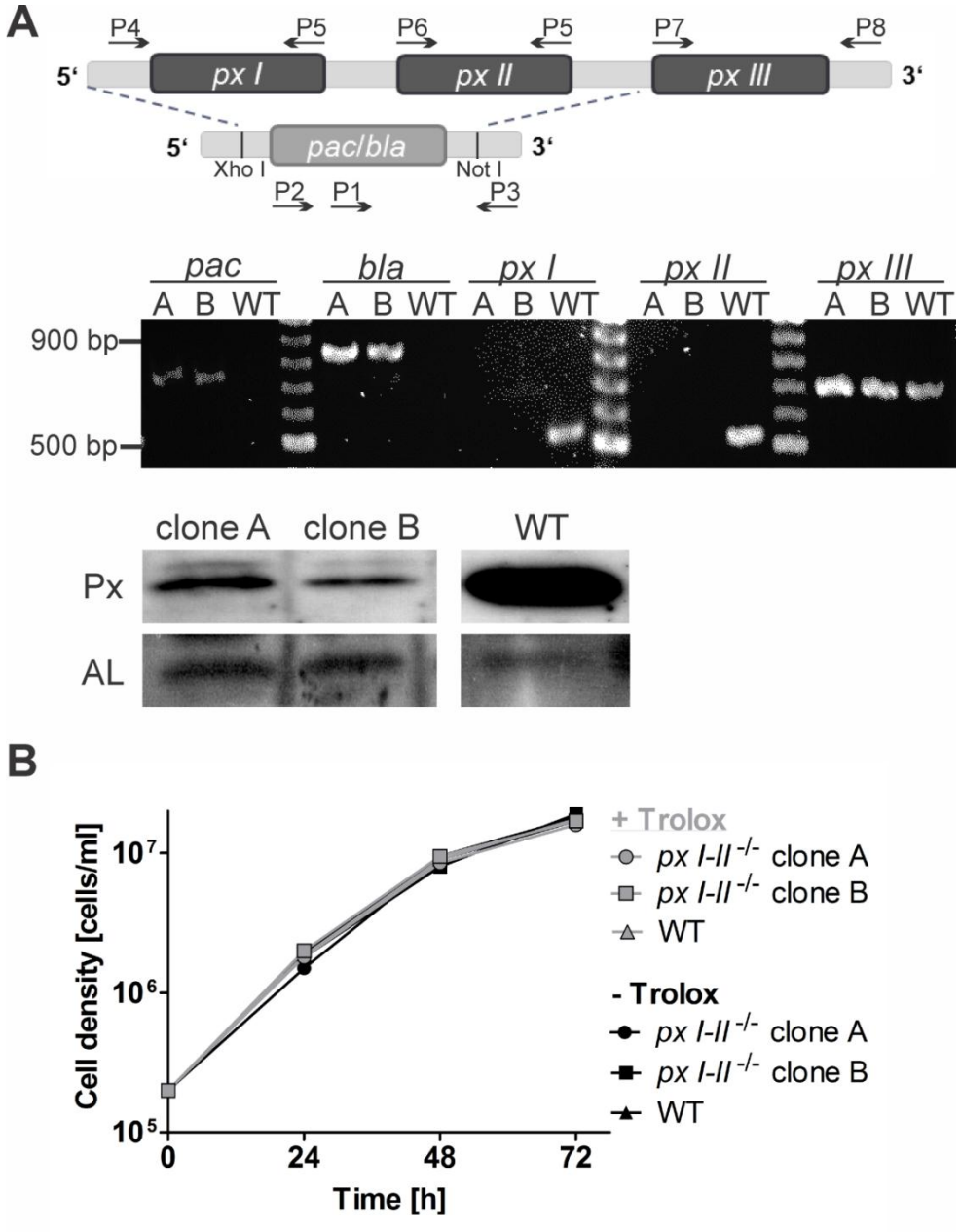

Figure 3.2: Generation and phenotypic analysis of PC *px I-II*$^{-/-}$ *T. brucei*. A. Upper part. Genomic *px* locus. The *px I-II* genes were replaced by transfecting the parasites with constructs containing a puromycin and blasticidin resistance gene, respectively, flanked by 5′*Xho*I/3′*Hind*III and 5′*Pst*I/3′*Not*I restriction sites 5′ and 3′ of the resistance gene, respectively, generated previously (Diechtierow and Krauth-Siegel, 2011). Middle part. To verify the specific removal of the *px I-II* alleles and correct insertion of the resistance genes after the two consecutive transfections, genomic DNA of two *px I-II*$^{-/-}$ cell lines (clones A and B) and WT parasites was subjected to PCR with different primer pairs (*pac*: P1 and P3, *bla*: P2 and P3, *px I*: P4 and P5, *px II*: P6 and P5, and *px III*: P7 and P8). Lower part. Western blot analysis of the two *px I-II*$^{-/-}$ clones and WT cells against Px and aldolase (AL) as loading control. The remaining comparably weak band corresponds to the mitochondrial Px III. **B.** Proliferation of the *px I-II*$^{-/-}$ cell lines (clone A and B) and WT cells in the presence (+) and absence (–) of 100 µM Trolox. The data are representative of three independent experiments giving identical results. The figure and legend were taken from Figure S1 in Hiller *et al.* 2014. The Western blot in **A.** and the cell viability analysis in **B.** were performed by Amrei Nißen. doi:10.1371/journal.ppat.1004075.s001 The primers described here are the following: P1 = PuroF_CH2, P2 = Bla-F_MD, P3 = P22r_CH, P4 = P7_MD, P5 = P18_MD, P6 = P26_MD, P7 = P22_MD, and P8 = P31_MD. Clone A = 4C4 and clone B = 4C2.

In contrast, PC *px I-II*$^{-/-}$ parasites generated and studied by Amrei Nißen did not show any growth defect after Trolox withdrawal (Figure 3.2) [Hiller *et al.*, 2014; Nißen, 2014]. "This may at least partially be due to the lower endocytosis rate in the insect form which is down-regulated approximately 10-fold compared to that of the BS form [Natesan *et al.*, 2007]. Because of the extremely rapid cell lysis observed at the normal culture temperature of 37 °C, the uptake studies described in the following sections were conducted at RT to allow acquisition of reliable data." [Hiller *et al.*, 2014]

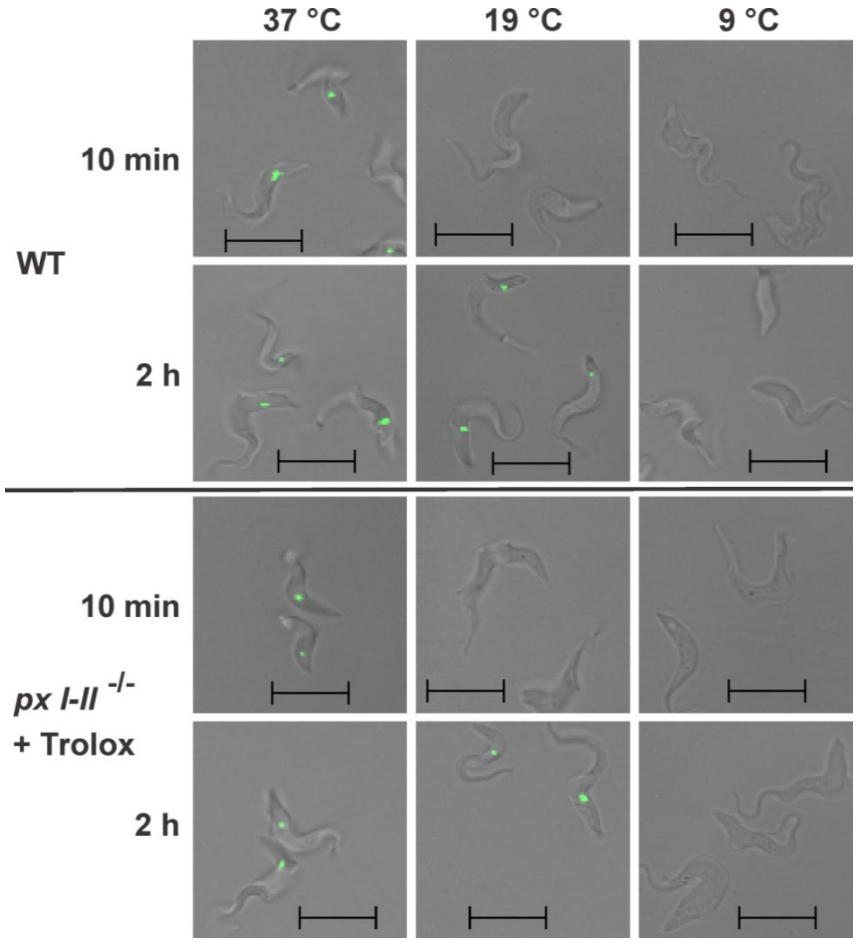

Figure 3.3: Temperature-dependent uptake of fluorescent dextran by WT and *px I-II*$^{-/-}$ BS parasites. Living cells were incubated in standard medium with 2.5 mg/ml Alexa Fluor-488 conjugated dextran at 37 °C, 19 °C, and 9 °C for 10 min and 2 h. In the case of the *px I-II*$^{-/-}$ cells, the medium was supplemented with 100 µM Trolox. The major phenotype of the respective cell populations is displayed. At 37 °C, already after 10 min, the whole cell population displayed lysosomal staining. At 19 °C, after 10 min practically none of the cells showed a fluorescent signal, but after 2 h, the picture was indistinguishable from that at 37 °C. At 9 °C, no significant staining was observed. No difference was noticed between WT and mutant parasites. (Scale bar: 10 µm). The figure and legend were taken from Figure S2 in Hiller *et al.* 2014 doi:10.1371/journal.ppat.1004075.s002

"Endocytosis by BS *T. brucei* is highly sensitive to temperature [Brickman *et al.*, 1995]. To verify that under our conditions, cargo is still delivered to the lysosome, we followed the

uptake of Alexa Fluor 488-conjugated dextran by living WT and *px I-II*$^{-/-}$ cells (the latter ones in the presence of Trolox) at different temperatures. Whereas after 10 min incubation at 37 °C, all parasites displayed a discrete lysosomal staining, practically none of the cells was stained at 19 °C and 9 °C. After 2 h at 19 °C, but not at 9 °C, labeling of the cells was identical to that at 37 °C in accordance with the dextran reaching the lysosomal compartment albeit at a much slower rate compared to 37 °C (Figure 3.3)." [Hiller *et al.*, 2014]

3.1.2 Disruption of the lysosome occurs prior to the lysis of the px I-II$^{-/-}$ *cells*

Michael Diechtierow could show an altered morphology during the lysis of *px I-II*$^{-/-}$ parasites. The cells appeared to be bloated and to lose membrane integrity before they finally lyse [Diechtierow and Krauth-Siegel, 2011]. To reveal the underlying mechanism of the phenotypic changes and to identify the organelles involved in the swelling of the parasites, mutant and WT cells were fed with Alexa Fluor 488-conjugated dextran to inspect the morphology of the lysosome using fluorescence microscopy. "In the mutants kept with Trolox as in WT cells, the fluid-phase marker was discretely located in the post-nuclear region of the parasite consistent with lysosomal delivery (1 in Figure 3.4A). As expected, in the absence of Trolox, the *px I-II*$^{-/-}$ cells progressively lysed. Of the remaining fluorescent parasites, 40 to 60% displayed a signal that was spread over the whole cell body (3 in Figure 3.4A). The enlarged but still confined fluorescence observed in 5 - 10% of the cells (2 in Figure 3.4A) suggests that swelling of the organelle can occur as an intermediate step. This has been observed in parasites that were treated with protease inhibitors or human serum or upon ablation of p67, a lysosomal transmembrane glycoprotein [Peck *et al.*, 2008; Scory *et al.*, 2007; Vanhollebeke *et al.*, 2007]. Trypanolysis caused by apoL-I, crucial component of the trypanolytic factor present in human serum, involves the formation of anion-selective pores in the lysosomal membrane of the parasite, a process which is abolished by addition of 1 mM 4,4-diisothiocyanatostilbene-2,2-disulfonic acid (DIDS) to the culture medium [Pérez-Morga *et al.*, 2005; Vanhollebeke *et al.*, 2007]. In the case of the *px I-II*$^{-/-}$ cells, 0.1 mM or 0.5 mM DIDS had no protective effect and 1 mM DIDS even proved to be lethal for both WT and mutant parasites (Figure 3.5). Thus, the loss of lysosomal integrity in the *px I-II*$^{-/-}$ cells does not appear to involve membrane pore formation." [Hiller *et al.*, 2014]

"To further dissect the role of the lysosome, the *px I-II*$^{-/-}$ cells were treated with LysoTracker, a fluorescent acidotropic reagent that traces acidic organelles in living cells and has previously been used to stain the parasite lysosome [Kieft *et al.*, 2010]. Cells that were kept at

37 °C for up to 30 min without Trolox or for 60 min in the presence of the antioxidant showed a discrete lysosomal staining." [Hiller *et al.*, 2014]

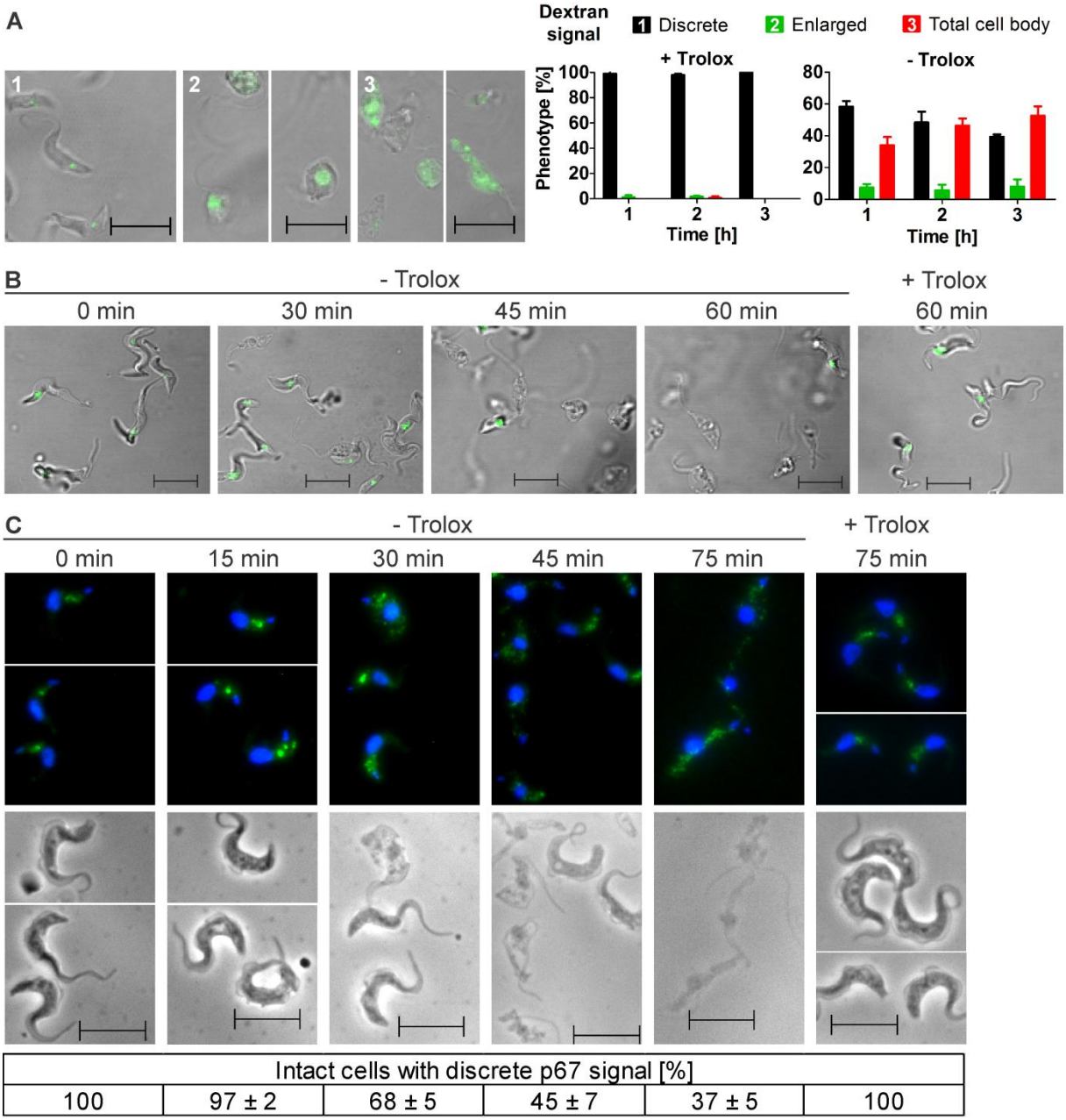

Intact cells with discrete p67 signal [%]					
100	97 ± 2	68 ± 5	45 ± 7	37 ± 5	100

Figure 3.4: Withdrawal of Trolox results in morphological changes of the *px I-II*$^{-/-}$ BS cells. A. Living parasites were fed at 37 °C with Alexa Fluor-488 conjugated dextran and then kept at RT in medium with (+) or without (-) 100 µM Trolox as outlined under Materials and Methods. On the left site, representative cells for the three different phenotypes observed in the remaining intact and fluorescent parasites are shown. The pictures were taken from cells incubated (1) 1 h, + Trolox, (2) 1 and 2 h, - Trolox, and (3) 2 h, - Trolox. On the right site, the quantitative analysis is provided. At each time point, ≥60 parasites were analyzed in three independent experiments and the mean ± SD was calculated. **B.** LysoTracker Green staining of living parasites incubated for the indicated times at 37 °C in the presence or absence of Trolox. **C.** Immunofluorescence analysis of cells stained with antibodies against p67 (green) and DAPI (blue) to visualize nuclear (large dot) and kinetoplast (small dot) DNA (upper panel) and the corresponding phase contrast pictures (lower panel). At each time point, the p67 signal of at least 130 parasites was analyzed in each of three independent experiments and the mean ± SD was calculated (below). (Scale bar: 10 µm). The figure and legend were taken from Figure 2 in Hiller *et al.* 2014 doi:10.1371/journal.ppat.1004075.g002

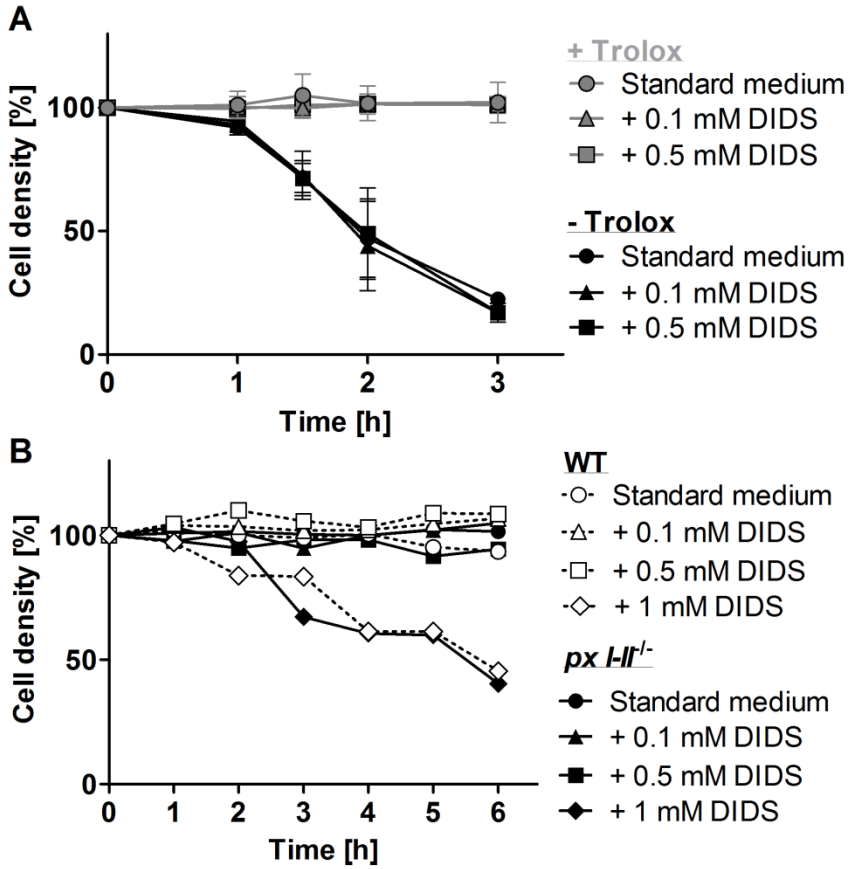

Figure 3.5: DIDS does not protect the *px I-II*$^{-/-}$ BS cells from lysis. A. The mutant cells were incubated in standard medium ± 100 µM Trolox containing none, 0.1, and 0.5 mM DIDS. The data represent the mean ± SD of three independent experiments. The figure and legend were taken from Figure S3 in Hiller *et al.* 2014. doi:10.1371/journal.ppat.1004075.s003 **B.** Different concentrations of DIDS (kill curve) were tested on *px I-II*$^{-/-}$ in the presence of Trolox and WT 449 BS cells.

"In contrast, after 45 and 60 min in Trolox-free medium, many and virtually all, respectively, parasites had lost the fluorescent signal (Figure 3.4B). This finding confirmed that disintegration of the lysosomal compartment preceded cell lysis. Antibodies against p67 typically stain a prominent vesicular compartment between the nuclear and mitochondrial (kinetoplast) DNA, although sometimes also multiple discrete vesicles in the same region are visualized [Alexander *et al.*, 2002; Peck *et al.*, 2008]. *Px I-II*$^{-/-}$ cells that were harvested up to 15 min after transfer into Trolox-free medium or kept in the presence of the antioxidant displayed a lysosomal p67 staining (Figure 3.4C). In contrast, when kept in Trolox-free medium, an increasing percentage of parasites lacked an intense and well defined signal. Many cells showed a dispersed staining which was reminiscent of parasites depleted of the Rab4 protein, a regulator of lysosomal trafficking [Hall *et al.*, 2004]. These signals however were hardly to distinguish from the background fluorescence of cells treated only with the

secondary antibody. Therefore, the quantitative analysis was based on cells with a vesicular p67 staining between the two DAPI signals. Taken together, the three different approaches strongly suggested that damage of the lysosomal membrane is a primary event caused by the absence of the cytosolic peroxidases." [Hiller *et al.*, 2014]

The alteration in lysosomal morphology was also analyzed by flow cytometry to quantify the phenotype presenting the enlarged lysosomal signal (2 in Figure 3.4A). *Px I-II*$^{-/-}$ cells were treated with Alexa Fluor 488-conjugated dextran and DAPI and kept at RT in the presence and absence of Trolox in PBS ± FCS for different times (30, 50, 70, and 90 min). The parasites with enlarged lysosome should be DAPI negative as they are still intact and Alexa Fluor 488 positive, but show altered cell morphology. However, a prominent third population representing an altered cell morphology was not observed in the density plot using forward and side scatter (data not shown). As expected with prolonged incubation time, the number of dead cells increased only in the Trolox-free PBS + FCS condition. The dead cells displayed after 90 min a 55% decrease of the Alexa Fluor 488 signal intensity which probably reflects the complete lysis of these parasites. As shown in Figure 3.4A parasites presenting the enlarged lysosome were however a minor and not enriched population. Due to their already partially damaged membranes, they were expected to be susceptible to rupture and hardly to detect.

3.1.3 Cell lysis is accelerated by exogenous iron

The previous experiments indicated that the cell damage is related to the lysosome and probably to endocytosis. Iron can lead to the production of free radicals involved in membrane damage and is taken up via endocytosis of transferrin in BS *T. brucei* [Steverding, 1998; Widener *et al.*, 2007]. Thus, the effect of iron on the lysis of the *px I-II*$^{-/-}$ parasites was studied. "Supplementation of the medium with 100 μM iron chloride had no effect on the viability of the *px I-II*$^{-/-}$ cells provided the presence of Trolox. In the absence of the antioxidant, iron strongly accelerated cell lysis (Figure 3.6A). To further evaluate the role of iron, the parasites were treated with deferoxamine, a potent iron chelator that in mammalian cells is preferentially taken up by fluid-phase endocytosis [Doulias *et al.*, 2003]. Deferoxamine primarily prevents iron incorporation into newly synthesized proteins. In Trolox-free medium, indeed the chelator slowed down cell lysis and thus protected the *px I-II*$^{-/-}$ cells (Figure 3.6B). In the presence of Trolox, deferoxamine had no effect on the short-term viability of the mutant cells but inhibited the long-term cell proliferation, as it has

previously been shown for WT parasites [Breidbach *et al.*, 2002; Comini *et al.*, 2008]. Neither iron nor deferoxamine affected the short-term viability of WT cells independent of the presence or absence of Trolox" [Hiller *et al.*, 2014] (Figure 3.7).

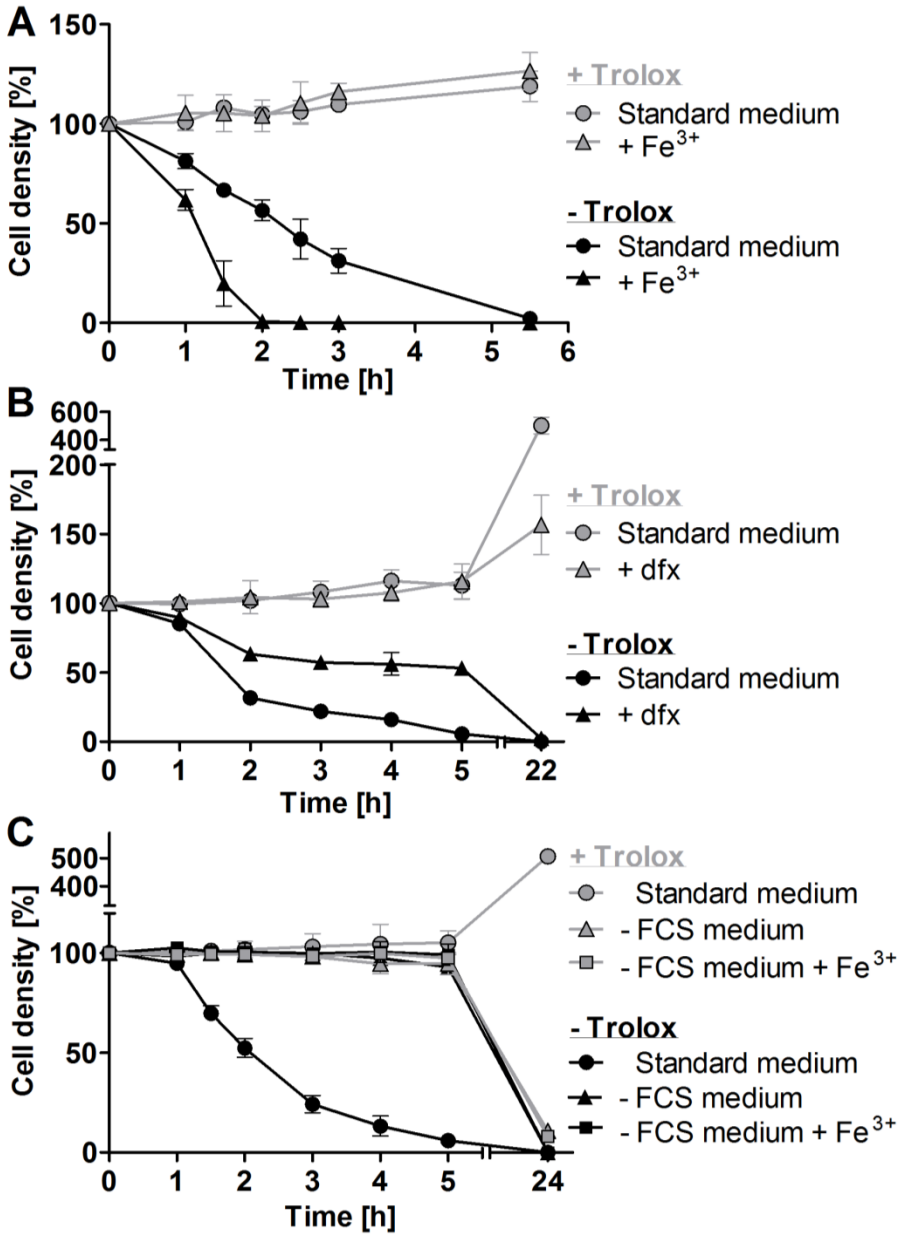

Figure 3.6: Exogenous iron promotes lysis of the *px I-II*$^{-/-}$ BS cells. A. The mutant parasites were incubated for up to 5.5 h at 19 °C in standard medium ± 100 µM Trolox in the presence and absence of 100 µM Fe^{3+}. WT cells behaved like the mutant cells in the presence of Trolox. **B.** The *px I-II*$^{-/-}$ cells were incubated for 5 h at 22 °C and then cultured overnight at 37 °C in medium ± 100 µM Trolox in the presence and absence of 100 µM deferoxamine (dfx). WT behaved like the mutant cells in the presence of Trolox. **C.** The *px I-II*$^{-/-}$ cells were incubated for 5 h at 19 °C and then cultured overnight at 37 °C in medium ± 10% FCS and/or 100 µM Trolox in the presence and absence of 100 µM Fe^{3+}. The behavior of WT cells in the absence of FCS was identical to that of the mutant cells. At the different time points, living cells were counted. The values represent the mean ± SD of three independent experiments. The figure and legend were taken from Figure 3 in Hiller *et al.* 2014 doi:10.1371/journal.ppat.1004075.g003

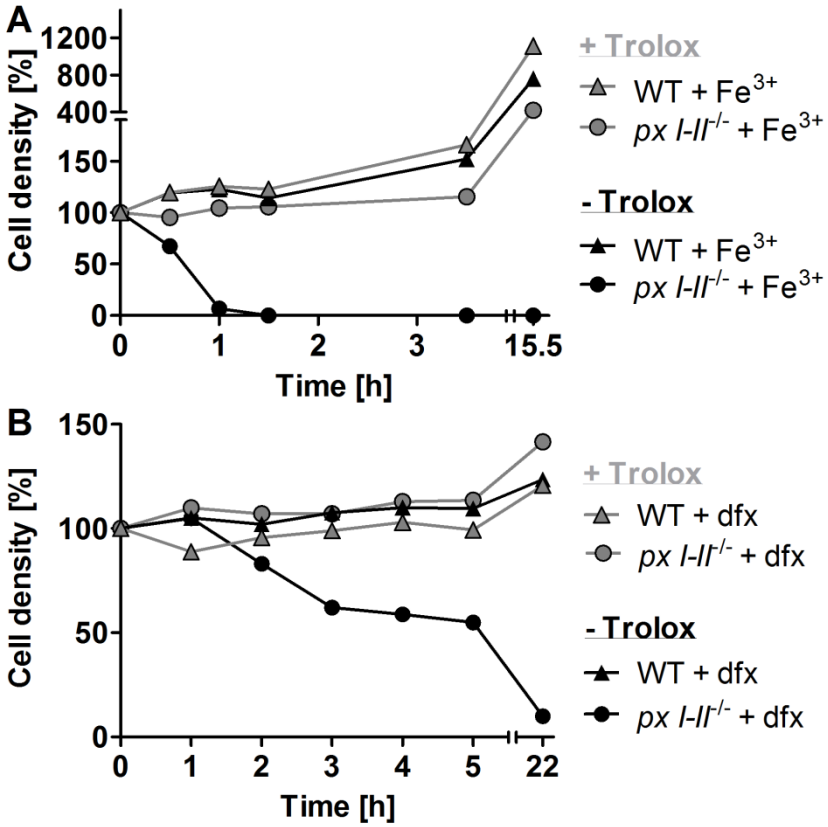

Figure 3.7: BS WT cells were unaffected by exogenous iron and deferoxamine treatment in the short-term. BS WT 449 and *px I-II*$^{-/-}$ parasites were kept in medium ± Trolox and **A. ±** 100 µM Fe^{3+} at 37 °C and **B.** ± 100 µM deferoxamine (dfx) at 22 °C.

To assess if the peroxidases would be even up-regulated under iron-induced stress, BS WT cells were treated each with 100 µM of either $FeCl_3$ or ammonium iron citrate, for 24 and 48 h. Parasites were harvested and 5 x 10^6 cells were loaded on a SDS gel and subjected to Western blot analysis (Figure 3.8). The level of expressed peroxidases did not change upon iron treatment independent of the duration or iron source. Post-transcriptional gene expression control of the Px-type enzymes does not seem to occur in iron-stressed trypanosomes.

3.1.4 The lethal phenotype requires a serum component

"BS *T. brucei* are cultured in HMI-9 medium which contains 10% of FCS. In accordance with our previous observations, *px I-II*$^{-/-}$ cells kept in this standard medium rapidly died, and after 2 h, the culture displayed only 50% of the starting cell density (Figure 3.6C). In medium lacking FCS, however, the mutant parasites remained viable and, remarkably, were insensitive towards exogenous iron, even in Trolox-free medium. Overnight cultivation in medium without FCS resulted in complete cell death due to the lack of essential nutrients and growth factors." [Hiller *et al.*, 2014]

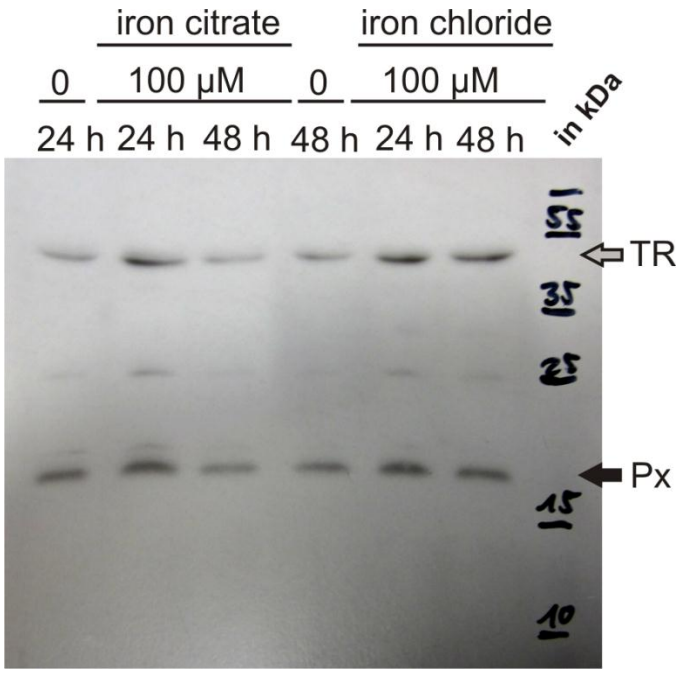

Figure 3.8: Protein expression of Px I-III is not up-regulated by exogenous iron in WT cells. BS WT 449 parasites were treated with and without 100 µM $FeCl_3$ (iron chloride) and ammonium iron citrate (iron citrate) for 24 and 48 h. After harvesting, 5 x 10^6 cells were subjected to Western blot analysis using antisera against Px as well as TR as loading control. The Px proteins run at ~19 kDa (black arrow) and TR at ~53 kDa (grey arrow).

"In conclusion, the iron-induced cell lysis clearly required the presence of (a component of) FCS. BS *T. brucei* acquire heme by receptor mediated endocytosis of the haptoglobin-hemoglobin complex [Vanhollebeke *et al.*, 2008]. In the absence of Trolox, supplementing the medium with 1 mg/ml of hemoglobin resulted in a minor, but detectable, acceleration of cell lysis (Figure 3.9). This only moderate effect may at least partially be due to the fact that in the serum, haptoglobin is already essentially saturated with hemoglobin." [Hiller *et al.*, 2014]

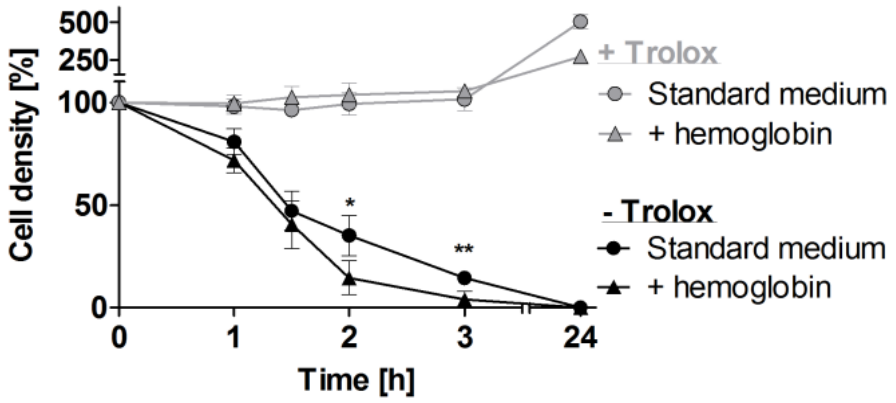

Figure 3.9: Supplementing the medium with hemoglobin slightly induces lysis of the *px I-II*$^{-/-}$ BS parasites. Cells were cultured in standard medium in the presence and absence of 100 µM Trolox and 16 µM hemoglobin at 21 °C and subsequently incubated overnight at 37 °C. WT cells behaved like the mutant parasites with Trolox (not shown). The values represent the mean ± SD of three independent experiments. For the -Trolox data sets, the p-values were calculated by paired two-tailed student's test. Statistically significant differences are marked (* $p \leq 0.1$; ** $p \leq 0.05$). The figure and legend were taken from Figure S4 in Hiller *et al.* 2014 doi:10.1371/journal.ppat.1004075.s004

3.1.5 Transferrin is involved in the lysis of px I-II$^{-/-}$ cells

Transferrin is another iron-containing serum component and taken up by the parasites via the heterodimeric transferrin receptor to fulfill their iron needs [Chaudhri *et al.*, 1994; Ligtenberg *et al.*, 1994; Steverding *et al.*, 1994; Steverding *et al.*, 1995]. "FCS contains about 25 μM transferrin and the iron saturation of transferrin ranges from 55 to 92% [Kakuta *et al.*, 1997]. To mimic these conditions, the medium was supplemented with 25 μM holo-transferrin. In the absence of Trolox, this treatment stimulated lysis of the *px I-II*$^{-/-}$ cells (Figure 3.10A). In contrast, apo-transferrin slowed down cell lysis in the absence of Trolox (Figure 3.10B). Parasites incubated overnight with apo-transferrin in medium containing Trolox remained viable but did not proliferate. Competition between holo- and apo-transferrin for the parasite transferrin receptor results in reduced iron uptake [Steverding, 1998]. This should directly affect the synthesis of DNA precursors by the iron-dependent ribonucleotide reductase. Incubation of the mutant parasites with holo-transferrin in medium lacking both FCS and Trolox induced the cell lysis (Figure 3.10C). However, a 10-fold higher concentration of holo-transferrin (25 μM) was required for an effect comparable to that observed in the presence of 10% FCS. This suggests that in the absence of FCS, the overall metabolism of the parasite is affected and/or another serum component contributes to the lethal phenotype. To get a deeper insight in the mechanism, we prepared transferrin-depleted medium. Purified antibodies against bovine transferrin were covalently linked to sepharose and HMI-9 medium was chromatographed on this matrix. Western blot analysis confirmed the successful removal of transferrin from the medium (Figure 3.11A). As expected, in the presence of Trolox, the *px I-II*$^{-/-}$ cells did not show any lysis in the transferrin-depleted medium with or without supplementation by 25 μM transferrin (Figure 3.10D). However, in the absence of Trolox, the *px I-II*$^{-/-}$ cells displayed lysis. This may be due to the uptake of hemoglobin, which occurs via endocytosis of the hemoglobin/haptoglobin complex, again resulting in lysosomal iron [Vanhollebeke *et al.*, 2007]. In addition, we cannot rule out that the medium still contained residual transferrin that was not detected in the Western blot. Even when assuming 99% depletion, the remaining transferrin may still be efficiently internalized due to the high affinity of the parasite transferrin receptor [Steverding, 1998]." [Hiller *et al.*, 2014]

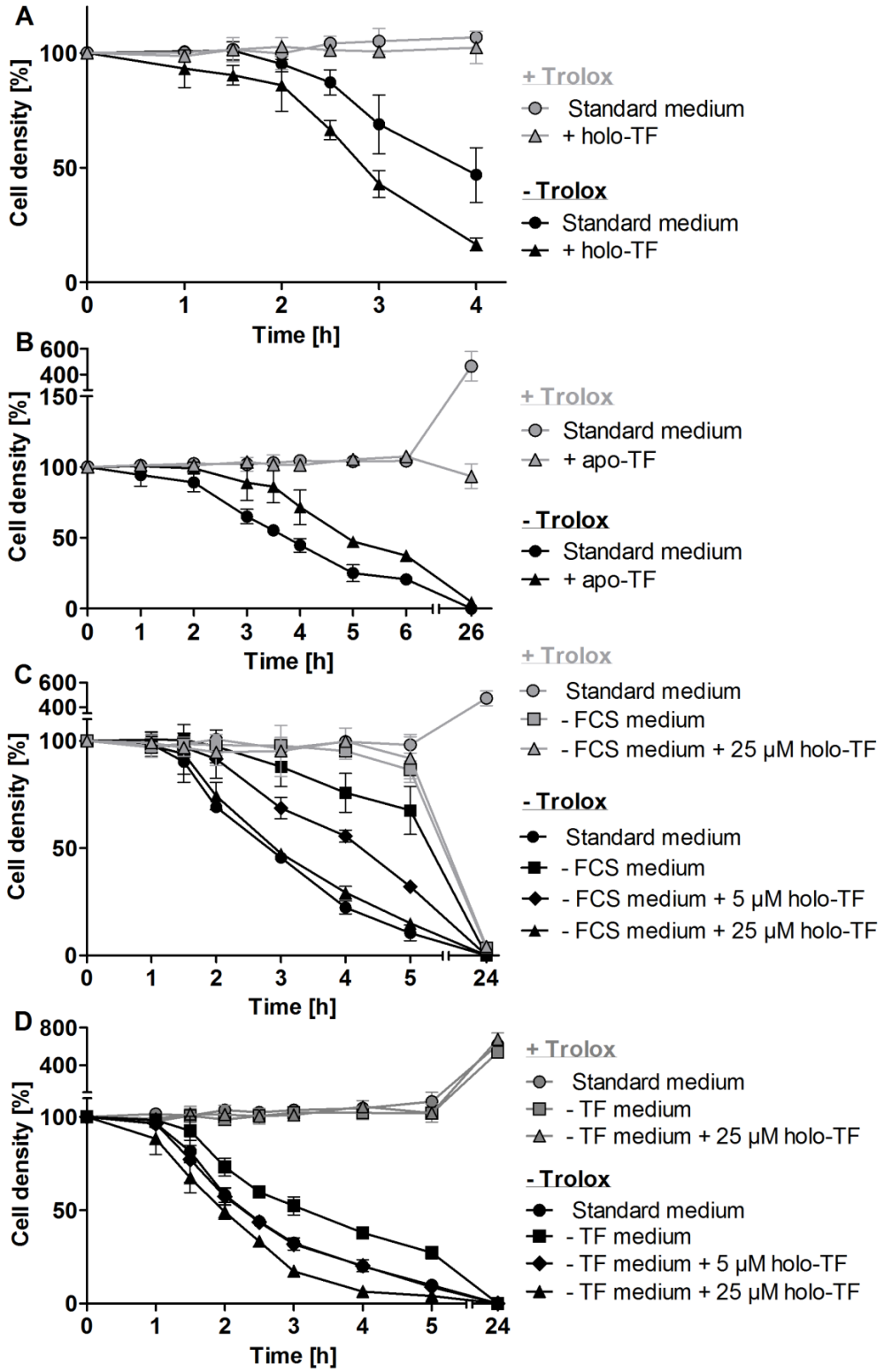

Figure 3.10: Holo-transferrin induces, whereas apo-transferrin slows down lysis of the *px I-II*$^{-/-}$ BS parasites. The mutant cells were incubated **A.** for 4 h at RT in standard medium ± 100 µM Trolox in the presence and absence of 25 µM holo-transferrin (holo-TF), **B.** for 6 h at RT and then cultured overnight at 37 °C in medium ± 100 µM Trolox in the presence and absence of 320 µM apo-transferrin (apo-TF), **C.** for 5 h at RT followed by overnight cultivation at 37 °C in standard medium as well as in FCS-free medium ± 100 µM Trolox in the presence and absence of 5 µM and 25 µM holo-TF, and **D.** for 5 h at 20 °C in standard medium as well as in transferrin-depleted medium (-TF medium) ± 100 µM Trolox in the presence and absence of 5 µM and 25 µM holo-TF. The values represent the mean ± SD of three independent experiments. The figure and legend were taken from Figure 4 in Hiller *et al.* 2014 doi:10.1371/journal.ppat.1004075.g004

To verify the incomplete depletion of transferrin, the 1x transferrin-depleted medium was subjected again to the immune column to generate 2x transferrin-depleted medium (Figure 3.11B). In 0.5 µl of the 1:10 diluted samples of the depleted media, transferrin was not observed. However, upon loading of a 600-fold amount (30 µl of undiluted medium) the protein was detectable in the 1x transferrin-depleted medium. This protein amount could still provide enough transferrin for sufficient binding to the receptor with a K_D of 131 nM for ES1.3A of the EATRO 1125 stock and 3.6 nM for the clone MITat 1.4 from Lister strain 427 [Steverding *et al.*, 1995]. For further generation of depleted media, two consecutive immune columns are recommended to completely remove the remaining protein.

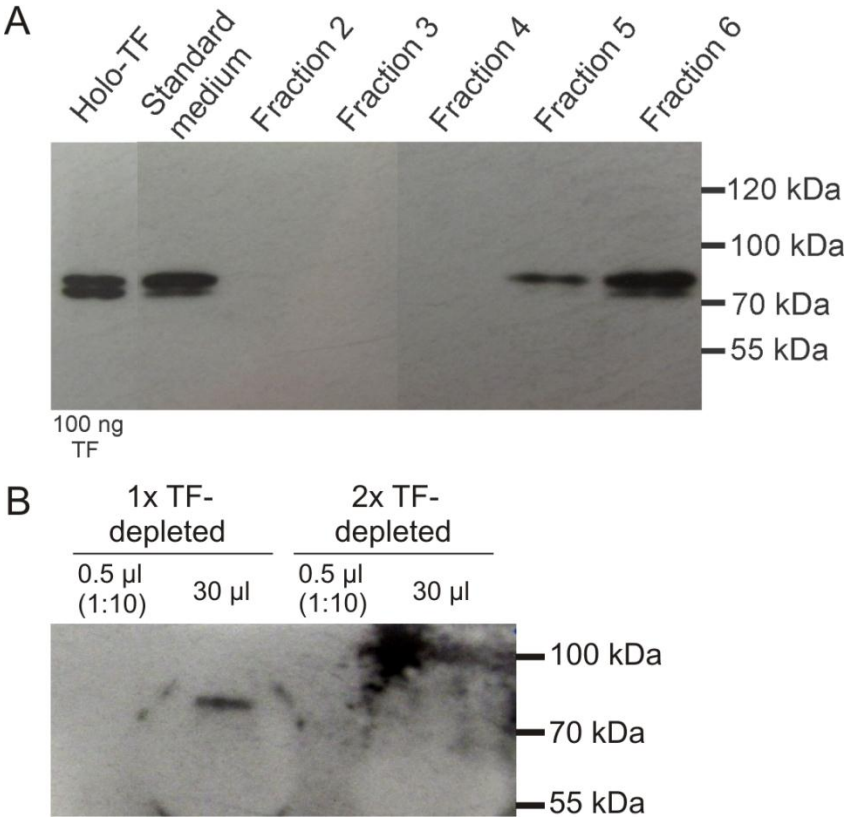

Figure 3.11: Western blot analysis of transferrin-depleted medium. A. Commercial holo-TF (100 ng) and 0.5 µl of the standard medium (corresponding to 100 ng TF) as well as of the fractions collected from the anti-TF column were subjected to Western blot analysis using the polyclonal antibodies against bovine TF. Fraction 1 was the FCS-free medium used for equilibration (not shown), fractions 2 to 4 represented TF-free medium whereas in fractions 5 and 6, TF was again detectable. The figure and legend were taken from Figure S5 in Hiller *et al.* 2014 doi:10.1371/journal.ppat.1004075.s005 **B.** Western blot analysis of the 1x and 2x TF-depleted medium. 1x TF-depleted, pooled TF-free medium fractions from the first column; 2x TF-depleted, 1x depleted medium was subjected again on the immune column and one "2x TF-free" fraction was used. Either 0.5 µl of a 1:10 diluted medium sample was applied onto the 10% gel or 30 µl of an undiluted sample. Remaining TF was still detectable in in the undiluted sample of the 1x TF-depleted medium.

"The contribution of transferrin to cell lysis could be clearly demonstrated: Supplementing the transferrin-depleted medium with transferrin accelerated cell lysis. Upon overnight cultivation in Trolox-supplemented transferrin-depleted medium, the mutant parasites proliferated, again indicating that the medium contained an iron source. This is in accordance with previous work showing that WT *T. brucei* can grow in TF-depleted medium [Salmon *et al.*, 2005]. Taken together, the data suggest that transferrin as well as hemoglobin contribute to the lethal phenotype of the *px I-II*$^{-/-}$ cells in the absence of the exogenous antioxidant, both resulting in the generation of free lysosomal iron." [Hiller *et al.*, 2014]

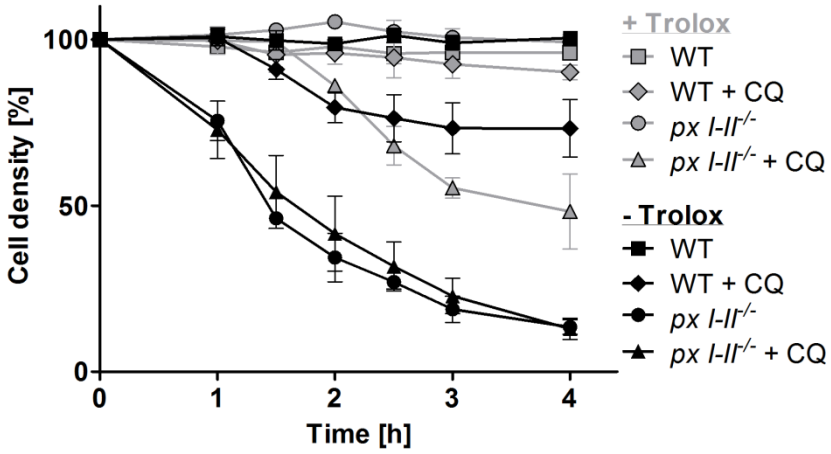

Figure 3.12: Lysis of the *px I-II*$^{-/-}$ cells is not slowed down by supplementing the medium with of chloroquine. BS WT and *px I-II*$^{-/-}$ cells were pre-incubated with 50 µM chloroquine (CQ) at 37 °C for 30 min. Then transferred into standard medium ± 100 µM Trolox and 50 µM CQ and incubated at 20 °C. After different times, viable cells were counted. The values represent the mean ± SD of three individual experiments.

Ferric iron bound to transferrin is released within the lysosome which is facilitated at this low pH [Aisen and Listowsky, 1980]. Proteolytic digest of transferrin by lysosomal proteases like the cathepsin B-like enzyme should be decreased at higher pH [Steverding *et al.*, 2012; Yoshinari and Taurog, 1985]. Thus, the neutralization of the lysosomal pH by lysomotropic agents should slow down trypanolysis as shown for the TLF studies on trypanosomes [Brickman *et al.*, 1995; Hager *et al.*, 1994]. Chloroquine (50 µM) was added to standard medium ± Trolox (Figure 3.12). Within the 4 h observation time at 20 °C, chloroquine induced lysis of about 50% of the mutant cells in the presence of Trolox as well as of about 25% of WT cells in the normal medium. In contrast, towards the *px I-II*$^{-/-}$ parasites in Trolox-free medium, it displayed a minor, but not significant, protective effect. Yet, if exerting an exclusively toxic effect, one would have expected that chloroquine induced lysis of the *px I-II*$^{-/-}$ cells also in the Trolox-free medium. Clearly, this is not the case. Most probably, the toxic

effect is partially compensated by a protective one, namely the pH rise in the endosomal/lysosomal compartment. Addition of 5 mM ammonium chloride or 10 µM chloroquine showed a similar effect (see appendix). Chloroquine was not suitable for the phenotypical analysis of this mechanism. This rather complex result is probably due to the fact that upon extended incubation with chloroquine, BS *T. brucei* lose their normal morphology and motility; and lysosomal swelling is induced leading most likely to a faster rupture of the damaged membrane [Brickman *et al.*, 1995; Peck *et al.*, 2008]. In addition, in mammalian cells, chloroquine has been reported to destabilize the lysosomal membrane [Zhao *et al.*, 2005].

3.1.6 Disintegration of the lysosome precedes other cellular membrane damage

To analyze cellular damages preceding cell lysis in more detail, the mitochondrion was visualized using the MitoTracker Red staining. As a result of lipid peroxidation and membrane disintegration, the membrane potential should collapse resulting in a loss of the MitoTracker signal. "The *px I-II*$^{-/-}$ cells were transferred from Trolox-supplemented into medium and after different time points subjected to immunofluorescence microscopy with MitoTracker, p67 antibodies, and DAPI (Figure 3.13A). The parasites were subdivided into four groups that displayed a) both MitoTracker and discrete p67 staining; b) MitoTracker staining, but no discrete p67 signal; c) no MitoTracker staining, but discrete p67 signal; and d) neither MitoTracker nor p67 staining (Figure 3.13B). *Px I-II*$^{-/-}$ cells kept for up to 15 min in Trolox-free medium and those in the presence of the antioxidant displayed perfect mitochondrial and lysosomal signals. In contrast, incubation of the *px I-II*$^{-/-}$ parasites in Trolox-free medium for >15 min resulted in the progressive formation of cells that lacked both signals. About 12% of the cells showed MitoTracker staining but no discrete p67 signal. The reverse phenotype, namely parasites that lacked the MitoTracker staining but had a discrete p67 signal, was practically not observed. Thus, lysosomal disintegration precedes the damage of the mitochondrion." [Hiller *et al.*, 2014]

A

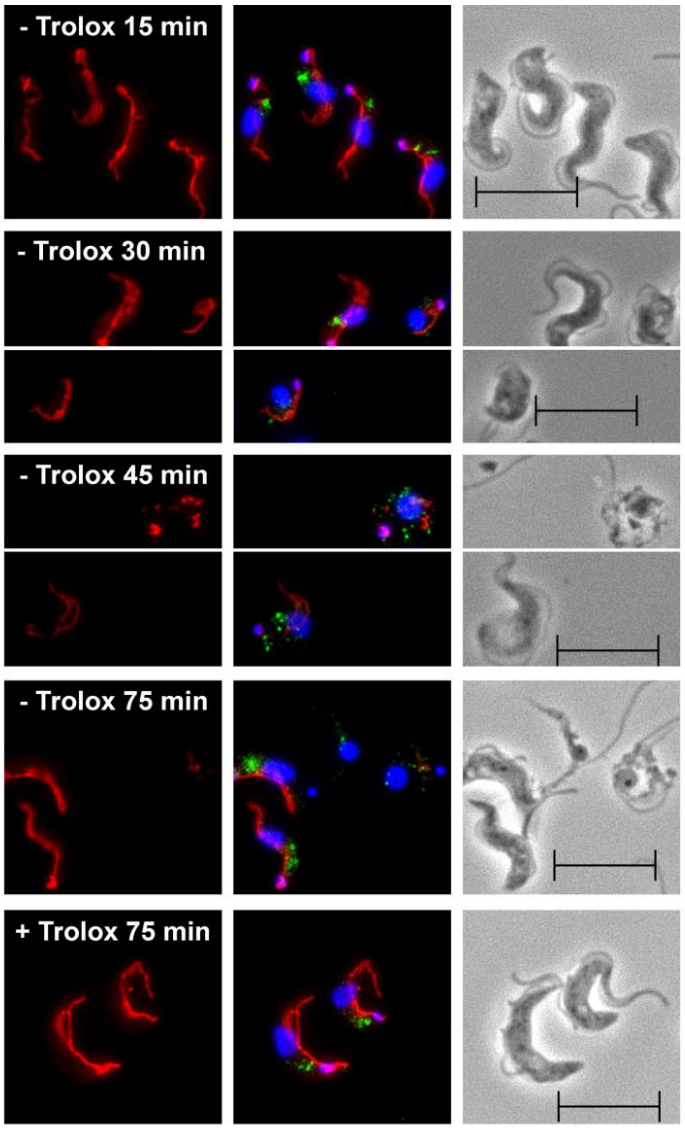

B

I	- Trolox [%]					+ Trolox [%]
Phenotype	0 min	15 min	30 min	45 min	75 min	75 min
Mito+ Lyso+	100	**95**	**77**	70	**53**	**99**
Mito+ Lyso-	0	5	**12**	**12**	14	<1
Mito- Lyso+	0	0	0	<1	<1	0
Mito- Lyso-	0	0	11	18	**33**	<1

II	- Trolox [%]					+ Trolox [%]
Phenotype	0 min	15 min	30 min	45 min	75 min	75 min
Mito+ Lyso+	99	96	75	75	56	99
Mito+ Lyso-	0	3	12	12	13	0
Mito- Lyso+	<1	0	<1	<1	<1	<1
Mito- Lyso-	0	1	13	13	31	<1

Figure 3.13: Lysosomal disintegration precedes damage of the mitochondrion. The *px I-II*$^{-/-}$ BS cells were kept for the indicated times at 37 °C in medium ± Trolox and then subjected to immunofluorescence analysis. **A.** MitoTracker staining (left), overlay of the signals for MitoTracker (red), p67 (green), and DAPI (blue) (middle), and phase contrast images (right). **B.** Quantitative analysis of the staining pattern of the cells (for details see text). The phenotypes visible in the respective pictures in (**A**) are highlighted by bold numbers. For each time point, at least 194 cells were inspected. Two independent sets of experiments are presented (I and II). (Scale bar: 10 mm). The figure and legend were taken from Figure 5 in Hiller *et al.* 2014 and modified. doi:10.1371/journal.ppat.1004075.g005

3.2 The functional role of Px I-III in PC parasites

The text, figures, and figure legends of the following chapter 3.2 are part of the unpublished manuscript of Schaffroth *et.al.* 2015.

3.2.1 The insect stage of T. brucei is fully viable in the absence of the cytosolic form of the Tpx peroxidase

Recently Amrei Nißen showed that – in contrast to the mammalian BS form of the parasite – PC *T. brucei* that specifically lack the cytosolic peroxidases are fully viable and proliferate like WT cells independent of the presence or absence of Trolox [Hiller *et al.*, 2014]. To get a deeper insight in the putative physiological role of the cytosolic enzymes in the insect stage of the parasite, the *px I-II*$^{-/-}$ cells were treated with exogenous Fe^{2+} and Fe^{3+}. No significant effect on the proliferation of the mutants could be observed (Figure 3.14). This contrasts significantly with the situation in the BS form of the parasite. Treating BS *px I-II*$^{-/-}$ cells with exogenous Fe^{3+} accelerates lysis of the parasites in Trolox-free medium (Figure 3.6A).

To further stress the PC *px I-II*$^{-/-}$ parasites, a huge excess of 500 µM ferric iron was supplemented to the MEM-Pros medium in the presence and absence of Trolox (Figure 3.14C). In the short-term (inset), the mutant cells kept in Trolox-free medium with iron displayed a greater proliferation defect compared to the cells in medium + Trolox and iron. WT cells behaved like the mutant cells in the presence of Trolox. After overnight incubation, the proliferation defect was even more severe whereas after 48 h, the parasites grew normally again. This excess of exogenous iron may likely lead to an unspecific damage of the plasma membrane which is mainly prominent in the stressed mutant cells without the membrane-protective antioxidant.

3.2.2 Deletion of the complete px locus is lethal for PC T. brucei in the absence of Trolox

Previous RNAi experiments, which targeted the whole locus, showed a severe proliferation defect in the insect form of the parasite [Schlecker *et al.*, 2005]. To prove if the insect form of *T. brucei* requires these peroxidases at all, we decided to delete the complete *px* locus.

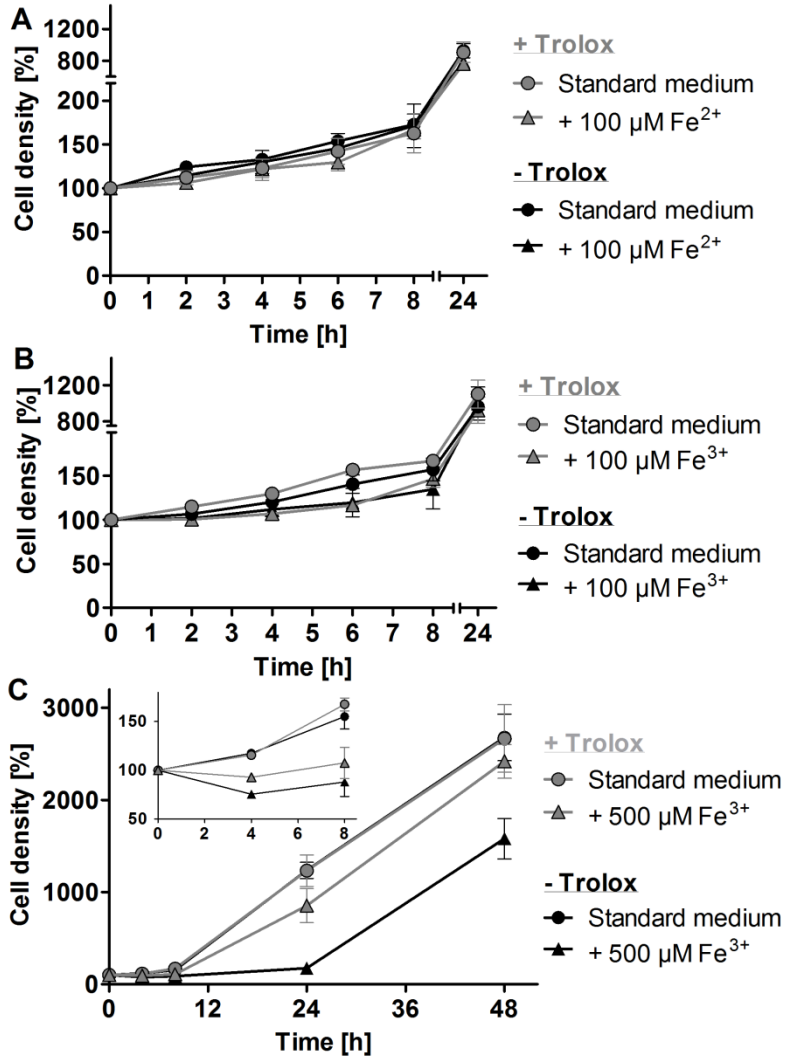

Figure 3.14: PC *px I-II*$^{-/-}$ cells are insensitive towards exogenous iron but show unspecific damage at high iron concentrations. The *px I-II*$^{-/-}$ parasites were cultivated at 27 °C in MEM-Pros medium ± Trolox supplemented with **A.** 100 µM Fe^{2+}, **B.** 100 µM Fe^{3+}, and **C.** 500 µM of Fe^{3+}. After different times, living cells were counted. The data represent the mean ± SD of three independent experiments.

To delete the whole *px I-III* locus in the insect stage of *T. brucei*, a 520 bp stretch of the 3'UTR of *px III* was amplified from pHD1747_KO*pxIII* using the primer pair KO_Px I-III_3'_F and KO_Px I-III_3'_R. The PCR product as well as the pHD1747_KO*pxI(I-II)* and pHD1748_KO*pxI(I-II)* vectors (to remove the 3'UTR of *px II*) were digested with *Pst*I and *Not*I, purified, and ligated. The plasmids obtained encoded the 5'UTR of *px I*, followed by the resistance gene and the 3'UTR of *px III* and were named pHD1747_KO*pxI-III* and pHD1748_KO*pxI-III*. PC *T. brucei* 449 cells were transfected with the *Xho*I/*Not*I-digested constructs and selected for blasticidin and/or puromycin resistance in Trolox-containing medium as outlined in Materials and Methods. Clones, in which one allele of the *px I-III* locus was replaced by the resistance gene, were obtained by serial dilution.

These single KO cells were subsequently transfected with the respective other construct, cloned again, yielding double-resistant cell lines.

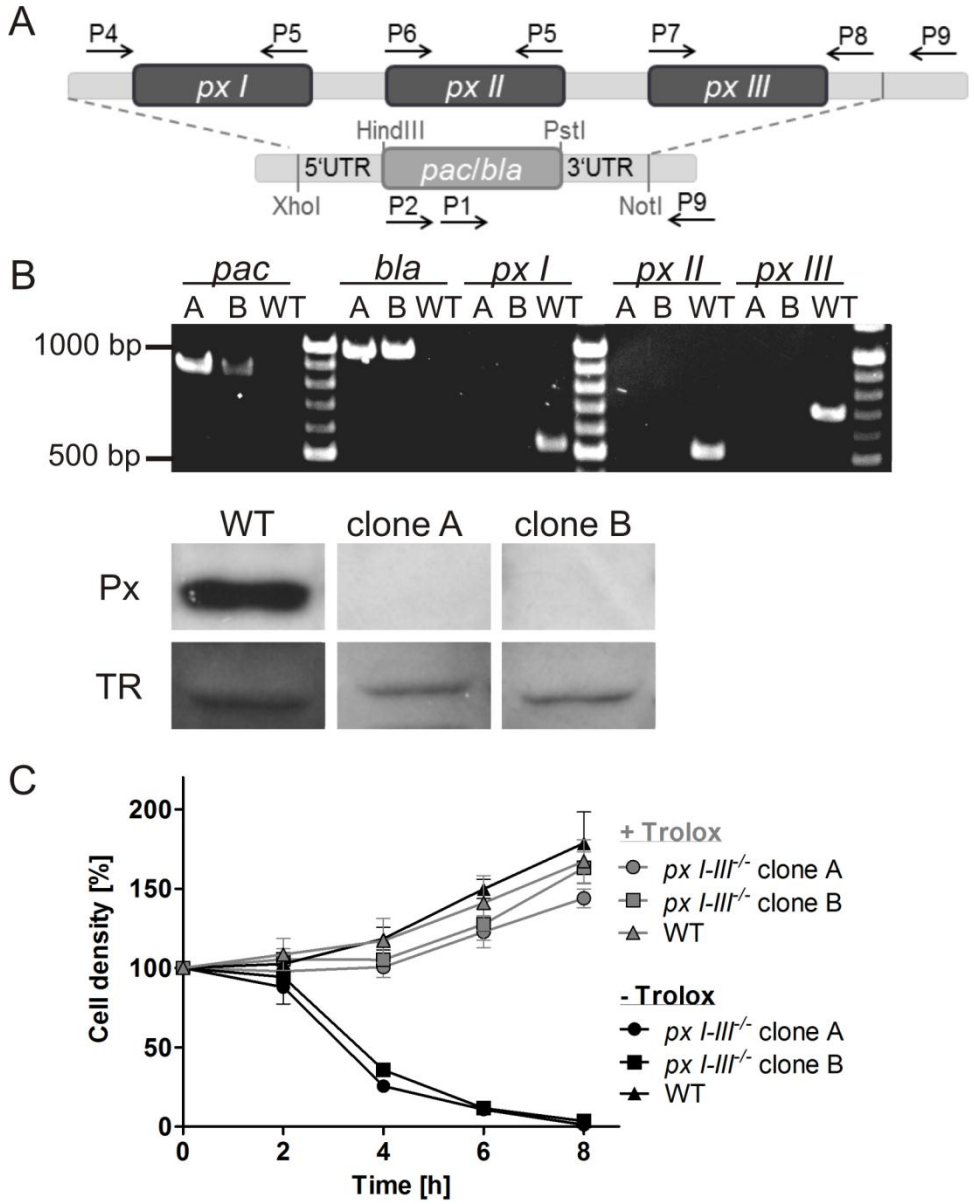

Figure 3.15: Generation and analysis of PC *px I-III*$^{-/-}$ cells. A. Scheme for the replacement of the whole genomic *px* locus by blasticidin (*bla*) and puromycin (*pac*) resistance genes. For details see Materials and Methods. The primers described here are the following: P1 = PuroF_CH2, P2 = Bla-F_MD, P4 = P7_MD, P5 = P18_MD, P6 = P26_MD, P7 = P22_MD, P8 = P31_MD, and P9 = 3UTR_PxIII_R1. **B.** Upper part. PCR analysis of genomic DNA isolated from two *px I-III*$^{-/-}$ cell lines (A: clone 2D4 and B: clone 1C5) and WT *T. brucei* with different primer pairs (*pac*: P1 and P9, expected amplicon 858 bp; *bla*: P2 and P9, 979 bp; *px I*: P4 and P5, 525 bp; *px II*: P6 and P5, 510 bp; *px III*: P7 and P8, 697 bp). The elongation time was adjusted to the expected PCR product size. Lower part. Western blot analysis of the *px I-III*$^{-/-}$ clones grown in the presence of 100 µM Trolox as well as of WT cells (4 x 10^6cells per lane) using antisera against Px as well as TR as loading control. **C.** Incubation of the *px I-III*$^{-/-}$ and WT *T. brucei* in MEM-Pros medium ± 100 µM Trolox at 27 °C. After different times, living cells were counted. The data represent the mean value ± SD of three independent experiments.

The successful replacement of the *px* genes was verified by different PCR analyses of genomic DNA from WT and KO clones; the absence of the protein was confirmed by Western blot analysis (Figure 3.15B). In the presence of Trolox, the *px I-III*$^{-/-}$ cells displayed a proliferation rate similar to that of WT cells (Figure 3.15C). However, the mutant parasites died within a few hours after withdrawal of the antioxidant from the medium. Thus, the removal of the complete *px* locus in the insect stage of the parasite is lethal.

3.2.3 In the PC px I-III$^{-/-}$ *parasites, loss of the mitochondrial membrane potential precedes damage of other organelles and cell lysis*

To identify the cellular compartment that is primarily affected in cells lacking all three peroxidases, the *px I-III*$^{-/-}$ parasites were transferred into Trolox-free medium and after different times subjected to immunofluorescence microscopy. The mitochondrial membrane potential-sensitive MitoTracker Red was used as marker for an intact mitochondrion, antibodies against the lysosomal membrane protein p67 as lysosomal marker, and DAPI for staining the nuclear and mitochondrial (kinetoplast) DNA (Figure 3.16). The cells were grouped according to four different phenotypes observed. They displayed signals for i) MitoTracker and p67; ii) only p67; iii) only MitoTracker; iv) neither p67 nor MitoTracker. More than 90% of the mutant parasites when kept in the presence of the antioxidant or for only 1 h in medium lacking Trolox showed both, lysosomal and mitochondrial staining. Prolonged incubation in Trolox-free medium resulted in an increasing number of cells without MitoTracker signal as well as cells devoid of both signals. Remarkably, cells lacking the lysosomal signal but keeping the mitochondrial one were virtually not observed (≤ 1%). In contrast, after 4 h in Trolox-free medium, nearly 40% of the cells lacked a mitochondrial signal, but still displayed a discrete p67 staining. Parasites that had lost only the MitoTracker signal displayed either the normal elongated shape or a more roundish morphology (compare the phase contrast pictures of -Trolox 1 h and 2 h, respectively, in Figure 3.16). Upon longer incubation in Trolox-free medium, the latter type of cells became more prominent while cells with normal morphology were less abundant. Taken together, the immunofluorescence data showed that PC parasites which lack the complete *px* locus lose their mitochondrial membrane potential. This process preceded damage of the lysosome.

A

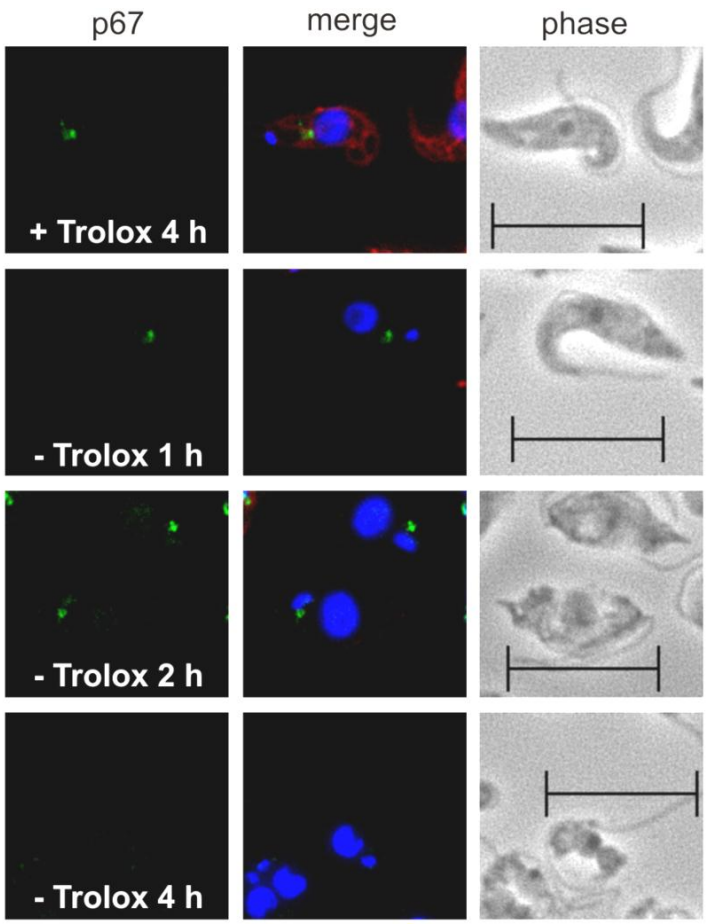

B

I	- Trolox [%]						+ Trolox [%]
Phenotype	0 h	0.5 h	1 h	1.5 h	2 h	4 h	4 h
Mito+ Lyso+	99	99	85	66	48	10	99
Mito- Lyso+	<1	0	6	19	26	28	<1
Mito+ Lyso-	<1	<1	<1	<1	1	0	<1
Mito- Lyso-	0	0	8	15	24	62	0

II	- Trolox [%]						+ Trolox [%]
Phenotype	0 h	0.5 h	1 h	1.5 h	2 h	4 h	4 h
Mito+ Lyso+	99	98	94	63	39	5	**99**
Mito- Lyso+	<1	1	**2**	16	**29**	38	<1
Mito+ Lyso-	<1	0	<1	1	<1	0	0
Mito- Lyso-	0	<1	3	20	31	**57**	0

Figure 3.16: PC *px I-III*$^{-/-}$ parasites rapidly lose their mitochondrial membrane potential. A. The cells were cultivated for the indicated times at 27 °C in medium ± Trolox and then subjected to immunofluorescence microscopy analysis using MitoTracker (red), antibodies against the lysosomal membrane protein p67 (green) as well as DAPI (blue) for visualizing the nuclear and kinetoplast DNA. Merge, overlay of all three signals; phase, phase contrast image (for details see text). **B.** Quantitative analysis of the different phenotypes observed. Between 333 and 413 cells were evaluated at each time point. Phenotypic cells shown in **A.** are highlighted by bold numbers. Two independent sets of experiments are presented (I and II). (Scale bar: 10 µm)

Since the *px III* gene encodes in addition to an N-terminal MTS also a putative glycosomal targeting signal, the lack of Px III could also affect glycosomal membranes. Thus, the *px I-III*$^{-/-}$ cells were subjected to immunofluorescence analysis as described above using aldolase as glycosomal marker (Figure 3.17). Independent of the presence or absence of Trolox, the cells kept punctured glycosomal staining. After 4 h without Trolox when ≥50% of the cells had lost their lysosomal as well as mitochondrial signals (Figure 3.16), they still displayed a proper aldolase staining. Thus, the glycosomes do not seem to be a primary site of cellular membrane damage.

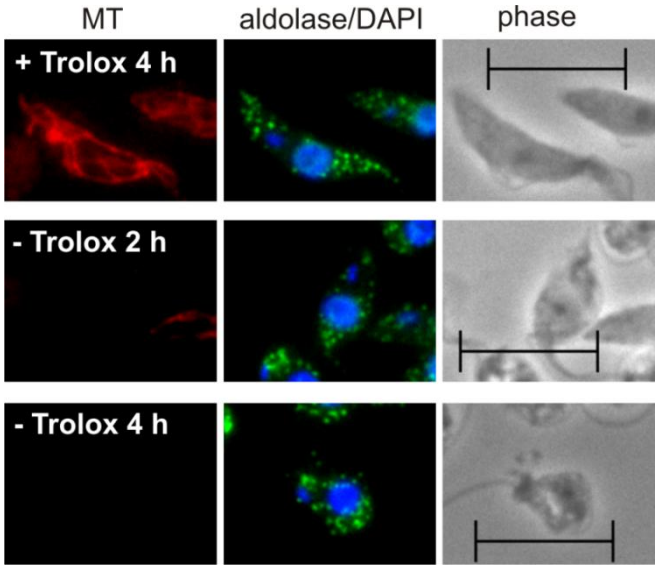

Figure 3.17: Glycosomal staining persists until the PC *px I-III*$^{-/-}$ cells completely lyse. The parasites were kept at 27 °C in medium ± Trolox for the indicated times and then, subjected to immunofluorescence microscopy analysis. MT, MitoTracker (red) staining; aldolase/DAPI, an overlay of the pictures obtained upon immuno-staining of the glycosomal marker protein aldolase (green) and the DAPI signals (blue); phase, phase contrast image (for details, see text). The immunofluorescence analysis depicted is a representative of two individual experiments. (Scale bar: 10 µm)

To evaluate the mitochondrial morphology in more detail, two different proteins of the mitochondrion were stained by immunofluorescence analysis (Figure 3.18). ASCT is a monomeric matrix protein whereas LipDH is a component of four mitochondrial multienzyme complexes. With prolonged incubation time in Trolox-free medium, the signal intensity of both mitochondrial proteins intensively decreased while the MitoTracker staining was still detectable in the *px I-III*$^{-/-}$ cells. As an example of the LipDH staining, a parasite with normal LipDH signal is presented at the top (- Trolox 1 h) whereas in the lower right corner, a cell with decreased signal is displayed. At later time points when the MitoTracker signal was lost, the signals of both mitochondrial proteins formed clusters and increased (- Trolox 4 h) which seemed not to be originated by the secondary antibody reaction alone (see appendix). These clusters may resemble autophagy vesicles as shown for Chinese hamster ovary cells [Gutierrez *et al.*, 2007]. Thus, autophagy-specific markers should be used to further dissect the mechanism of this cell lysis.

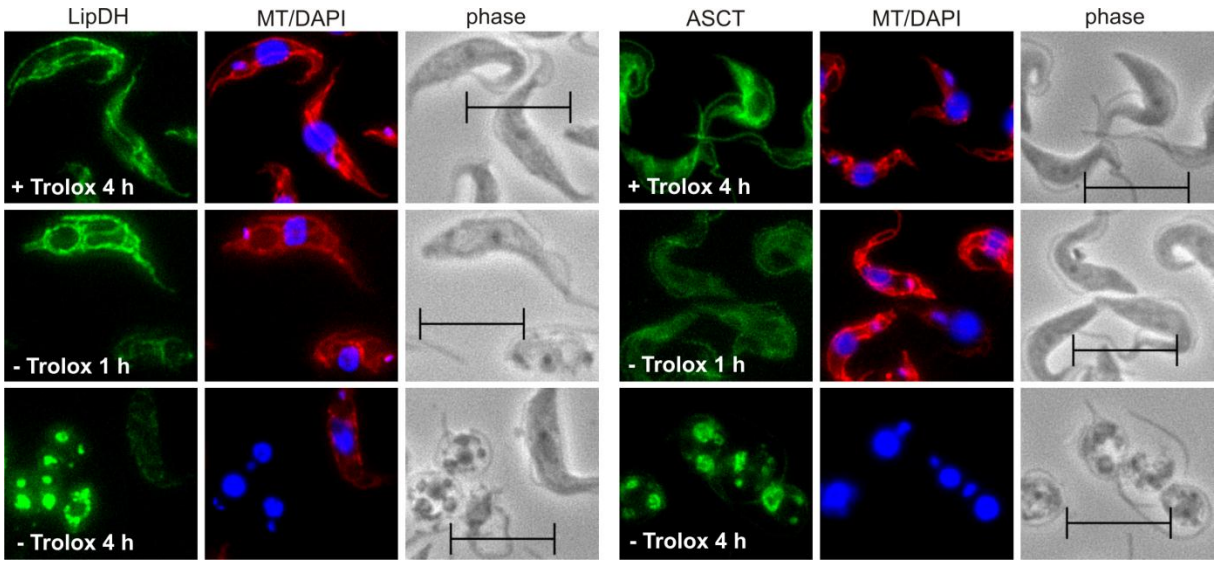

Figure 3.18: Two mitochondrial proteins show signal reduction followed by a prominent clustered staining in the PC *px I-III*$^{-/-}$ parasites. The cells were transferred into medium ± Trolox and kept at 27 °C for different times. Immunofluorescence microscopy displayed LipDH (left) and ASCT (right) staining (green), an overlay of pictures of MitoTracker (MT, red) and DAPI (blue) staining, and phase contrast image (phase). (Scale bar: 10 µm)

To analyze further which cellular organelles are affected by lipid peroxidation, the Click-iT Lipid Peroxidation Detection kit (Life Technologies) was ordered. The company stated that the procedure of the kit is able to detect lipid-peroxidation-derived protein modifications in the cell. After incubation of the cells with LAA, the incorporated lipid derivative should produce unsaturated aldehydes upon stress by cumene hydroperoxide. These aldehydes should modify adjacent proteins and be detectable by a fluorescent azide reaction with the alkyne via click chemistry. The method was performed by Samantha Ebersoll to monitor lipid peroxidation on a subcellular level. However, upon induction of cellular stress by the suggested cumene hydroperoxide or HpODE, no great changes in signal intensity of the LAA reaction was observed in WT cells (see appendix). In order to visualize lipid peroxidation in the PC *px I-III*$^{-/-}$ cell line, parasites were fed with LAA and kept in medium ± Trolox. No change in signal intensity was observed in the damaged mutant parasites after 2 h in the absence of Trolox (see appendix). This kit was not suitable for the detection of lipid peroxidation in trypanosomes.

3.2.4 Lysis of the PC px I-III$^{-/-}$ *parasites is stimulated by exogenous iron or hemin*

As an initial study, different concentrations of iron and hemin were tested on PC WT cells to identify the concentration range to be used in the further experiments (see appendix). To study the putative involvement of iron in the lethal phenotype of the PC *px I-III*$^{-/-}$ cells, the medium was supplemented with 100 µM iron nitrate (Fe^{3+}) and iron sulfate (Fe^{2+}),

respectively (Figure 3.19). In the presence of Trolox, short-term viability and even overnight proliferation remained unaffected whereas after Trolox removal, both ferrous and ferric iron accelerated cell lysis to almost the same extent (Figs. 3.19A and C). This does, however, not imply that the parasites incorporate ferric iron. PC *T. brucei* have been shown to actively take up ferrous iron and rapidly reduce ferric iron prior to transport [Mach *et al.*, 2013].

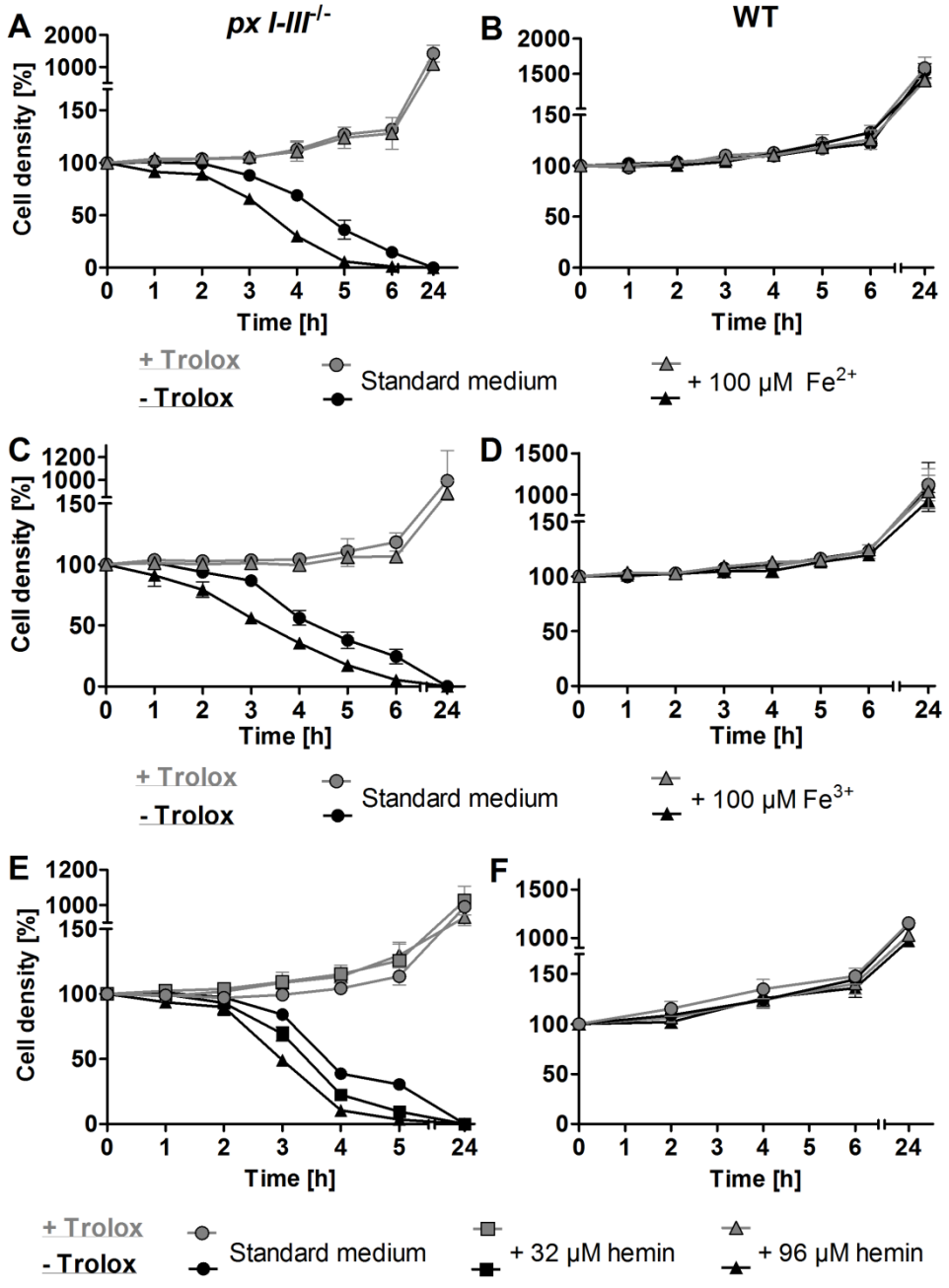

Figure 3.19: Lysis of PC *px I-III*$^{-/-}$ cells in the absence of Trolox is accelerated by exogenous iron or hemin. PC *px I-III*$^{-/-}$ and WT parasites were cultivated for 24 h at 27 °C in MEM-Pros medium (which contains 11 µM hemin) ± 100 µM Trolox supplemented with **A.** and **B.** 100 µM Fe^{2+}, **C.** and **D.** 100 µM Fe^{3+}, and **E.** and **F.** additional 32 and 96 µM hemin. At the indicated time points, living cells were counted. The values are the mean ± SD of three individual experiments.

The MEM-Pros medium we use for the cultivation of PC *T. brucei* contains about 11 µM hemin but no additional iron source. Either the minute amount of free iron present in the FCS is sufficient for proper proliferation or the parasites can obtain iron from heme despite they probably lack a heme oxygenase [Korený *et al.*, 2013]. The latter mechanism has been reported for *L. infantum* [Carvalho *et al.*, 2009]. Supplementing the medium with increasing concentrations of hemin also accelerated lysis of the PC *px I-III*$^{-/-}$ cells in Trolox-free medium (Figure 3.19E). In contrast, the proliferation of WT cells was not affected by any of these treatments (Figure 3.19B, D, and F).

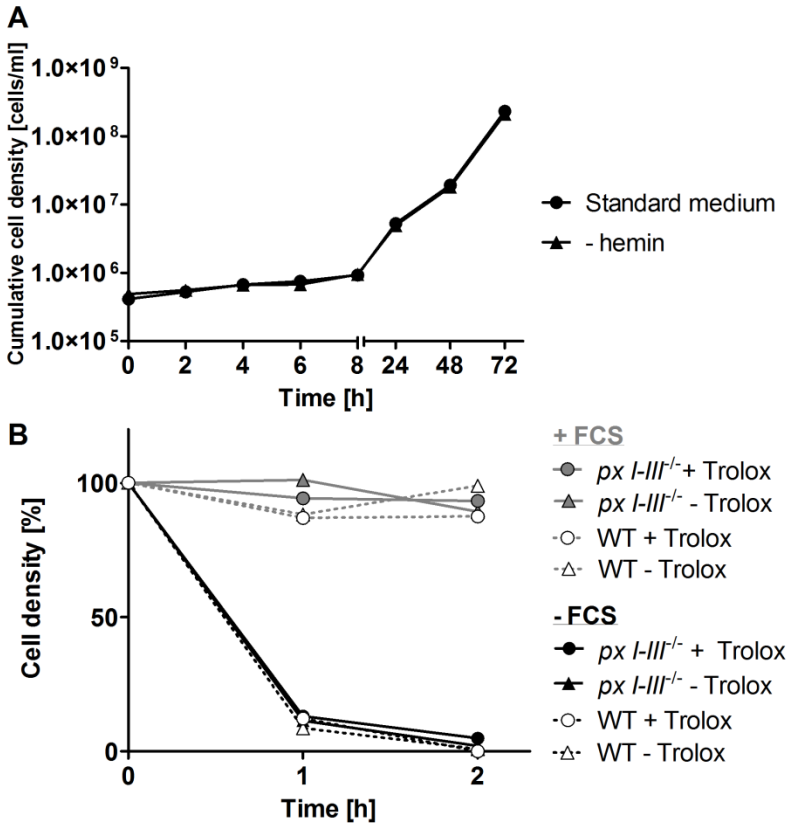

Figure 3.20: PC *T. brucei* lacking hemin and FCS. A. WT cells were washed six times with 5 ml of 1x PBS and transferred to MEM-Pros standard medium ± supplemented 11 µM of hemin. The cell proliferation was analyzed for three days. **B.** PC *px I-III*$^{-/-}$ and WT parasites were cultivated for 2 h at 27 °C in MEM-Pros medium ± FCS and Trolox.

To further dissect the effect of heme, PC WT parasites were cultured in medium without exogenous added hemin for several weeks. There was no proliferation difference between WT cells in standard medium and hemin-free medium (Figure 3.20A). This suggests that the parasites take up traces of heme from the FCS. In the absence of the antioxidant, the *px I-III*$^{-/-}$ parasites still died in the short-term when kept in hemin-free medium (data not shown). To

remove completely heme from the medium, WT and *px I-III*$^{-/-}$ cells were transferred to hemin- and FCS-free medium in the presence or absence of Trolox. KO as well as WT parasites without FCS died within two hours irrespective of the presence of Trolox (see appendix). Also in hemin supplemented but FCS-free medium, WT and mutant parasites died rapidly independent of Trolox (Figure 3.20B). The short-term withdrawal of the FCS from the medium was not possible for phenotypic analyses in PC cells.

3.2.5 The iron-induced lysis of the PC px I-III$^{-/-}$ *cells is not linked to lysosomal damage*

Supplementing the Trolox-free medium with the iron chelator deferoxamine prevented lysis of the PC *px I-III*$^{-/-}$ cells and even allowed modest proliferation upon overnight incubation (Figure 3.21A). Deferoxamine enters the cell via fluid-phase endocytosis and mainly resides inside the lysosomal compartment [Kurz *et al.*, 2006]. However, at high concentrations, enough deferoxamine may enter the cytosol and other cellular compartments to chelate iron and protect the cells [Zhang and Lemasters, 2013].

In contrast to deferoxamine, starch-deferoxamine is membrane-impermeable and thus, should stay in the endosomal/lysosomal compartments [Zhang and Lemasters, 2013]. Indeed, compared to the full protection exerted by the free chelator, supplementing the medium with 100 µM of starch-deferoxamine only slightly delayed lysis of the PC *px I-III*$^{-/-}$ cells in the absence of Trolox (Figure 3.21C). Notably, this minor protective effect became only visible after 4 h of incubation. This may suggest that starch-deferoxamine became partially hydrolyzed in the lysosome.

To demonstrate that both chelators would be equally protective if the lysosome was the major site of iron-mediated damage, we studied their effect towards BS *px I-II*$^{-/-}$ parasites. For these cells, it was shown in section 3.1 that the lysosome is highly sensitive to iron-induced oxidative damage and deferoxamine protects the cells from lysis. Indeed, supplementing the Trolox-free HMI-9 medium with 100 µM of either deferoxamine or starch-deferoxamine slowed down lysis of BS *px I-II*$^{-/-}$ cells to the same extent (Figure 3.21E). Thus, the iron-mediated lysis of the PC *px I-III*$^{-/-}$ cells is not linked to damage of the lysosome. In the presence of Trolox, the chelators did not have any effect on the short-term viability of the mutant cell lines consistent with WT analysis (Figure 3.21B, D, and F).

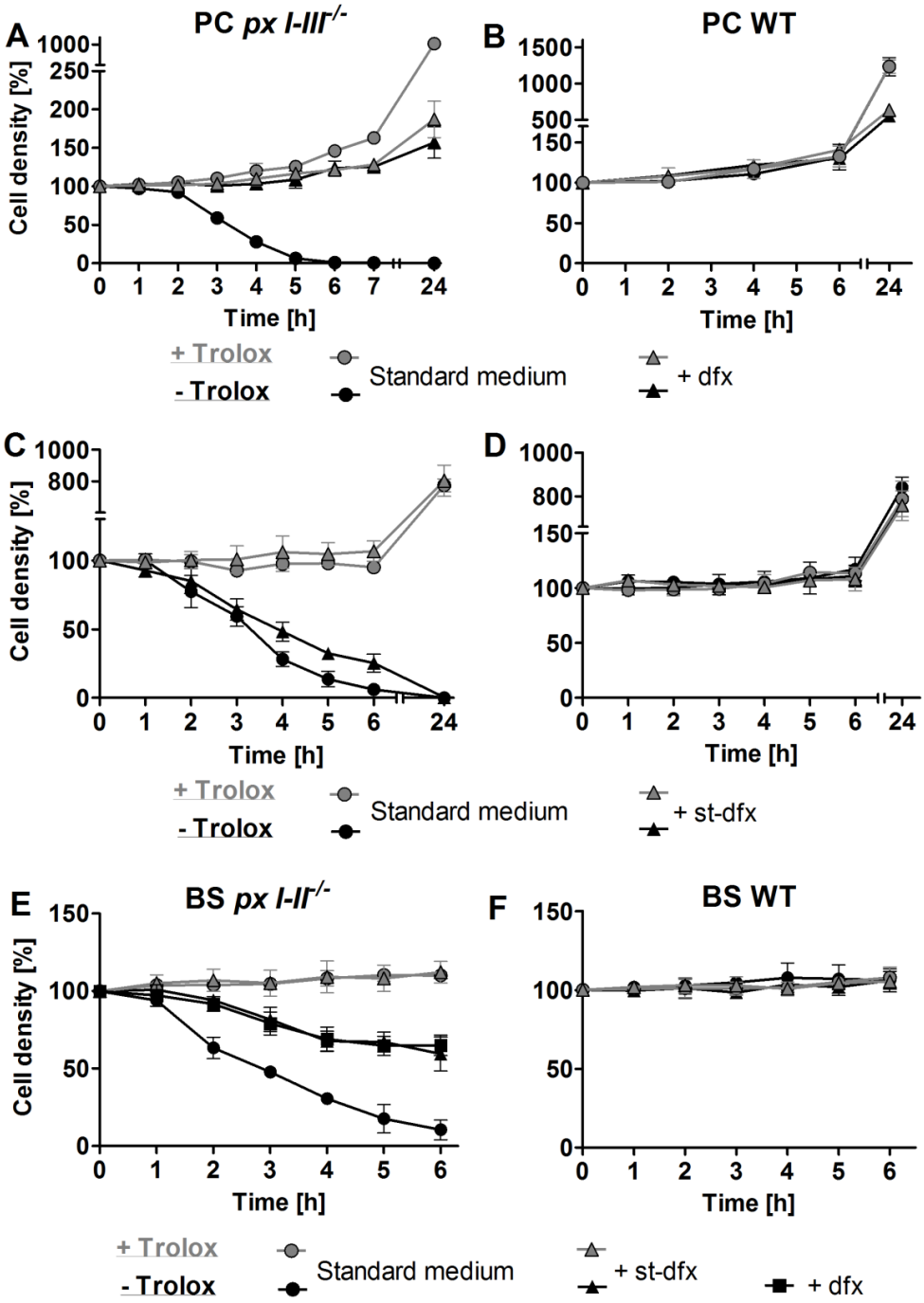

Figure 3.21: Deferoxamine − but not starch-coupled deferoxamine − protects PC *px I-III*$^{-/-}$ cells from lysis. The parasites were kept in medium ± 100 µM Trolox. **A.** and **B.** PC *px I-III*$^{-/-}$ and WT cells were incubated ± 100 µM deferoxamine (dfx) at 27 °C. **C.** and **D.** PC *px I-III*$^{-/-}$ and WT parasites were incubated ± 100 µM starch-deferoxamine (st-dfx) at 27 °C. **E.** and **F.** As a control, BS *px I-II*$^{-/-}$ and WT cells were treated ± 100 µM dfx and st-dfx at 23 °C. In this case, both chelators attenuated cell lysis to the same degree. The data represent the mean value ± SD of three independent experiments.

3.2.6 MitoQ and decylubiquinone prevent lysis of PC px I-III$^{-/-}$ and BS px I-II$^{-/-}$ cells to different degrees.

MitoQ is a ubiquinone derivative that is specifically targeted to the mitochondrial matrix by its positively charged triphenylphosphonium ligand [Jauslin *et al.*, 2003; Ross *et al.*, 2008]. As MitoQ is routinely used in low nM concentrations on mammalian cells, the effect of low concentrations of Trolox was first evaluated on PC and BS mutant parasites (Figure 3.22). Only the standard supplementation of 100 µM Trolox was sufficient to rescue the PC *px I-III*$^{-/-}$ and BS *px I-II*$^{-/-}$ cells. This vitamin E-analog was not efficient enough to prevent cell lysis in the nM range.

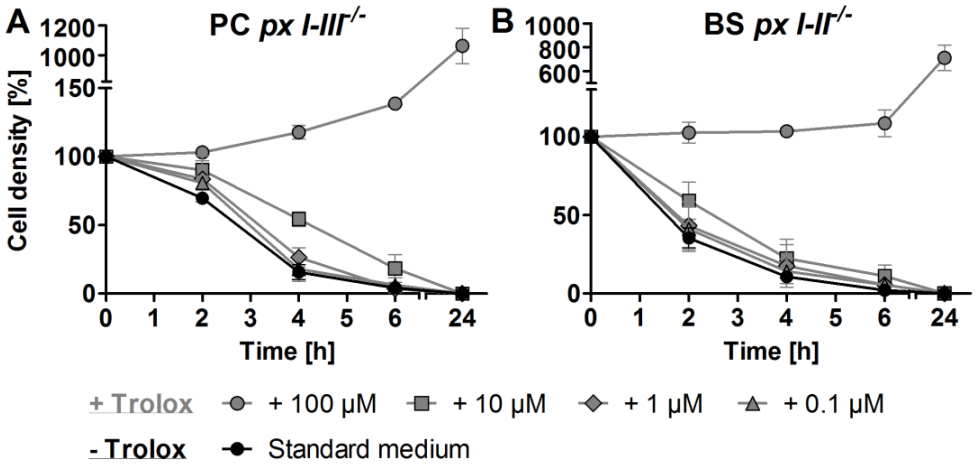

Figure 3.22: The BS and PC KO cells do not tolerate low Trolox concentrations. A. PC *px I-III*$^{-/-}$ and **B.** BS *px I-II*$^{-/-}$ parasites were kept in standard medium supplemented with 0.1, 1, 10, and 100 µM Trolox. The data display the mean ± SD of three independent experiments.

As a second study, coenzyme Q10 was used to rescue the cells in a concentration of 10 and 1 µM (see appendix). However, coenzyme Q10 was not able to prevent cell lysis in the PC *px I-III*$^{-/-}$ and BS *px I-II*$^{-/-}$ cells.

Initial studies revealed that the supplementation of 10 µM MitoQ instead of Trolox was lethal to BS and PC parasites whereas 10 µM decylubiquinone did not affect the growth of BS and PC WT cells and even supported proliferation of BS and PC mutant parasites in the absence of Trolox (Figure 3.23). In addition, 10 nM MitoQ did not protect the PC *px I-III*$^{-/-}$ cells from lysis in Trolox-free medium (data not shown) and at a concentration of 100 nM, MitoQ slightly affected the overnight proliferation of WT cells (Figure 3.23E and F). Thus, to allow a direct comparison, MitoQ and free decylubiquinone were investigated at fixed concentrations of 30 nM and 100 nM.

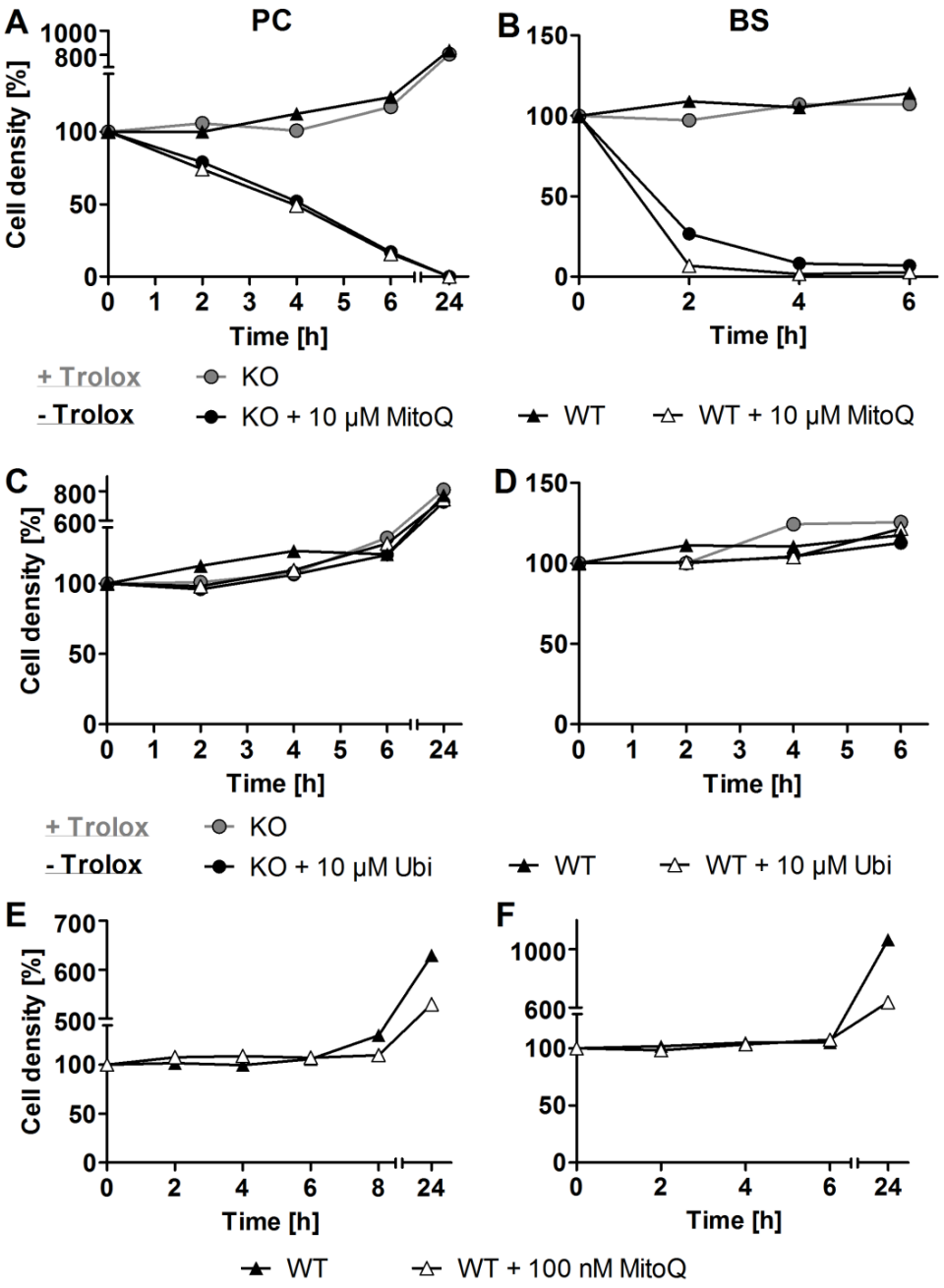

Figure 3.23: The toxic and protective effect of MitoQ and decylubiquinone, respectively, on PC and BS mutant and WT cells in Trolox-free medium. A. and **B.** PC *px I-III*$^{-/-}$ and BS *px I-II*$^{-/-}$ parasites as well as WT cells were kept in standard medium ± Trolox ± 10 µM MitoQ. **C.** and **D.** PC *px I-III*$^{-/-}$ and BS *px I-II*$^{-/-}$ parasites as well as WT cells were kept in standard medium ± Trolox ± 10 µM decylubiquinone (Ubi). **E** and **F.** PC and BS WT parasites were kept for 24 h in standard medium ± 100 nM MitoQ.

The PC *px I-III*$^{-/-}$ cells were transferred into Trolox-free medium, MitoQ or decylubiquinone was added, and living parasites were counted. A concentration of 100 nM MitoQ completely and decylubiquinone largely, rescued the short-term viability of the mutants (Figure 3.24A). However, whereas 30 nM MitoQ still prevented lysis of the parasites, at the same

concentration, decylubiquinone was virtually inactive. Indeed MitoQ was superior in protecting the cells compared to the free ubiquinone. To further assess the mitochondrion as origin of the cellular damage in the PC *px I-III*$^{-/-}$ cells, BS *px I-II*$^{-/-}$ parasites − which display damage of the lysosome as primary event − were also exposed to both antioxidants. Surprisingly, again MitoQ proved to be more efficient compared to decylubiquinone (Figure 3.24B). This can, however, be due to the fact that the uptake of MitoQ into the cytoplasm is driven by the plasma membrane potential resulting in a 5-10 fold accumulation [Jauslin *et al.*, 2003]. The direct comparison of both mutant cell lines showed that 30 nM MitoQ protected the PC *px I-III*$^{-/-}$ cells but lysis of the BS *px I-II*$^{-/-}$ mutant is only marginally slowed down (compare Figure 3.24A and B). A higher concentration of MitoQ is probably needed to protect the lysosomal membrane compared to the mitochondrial one.

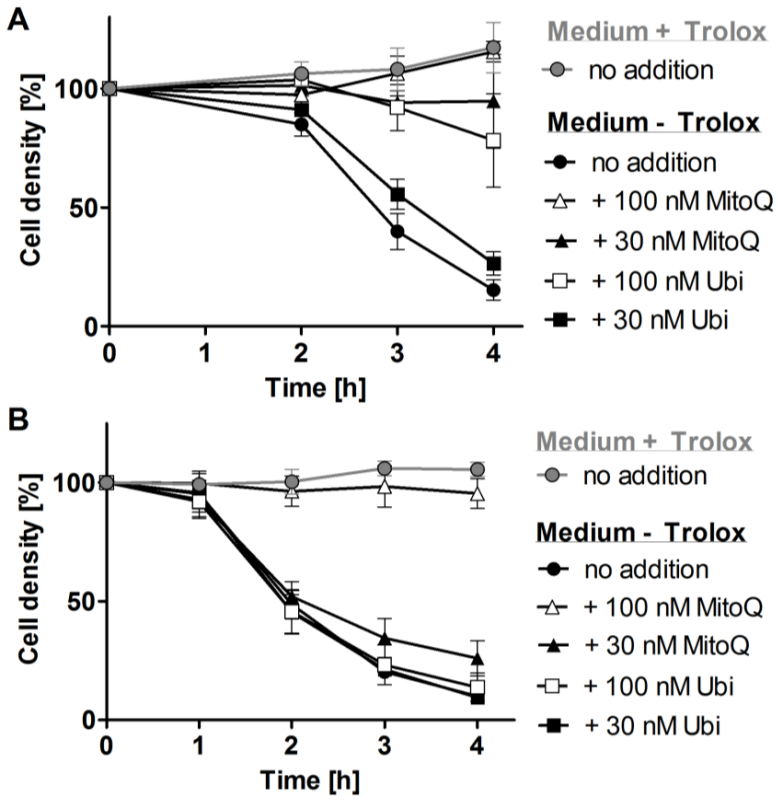

Figure 3.24: Effect of MitoQ and decylubiquinone on the short-term viability of the PC *px I-III*$^{-/-}$ and BS *px I-II*$^{-/-}$ parasites in Trolox-free medium. The cells were transferred into the respective Trolox-free medium and MitoQ and decylubiquinone (Ubi), respectively, was added. **A.** PC *px I-III*$^{-/-}$ cells were incubated at 27 °C and **B.** BS *px I-II*$^{-/-}$ parasites at 22 °C. Viable cells were counted after different incubation times. As controls, the mutant cells were kept in Trolox-supplemented medium. The data are the mean ± SD of three independent experiments.

3.2.7 PC T. brucei require either the cytosolic or the mitochondrial Px-type enzyme for viability in Trolox-free medium

As outlined above, PC *px I-II*$^{-/-}$ cells perfectly proliferate in Trolox-free medium whereas *px I-III*$^{-/-}$ cells are only viable in the presence of the exogenous antioxidant. This suggests that the insect form requires only the mitochondrial Px III or alternatively either the cytosolic or the mitochondrial form of these enzymes. Previous results of Amrei Nißen showed that the KO of *px III* and partially *px II* does not resulted in a lethal phenotype [Nißen, 2014]. To generate a pure *px III*$^{-/-}$ cell line in the insect stage of the parasite, WT 449 cells were transfected again consecutively with the pHD1747_KO*pxIII* and pHD1748_KO*pxIII* and *vice versa*. In total, 16 clones were obtained. The replacement of the *px III* gene by the two resistance cassettes was verified (see appendix). Because of the extreme sequence conservation within the *px* locus and even of the intergenic regions, a PCR was performed to evaluate if the *px III*$^{-/-}$ cell lines lost not only the *px III* gene but also the *px II* gene (for scheme, see Figure 3.25A). Three PC *px III*$^{-/-}$ clones were analyzed as well as the BS *px III*$^{-/-}$ cell line generated in the infective form of the parasites by Michael Diechtierow (Figure 3.25B). Compared to PC WT 449 cells, all *px III*$^{-/-}$ clones displayed a band at 1981 bp (black arrow) and 1045 bp (white arrow) indicating the loss of only *px III* and the combined loss of *px II* and *px III*.

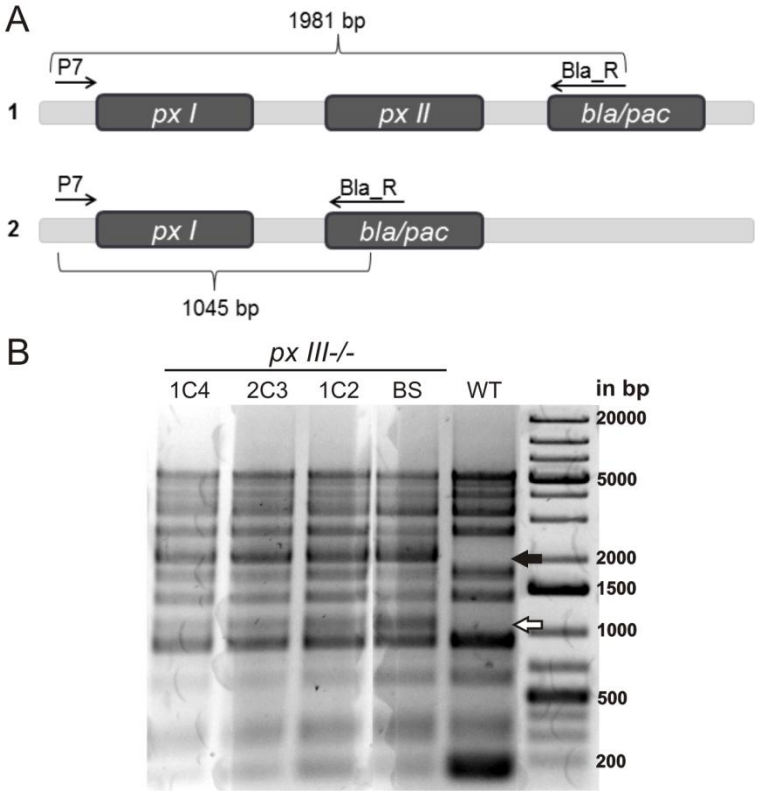

Figure 3.25: PC *px III*$^{-/-}$ cell lines generated by the pHD1747/48_ KO*pxIII* vectors appear to be also partially *px II*$^{+/-}$. A. Schematic *px* locus including the used primer pair (P7 and Bla_R_MD) and the length of the PCR products to differentiate between the loss of only *px III* (1) or *px II/III* (2). **B.** Genomic DNA of PC *px III*$^{-/-}$ clones 1C4, 2C3, and 1C2 generated by pHD1747/48_KO*pxIII* plasmids, BS *px III*$^{-/-}$ parasites clone Z11 from M. Diechtierow (BS), and PC WT cells were isolated and subjected to PCR analysis with the primer pair P7 and Bla_R_MD. The PCR products were analyzed on a 1% agarose gel (*px III* out, 1981 bp (black arrow); *px II/III* out, 1045 bp (white arrow)). The primer pair showed many cross-reactions bands.

This finding suggested that each cell line consists of parasites with different genotypes (mixed cell lines) namely: parasites that have lost *px II* and *px III* on both alleles, only lost *px III* on both alleles, and lost *px II* and *px III* on one allele while the other allele lacks only *px III*.

Southern blot analysis was performed to analyze the genotypes of the mixed cell lines in more detail. The digestion with *Hpa*I and *Pst*I as well as *Hpa*I and *Sca*I should result in two fragments with different length for each allele, *pac* and *bla* (see Materials and Methods, Table 2.4). Through the different sizes, one can differentiate between a loss of only *px III* or *px II* and *III*. WT cells served as a control for proper DNA restriction whereas BS *px III*$^{-/-}$ cells were used as a positive control. Thus, genomic DNA of two PC *px III*$^{-/-}$ clones (2D4 and 1C4), the BS *px III*$^{-/-}$ clone Z11 from M. Diechtierow, and PC WT cells were isolated and 12 µg of each DNA was double digested with either *Hpa*I and *Pst*I or *Hpa*I and *Sca*I (For the detailed procedure see Materials and Methods, chapter 2.2.4.4). However, the blot developed with the probe against the *px* locus did not show any signal (data not shown). The blot was re-developed with the *β-tubulin* probe to verify the restriction digest and the transfer of the genomic DNA (Figure 3.26). The obtained DNA fragments should be at 775 and 2859 b for the *Hpa*I/*Pst*I digest and at 3944 b for the *Hpa*I/*Sca*I digest. Tubulin fragments were only faintly detectable in the *Hpa*I/*Pst*I digest at ~787 b originated by a double *Pst*I restriction (black arrow). The result was not able to confirm the proper digest by *Hpa*I and *Sca*I but indicated that the used DNA amount was below the detection limit for the *px* locus as the expected *px* signal should be four times less than the one of the β-tubulin (4 identical *β-tubulin* genes vs 1 *px* locus).

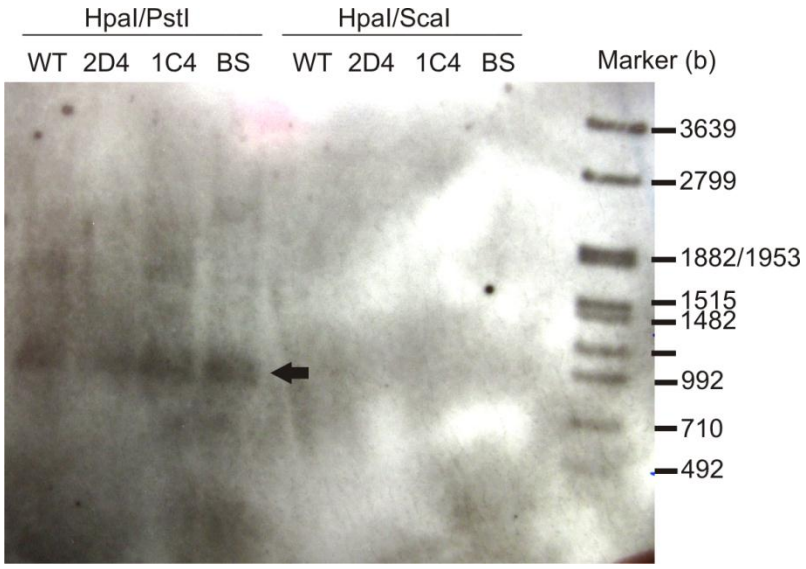

Figure 3.26: Southern blot analysis of PC *px III*$^{-/-}$ clones using the *β-tubulin* probe. Genomic DNA (12 µg) of PC WT cells, PC *px III*$^{-/-}$ clones 2D4 and 1C4 generated with the pHD1747/48_KO*pxIII* vectors, and BS *px III*$^{-/-}$ parasites clone Z11 from M. Diechtierow (BS) were double digested by either *Hpa*I and *Pst*I or *Hpa*I and *Sca*I. The DNA fragments were subjected to Southern blot analysis (see Materials and Methods). The blot was developed with the probe against the *β-tubulin* genes.

To specify the homologous recombination event in the parasites, the transfection vectors pHD1747_KO*pxIII*+MTS and pHD1748_KO*pxIII*+MTS were created (for scheme see Figure 2.2B). As template the pHD1747/8_KO*pxI-III* were used where the 5'UTR of *px I* was replaced by a DNA sequence containing 162 bp of the 3'UTR of *px II* followed by the MTS of *px III* (24 bp) to enhance the probability of a pure *px III* gene depletion. However, it showed the same result as the original pHD1747/8_KO*pxIII* vectors discussed before (data not shown).

The extreme sequence conservation of the UTRs made it difficult to create a proper *px III*$^{-/-}$ cell line. Thus, I tried to re-introduce the *px I* + 3'UTR + *px II* + 3'UTR locus into the PC *px I-III*$^{-/-}$ cell line. As the intergenic regions are so similar, I created mixed transfection vectors containing *px I* + 3'UTR or the whole *px I* + 3'UTR + *px II* + 3'UTR locus (data not shown; for scheme see Figure 2.2C). I was not able to separate them appropriately without any doubt. Finally, I only re-introduced the *px II* + 3'UTR of *px II* locus into the PC *px I-III*$^{-/-}$ cell line as the cloning primers (P26RS_Fw and Px I-II in NeRv) were more specific. Previous data showed that the cytosolic protein Px I displays no enzymatic activity in *T. b brucei* Lister 427 due to a mutation in the active site [Diechtierow and Krauth-Siegel, 2011]. Thus, the absence of the respective gene should not result in any phenotypic changes.

First, a transfection vector with more restrictions sites was created which originated from the transfection vector pHD1748_KO*pxI-III* (see chapter 3.2.2). The blasticidin resistance gene in pHD1748_KO*pxI-III* was replaced by the neomycin resistance gene introducing *Mlu*I and *Xba*I as additional restriction sites by the use of the primer pair PxIIIKONeoFw and PxIIIKONeoRv resulting in pHD1748-Neo. The *px II* gene and its 3'UTR were amplified from genomic DNA using P26RS_Fw and Px I-II in NeRv as primers and inserted upstream into the pHD1748_KO*pxI-III* vector yielding pHD1748-Neo_re-insert*pxII* (see Figure 2.2D). A second transfection vector was created by exchanging the neomycin resistance gene from the pHD1748-Neo_re-insert*pxII* vector with the puromycin one amplified from pHD1747_KO*pxI-III* using the primer pair PuroPxIII_Fw and PuroPxIII_Rv resulting in pHD1748-Pac_re-insert*pxII*. PC *px I-III*$^{-/-}$ cells were transfected with the *Xho*I/*Not*I-digested pHD1748-Neo_re-insert*pxII* in the presence of Trolox and blasticidin to selectively exchange the locus with the puromycin resistance. For subsequent selection, G418 was added to the serial dilutions. Four clones from the *px I*$^{-/-}$/*II*$^{+/-}$/*III*$^{-/-}$ cell line were obtained: 2D6, 2D4, 4D4, and 2C1.

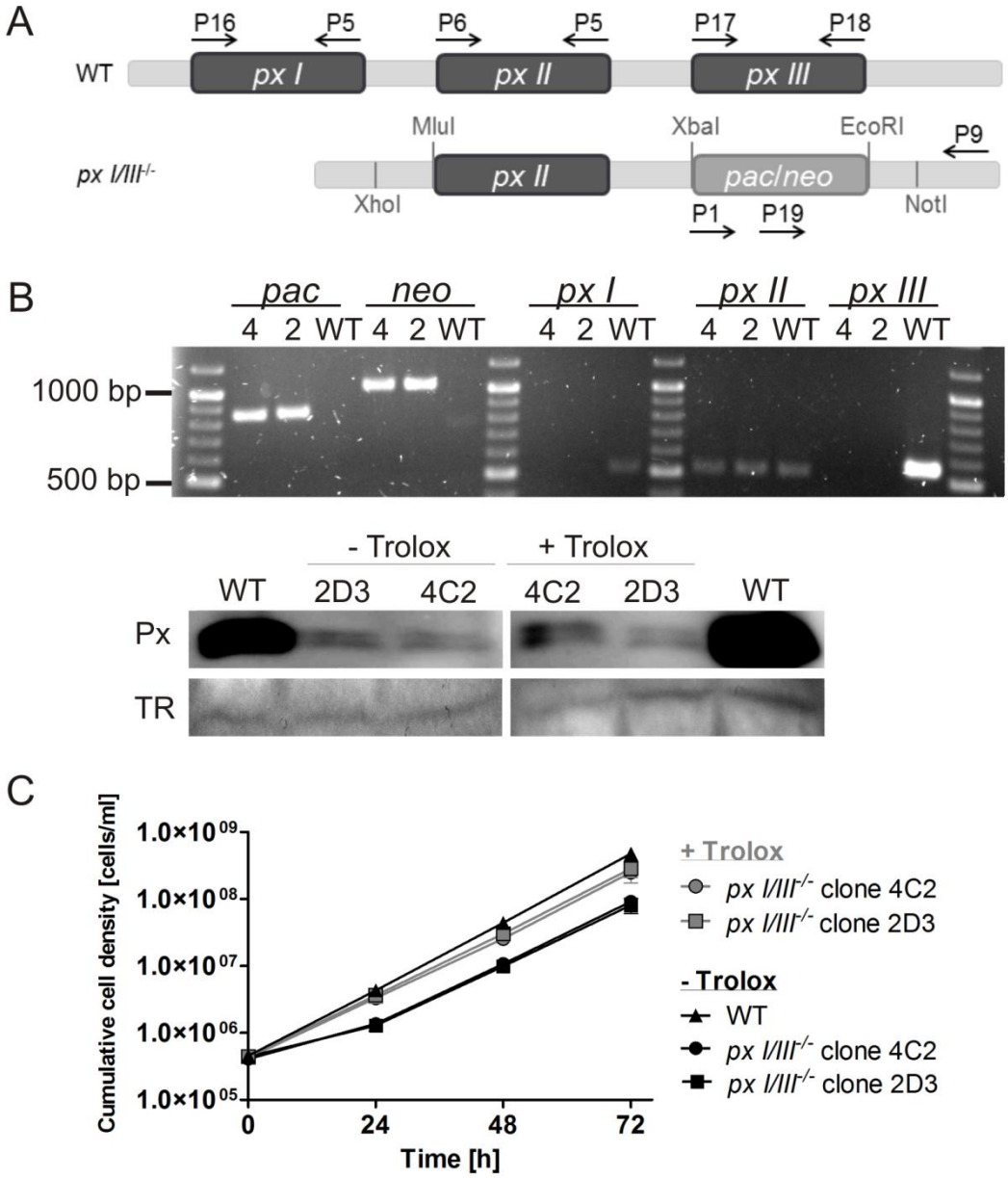

Figure 3.27: Analysis of the PC *px I/III*$^{-/-}$ cell lines. A. Scheme for the PCR analysis with the used primer pairs. The primers described here are the following: P1 = PuroF_CH2, P5 = P18_MD, P6 = P26_MD, P9 = 3UTR_PxIII_R1, P16 = Px I-II in NeFw, P17 = P1_MD, P18 = P24_MD, and P19 = NeoF_BM. **B.** Upper part. PCR analysis of genomic DNA isolated from clone 4C2 and 2D3 of the *px I/III*$^{-/-}$ cell lines as well as WT *T. brucei* with the primer pairs mentioned above (*pac*: P1 and P9, expected amplicon 858 bp; *neo*: P19 and P9, 1031 bp; *px I*: P16 and P5, 511 bp; *px II*: P6 and P5, 510 bp; *px III*: P17 and P18, 548 bp). The elongation time of the PCR program was adjusted to the amplicon size. Lower part. 1.5 x 10^7cells of the *px I/III*$^{-/-}$ clones grown in medium ± 100 µM Trolox as well as of WT parasites were harvested at day three presented in **C**. Western blot analysis was performed using antisera against Px as well as TR as loading control. **C.** *Px I/III*$^{-/-}$ and WT *T. brucei* were cultivated in standard MEM-Pros medium ± 100 µM Trolox at 27 °C. Living cells were counted each day. The data represent the mean value ± SD of three independent cumulative growth curves.

The second transfection was performed with the clone 4D4 by the pHD1748-Pac_re-insert*pxII* vector in the presence of Trolox and G418 while puromycin was supplemented to

the medium during the selection procedure. I obtained five *px I/III*$^{-/-}$ clones (4C4, 2D3, 4C2, 2D2, and 2C3) which were verified by PCR and Western blot analyses, particularly clone 4C2 and 2D3 are shown in Figure 3.27.

To analyze the proliferation of the *px I/III*$^{-/-}$ cell line, the clones 2D3 and 4C2 as well as the clones 2D6 and 4D4 from the *px I*$^{-/-}$*/II*$^{+/-}$*/III*$^{-/-}$ cell line were selected. The proliferation of the mutant cell lines in medium ± Trolox compared to PC WT 449 cells was analyzed for three days (Figure 3.27C and 3.28A). In the case of the *px I/III*$^{-/-}$ cell line, parasites in medium supplemented with Trolox displayed almost no difference in proliferation compared to PC WT cells whereas in the absence of the antioxidant, the *px I/III*$^{-/-}$ cells showed a transient proliferation defect resulting after 24 h in a cell density of 50% compared to that in the presence of Trolox (Figure 3.27C). Remarkably, from day 2 onwards, this phenotype disappeared and the parasite proliferated comparable to that in Trolox-supplemented medium. PC African trypanosomes appear to require either the cytosolic or the mitochondrial form of the peroxidase.

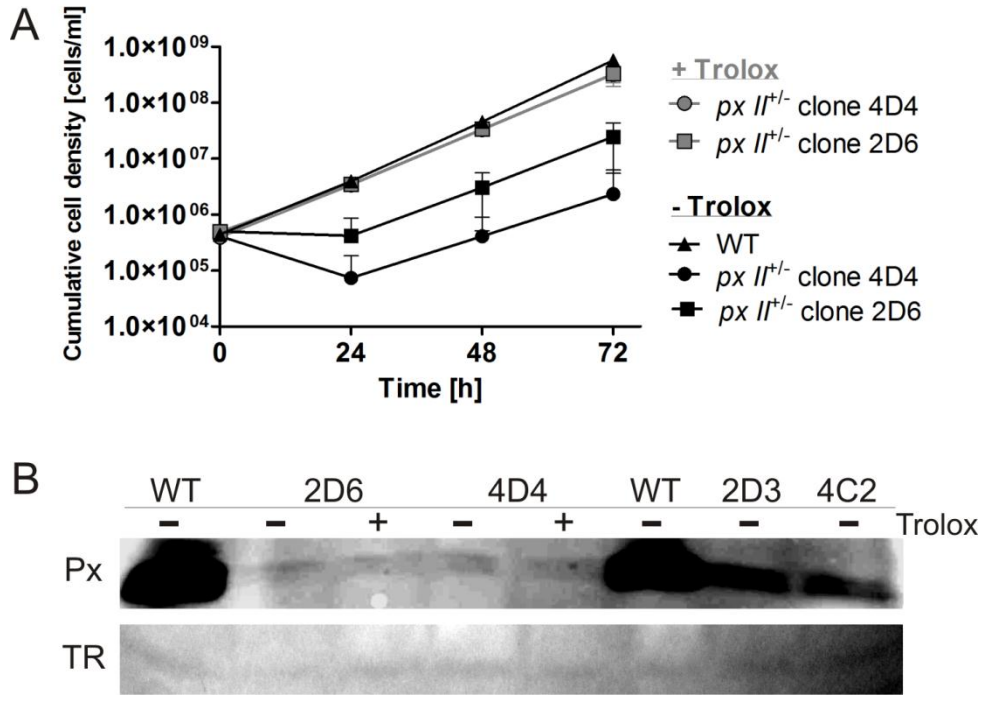

Figure 3.28: PC *px I*$^{-/-}$*/II*$^{+/-}$*/III*$^{-/-}$ cell lines proliferate and express low levels of Px II independent of Trolox supplementation. A. Incubation of the *px I*$^{-/-}$*/II*$^{+/-}$*/III*$^{-/-}$ clones 4D4 and 2D6 ± 100 µM Trolox and WT *T. brucei* in MEM-Pros medium at 27 °C. Living cells were counted each day. The data display the mean value ± SD of three independent cumulative growth curves. **B.** 1.5 x 10^7 cells of the *px I*$^{-/-}$*/II*$^{+/-}$*/III*$^{-/-}$ (named *px II*$^{+/-}$) clones 4D4 and 2D6 ± Trolox and *px I-III*$^{-/-}$ clones 4C2 and 2D3 - Trolox as well as WT parasites were harvested at day 3 in **A.** and Figure **27.C** and subjected to Western blot analysis using antisera against Px and TR as loading control.

In the absence of Trolox, the protein level of the cytosolic peroxidase did not significantly increased (Figure 3.27B) and cannot explain the change in the proliferation rate after 24 h. Interestingly, the overall level of Px II is rather low compared to the over-saturated WT signal. Thus, this minor expression is sufficient for the parasite to survive.

In the case of the *px I*$^{-/-}$*/II*$^{+/-}$*/III*$^{-/-}$ clones, both cell lines proliferated nearly comparable to the WT cells in the presence of Trolox. After Trolox removal, the two clones started dying after 24 h but returned to a normal growth rate after 2 - 3 days. The adaptation process was not linked to an increase in Px II levels as shown by Western blot analysis in Figure 3.28B. Intriguingly, the mutant parasites can survive although they express about 5x less Px II compared to the *px I/III*$^{-/-}$ clones 2D3 and 4C2 without Trolox. As the signals of the WT samples were already saturated, the Western blot has to be repeated with 5x to 10x less cells for better comparison. This minute expression level of the peroxidase seems not to be really sufficient as especially clone 4D4 displayed mostly a severe proliferation defect which could lead to an altered expression level of other related genes to compensate the essential enzyme.

As Px III exhibits also a glycosomal targeting sequence (ARL), transfection vectors to insert the *px III* gene lacking the ARL sequence into the PC *px I-III*$^{-/-}$ parasites were generated. For this purpose, the truncated *px III* gene was amplified from genomic DNA of the PC *px I-II*$^{-/-}$ cells using 4UTR_Fw_CH and PxIII-ARL_Rv_CH as primers, digested with *Xba*I and *Eco*RI, and inserted into the pHD1748-Neo vector by exchanging the neomycin resistance cassette yielding pHD1748_re-insert*pxIII*-ARL. In a second step, a neomycin resistance gene was amplified from pHD1748-Neo using the primers NeoClon_Fw_CH and NeoClon_Rv_CH. The PCR product was digested with *Mlu*I and *Xba*I and ligated into pHD1748_re-insert*pxIII*-ARL resulting in pHD1748-Neo_re-insert*pxIII*-ARL (for scheme see Figure 2.2E). The plasmid (clone 4) was recently sequenced. In addition, the second transfection vector encoding the puromycin resistance gene as well as vectors for the insertion of the *px III* gene lacking the MTS should be created to investigate the influence of the mitochondrial or glycosomal localization of Px III on this interesting phenotype.

3.3 The functional role of Px IV

3.3.1 Sequence analysis of T. brucei Px IV

In the TriTryp database, Px IV (Tb427tmp.01.7560) from Lister strain 427 is annotated as a putative glutathione peroxidase with mass of 17341 Da and an isoelectric point of 8.41. The DNA sequence is 471 bp in length. ClustalW2 alignment of Kinetoplastida proteins (Figure 3.29) revealed that the Px IV protein sequence from *T. brucei* showed 64% identity to the respective protein of *T. congolense*, 58% to *T. cruzi*, 47% to *L. major*, and 49% to *C. fasciculata*. The *T. b. brucei* Px IV sequence is identical to that of *T. b. gambiense*. Px IV possesses eight cysteines of which those at positions 37, 66, and 127 are highly conserved.

```
T. brucei MNGGAIFSHSVLMDGNAVMLSKYAGCVTVLVNTASLCSFTSSNIQHLIHVQQKWASRSFT 60
T. congo  MNGVSVFSHLALMDGSPVPLAKYGGNVTIIVNTASLCSFAASNIRHLTQMQRSWGTRGFT 60
T. cruzi  MGSSTVFAYSALMGGKSVALSNYTGRVTVVVNTASLCSFANSSLQQLTHVQETYGPRGFT 60
L. major  --MASVFTYSAVQNGKTVVLQKYSGYATLIVNVASRCSLASTNIEMLNEVQQAYGSRRFT 58
C. fasci  --MTSIFAYSAAQEGKMILLQRYTGCVTLIVNVASRCSFTTANLEMLNEVQQTYGSRKFT 58
              ::*:: .   *. : * .* * .*::**.** **:: :.:. * .:*. :..* **

T. brucei VLAFPCSQFGNQEPKKRDEICCWVARNGINFPVFDKVNLKGPNTHPLFQMIQSSLGPIRW 120
T. congo  ILAFPCSQFANQEPKSAEEISSWVASSGINFPVFDKVKVSGPDAHPLFKGLQSSLGPIRW 120
T. cruzi  ILAFPCAQFANQEPKSNEEIAVWAQTCGLNFPLFDKVKVKGPDAHPLFQMLQASLGPIRW 120
L. major  VLAFPCAQFANQEPLNNTEIAQWCEDLGLLFPVFDRVNVKGSSADPLFQMLRAQQGAPLW 118
C. fasci  VLGFPCSQFANQEPLSNAEIAQWRQERPVLFPVFDKINVKGPQADPLFQMLRAQQGAPVW 118
          :*.***:**.**** .  **. *     : **:**::::.*.:.***: :::. *.  *

T. brucei NYTKVVCNRAGLPCVKLQPGSSLEELERYVSQLCDE---- 156
T. congo  NYTKFVCSRAGMPYAKFHPTSGIDEVERCVSLLCEE---- 156
T. cruzi  NYTKFICDREGIPLVKLDSSSFLEELRRSIEQACGPQRGA 160
L. major  NYTKYLCDRSGVPRRKLEPGCSMDALRQSIECVL------ 152
C. fasci  NYTKYLCDRGGVPVRKLEPGCSLDTLKRAIECVL------ 152
          **** :*.* *:*  *:.. . :: :.: :.
```

Figure 3.29: Multiple sequence alignment of Px IV from different trypanosomatids species. *T. brucei* = *T. b. brucei* Lister strain 427; *T. congo* = *T. congolense* IL3000; *T. cruzi* = *T. cruzi* CL Brener Non-Esmeraldo-like; *L. major* = *L. major* strain Friedlin; *C. fasci* = *C. fasciculata* strain Cf-Cl. The numbers on the right give the position of the residue in the respective protein. Amino acids conserved in all sequences are shown with grey background and marked by *. Cysteine residues of *T. brucei* Px IV are highlighted in yellow.

For a functional analysis, a sequence alignment with related peroxidases was conducted (Figure 3.30). The catalytic triad (Cys 37, Gln 72, and Trp 120) in *T. brucei* Px IV, is conserved except for GPx8. For the enzymatic activity, even a tetrad instead of a triad is reported which would include the highly conserved Asn 121 [Tosatto *et al.*, 2008]. The overall identity to the human GPx7/8 and *T. brucei* Px III is only 33 and 30%, respectively. Another cysteine found in all Kinetoplastida Px IV sequences (Cys 66) is also conserved in the other peroxidases. Intriguingly, except for *T. cruzi*, all Kinetoplast Px IV display a cysteine at the third last position of the C-terminus. Neither a classic ER retention signal,

present in GPx7 and 8, nor an MTS, as in Px III, was found in Px IV. Different prediction algorithm yielded a variety of putative subcellular localizations.

```
Px IV    ----------------------------------------MNGGAIFSHSVLMDGNAV 18
Px III   --------------------------------MLRSSRKKMSAASSIFDFEVLDADHKPY 28
GPx7     --------------------MVAATVAAAWLLLWAAACAQQEQD-FYDFKAVNIRGKLV 38
GPx8     MEPLAAYPLKCSGPRAKVFAVLLSIVLCTVTLFLLQLKFLKPKINSFYAFEVKDAKGRTV 60
                                                     .     .      .

Px IV    MLSKYAGCVTVLVNTASLCSFTSSNIQHLIHVQQKWASRSFTVLAFPCSQFGNQEPKKRD 78
Px III   NLVQHKGSPLLIYNVASKCGYTKGGYETATTLYNKYKSQGFTVLAFPCNQFGGQEPGNEE 88
GPx7     SLEKYRGSVSLVVNVASECGFTDQHYRALQQLQRDLGPHHFNVLAFPCNQFGQQEPDSNK 98
GPx8     SLEKYKGKVSLVVNVASDCQLTDRNYLGLKELHKEFGPSHFSVLAFPCNQFGESEPRPSK 120
          * :: *   :: *.** *  *.        : ..  .  *.******.*** .**   .

Px IV    EICCWVARN-GINFPVFDKVNLKGPNTHPLFQMIQSS-----LG-PIRWNYTKVVCNRAG 131
Px III   EIKEFVCTKFKAEFPIMAKINVNGENAHPLYEYMKKTKPGILATKAIKWNFTSFLIDRDG 148
GPx7     EIESFARRTYSVSFPMFSKIAVTGTGAHPAFKYLAQT-----SGKEPTWNFWKYLVAPDG 153
GPx8     EVESFARKNYGVTFPIFHKIKILGSEGEPAFRFLVDS-----SKKEPRWNFWKYLVNPEG 175
         *:  :.  .    **:: *: : *   .* :. : .:          *: . :    *

Px IV    LPCVKLQPGSSLEELERYVSQLCDE--------- 156
Px III   VPVERFSPGASVKDIEEKLIPLLGSARL------ 176
GPx7     KVVGAWDPTVSVEEVRPQITALVRKLILLKREDL 187
GPx8     QVVKFWRPEEPIEVIRPDIAALVRQVIIKKKEDL 209
               *  .:: :.  :  *  .
```

Figure 3.30: Alignment of Px IV with related peroxidases. Px IV = Px IV from *T. b. brucei* Lister strain 427; Px III = Px III from *T. b. brucei* Lister strain 427; GPx7 = human GPx7; GPx8 = human GPx8. The numbers belonging to the amino acid position are presented on the right site. Strictly conserved residues are highlighted by a grey background and *. The MTS and the glycosomal targeting sequence of Px III are shown in blue and green, respectively. The ER retention signals in the human proteins are given in orange. The catalytic triad is given in bold letters and all cysteines of *T. brucei* Px IV are shown with a yellow background.

3.3.2 Isolation of genomic px IV DNA from T. brucei

For the *in vitro* characterization of recombinant Px IV, the coding region of *px IV* was cloned into the pETtrx-1b vector yielding a Trx-Px IV fusion construct (see chapter 2.2.1). DNA of PC WT 449 *T. brucei* was isolated and served as template to amplify the coding region of *px IV* by PCR with *Nco*I and *Acc*65I restriction sites. The ATG of the *Nco*I site was used as the first residue of *px IV*. This procedure led to an insertion of an additional second amino acid, glycine, after the methionine which should not influence the protein function. NovaBlue competent *E. coli* were transformed with the pETtrx-1b_PxIV vector and two clones, 1A and 1D were obtained. Plasmids were extracted for test digestion and agarose gel electrophoresis (Figure 3.31). Sequencing of clone 1A confirmed the sequence (see appendix).

3.3.3 Recombinant Px IV is not soluble

Different *E. coli* strains were transformed with the pETtrx-1b_PxIV clone 1A plasmid. Various test expressions yielded only small amounts of soluble protein (Table 3.1).

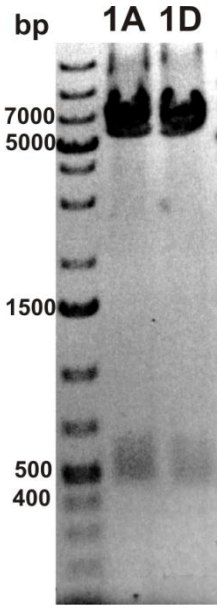

Figure 3.31: Cloning of *px IV* into the pETtrx-1b vector. The pETtrx_PxIV clones 1A and 1D were digested with *Nco*I and *Acc*65I and subjected to agarose gel electrophoresis. The restriction products of 470 bp for *px IV* and 5685 bp for the digested vector had the expected size.

Using lysis buffers that were titrated with HCl and NaOH to a pH of 2, 4, 6, 7, 7.5, 8, and 10 did not increase the amount of protein in the supernatant (data not shown). None of the different conditions using the pETtrx-1b_PxIV construct significantly improved the expression of soluble protein.

Table 3.1: Conditions employed for the expression of recombinant *T. brucei* Px IV. Different Px IV plasmids, *E. coli* strains, media, and the cell density (OD_{600}) at which expression was induced by IPTG induction were tested. In addition, the IPTG concentration and temperature for overnight cultivation after induction were varied.

Construct	*E. coli* strain	Medium	OD_{600}	IPTG [mM]	Temperature [°C]
pETtrx-1b_PxIV	**BL21 (DE3)**	LB	0.4-0.6	0.2	27
				1	
			0.4-0.6	0.2	18
			0.5		15
			0.4-0.6	1	18
		2-YT	0.4	0.2	15
		Minimal			
	BL21 (DE3) pLysS	LB	0.6	0.2	15
		2-YT			
		Minimal	0.5		
	Rosetta (DE3) pLysS	LB	0.4	0.2	15
		2-YT	0.5		
		Minimal	0.4		
	Origami 2 (DE3)	2-YT	0.7	0.2	15
	SHuffle T7 Express	LB	0.6	0.2	15
	Tuner (DE3)	LB	0.4	0.2	15

pETtrx-1b_Δ1-18-PxIV	BL21 (DE3)	LB	0.5	0.2	15
pQE-30_PxIV	BL21 (DE3)	2-YT	0.5	0.2	15
			1		
		LB	0.4-0.5		
			1		
pETtrx_C26/81/134S-PxIV (mutant)	BL21 (DE3)	LB	0.4-0.6	0.2	27
pETNusA-1a_PxIV	BL21 (DE3)	LB	0.4-0.6	0.2	18
pETMBP-1a_PxIV	BL21 (DE3)	LB	0.4-0.6	0.2	18
pETZZ-1a_PxIV	BL21 (DE3)	LB	0.4-0.6	0.2	18
pETGB-1a_PxIV	BL21 (DE3)	LB	0.4-0.6	0.2	18

Two representative expressions are displayed in Figure 3.32. 2-YT and minimal medium (500 ml) were inoculated with the pETtrx-1b_PxIV transformed BL21 pLysS and BL21 cells, respectively (conditions are highlighted in bold in Table 3.1). The cells were treated essentially as described for the preparative expression in Materials and Methods (chapter 2.2.3.2). Total lysates of the uninduced cells as well as supernatant and pellet samples of the induced bacterial cultures were subjected to SDS-PAGE.

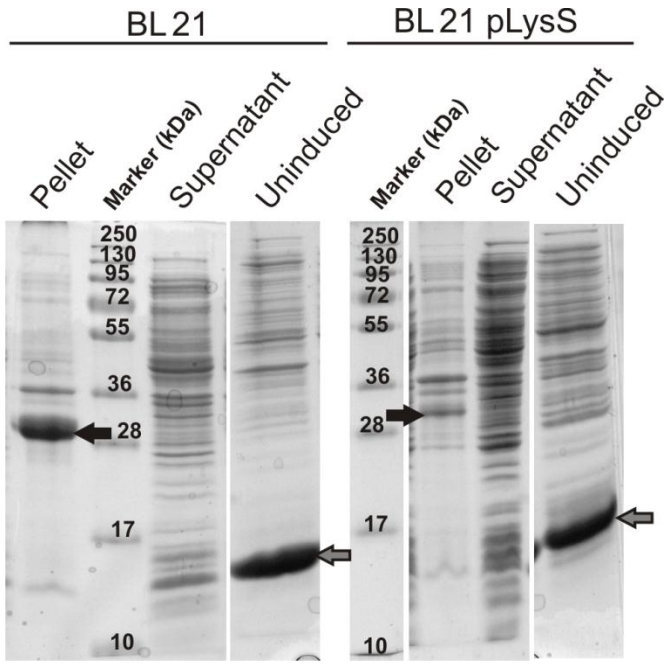

Figure 3.32: Test expression of the Trx-Px IV fusion protein. Minimal and 2-YT medium was inoculated with BL21 (DE3) and BL21 (DE3) pLysS *E. coli* cells, respectively, transformed with the pETtrx_PxIV plasmid clone 1A. The detailed procedure is described under Materials and Methods (chapter 2.2.3.2) and the conditions are highlighted in bold in Table 3.1. Uninduced represent cell extracts prior to IPTG induction treated with lysozyme (at ~13 kDa, grey arrow). The induced samples after overnight incubation were lysed and separated into pellet and supernatant fractions. All samples were subjected to SDS-PAGE on a 14% gel and Coomassie staining. The black arrows mark the Trx-Px IV fusion protein.

Prior to IPTG induction (uninduced) no expression was observed. BL21 cells led to a high expression of the fusion protein in the pellet fraction (black arrow, BL21) but the protein was undetectable in the supernatant. The BL21 pLysS yielded low amounts of protein in the pellet

(black arrow, BL21 pLysS). A prominent protein band was also not obtained in the supernatant. With the pETtrx-1b_PxIV expression vector, the protein was almost insoluble under all conditions studied. Although the fusion protein was not visible in the supernatant, a low amount of soluble Px IV might have been expressed. Thus, a preparative purification by affinity chromatography was performed with the aim to enrich some protein for kinetic analysis.

š

3.3.4 Purification of recombinant Px IV results in little, impure protein

Recombinant Px IV was purified from 4 l bacterial culture by two-step chromatography on Ni^{2+}-NTA sepharose as described in chapter 2.2.3.2. The elution profiles are shown in Figure 3.33A. Aliquots of the different purification steps were subjected to SDS-PAGE and Coomassie staining (Figure 3.33B). A strong Trx-Px IV expression was not detectable in the induced total lysate or in the pellet and supernatant (crude soluble extract) fractions after cell lysis. The fusion protein was bound to the column with its His-tag and not eluted during the two washing steps. The elution fraction of the first column showed a band of the expected 31.7 kDa for the fusion protein (grey arrow). Prominent larger proteins could be co-purified chaperones. After overnight cleavage with TEV, tag-free Px IV with a theoretical mass of 17.3 kDa was detectable. In the flow-through and the wash 1 fraction of the second column, small amounts of recombinant Px IV (0.2 mg/1 l bacterial culture) were eluted (black arrow). Both fractions were pooled and used for kinetic studies. The cleaved fusion partner (His-tagged Trx, 13 kDa), the His-tagged TEV protease (33 kDa) as well as uncleaved Trx-Px IV were eluted by high imidazole concentration (Wash 2). Most of the other contaminants like potential chaperones were co-purified probably bound to the undigested fusion protein.

3.3.5 Identification of putative Px IV substrates

The activity of recombinant Px IV was measured with 50 µM of H_2O_2 and HpETE as substrates using the peroxidase assay described for Px I-III [Diechtierow and Krauth-Siegel, 2011]. With H_2O_2, no activity was detectable even not when the concentrations of Tpx and TR were doubled to 20 µM and 450 mU, respectively. As a control, the assay was performed with Prx and H_2O_2 and a specific activity of 15 U/mg was measured. Under normal assay conditions, HpETE also did not yield activity. At twice the concentration of Tpx (20 µM) and Px IV (6.6 µM), a low specific activity of 0.049 U/mg was obtained. In comparison, a stored sample of recombinant Px III without MTS showed a specific activity of 4.8 U/mg and the theoretical value for a fresh sample would be around 11 U/mg (Natalie Dirdjaja, personal

communication). Thus, both assays worked using the control proteins. Future work should focus on the preparation of pure and properly folded protein for detailed kinetic analyses.

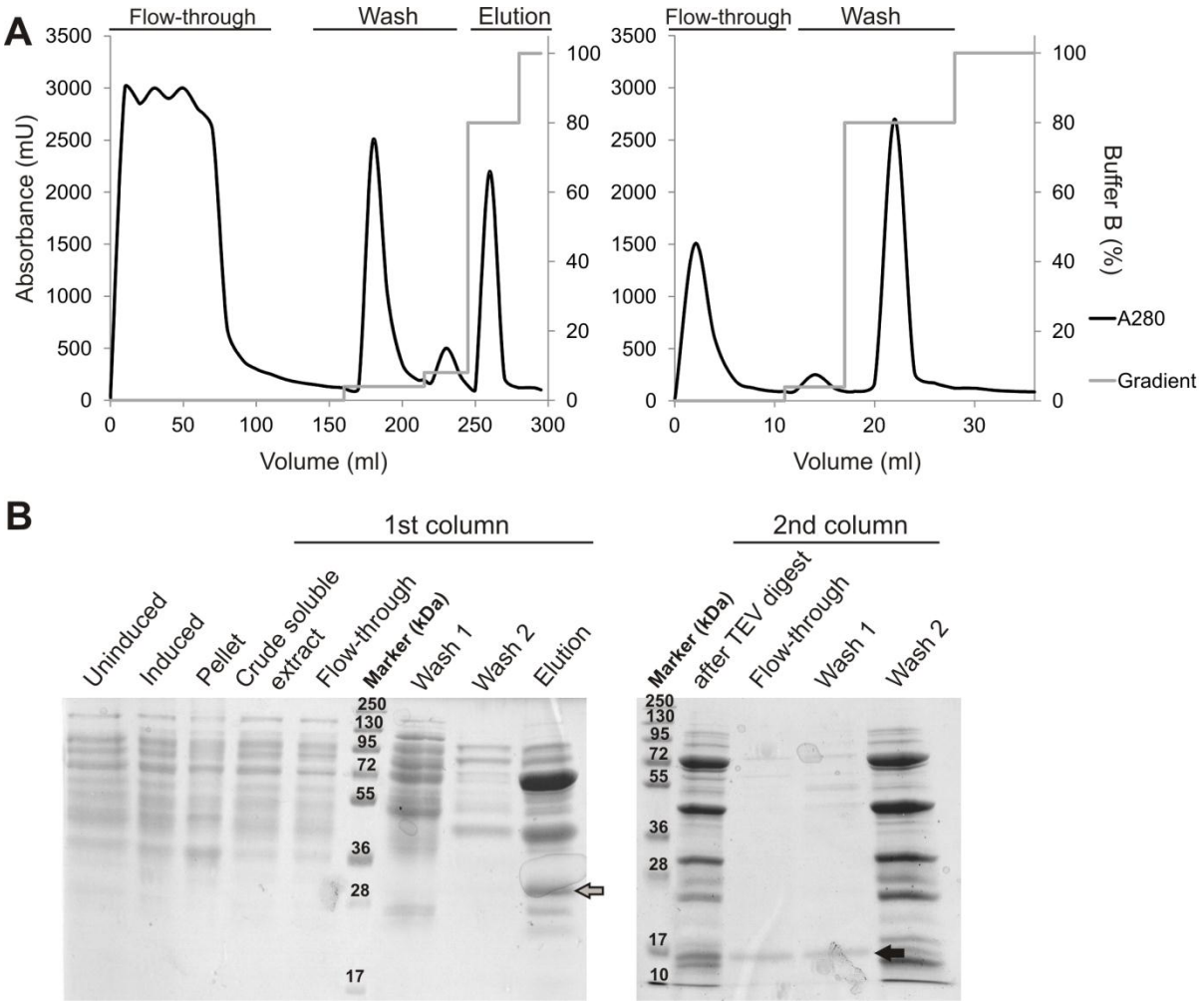

Figure 3.33: Preparation of Px IV from a 4 l bacterial culture yields small protein amounts. A. FPLC elution profiles of the first (*left*) and second (*right*) Ni^{2+}-NTA column showing absorbance at 280 nm (black) and the concentration of buffer B (grey). **B.** SDS gels (12%) showing the two-step preparative purification on an 8 ml (*left*) and 1 ml (*right*) Ni^{2+}-NTA column. *Left gel.* Extract of cells collected before IPTG addition directly boiled as total lysate in sample buffer (uninduced); the instantly boiled total lysate of the induced culture after overnight incubation (induced); pellet and crude soluble cell extract after lysis (crude soluble extract was applied on the column); flow-through from the 1st column; wash 1 and 2 washing with 56 ml of 4% (10 mM imidazole) and 32 ml of 8% (20 mM) buffer B, respectively; elution with 80% (200 mM) buffer B. The Trx-Px IV fusion protein is marked by grey arrow. *Right gel*. Sample after TEV digest; flow-through of the 2nd column; wash 1 and 2 washing with 6.6 ml of 4% (10 mM) and 11 ml of 80% (200 mM) buffer B, respectively. The maximal volume of the flow-through and wash 1 were applied onto the gel. The flow-through and wash 1 fractions contained untagged Px IV (black arrow).

3.3.6 Truncated Px IV or His_6-Px IV do not yield higher amounts of soluble protein

For the truncated protein, 18 amino acids (M1-V18) from the N-terminus were deleted. The truncated and full-length sequences of Px IV were cloned into the pETtrx-1b and the pQE-30 plasmid, respectively. After verifying the correctness of the sequences, clone 6 of the Δ1-18-

Px IV (pETtrx_Δ1-18-PxIV) and clone 2 of pQE-30_HisPxIV plasmid were used for protein expression in bacteria. The test expressions were performed as described in Table 3.1. For the His_6-Px IV, cells were cultivated in LB media and expression was induced at an OD_{600} of 0.4. Pellet and supernatant samples were subjected to SDS-PAGE (Figure 3.34).

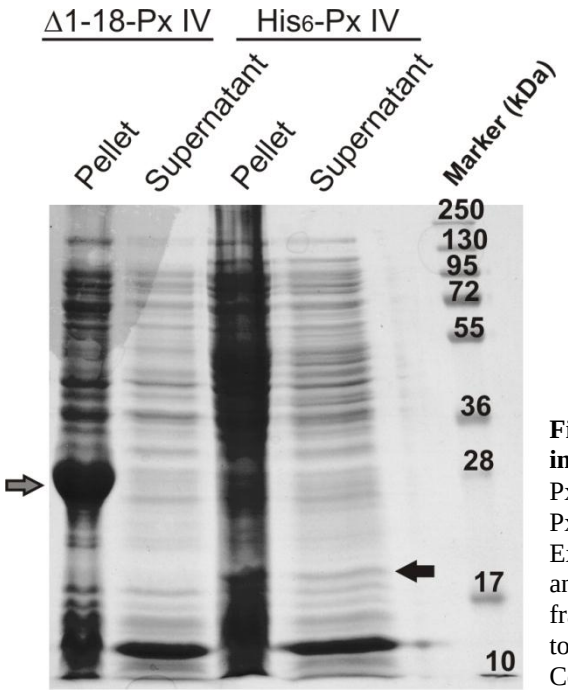

Figure 3.34: His_6-Px IV is probably expressed in the supernatant. Test expression of truncated Px IV (Δ1-18-Px IV, grey arrow) and His-tagged Px IV (His_6-Px IV, black arrow) were analyzed**.** Expression conditions were described in the text and Table 3.1. The supernatant and pellet fractions of the induced cultures were subjected to SDS-PAGE onto a 12% SDS gel and Coomassie staining.

The Trx-Δ1-18-Px IV fusion protein has a theoretical mass of 29.9 kDa (grey arrow) and the His_6-Px IV of 18.3 kDa (black arrow). The truncated Px IV fusion protein yielded high protein amounts in the pellet fraction but no over-expression was detectable in the supernatant. In contrast, His_6-Px IV showed some protein in the supernatant (black arrow). Thus, a preparative purification from a 2 l bacterial culture was performed (Figure 3.35). Expression of His_6-Px IV was not detectable in the pellet and crude soluble extract fraction. The three washing steps resulted in the removal of many proteins. However, the elution fraction contained in addition to His_6-Px IV (black arrow) contaminating bands (grey arrows) of which at least one (~25 kDa) appeared to be co-enriched. Besides, the elution fraction contained only 1.2 mg total protein/1 l bacterial culture corresponding to an estimated Px IV yield of 0.6 mg from a 2 l culture.

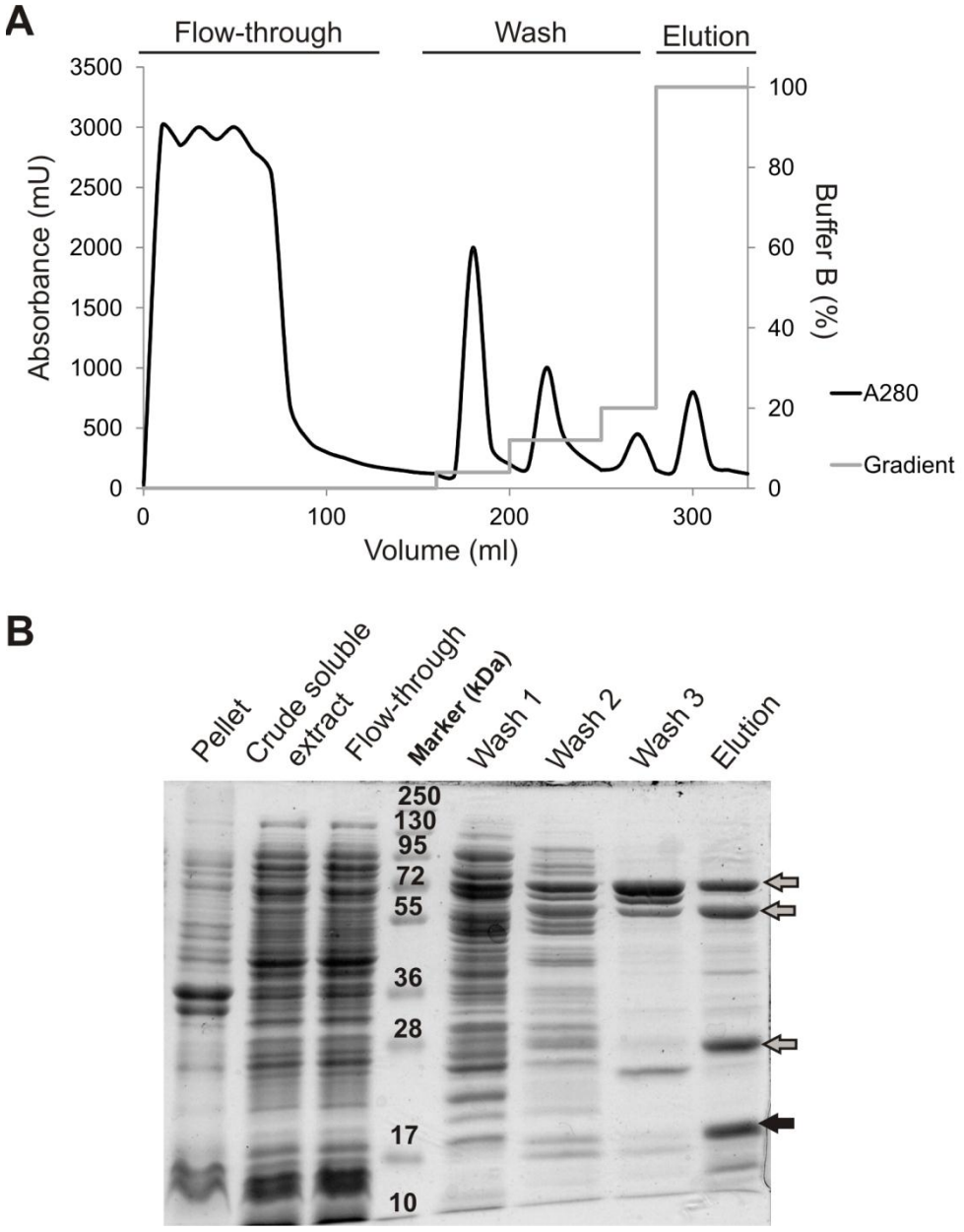

Figure 3.35: Preparative expression of His_6-Px IV yields a small amount of impure recombinant protein. A. The profile of the FPLC, absorbance measurement at 280 nm (black) and the imidazole gradient (grey). **B.** The crude soluble extract of a 2 l culture of BL21 (DE3) *E. coli* transformed with the pQE-30_PxIV plasmid was applied onto an 8 ml Ni^{2+}-NTA column and samples obtained from the different purification steps were subjected to SDS-PAGE on a 12% gel and Coomassie staining. The pellet and crude soluble cell extract of the induced culture after lysis as well as the flow-through from the column are shown. Wash 1, 2, and 3 are the washing steps in buffer B with 35 ml of 4% (10 mM), 40 ml of 12% (30 mM), and 30 ml of 20% (50 mM), respectively. The elution fraction contained His_6-Px IV (black arrow) but also several prominent contaminants (grey arrows).

3.3.7 Px IV shows a reduced and non-reduced form

Recombinant His_6-Px IV was diluted in sample buffer ± reducing agent and subjected to SDS-PAGE (Figure 3.36A). Under non-reducing conditions, the protein runs at a lower apparent mass of ~13 kDa (grey arrow) compared to the reduced Px IV sample (black arrow).

A

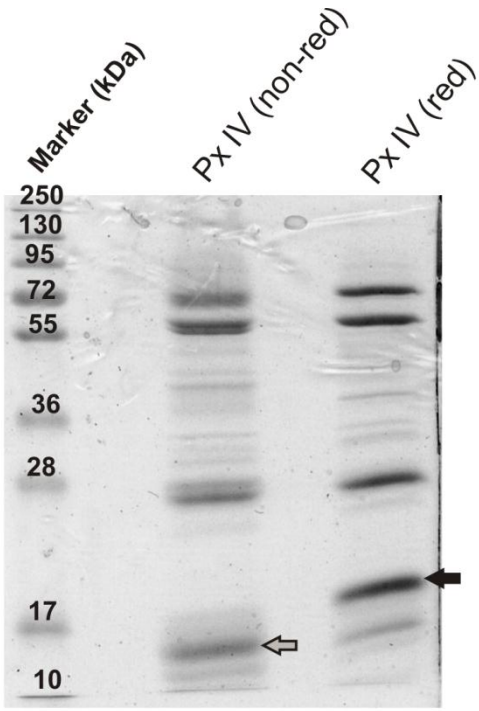

B

Experiment	Cys 26	Cys 37	Cys 66	Cys 81	Cys 82	Cys 127	Cys 134	Cys 154
1	missing	missing	both	both	both	IAM	IAM	NEM
2	IAM	IAM	NEM	IAM	IAM	IAM	missing	NEM
3	IAM	IAM	IAM	IAM	IAM	IAM	IAM	IAM
4	no label	no label	no label	IAM	IAM	IAM	no label	missing
state	bridge	bridge	free	free?	free?	free?	bridge	free

Figure 3.36: Px IV exists in reduced and non-reduced forms. A. SDS-PAGE of His_6-Px IV dissolved in SDS sample buffer in the absence (Px IV non-red, grey arrow) and presence of 2-mercaptoethanol (Px IV red, black arrow). The samples were run on a 12% gel and Coomassie stained. **B.** Treatment of Px IV with NEM and IAM under different experimental conditions to evaluate the thiol state in the non-reduced protein. The cysteine residues were assigned to the position in the protein and the different experiments to 1 - 4. Some cysteine-containing peptides were not found in the analysis (missing). The thiol state (state) displayed the presence of a disulfide bond (bridge), of a free thiol group (free) or of an unclear result (?) in the non-reduced protein.

To identify the cysteine residues involved in the putative intramolecular disulfide bridge(s), Px IV was subjected to MALDI-TOF-MS. Four different experiments were performed: The protein (18 µg) was **1)** treated with 3 mM of DTT followed by 20 mM of NEM. After reducing SDS-PAGE, the protein band was excised and treated again with 10 mM of DTT and 55 mM of IAM (for more details see chapter 2.2.4.13). **2)** treated with NEM, loaded on a non-reducing SDS gel, and then treated afterwards with DTT and IAM. **3)** run on a non-reducing gel and treated with DTT and IAM. **4)** subjected to a non-reducing SDS-PAGE and subsequently treated with IAM without prior reduction. Tryptic digest and MALDI-TOF-MS were performed with all protein bands and the peptides analyzed by the MASCOT software as outlined in Figure 3.36B. Not all cysteine-containing peptides could be found in all

experiments. In the first approach, all cysteine residues should have been labeled with NEM. However, some peptides showed both labels. Either reduction by DTT or the NEM-labeling was not complete. In the second approach, accessible free thiol groups should have been NEM-labeled and cysteines part of a disulfide bridge should have been labeled with IAM. The analysis yielded mainly IAM-labeled peptides indicating an inefficient NEM-treatment. The third experiment displayed that in the denatured protein, all cysteines were perfectly susceptible to reduction and labeling by IAM. In the fourth analysis, only free thiol groups present in the non-reduced protein should have been labeled with IAM. The peptide labeling obtained was not in agreement with the results from experiment 2. When assuming that the NEM-labeling was not complete, the fourth approach is the more conclusive one. The results are presented in Figure 3.36B. Cys 81, 82, and 127 gave contradicting results in experiments 2 and 4 and thus, were defined as unclear. Cys 66, 134, and 154 seem to be in the thiol state whereas Cys 26, 37, and 134 may form a disulfide bridge. However, Cys 26 and 134 are not conserved and thus, unlikely to be involved in a functional disulfide bridge. Clearly, this experiment has to be repeated with pure protein improving the NEM-labeling step.

3.3.8 Antibodies against T. brucei Px IV hardly recognize the protein

Recombinant untagged Px IV was used to immunize a rabbit (see Materials and Methods). Up to 1 µg protein from the elution fraction of recombinant His_6-Px IV (chapter 3.3.6) was hardly detectable using the large or the final bleeding in a 1:500 dilution (see appendix). Low specificity of the antibody was indicated by several cross-reactions and a protein band of the respective size was not observed in lysates of 3 x 10^6 BS *T. brucei*.

3.3.9 Other fusion proteins of Px IV display higher solubility

Px IV possesses eight cysteine residues which may interfere with folding of the recombinant protein. Thus, Natalie Dirdjaja cloned the pETtrx_triple-mut-PxIV plasmid using the pETtrx-1b_PxIV vector and mutated Cys 26, 81, and 134 into serines. However, the test expression showed no increase in solubility (see appendix, for conditions see Table 3.1).

As the Trx-Px IV fusion protein was poorly soluble, other vectors for the expression with different fusion partners were obtained from Gunter Stier. The coding sequence of *px IV* was cloned into the pETMBP, pETNusA, pETZZ, and pETGB plasmids using *Nco*I and *Acc*65I restriction sites. A glycine was again introduced as second residue in the *px IV* sequence as described in chapter 3.3.2. Thus, the PCR product of the pETtrx_PxIV was ligated with the

*Nco*I- and *Acc*65I-digested pET-1a vectors. Expression of the respective fusion proteins was induced as listed in Table 3.1 and pellet and supernatant fractions were analyzed by SDS-PAGE and Coomassie staining (Figure 3.37). Except for the leaky expression of NusA-Px IV, all other fusion proteins displayed a prominent band in the soluble fraction. The GB-Px IV was subjected to preparative protein purification. However, there was no good expression in the crude soluble extract compared to the small test expression (data not shown). After the second Ni^{2+}-NTA column, untagged recombinant protein was not detectable in the elution fraction. Clearly, the expression conditions need further optimization.

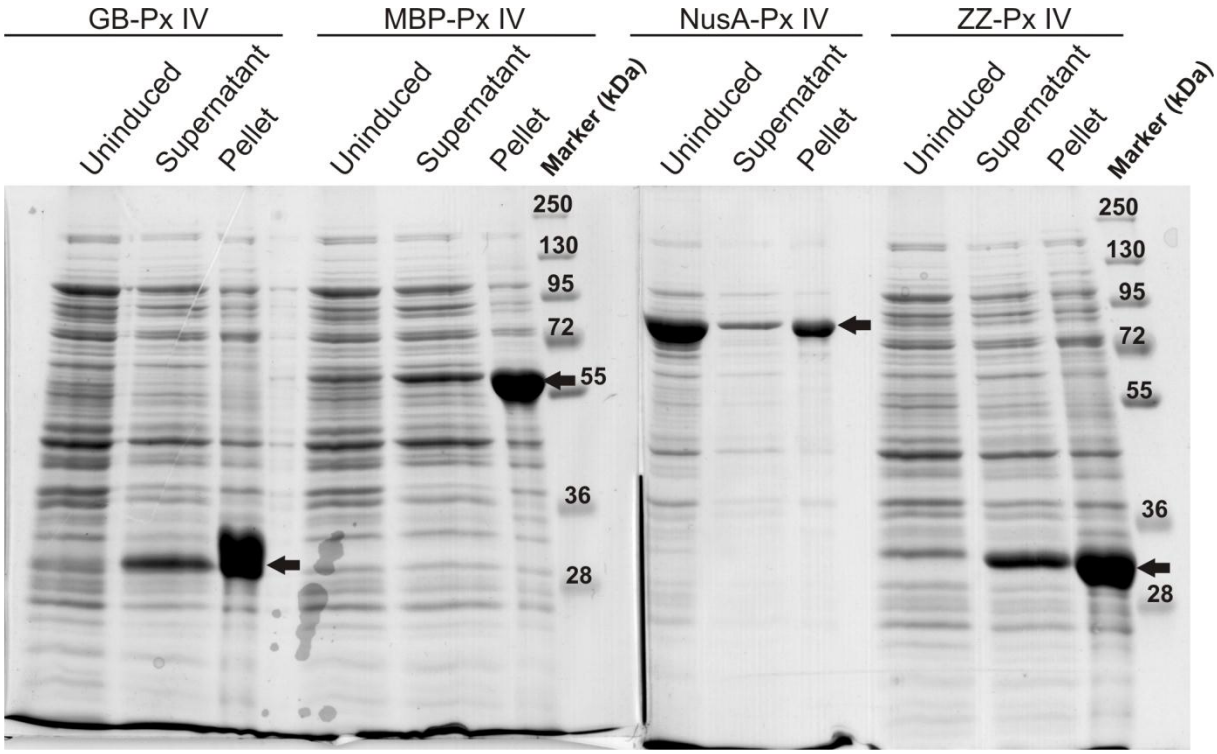

Figure 3.37: Different fusion partners increase the solubility of Px IV. BL21 (DE3) cells were transformed with the pET-1a plasmids encoding Px IV with GB, MBP, NusA or ZZ as N-terminal fusion partners. For detailed expression conditions see Table 3.1. Uninduced total lysates were collected prior to the addition of IPTG and directly boiled in sample buffer (uninduced). Boiled pellet and supernatant fractions of the induced cultures were applied onto a 10% SDS gel and stained by Coomassie. The black arrows mark the expressed fusion proteins.

3.3.10 Generation of a px IV$^{-/-}$ cell line

Ilon Liu created two single KO *px IV* cell lines (*px IV*$^{+/-}$) introducing the pHD1747_KO*pxIV* plasmid into BS WT 449 as well as B2T1 cells inducibly expressing c-myc tagged Px IV [Liu, 2015]. I tried to transfect these cells several times with the second pHD1748_KO*pxIV* construct in the presence of Trolox but did not obtain clones. In the case of the B2T1 *px IV*$^{+/-}$ cells, expression of the c-myc-Px IV was induced using doxycycline and different

concentrations of tetracycline (Figure 3.38). After 24 h as well as 72 h, the myc-tagged protein was expressed upon both, tetracycline and doxycycline treatment independently of the concentration used. No leaky expression was observed in the absence of the inducer.

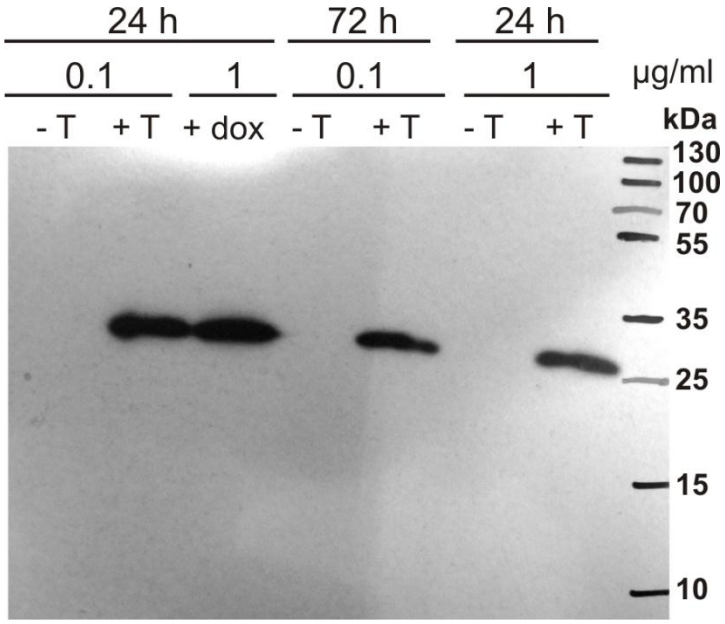

Figure 3.38: Expression of c-myc tagged Px IV in the *px IV*$^{+/-}$ cells by tetracycline and doxycycline. *Px IV* $^{+/-}$ cells (clone 2A1) allowing the inducible expression of c-myc-tagged Px IV were treated with 0.1 and 1 µg/ml tetracycline (T) or 1 µg/ml doxycycline (dox) for 24 and 72 h. 1.2 x 10^6 (for 1 µg/ml ± T) and 5 x 10^6 cells (all other conditions) were harvested and the total lysates were subjected to Western blot analysis using the monoclonal myc antibodies.

To verify the proper expression of the blasticidin resistance gene in the *px IV* locus, BS WT 449 parasites were transfected with pHD1748_KO*pxIV* plasmid to obtain single KO clones. This transfection experiment was repeated twice without success. Thus, we decided to use the neomycin resistance cassette to generate *px IV* KO cell lines. Under my supervision, Samantha Ebersoll replaced the puromycin by the neomycin selection gene to yield the pHD1747-Neo_KO*pxIV* vector using *Eco*RI and *Hind*III restriction sites. BS WT 449 parasites were transfected and after the selection process by a serial dilution, we obtained three clones: 1D2, 2C4, and 2C5. The correct replacement was verified by PCR analysis and Samantha Ebersoll transfected the puromycin-resistant *px IV*$^{+/-}$ 2D3 clone (from Liu, chapter 2.1.6) with the pHD1747-Neo_KO*pxIV* in the presence Trolox. After dilution in 24-well plates in medium ± Trolox, living but slowly moving parasites were transferred into 5 ml culture flasks. Some clones died immediately, others were proliferating and lysing to the same extent. After two weeks without seeding, one clone (1C1) survived in the presence of Trolox but did not display proper proliferation. After another week, when the *px IV*$^{-/-}$clone was grown to sufficient density, genomic DNA was isolated, and subjected to PCR analysis. To verify the correct replacement of the *px IV* alleles by the resistance genes, I used a forward primer inside the resistance cassette and a primer outside of the cloning region: for *neo*, NeoF_BM

and PxIV_3'UTR_Ext, and for *pac*, PuroF_CH1 and PxIV_3'UTR_Ext. Both PCR analyses yielded the expected bands, 928 bp (*neo*) and 788 bp (*pac*) (Figure 3.39). The absence of the *px IV* gene was verified by two internal primers. The PCR product of the WT DNA displayed the *px IV* gene (409 bp). The DNA of the mutant showed no band with the correct size which is a strong indication of a real *px IV*$^{-/-}$clone. The two additional bands of around 300 and 700 bp are probably unspecific bands. However, the PCR reactions using only one primer resulted not in these cross-reaction bands (Figure 3.39B).

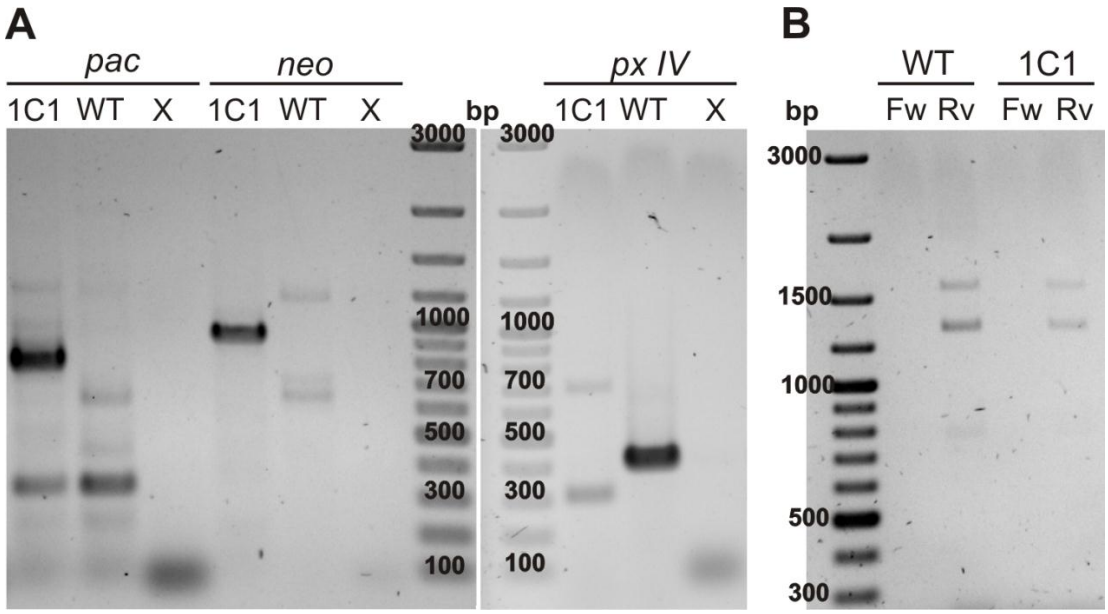

Figure 3.39: PCR analysis of the single *px IV*$^{-/-}$ clone 1C1. Genomic DNA of WT and *px IV*$^{-/-}$ (clone 1C1) cells was isolated and subjected to PCR followed by electrophoresis on a 1% agarose gel. **A.** Different primer pairs were used (*pac*: PuroF_CH1 and PxIV_3'UTR_Ext, 788 bp; *neo*: NeoF_BM and PxIV_3'UTR_Ext, 928 bp; *px IV*: Px4 Internal Fw and Px4 Internal Rv, 409 bp). PCR reaction without DNA to exclude contaminations (X). **B.** PCR with either the Px4 Internal Fw or Px4 Internal Rv primer on WT and mutant DNA.

3.3.11 Proliferation of the px IV$^{-/-}$ *cells is Trolox-independent*

To analyze if the *px IV*$^{-/-}$ 1C1 cell line required Trolox for viability as it is the case for the BS *px I-II*$^{-/-}$ and PC *px I-III*$^{-/-}$ parasites, the antioxidant was removed from the medium and the short-term (for 6 h) and long-term (for 72 h) proliferation were followed at 37 °C (Figure 3.40A and B). Puromycin and G418 were always removed prior to the experiment to exclude antibiotic-related proliferation defects. The mutant parasites were fully viable after the withdrawal of Trolox. The KO of *px IV* was not lethal in this single cell line which points to the dispensability of the protein under culture conditions. However, the BS *px IV*$^{-/-}$ 1C1 cell line showed a clear proliferation defect when compared to WT 449 cells. Every 24 h, the cultures were diluted back to the start density of ~1 x 10^5 cells/ml. The mutant cells grew 30%

slower than the WT cells independent of Trolox (Figure 3.40C). Thus, the lack of Px IV results in an impaired proliferation.

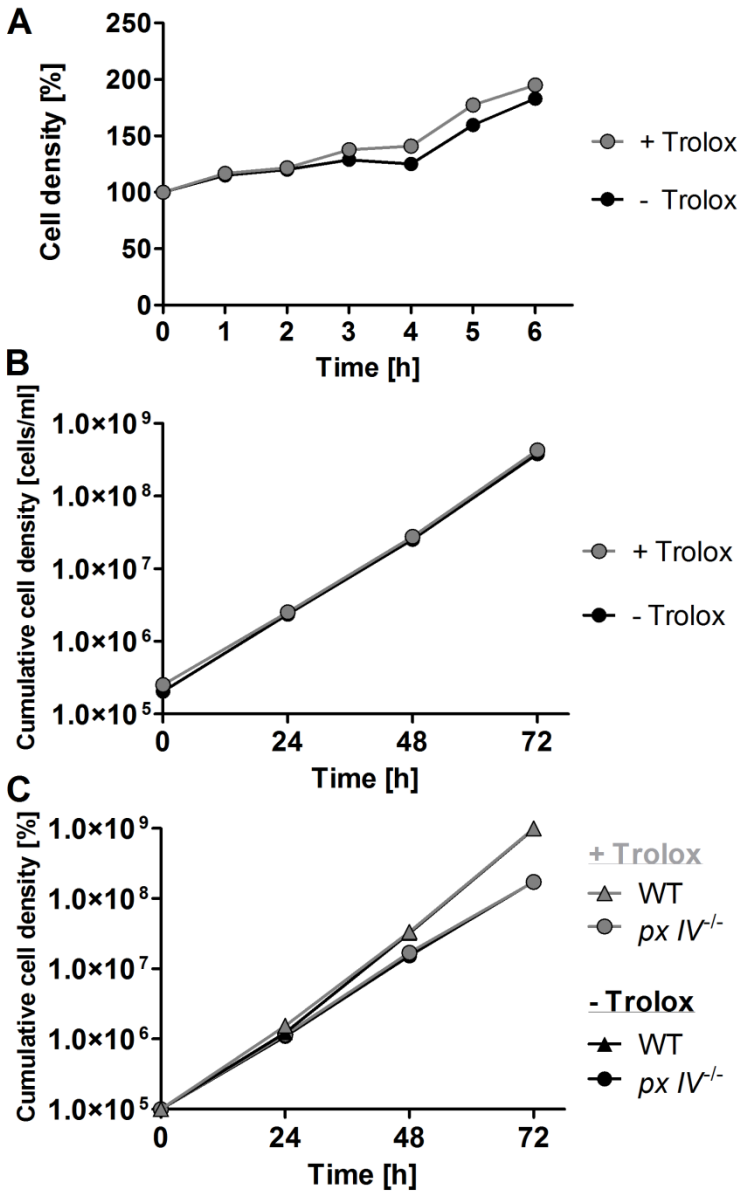

Figure 3.40: Deletion of Px IV results in a growth defect of BS *T. brucei* that cannot be rescued by Trolox. *Px IV*$^{-/-}$ cells were cultured in the presence of 100 µM Trolox. Cell viability experiments were performed in medium ± Trolox and without the antibiotics puromycin and G418 at 37 °C for **A.** 6 h and **B.** 72 h. **C.** WT and *px IV*$^{-/-}$ cells were cultured in medium ± Trolox at 37 °C for 72 h and every 24 h diluted back to the starting cell density.

3.3.12 Cloning of the untagged Px IV over-expressing plasmid

To create BS *px IV*$^{-/-}$ parasites with an inducible system to express an ectopic copy of Px IV, Philippa Lantwin under my supervision cloned the respective pHD1700 vector. The coding region of *px IV* was isolated from genomic DNA and ligated into the vector using *Mlu*I and *Bam*HI restriction sites. The pHD1700_PxIV plasmid was sequenced confirming the complete and correct sequence of *px IV* including the stop codon, the tetracycline operator, and almost the whole sequence of the GPEET promoter. The adjacent region upstream of the *px IV* gene as well as the adjacent region downstream corresponding to the myc-tag could not be clearly sequenced three times and showed overlapping signals for different bases. The original pHD1700 plasmid seemed to be contaminated or damaged. Thus, the cloning will be repeated using another pHD1700 stock.

4 Discussion and Outlook

The text of the following chapter 4.1 has been taken from Hiller *et. al.* 2014 and has been originally written by myself:

4.1 The functional role of thiol peroxidases in BS parasites

"African trypanosomes express three virtually identical Px-type proteins in the cytosol (Px I-II) and mitochondrion (Px III). The closest related enzyme in higher organisms is GPx4 [Brigelius-Flohé and Maiorino, 2013; Ursini *et al.*, 1999]. Both types of enzymes have in common that they are monomeric proteins, prefer lipid-derived hydroperoxides as substrates, and their physiological functions can be replaced by α-tocopherol or Trolox but not by water-soluble antioxidants [Diechtierow and Krauth-Siegel, 2011; Seiler *et al.*, 2008; Yoo *et al.*, 2010]. In contrast to GPx4, the parasite Px I-III do not contain a selenocysteine but a cysteine residue in the active site and obtain their reducing equivalents from the kinetoplast-specific trypanothione/tryparedoxin system, not from glutathione [Hillebrand *et al.*, 2003; Schlecker *et al.*, 2005]. In mammals, the cytosolic GPx4 is the only known glutathione peroxidase that is essential. The inducible inactivation of the cytosolic GPx4 in mice revealed that the enzyme counteracts the activity of 12/15 lipoxygenase which catalyzes hydroperoxide formation in membranes and triggers an apoptosis-inducing factor-mediated cell death [Seiler *et al.*, 2008]. Intriguingly, the mechanism of cell death remained unclear since the canonical markers of programmed cell death (e.g. caspase 3 activation, phosphatidylserine exposure) were not detected. Only disruption of the mitochondrial membrane potential was observed as a late event upon induction of the GPx4 KO [Seiler *et al.*, 2008]." [Hiller *et al.*, 2014]

"Here we show that the lethal phenotype of BS *px I-II*$^{-/-}$ trypanosomes originates from the damage of their lysosome. *Px I-II*$^{-/-}$ cells deprived of Trolox and treated with Alexa Fluor-conjugated dextran became completely fluorescent with time; and cells fed with LysoTracker lost the fluorescent signal totally. The enlarged but still confined fluorescent signal observed in a fraction of the dextran-fed *px I-II*$^{-/-}$ parasites indicates that lysosomal swelling may precede rupture of the organelle. Our data did not support a specific pore formation in the lysosomal membrane as it is the case in parasites treated with the TLF component apoL-I [Pérez-Morga *et al.*, 2005; Vanhollebeke *et al.*, 2007]. Probably a reduced rate of export

and/or recycling of (the damaged) membrane and content contributes to the enlargement of the lysosome, a mechanism discussed in the context of p67-ablated parasites [Peck *et al.*, 2008]. Accordingly, the immunofluorescence analysis of *px I-II*$^{-/-}$ cells with p67 as lysosomal marker showed a progressive loss of the discrete organelle signal. All these findings strongly suggest that cell death starts with disintegration of the lysosome and likely evolves to massive membrane damages, as shown here for the mitochondrion. The absence of these cytosolic peroxidases probably affects the integrity of all (sub)cellular membranes. The Px-type enzymes use trypanothione as substrate suggesting that a decrease of the low molecular weight thiol should cause a similar phenotype. Indeed, the ultrastructural analysis of *T. brucei* depleted of trypanothione synthetase indicates membrane damage at several organelles [Comini *et al.*, 2004]. However, lowering the trypanothione level will affect also the Prx-type peroxidase and many other redox pathways and therefore the overall cellular redox state." [Hiller *et al.*, 2014]

"Lysosomes are oxidizing rather than reducing compartments [Austin *et al.*, 2005] and therefore should require the presence of effective antioxidant systems. Dietary vitamin E has been reported to result in increased α-tocopherol levels in the lysosomal fractions and to prevent lysosomal release [Mukherjee *et al.*, 1997]. The full rescue of the lethal phenotype of the *px I-II*$^{-/-}$ parasites by Trolox strongly suggests that one physiological role of the cytosolic peroxidases is protection of the lysosomal membrane from peroxidation." [Hiller *et al.*, 2014]

"Both free iron and heme are known to react with hydrogen peroxide to generate highly oxidizing species that are capable of initiating lipid peroxidation [Higdon *et al.*, 2012; Widener *et al.*, 2007]. Indeed, supplementing Trolox-free medium with iron or holo-transferrin accelerated lysis of the *px III*$^{-/-}$ cells whereas the removal of FCS or addition of apo-transferrin slowed down trypanolysis. In addition, the use of transferrin-depleted medium suggests that also iron derived from the uptake and degradation of hemoglobin contributes to the lethal phenotype of the *px I-II*$^{-/-}$ cells in the absence of Trolox. The lysosomal iron probably induces damage of the organelle membrane by inducing a Fenton-like reaction as described previously [Widener *et al.*, 2007]. In line with a key role of iron in lysosomal damage, treatment of *px I-II*$^{-/-}$ cells with the iron chelator deferoxamine [Breidbach *et al.*, 2002; Comini *et al.*, 2008] increased their short-term viability in Trolox-free medium. In human epithelial cells and lysosome-rich murine macrophage-like J774 cells, deferoxamine localizes almost exclusively within these organelles [Doulias *et al.*, 2003; Persson *et al.*,

2003]. Also for *T. brucei*, the lysosome has been suggested as an iron storage organelle [Lu *et al.*, 2007] and a mucolipin 1 orthologue has been implicated in iron transport into the cytosol [Taylor *et al.*, 2013]. Intralysosomal iron can powerfully synergize oxidant-induced cellular damage. The steps associated with cell collapse in different mammalian cell lines were not fully understood [Denamur *et al.*, 2011; Doulias *et al.*, 2003] although it was clear that lysosomal disruption entailed cell death [Kurz *et al.*, 2006].“ [Hiller *et al.*, 2014]

“In BS *px I-II*$^{-/-}$ *T. brucei*, the cellular damage is apparently linked to endocytosis. This is supported by several observations. In the absence of FCS, the *px I-II*$^{-/-}$ cells do not require Trolox for short-term viability and are even insensitive towards exogenous iron. This would not be expected if the cellular damage started at other membranes such as e. g. that of the glycosomes or mitochondrion or the plasma membrane. Disintegration of the cell membrane as primary event could be ruled out also by the fact that after feeding with fluorescent dextran and transfer into Trolox-free medium, a large proportion of the *px I-II*$^{-/-}$ cells became completely stained. Since in a variety of other cell types, the mitochondrion is the origin of endogenous oxidative stress we studied the damage of the lysosome and mitochondrion in more detail. In the *px I-II*$^{-/-}$ parasites, mitochondrial damage occurs but follows the disintegration of the lysosome. The order of events is thus opposite to that in cells with injured mitochondria where externalization of cardiolipin to the outer mitochondrial membrane acts as an elimination signal for the mitochondrion by autophagy [Chu *et al.*, 2013].” [Hiller *et al.*, 2014]

“Notably, any treatment, such as with exogenous iron, hemoglobin or transferrin affected the viability of the *px I-II*$^{-/-}$ cells only in the absence of Trolox. All of these compounds enter the parasite via the endocytic pathway suggesting that the extremely fast lethal phenotype of BS trypanosomes that lack the cytosolic peroxidases is linked to their high endocytic rate. Taken together, disintegration of other intracellular membranes and the plasma membrane appears to be a secondary event or is at least much slower than lysosomal damage.“ [Hiller *et al.*, 2014]

“Parasites inhabiting the insect vector harbor a fully developed mitochondrion rich in cytochromes and Krebs cycle enzymes, many of which require iron or iron/sulfur complexes as cofactors [Dellibovi-Ragheb *et al.*, 2013]. Strikingly, in the insect stage, the cytosolic Px I-II proved to be entirely dispensable under culture conditions. One reason may be the lower endocytic activity of the PC cells compared to BS parasites [Natesan *et al.*, 2007]. In addition,

PC *T. brucei* do not express a transferrin receptor [Ligtenberg *et al.*, 1994] but can take up iron via specific transporters [Mach *et al.*, 2013] or extract it from internalized hemin as it is the case in *L. infantum* [Carvalho *et al.*, 2009]. *L. amazonensis* has been shown to express a heme transporter (LHR1) in both the plasma membrane and acidic endocytic compartments; and highly syntenic, close homologs are present in *T. brucei* [Huynh *et al.*, 2012]. The direct delivery to the cytosol and/or the rapid transport from the lysosome into the mitochondrion probably precludes lysosomal iron accumulation in the PC cells and thus, renders Px I-II not necessary for protection of this organelle towards iron-mediated lipid peroxidation. On the other hand, these stage-specific differences highlight the biological role of the cytosolic peroxidases at the interface between iron homeostasis and protection against iron-induced and lipid-derived oxidative stress in the pathogenic stage of the parasites." [Hiller *et al.*, 2014]

"BS *T. brucei* lack an active respiratory chain [Tielens and Van Hellemond, 1998] and, although obligate, mitochondrial iron-sulfur cluster biosynthesis is much lower compared to the insect stage [Kovárová *et al.*, 2013; Taylor and Kelly, 2010]. These may be main reasons why BS parasites in which the mitochondrial *px III* gene has been knocked out do not display any strong proliferation phenotype [Diechtierow and Krauth-Siegel, 2011]. The *in vivo* data presented" in Hiller *et al.* 2014 "revealed that the Px III is not essential for infectivity and survival although mutant parasites grown *in vitro* prior to infection displayed a slightly delayed proliferation and disease development compared to WT pathogens. The cytosolic isoenzymes are probably sufficient for protecting the membranes of the metabolically repressed mitochondrion of BS parasites." [Hiller *et al.*, 2014]

"As shown here for African trypanosomes, cytosolic glutathione peroxidase-type enzymes are responsible for protecting the lysosome from oxidative membrane damage. To our knowledge, this is the first report demonstrating such function for cytosolic thiol peroxidases. The underlying molecular mechanism is not yet known and we can only speculate. Peroxidized phospholipids formed in the inner leaflet of the organelle membrane may be exchanged with lipids in the outer leaflet to allow the subsequent repair by the cytosolic peroxidases. In addition, it remains elusive if this lipid exchange would be a spontaneous or catalyzed process. At least for the plasma membrane of different *Leishmania* species, a phospholipid scramblase activity has been described [dos Santos *et al.*, 2013]. In addition, cardiolipin externalization to the outer mitochondrial membrane has been demonstrated recently [Chu *et al.*, 2013]. Although not yet investigated in detail, it is worth to note that

other human pathogens such as *Trichomonas*, *Toxoplasma*, and *Entamoeba* can acquire iron via endocytic uptake of host Fe-binding proteins such as transferrin, lactoferrin, and ferritin (for reviews see [López-Soto *et al.*, 2009; Ortíz-Estrada *et al.*, 2012]) and the genomes of *T. vaginalis* and *T. gondii* encode Px homologues. Future work by others may reveal if our findings are extensible to these pathogens and the mammalian GPx4." [Hiller *et al.*, 2014]

4.2 The physiological role of Px I-III in PC parasites

In the mammalian form of African trypanosomes, KO of the cytosolic peroxidases (Px I-II) is lethal but cell viability and proliferation can be fully rescued by supplementing the medium with Trolox [Diechtierow and Krauth-Siegel, 2011]. In contrast, the mitochondrial Px III is dispensable *in vitro* and in an *in vivo* mouse model [Diechtierow and Krauth-Siegel, 2011; Hiller *et al.*, 2014]. Earlier RNAi approaches – which cause the simultaneous depletion of all three (virtually identical) peroxidase mRNAs – had revealed severe growth defects in both BS and PC parasites [Schlecker *et al.*, 2005; Wilkinson *et al.*, 2003]. This indicated that also in the insect stage at least one of the peroxidases is essential. Recently, Amrei Nißen generated PC *T. brucei* specifically lacking the cytosolic peroxidases [Nißen, 2014]. These *px I-II*$^{-/-}$ cells proved to be fully viable in standard MEM-Pros medium independent of the presence or absence of Trolox. As shown here, even supplementing the medium with exogenous Fe^{2+} and Fe^{3+} did not affect the short-term viability of PC *px I-II*$^{-/-}$ cells. To evaluate if in the mutants some of the mitochondrial Px III might have resided in the cytosol, Natalie Dirdjaja subjected the mutant cells to a fractionated digitonin lysis and subsequent Western blot analysis using LipDH and Tpx as mitochondrial matrix and cytosolic marker proteins, respectively (data not shown). At low digitonin concentrations which solubilized Tpx, the peroxidase was undetectable in the soluble fractions. Instead, Px III co-eluted with LipDH at high digitonin concentrations. Thus, the cytosolic forms of the peroxidases are dispensable in the PC parasites at least under culture conditions. Next, we generated PC *T. brucei*, which lacked the mitochondrial peroxidase as well as the *px I* gene (*px I/III*$^{-/-}$ cells). Due to a mutation in the active site, Px I has no peroxidase activity in Lister strain 427 and should not alter the phenotype [Diechtierow and Krauth-Siegel, 2011]. The PC *px I/III*$^{-/-}$ cell line displayed only a transient proliferation defect. Px III seems not to be necessary for cell survival and proliferation although the absence of defects in the *px I-II*$^{-/-}$ may imply that Px III is more important than the cytosolic counterparts. The transient proliferation defect is probably overcome by the upregulation of an antioxidant protein or a low molecular mass thiol.

Finally, we replaced the complete genomic locus by resistance genes. In medium supplemented with Trolox, these PC *px I-III*$^{-/-}$ cells were fully viable and proliferated as WT controls. However, in Trolox-free medium, the mutant cells lysed within 4 h. At least one of the peroxidases appears to be essential in accordance with the RNAi experiments described above. Interestingly, the novel data suggest that PC *T. brucei* require either the cytosolic or the mitochondrial isoenzyme for survival and proliferation in culture. In BS *px I-II*$^{-/-}$ trypanosomes, the cellular alterations and finally the lysis observed upon transfer into Trolox-free medium originates from damages within the lysosome as discussed in the previous section 4.1. To get an insight in the order of morphological changes linked to the deletion of the whole *px* locus in the insect stage of *T. brucei*, the PC *px I-III*$^{-/-}$ cells were incubated in Trolox-free medium and after various times investigated by immunofluorescence microscopy. Antibodies against p67 and aldolase were used to visualize the lysosome and the glycosomes, respectively, and MitoTracker Red as an indicator for a fully functional mitochondrion. Intriguingly, the mutant parasites lost their mitochondrial membrane potential prior to the disappearance of the lysosomal signal. Moreover, the glycosomes maintained an accurate aldolase staining even after 4 h in Trolox-free medium when the majority of remaining intact cells had already lost the mitochondrial as well as lysosomal signals. Thus, as in most other cell types (for reviews see [Kowaltowski *et al.*, 2009; Murphy and Smith, 2007; Turrens, 2003]), in the insect form of African trypanosomes, the mitochondrion appears to be the main source of ROS and site of intracellular membrane damage. The finding that the glycosomes did not display any damage in the *px I-III*$^{-/-}$ cells was rather intriguing as the Px III possesses a putative C-terminal glycosomal targeting signal and the protein had been identified in the proteome analysis of PC glycosomes [Colasante *et al.*, 2006]. Nevertheless, the data presented here show that the protein does not play a crucial role in PC *T. brucei* under culture conditions.

Supplementing the medium with Fe^{2+} or Fe^{3+} accelerated the lysis of PC *px I-III*$^{-/-}$ parasites. PC *T. brucei*, unlike the infective form, do not possess a transferrin receptor but take up iron from ferric complexes via a reductive mechanism [Mach *et al.*, 2013]. At a concentration of 100 µM, both iron ions lowered the viability of the *px I-III*$^{-/-}$ cells to the same extent. This may suggest that reduction of Fe^{3+} by the putative ferric reductase is fast compared to the subsequent transport of Fe^{2+} across the plasma membrane. Alternatively, at the high concentration, iron may enter the cell independent of the transporter. Anyhow the accelerated lysis observed should be related to iron inside the cell. An unspecific damage of the plasma

membrane by the exogenous iron is unlikely as the PC *px I-II*$^{-/-}$ as well as WT cells were completely unaffected by this treatment. Iron taken up by PC cells is transported to, and used in, the mitochondrion [Mach *et al.*, 2013]. The transport may be mediated by MCP17, displaying similarities to human and yeast iron carriers [Colasante *et al.*, 2009]. Another protein importing iron from the cytosol into the organelle is the MCU as shown in hepatocytes [Uchiyama *et al.*, 2008; Zhang and Lemasters, 2013]. If the MCU of *T. brucei* [Huang *et al.*, 2013] has a respective function remains to be investigated. Thus, one may speculate that the mitochondrial iron pool contributes to the lethal phenotype of the PC *px I-III*$^{-/-}$ cells.

The MEM-Pros medium we used for the cultivation of PC *T. brucei* is supplemented with 11 µM of hemin but does not contain any added iron salt. Thus, either the free iron present in the FCS is sufficient or the parasites acquire iron from hemin. In trypanosomatids, a heme oxygenase gene has not yet been identified [Korený *et al.*, 2013]. However, iron can be released from heme by reductive (e.g. glutathione; [Atamna and Ginsburg, 1995]) or oxidative agent (e.g. hydrogen peroxide [Gutteridge, 1986; Nagababu and Rifkind, 2000]). Heme as iron source has been reported for *L. infantum* [Carvalho *et al.*, 2009]. Trypanosomes are heme-auxotroph and so, require heme as a co-factor for many mitochondrial proteins [Korený *et al.*, 2010; Tripodi *et al.*, 2011]. As in the case of free iron, high concentrations of exogenous hemin further augmented lysis of the PC *px I-III*$^{-/-}$ in Trolox-free medium but did not have any effect in the presence of the antioxidant as well as against WT cells. Most probably, the harmful effect exerted by heme at high concentrations is probably unrelated to the physiological uptake mechanisms for heme but due to a spontaneous association with and efflux from the membrane lipid bilayer as shown for liposomes of variety of compositions [Cannon *et al.*, 1984]. *L. infantum* have been shown to bind hemin with a dissociation constant as low as 44 pM [Carvalho *et al.*, 2009], the respective transporter is probably LHR1, an essential transmembrane protein located in the plasma membrane as well as late endosomes/lysosomes for which a close homolog is present in *T. brucei* [Huynh *et al.*, 2012]. Thus, the putative heme transporter should be saturated at submicromolar heme concentrations. Heme uptake in form of hemoglobin as in BS *T. brucei* does not occur as the insect stage lacks the haptoglobin/hemoglobin receptor [Vanhollebeke *et al.*, 2008]. Taken together, the increase of lysis of the PC *px I-III*$^{-/-}$ cells observed upon supplementing the medium with 100 µM of either ferrous or ferric iron as well as hemin reinforced the conclusion that lysis of the PC *px I-III*$^{-/-}$ cells in Trolox-free medium is linked to the cellular

iron metabolism. However, more importantly, the lethal phenotype is only slightly slower in the absence of additional external stressors.

To further corroborate the role of intracellular iron in the process, the parasites were treated with iron chelators. Deferoxamine is a polar iron chelating agent that mainly localizes within lysosomal compartments [Persson *et al.*, 2003]. At high concentrations, however, deferoxamine might be distributed to a minor extent in the cytosol and other cellular organelles [Zhang and Lemasters, 2013]. In contrast, starch-deferoxamine should exclusively be taken up by fluid-phase endocytosis and accumulate in the lysosome. Deferoxamine prevented the lysis of the PC *px I-III*$^{-/-}$ cells in Trolox-free medium unlike starch-deferoxamine which showed only a marginal protective effect. In comparison, BS *px I-II*$^{-/-}$ cells were equally protected by starch-deferoxamine as well as deferoxamine. These findings are in accordance with our previous results that in BS cells the lysosome is the primary site of iron-mediated cellular damage. In contrast, in PC parasites the iron-induced oxidative stress originates from another organelle. To further corroborate that this subcellular structure is the mitochondrion, we studied the effect of MitoQ and free ubiquinone towards the mutant parasites.

MitoQ (Mitoquinone) is a ubiquinone conjugated to a delocalized cation (triphenylphosphonium) which is highly efficient in suppressing mitochondrial oxidative damage [Jauslin *et al.*, 2003]. In Trolox-free medium, 30 or 100 nM MitoQ completely restored the short-term viability of the PC *px I-III*$^{-/-}$ cells. As expected, MitoQ was more effective than the untargeted decylubiquinone. Interestingly, MitoQ was also superior in protecting the BS *px I-II*$^{-/-}$ against cell death. This may be explained by the fact that, driven by the membrane potential of the plasma membrane, the positively charged MitoQ is selectively taken up into the cytosol resulting in a 5 - 10 fold accumulation [Jauslin *et al.*, 2003; Murphy, 2008]. This could explain the higher efficiency of MitoQ in protecting other subcellular membranes [Murphy and Smith, 2007] such as the lysosome in the case of BS *px I-II*$^{-/-}$ cells. These data, however, also revealed that the higher protective power of MitoQ compared to ubiquinone does not necessarily allow the conclusion that the mitochondrion is the targeted organelle.

Small pools (< 20 µM) of labile Fe^{2+} reside in the cytosol and the mitochondrial matrix as well as the lysosome of eukaryotic cells [Dixon and Stockwell, 2014]. These redox-active

iron pools are capable of directly catalyzing the formation of damaging free radicals from hydrogen peroxide via the Fenton reaction [Koskenkorva-Frank *et al.*, 2013]. These radicals can damage all biomolecules and cause further side reactions including the initiation of lipid peroxidation [Valko *et al.*, 2007]. Accumulation of hydrogen peroxide by exposing the cells to the oxidant or by deleting stress-responsive transcription factors and repair enzymes has been shown to arrest cell growth owing to Fenton chemistry-dependent DNA damage [Dixon and Stockwell, 2014]. As shown here, deletion of the lipid hydroperoxide-detoxifying enzymes results in an iron-mediated cell death in the absence of any additional stress. Thus, the levels of free iron and of ROS in the unstressed cell are sufficient to severely damage membranes. The requirement for lipid hydroperoxide detoxifying enzymes has also shown in mammalian cell where the lack of the cytosolic form of GPx4 results in 12/15-lipoxygenase-mediated lipid peroxidation and mitochondrial membrane potential disruption followed by apoptosis [Seiler *et al.*, 2008]. Thus, this closest related enzyme displays a conserved physiological function between humans and trypanosomes.

Iron acquisition pathways are different in both parasite forms. BS cells fulfill their iron demand by the receptor-mediated endocytosis of host transferrin [Schell *et al.*, 1991; Steverding, 1998; Steverding *et al.*, 1995] and release their iron probably by a mucolipin-type 1 import channel into the cytosol [Taylor *et al.*, 2013]. In contrast, the iron uptake mechanism in the insect stage is still not fully understood. It is proposed that ferrous iron post reduction is taken up via a transmembrane transporter through the plasma membrane [Mach *et al.*, 2013]. Another main difference between the two life cycle stages is the energy metabolism. BS parasites exclusively rely on glycolysis [Tielens and van Hellemond, 2009]. Here, the mitochondrion is of less importance as reflected in the kinetoplast loss of *T. evansi* and *T. equiperdum* [Lai *et al.*, 2008]. The differentiation to PC cells leads to a complex mitochondrial energy metabolism resulting in the development of an active cytochrome-containing respiratory chain and the expression of TCA cycle enzymes for ATP production [Tielens and van Hellemond, 2009]. This explains the higher iron needs of PC parasites compared to BS cells [Taylor and Kelly, 2010]. RNAi studies in PC reveal that the knockdown of Fe/S cluster containing proteins causes a switch towards a BS-like metabolism [Horváth *et al.*, 2005]. These results highlighted a direct linkage between the energy metabolism and the iron usage in *T. brucei* and explain the distinct phenotypes observed upon deletion of the Px-type enzymes in both life stages.

The iron storage in trypanosomes is not yet elucidated. The lysosome is proposed as a putative storage organelle [Lu *et al.*, 2007]. Recent studies also highlighted acidocalisomes as iron-containing organelles [Blaby-Haas and Merchant, 2014]. Acidocalisomes are rich in phosphorus compounds and cations in form of calcium, zinc, and iron [Docampo and Huang, 2014]. A proteomic analysis of *T. cruzi* identified a putative metal iron transporter [Ferella *et al.*, 2008b]. The mitochondrion is the main source of superoxide anion and H_2O_2 produced by the superoxide dismutase [Turrens, 2003]. Iron is not only present as labile pool in the mitochondrion; it can be also released from iron-containing proteins by superoxide as shown for the Fe/S-containing aconitase [Liochev and Fridovich, 1994; Vasquez-Vivar *et al.*, 2000]. Thus, this organelle is a putative source of Fenton-induced oxidative stress leading to membrane rupture by its iron pool [Koskenkorva-Frank *et al.*, 2013].

How the cytosolic peroxidases can protect subcellular membranes from lipid peroxidation which most probably occurs at the luminal face we do not know. We may speculate that peroxidized lipids are translocated from the inner to the outer mitochondrial membrane as it was described for cardiolipin in mitochondrial autophapy due to mitochondrial injuries [Chu *et al.*, 2013]. The exchange of phospholipids within a membrane bilayer is mediated by ATP-dependent flippases or ATP-independent scramblases [Pomorski and Menon, 2006]. Maybe these enzymes can also exchange oxidized versus intact phospholipids, anyhow they still need to be identified in trypanosomes. The *T. brucei* homologue of a putative yeast flippase is not required for the flipping of glycosylated dolichol in the ER but most probably acts as a chaperone [Jelk *et al.*, 2013]. Finally, lipid traffic between organelles could explain the exchange of damaged lipids and the protection by the differently located peroxidases [Holthuis and Menon, 2014].

4.3 Px IV, a challenging protein

In *T. cruzi*, Px IV is described as a glutathione-dependent peroxidase which is involved in the reduction of phospholipid and fatty acid hydroperoxides in the ER [Wilkinson *et al.*, 2002b]. The sequence analysis of Px IV revealed eight cysteines. The catalytic triad composed of cysteine, glutamine, and tryptophan is conserved in the proteins from different Kinetoplastida species. The prediction of subcellular localization yielded a variety of possibilities ranging from mitochondrial (43% MitoProt II), cytosolic (48% PSORT II, 53% ESLpred) or secreted (46% TargetP 1.1, 80% CELLO v.2.5) probably because the prediction programs are made

for proteins of higher eukaryotes. Ilon Liu showed in her MD thesis (2015) that c-myc tagged Px IV was found in the mitochondrion whereas the n-myc tagged protein was cytosolic suggesting a mitochondrial localization with a putative (unidentified) N-terminal MTS. Specific Px IV antibodies, that would allow immunofluorescence microscopy, are still missing to confirm this localization. In contrast to the mitochondrial Px III of *T. brucei*, a cleavable N-terminal MTS was not identified. In general, the MTS in trypanosomatids are much shorter compared to higher eukaryotes like animals and plants [Schneider *et al.*, 2008]. Six to eight residues comprising serine, leucine, and basic amino acids seem to be sufficient for protein import into the mitochondrion as for instance in *T. brucei* Px III (MLRSSRKK). The N-terminal residues of Px IV are MNGGAIFSHSVL; at least no acidic amino acids are present. An internal MTS as shown for the alternative oxidase [Hamilton *et al.*, 2014] can be virtually excluded because the mitochondrial targeting can be blocked by a myc-tag situated on the N-terminus of Px IV.

Px IV is only distantly related to the human GPxs and does not allow any conclusion regarding its function. The closest related human GPx7 and 8 show protein disulfide isomerase-dependent peroxidase activity involved in oxidative protein folding and ER-stress protection [Nguyen *et al.*, 2011; Ramming and Appenzeller-Herzog, 2013]. The enzymes contain ER-retention signals (REDL and KEDL). Whereas GPx7 exhibits an N-terminal signal peptide, GPx8 is a transmembrane protein with an annotated membrane region close to the N-terminus [Ramming and Appenzeller-Herzog, 2013]. *T. brucei* Px IV does not display a membrane-spanning or -associated sequence and lacks a conventional (KDEL) or trypanosomal (MDDL or KQDL) C-terminal ER-retention signal [Andres *et al.*, 1991; Bangs *et al.*, 1993]. However, for trypanosomes, divergent ER retention signals were proposed [Bangs *et al.*, 1993].

For the respective *T. cruzi* Px IV, ER-localization was suggested based on immunofluorescence microscopy by co-staining using *T. brucei* anti-BiP and *T. cruzi* anti-Px IV antibodies. Only two cells were depicted with different morphology. Both displayed a rather diffuse Px IV staining pattern which did not completely overlap with the one from the ER chaperone BiP [Wilkinson *et al.*, 2002b]. Although differences in localization and physiological function between the *T. cruzi* and *T. brucei* orthologue of Px IV might be possible, the immunofluorescence images did not give a clear picture. The pattern of BiP can structurally be similar to a mitochondrial signal in *T. cruzi* epimastigotes [Ferella *et al.*,

2008a; Leroux *et al.*, 2011; Paes *et al.*, 2013] as well as in PC *T. brucei* [Ferella *et al.*, 2008a; Leroux *et al.*, 2011]. The co-staining with MitoTracker or a mitochondrial protein would have been appropriate in addition to a DAPI staining to properly visualize the perinuclear ring of the ER staining. Wilkinson *et al.* also proposed the 22 N-terminal residues as putative ER signal peptide. In general, such signal peptides are rather diverse and do not show a clear consensus sequence but contain a positively charged stretch followed by a hydrophobic core [Zimmermann *et al.*, 2011]. However, no cluster of positively charged amino acids on the N-terminus is present in the *T. cruzi* or *T. brucei* protein. This is consistent with the finding that the score of the grand average of hydropathy (GRAVY) for the first 22 amino acids showed only a value of 0.9 and 0.8, respectively, and thus, a rather low hydrophobicity. All these findings would argue against ER localization and may support a mitochondrial one although no MTS was identified. Indeed, if specific Px IV antibodies recognize the endogenous protein in cell lysates, the mitochondrial localization could be inspected by a fractionated digitonin lysis and subsequent Western blot analysis. Another approach would be the generation of an *in-situ* tagged protein. Intriguingly, dual localization of proteins in the mitochondrion and ER was described in mammals [Anandatheerthavarada *et al.*, 1999; Stone *et al.*, 2009] while alternative splicing is discussed as a potential mechanism for a dual localization in trypanosomes but no ER- and mitochondrion-targeted protein was yet identified [Nilsson *et al.*, 2010; Zhang *et al.*, 2010].

The cytosolic expression of recombinant Px IV in *E. coli* did not yield large amounts of soluble and pure protein. Assuming a putative ER localization, secretion of the protein to the periplasm could enhance the solubility. The periplasm of *E. coli* represents an oxidizing environment facilitating the formation of disulfide bridges as well as possessing foldases like DsbA and DsbC [de Marco, 2009]. Another approach may be to secrete the protein into the medium as in the larger volume, aggregation is less likely [de Marco, 2012].

The purification of Px IV using Trx as fusion partner yielded a small amount of almost pure soluble protein. However, cleavage by the TEV protease seems to be rather inefficient as from the expected 4.3 mg of the fusion protein (out of 4 l) only 0.8 mg untagged Px IV was obtained representing a cleavage efficiency of only 20%. The purification of the His_6-Px IV could be also optimized by more extensive washing at higher imidazole concentrations. Clearly, a tag-free recombinant protein would be preferable. Thus, optimization of the

purification protocol using the other fusion partners like GB and MBP would be recommended.

On SDS-PAGE under non-reducing conditions, recombinant Px IV migrates faster indicating the formation of an intramolecular disulfide bridge. The disulfide bridge(s) may be involved in the activity of the enzyme as shown for the other *T. brucei* peroxidases (Px I-III) where two thiol groups are necessary for the reduction of lipid hydroperoxides [Diechtierow and Krauth-Siegel, 2011]. In the case of a mitochondrial localization of Px IV, the required oxidoreductase and the low molecular weight thiol required are not yet known. Although the preliminary kinetic analysis revealed a higher activity for lipid hydroperoxides compared to H_2O_2, the activity is only 0.049 U/mg. Wilkinson *et al.* showed for the *T. cruzi* protein a reasonable K_m of 0.7 µM for HpODE and a K_m of 5 mM for GSH. In addition, the significance *in vivo* of this reaction is not clear since the total GSH concentration in *T. cruzi* is between 0.2 - 2 mM [Krauth-Siegel and Comini, 2008; Wilkinson *et al.*, 2002b]. Therefore, the physiological function of Px IV is still elusive. Recent studies of GPx7 showed that the conserved Cys 86 can act as a non-canonical resolving cysteine for the Cys 57 oxidized by H_2O_2 [Wang *et al.*, 2014]. This finding suggests a putative function for the highly conserved Cys 66 in Px IV as well as depicted an interesting difference to the respective cysteine in Px I-III. Here, site-directed mutagenesis of Cys 76 (Px III) did not influence enzymatic activity and its function remained unknown [Schlecker *et al.*, 2007].

The MALDI-TOF-MS analysis of the recombinant Px IV revealed that the NEM-treatment might not be as efficient as the IAM-labeling. The duration, temperature or the NEM-concentration should be optimized to gain more reliable data. From the initial data and the amino acid conservation, a disulfide bridge between Cys 66 and 127 may be expected. However, Cys 37 should be clearly the active-site cysteine as shown by the sequence alignment with other peroxidases. To analyze this in more detail, the triple cysteine mutant of Px IV (C26/81/134S, generated by N. Dirdjaja) could be also subjected to reducing and non-reducing SDS-PAGE to further analyze the formation of the intramolecular disulfide.

In many cell types, the mitochondrion represents the primary source of endogenous ROS [Turrens, 2003] and so, the organelle responsible for oxidative damage concerning proteins, DNA, and lipids [Murphy and Smith, 2007]. If Px IV was involved in the detoxification of lipid hydroperoxides produced as side products of oxidative phosphorylation, the protein

should be more important in the insect stage of the trypanosomes compared to the BS cells that rely solely on glycolysis for their energy supply. Thus, it would be expected that Px IV is essential in PC. However, a high-throughput RNAi approach suggested that the protein is dispensable in the insect form but essential in BS cells [Alsford *et al.*, 2011]. The RNAi resulted in a significant loss of reads and consequently, loss-of-fitness of 92% (Z-score: 3.7) after three days in BS cells and 77% (Z-score: 4.2) after six days. The fitness of PC cells decreased by 85% (Z-score: 2.9) after induction which was stated as not significant. The statistical analysis was based on the Z-score defining a significant loss-of-fitness >3.3. This threshold is quite close to the results obtained for the BS and PC form and thus, the high-throughput data of the essentiality of Px IV may be not that conclusive compared to the Z-scores (three days: 5.3, six days: 10.6) obtained from the BS Px I-III data.

As the potency of RNAi constructs varies dependent on the chosen sequence, the knockdown might be ineffective and the RNAi phenotype is often not stable. The generation of KO cell lines by deletion of both *px IV* alleles should be more conclusive. PCR analysis of the single *px IV*$^{-/-}$ cell line obtained so far showed the replacement of both *px IV* alleles by resistance cassettes and the *px IV* gene was not detectable. However, the selection procedure after the transfection took more than two weeks which was rather unusual. The culture contained simultaneously proliferating and dying cells at a low density. After the adaptation time, the *px IV*$^{-/-}$ cells started growing but with a proliferation defect compared to WT cells. It cannot be excluded that the cell line altered its genomic integrity upon *px IV* deletion. To evaluate the essentiality of Px IV for BS parasites, clearly more cell lines are needed. It is possible that the KO of *px IV* is not lethal under culture conditions but might be fatal in the animal host.

For the case that a complete KO is not possible, cloning of a vector for the inducible expression of an ectopic copy of untagged Px IV in *T. brucei* was directed. Prior to the deletion of the second allele, the *px IV*$^{+/-}$ parasites should be transfected with the pHD1700 vector which integrates into the rRNA locus. However, in the case of an essential gene, conditional null mutants that express an inducible copy may become “leaky” in trypanosomes and may not yield conclusive data [Krieger *et al.*, 2000; Taylor *et al.*, 2013].

The primary structure of Px IV definitely shows the characteristics of glutathione peroxidase-type enzymes. Although the function of Px IV remains still elusive, future studies should focus not only on BS but also on PC cells.

5 References

A. Acosta-Serrano, E. Vassella, M. Liniger, C. Kunz Renggli, R. Brun, I. Roditi, and P. T. Englund (2001). The surface coat of procyclic *Trypanosoma brucei*: programmed expression and proteolytic cleavage of procyclin in the tsetse fly. Proc Natl Acad Sci U S A 98: 1513-1518.

P. Aisen, and I. Listowsky (1980). Iron transport and storage proteins. Annu Rev Biochem 49: 357-393.

D. L. Alexander, K. J. Schwartz, A. E. Balber, and J. D. Bangs (2002). Developmentally regulated trafficking of the lysosomal membrane protein p67 in *Trypanosoma brucei*. J Cell Sci 115: 3253-3263.

S. Alsford, R. B. Currier, J. A. Guerra-Assunção, T. G. Clark, and D. Horn (2014). Cathepsin-L can resist lysis by human serum in *Trypanosoma brucei brucei*. PLoS Pathog 10: e1004130.

S. Alsford, D. J. Turner, S. O. Obado, A. Sanchez-Flores, L. Glover, M. Berriman, C. Hertz-Fowler, and D. Horn (2011). High-throughput phenotyping using parallel sequencing of RNA interference targets in the African trypanosome. Genome Res 21: 915-924.

H. K. Anandatheerthavarada, G. Biswas, J. Mullick, N. B. Sepuri, L. Otvos, D. Pain, and N. G. Avadhani (1999). Dual targeting of cytochrome P4502B1 to endoplasmic reticulum and mitochondria involves a novel signal activation by cyclic AMP-dependent phosphorylation at ser128. EMBO J 18: 5494-5504.

D. A. Andres, J. D. Rhodes, R. L. Meisel, and J. E. Dixon (1991). Characterization of the carboxyl-terminal sequences responsible for protein retention in the endoplasmic reticulum. J Biol Chem 266: 14277-14282.

D. G. Arias, M. S. Cabeza, E. D. Erben, P. G. Carranza, H. D. Lujan, M. T. Téllez Iñón, A. A. Iglesias, and S. A. Guerrero (2011). Functional characterization of methionine sulfoxide reductase A from *Trypanosoma* spp. Free Radic Biol Med 50: 37-46.

P. Arosio, and S. Levi (2010). Cytosolic and mitochondrial ferritins in the regulation of cellular iron homeostasis and oxidative damage. Biochim Biophys Acta 1800: 783-792.

H. Atamna, and H. Ginsburg (1995). Heme degradation in the presence of glutathione. A proposed mechanism to account for the high levels of non-heme iron found in the membranes of hemoglobinopathic red blood cells. J Biol Chem 270: 24876-24883.

C. D. Austin, X. Wen, L. Gazzard, C. Nelson, R. H. Scheller, and S. J. Scales (2005). Oxidizing potential of endosomes and lysosomes limits intracellular cleavage of disulfide-based antibody-drug conjugates. Proc Natl Acad Sci USA 102: 17987-17992.

J. D. Bangs, L. Uyetake, M. J. Brickman, A. E. Balber, and J. C. Boothroyd (1993). Molecular cloning and cellular localization of a BiP homologue in *Trypanosoma brucei*. Divergent ER retention signals in a lower eukaryote. J Cell Sci 105 (Pt 4): 1101-1113.

S. Basu, D. J. Netz, A. C. Haindrich, N. Herlerth, T. J. Lagny, A. J. Pierik, R. Lill, and J. Lukeš (2014). Cytosolic iron-sulphur protein assembly is functionally conserved and essential in procyclic and bloodstream *Trypanosoma brucei*. Mol Microbiol 93: 897-910.

M. Berriman, E. Ghedin, C. Hertz-Fowler, G. Blandin, H. Renauld, D. C. Bartholomeu, N. J. Lennard, E. Caler, N. E. Hamlin, B. Haas, U. Bohme, L. Hannick, M. A. Aslett, J. Shallom, L. Marcello, L. Hou, B. Wickstead, U. C. Alsmark, C. Arrowsmith, R. J. Atkin, A. J. Barron,

F. Bringaud, K. Brooks, M. Carrington, I. Cherevach, T. J. Chillingworth, C. Churcher, L. N. Clark, C. H. Corton, A. Cronin, R. M. Davies, J. Doggett, A. Djikeng, T. Feldblyum, M. C. Field, A. Fraser, I. Goodhead, Z. Hance, D. Harper, B. R. Harris, H. Hauser, J. Hostetler, A. Ivens, K. Jagels, D. Johnson, J. Johnson, K. Jones, A. X. Kerhornou, H. Koo, N. Larke, S. Landfear, C. Larkin, V. Leech, A. Line, A. Lord, A. Macleod, P. J. Mooney, S. Moule, D. M. Martin, G. W. Morgan, K. Mungall, H. Norbertczak, D. Ormond, G. Pai, C. S. Peacock, J. Peterson, M. A. Quail, E. Rabbinowitsch, M. A. Rajandream, C. Reitter, S. L. Salzberg, M. Sanders, S. Schobel, S. Sharp, M. Simmonds, A. J. Simpson, L. Tallon, C. M. Turner, A. Tait, A. R. Tivey, S. Van Aken, D. Walker, D. Wanless, S. Wang, B. White, O. White, S. Whitehead, J. Woodward, J. Wortman, M. D. Adams, T. M. Embley, K. Gull, E. Ullu, J. D. Barry, A. H. Fairlamb, F. Opperdoes, B. G. Barrell, J. E. Donelson, N. Hall, C. M. Fraser, S. E. Melville, and N. M. El-Sayed (2005). The genome of the African trypanosome *Trypanosoma brucei*. Science 309: 416-422.

S. Biebinger, L. E. Wirtz, P. Lorenz, and C. Clayton (1997). Vectors for inducible expression of toxic gene products in bloodstream and procyclic *Trypanosoma brucei*. Mol Biochem Parasitol 85: 99-112.

W. Bitter, H. Gerrits, R. Kieft, and P. Borst (1998). The role of transferrin-receptor variation in the host range of *Trypanosoma brucei*. Nature 391: 499-502.

C. E. Blaby-Haas, and S. S. Merchant (2014). Lysosome-related organelles as mediators of metal homeostasis. J Biol Chem 289: 28129-28136.

T. Breidbach, S. Scory, R. L. Krauth-Siegel, and D. Steverding (2002). Growth inhibition of bloodstream forms of *Trypanosoma brucei* by the iron chelator deferoxamine. Int J Parasitol 32: 473-479.

M. J. Brickman, J. M. Cook, and A. E. Balber (1995). Low temperature reversibly inhibits transport from tubular endosomes to a perinuclear, acidic compartment in African trypanosomes. J Cell Sci 108 (Pt 11): 3611-3621.

R. Brigelius-Flohé, and M. Maiorino (2013). Glutathione peroxidases. Biochim Biophys Acta 1830: 3289-3303.

R. Brun, J. Blum, F. Chappuis, and C. Burri (2010). Human African trypanosomiasis. Lancet 375: 148-159.

H. Budde, L. Flohé, H. J. Hecht, B. Hofmann, M. Stehr, J. Wissing, and H. Lünsdorf (2003). Kinetics and redox-sensitive oligomerisation reveal negative subunit cooperativity in tryparedoxin peroxidase of *Trypanosoma brucei brucei*. Biol Chem 384: 619-633.

J. B. Cannon, F. S. Kuo, R. F. Pasternack, N. M. Wong, and U. Muller-Eberhard (1984). Kinetics of the interaction of hemin liposomes with heme binding proteins. Biochemistry 23: 3715-3721.

P. Capewell, C. Clucas, E. DeJesus, R. Kieft, S. Hajduk, N. Veitch, P. C. Steketee, A. Cooper, W. Weir, and A. MacLeod (2013). The TgsGP gene is essential for resistance to human serum in *Trypanosoma brucei gambiense*. PLoS Pathog 9: e1003686.

S. Carvalho, T. Cruz, N. Santarém, H. Castro, V. Costa, and A. M. Tomás (2009). Heme as a source of iron to *Leishmania infantum* amastigotes. Acta Trop 109: 131-135.

H. Castro, and A. M. Tomás (2008). Peroxidases of trypanosomatids. Antioxid Redox Signal 10: 1593-1606.

M. Chaudhri, D. Steverding, D. Kittelberger, S. Tjia, and P. Overath (1994). Expression of a glycosylphosphatidylinositol-anchored *Trypanosoma brucei* transferrin-binding protein complex in insect cells. Proc Natl Acad Sci U S A 91: 6443-6447.

C. T. Chu, J. Ji, R. K. Dagda, J. F. Jiang, Y. Y. Tyurina, A. A. Kapralov, V. A. Tyurin, N. Yanamala, I. H. Shrivastava, D. Mohammadyani, K. Z. Qiang Wang, J. Zhu, J. Klein-Seetharaman, K. Balasubramanian, A. A. Amoscato, G. Borisenko, Z. Huang, A. M. Gusdon, A. Cheikhi, E. K. Steer, R. Wang, C. Baty, S. Watkins, I. Bahar, H. Bayir, and V. E. Kagan (2013). Cardiolipin externalization to the outer mitochondrial membrane acts as an elimination signal for mitophagy in neuronal cells. Nat Cell Biol 15: 1197-1205.

A. B. Clarkson, Jr., E. J. Bienen, G. Pollakis, and R. W. Grady (1989). Respiration of bloodstream forms of the parasite Trypanosoma brucei brucei is dependent on a plant-like alternative oxidase. J Biol Chem 264: 17770-17776.

C. E. Clayton (1987). Import of fructose bisphosphate aldolase into the glycosomes of *Trypanosoma brucei*. J Cell Biol 105: 2649-2654.

C. Clayton, and M. Shapira (2007). Post-transcriptional regulation of gene expression in trypanosomes and leishmanias. Mol Biochem Parasitol 156: 93-101.

C. Colasante, M. Ellis, T. Ruppert, and F. Voncken (2006). Comparative proteomics of glycosomes from bloodstream form and procyclic culture form *Trypanosoma brucei brucei*. Proteomics 6: 3275-3293.

C. Colasante, P. Peña Diaz, C. Clayton, and F. Voncken (2009). Mitochondrial carrier family inventory of *Trypanosoma brucei brucei*: Identification, expression and subcellular localisation. Mol Biochem Parasitol 167: 104-117.

M. A. Comini, S. A. Guerrero, S. Haile, U. Menge, H. Lünsdorf, and L. Flohé (2004). Validation of *Trypanosoma brucei* trypanothione synthetase as drug target. Free Radic Biol Med 36: 1289-1302.

M. A. Comini, J. Rettig, N. Dirdjaja, E. M. Hanschmann, C. Berndt, and R. L. Krauth-Siegel (2008). Monothiol glutaredoxin-1 is an essential iron-sulfur protein in the mitochondrion of African trypanosomes. J Biol Chem 283: 27785-27798.

M. P. Cunningham, and K. Vickerman (1962). Antigenic analysis in the *Trypanosoma brucei* group, using the agglutination reaction. Trans R Soc Trop Med Hyg 56: 48-59.

C. De Greef, and R. Hamers (1994). The serum resistance-associated (SRA) gene of *Trypanosoma brucei rhodesiense* encodes a variant surface glycoprotein-like protein. Mol Biochem Parasitol 68: 277-284.

A. de Marco (2009). Strategies for successful recombinant expression of disulfide bond-dependent proteins in *Escherichia coli*. Microb Cell Fact 8: 26.

A. de Marco (2012). Recent contributions in the field of the recombinant expression of disulfide bonded proteins in bacteria. Microb Cell Fact 11: 129.

E. DeJesus, R. Kieft, B. Albright, N. A. Stephens, and S. L. Hajduk (2013). A single amino acid substitution in the group 1 *Trypanosoma brucei gambiense* haptoglobin-hemoglobin receptor abolishes TLF-1 binding. PLoS Pathog 9: e1003317.

T. A. Dellibovi-Ragheb, J. E. Gisselberg, and S. T. Prigge (2013). Parasites FeS up: iron-sulfur cluster biogenesis in eukaryotic pathogens. PLoS Pathog 9: e1003227.

S. Denamur, D. Tyteca, J. Marchand-Brynaert, F. Van Bambeke, P. M. Tulkens, P. J. Courtoy, and M. P. Mingeot-Leclercq (2011). Role of oxidative stress in lysosomal membrane

permeabilization and apoptosis induced by gentamicin, an aminoglycoside antibiotic. Free Radic Biol Med 51: 1656-1665.

M. Deponte (2013). Glutathione catalysis and the reaction mechanisms of glutathione-dependent enzymes. Biochim Biophys Acta 1830: 3217-3266.

M. Diechtierow (2011). The distinct functions of the tryparedoxin-dependent peroxidases in African trypanosomes. PhD thesis: Ruprecht-Karls-Universität Heidelberg.

M. Diechtierow, and R. L. Krauth-Siegel (2011). A tryparedoxin-dependent peroxidase protects African trypanosomes from membrane damage. Free Radic Biol Med 51: 856-868.

S. J. Dixon, and B. R. Stockwell (2014). The role of iron and reactive oxygen species in cell death. Nat Chem Biol 10: 9-17.

R. Docampo, and G. Huang (2014). Calcium signaling in trypanosomatid parasites. Cell Calcium, 10.1016/j.ceca.2014.10.015.

M. Dormeyer, N. Reckenfelderbäumer, H. Ludemann, and R. L. Krauth-Siegel (2001). Trypanothione-dependent synthesis of deoxyribonucleotides by *Trypanosoma brucei* ribonucleotide reductase. J Biol Chem 276: 10602-10606.

M. G. dos Santos, S. M. Muxel, R. A. Zampieri, T. G. Pomorski, and L. M. Floeter-Winter (2013). Transbilayer dynamics of phospholipids in the plasma membrane of the *Leishmania* genus. PLoS One 8: e55604.

P. T. Doulias, S. Christoforidis, U. T. Brunk, and D. Galaris (2003). Endosomal and lysosomal effects of desferrioxamine: protection of HeLa cells from hydrogen peroxide-induced DNA damage and induction of cell-cycle arrest. Free Radic Biol Med 35: 719-728.

N. A. Dyer, C. Rose, N. O. Ejeh, and A. Acosta-Serrano (2013). Flying tryps: survival and maturation of trypanosomes in tsetse flies. Trends Parasitol 29: 188-196.

J. E. Ellis (1994). Coenzyme Q homologs in parasitic protozoa as targets for chemotherapeutic attack. Parasitol Today 10: 296-301.

A. Escobar, V. Gaete, and M. T. Núñez (1992). Effect of ascorbate in the reduction of transferrin-associated iron in endocytic vesicles. J Bioenerg Biomembr 24: 227-233.

A. H. Fairlamb (2003). Chemotherapy of human African trypanosomiasis: current and future prospects. Trends Parasitol 19: 488-494.

A. H. Fairlamb, P. Blackburn, P. Ulrich, B. T. Chait, and A. Cerami (1985). Trypanothione: a novel bis(glutathionyl)spermidine cofactor for glutathione reductase in trypanosomatids. Science 227: 1485-1487.

M. Ferella, Z. H. Li, B. Andersson, and R. Docampo (2008a). Farnesyl diphosphate synthase localizes to the cytoplasm of *Trypanosoma cruzi* and *T. brucei*. Exp Parasitol 119: 308-312.

M. Ferella, D. Nilsson, H. Darban, C. Rodrigues, E. J. Bontempi, R. Docampo, and B. Andersson (2008b). Proteomics in *Trypanosoma cruzi*--localization of novel proteins to various organelles. Proteomics 8: 2735-2749.

M. A. Ferguson, S. W. Homans, R. A. Dwek, and T. W. Rademacher (1988). Glycosyl-phosphatidylinositol moiety that anchors *Trypanosoma brucei* variant surface glycoprotein to the membrane. Science 239: 753-759.

H. F. Gilbert (1990). Molecular and cellular aspects of thiol-disulfide exchange. Adv Enzymol Relat Areas Mol Biol 63: 69-172.

L. Gille, and H. Nohl (2000). The existence of a lysosomal redox chain and the role of ubiquinone. Arch Biochem Biophys 375: 347-354.

H. Gunshin, B. Mackenzie, U. V. Berger, Y. Gunshin, M. F. Romero, W. F. Boron, S. Nussberger, J. L. Gollan, and M. A. Hediger (1997). Cloning and characterization of a mammalian proton-coupled metal-ion transporter. Nature 388: 482-488.

A. Günzl, T. Bruderer, G. Laufer, B. Schimanski, L. C. Tu, H. M. Chung, P. T. Lee, and M. G. Lee (2003). RNA polymerase I transcribes procyclin genes and variant surface glycoprotein gene expression sites in *Trypanosoma brucei*. Eukaryot Cell 2: 542-551.

M. G. Gutierrez, H. A. Saka, I. Chinen, F. C. Zoppino, T. Yoshimori, J. L. Bocco, and M. I. Colombo (2007). Protective role of autophagy against *Vibrio cholerae* cytolysin, a pore-forming toxin from *V. cholerae*. Proc Natl Acad Sci U S A 104: 1829-1834.

J. M. Gutteridge (1986). Iron promoters of the Fenton reaction and lipid peroxidation can be released from haemoglobin by peroxides. FEBS Lett 201: 291-295.

K. M. Hager, M. A. Pierce, D. R. Moore, E. M. Tytler, J. D. Esko, and S. L. Hajduk (1994). Endocytosis of a cytotoxic human high density lipoprotein results in disruption of acidic intracellular vesicles and subsequent killing of African trypanosomes. J Cell Biol 126: 155-167.

B. S. Hall, A. Pal, D. Goulding, and M. C. Field (2004). Rab4 is an essential regulator of lysosomal trafficking in trypanosomes. J Biol Chem 279: 45047-45056.

L. C. Hamill, M. T. Kaare, S. C. Welburn, and K. Picozzi (2013). Domestic pigs as potential reservoirs of human and animal trypanosomiasis in Northern Tanzania. Parasit Vectors 6: 322.

V. Hamilton, U. K. Singha, J. T. Smith, E. Weems, and M. Chaudhuri (2014). Trypanosome alternative oxidase possesses both an N-terminal and internal mitochondrial targeting signal. Eukaryot Cell 13: 539-547.

M. W. Hentze, M. U. Muckenthaler, B. Galy, and C. Camaschella (2010). Two to tango: regulation of Mammalian iron metabolism. Cell 142: 24-38.

A. N. Higdon, G. A. Benavides, B. K. Chacko, X. Ouyang, M. S. Johnson, A. Landar, J. Zhang, and V. M. Darley-Usmar (2012). Hemin causes mitochondrial dysfunction in endothelial cells through promoting lipid peroxidation: the protective role of autophagy. Am J Physiol Heart Circ Physiol 302: H1394-1409.

H. Hillebrand, A. Schmidt, and R. L. Krauth-Siegel (2003). A second class of peroxidases linked to the trypanothione metabolism. J Biol Chem 278: 6809-6815.

C. Hiller, A. Nissen, D. Benítez, M. A. Comini, and R. L. Krauth-Siegel (2014). Cytosolic peroxidases protect the lysosome of bloodstream African trypanosomes from iron-mediated membrane damage. PLoS Pathog 10: e1004075.

A. Hofer, P. P. Schmidt, A. Gräslund, and L. Thelander (1997). Cloning and characterization of the R1 and R2 subunits of ribonucleotide reductase from *Trypanosoma brucei*. Proc Natl Acad Sci U S A 94: 6959-6964.

J. C. Holthuis, and A. K. Menon (2014). Lipid landscapes and pipelines in membrane homeostasis. Nature 510: 48-57.

D. Horn (2014). Antigenic variation in African trypanosomes. Mol Biochem Parasitol, 10.1016/j.molbiopara.2014.05.001.

A. Horváth, E. Horáková, P. Dunajcíková, Z. Verner, E. Pravdová, I. Slapetová, L. Cuninková, and J. Lukes (2005). Downregulation of the nuclear-encoded subunits of the complexes III and IV disrupts their respective complexes but not complex I in procyclic *Trypanosoma brucei*. Mol Microbiol 58: 116-130.

G. Huang, A. E. Vercesi, and R. Docampo (2013). Essential regulation of cell bioenergetics in *Trypanosoma brucei* by the mitochondrial calcium uniporter. Nat Commun 4: 2865.

C. Huynh, X. Yuan, D. C. Miguel, R. L. Renberg, O. Protchenko, C. C. Philpott, I. Hamza, and N. W. Andrews (2012). Heme uptake by *Leishmania amazonensis* is mediated by the transmembrane protein LHR1. PLoS Pathog 8: e1002795.

H. Imai, and Y. Nakagawa (2003). Biological significance of phospholipid hydroperoxide glutathione peroxidase (PHGPx, GPx4) in mammalian cells. Free Radic Biol Med 34: 145-169.

V. Jamonneau, H. Ilboudo, J. Kaboré, D. Kaba, M. Koffi, P. Solano, A. Garcia, D. Courtin, C. Laveissière, K. Lingue, P. Büscher, and B. Bucheton (2012). Untreated human infections by *Trypanosoma brucei gambiense* are not 100% fatal. PLoS Negl Trop Dis 6: e1691.

M. L. Jauslin, T. Meier, R. A. Smith, and M. P. Murphy (2003). Mitochondria-targeted antioxidants protect Friedreich Ataxia fibroblasts from endogenous oxidative stress more effectively than untargeted antioxidants. FASEB J 17: 1972-1974.

J. Jelk, N. Gao, M. Serricchio, A. Signorell, R. S. Schmidt, J. D. Bangs, A. Acosta-Serrano, M. A. Lehrman, P. Bütikofer, and A. K. Menon (2013). Glycoprotein biosynthesis in a eukaryote lacking the membrane protein Rft1. J Biol Chem 288: 20616-20623.

S. Jenkitkasemwong, C. Y. Wang, B. Mackenzie, and M. D. Knutson (2012). Physiologic implications of metal-ion transport by ZIP14 and ZIP8. Biometals 25: 643-655.

K. Kakuta, K. Orino, S. Yamamoto, and K. Watanabe (1997). High levels of ferritin and its iron in fetal bovine serum. Comp Biochem Physiol A Physiol 118: 165-169.

A. Kalén, B. Norling, E. L. Appelkvist, and G. Dallner (1987). Ubiquinone biosynthesis by the microsomal fraction from rat liver. Biochim Biophys Acta 926: 70-78.

P. G. Kennedy (2006). Diagnostic and neuropathogenesis issues in human African trypanosomiasis. Int J Parasitol 36: 505-512.

P. G. Kennedy (2013). Clinical features, diagnosis, and treatment of human African trypanosomiasis (sleeping sickness). Lancet Neurol 12: 186-194.

R. Kieft, P. Capewell, C. M. Turner, N. J. Veitch, A. MacLeod, and S. Hajduk (2010). Mechanism of *Trypanosoma brucei gambiense* (group 1) resistance to human trypanosome lytic factor. Proc Natl Acad Sci USA 107: 16137-16141.

T. Kirkegaard, and M. Jäättelä (2009). Lysosomal involvement in cell death and cancer. Biochim Biophys Acta 1793: 746-754.

L. Kořený, J. Lukeš, and M. Oborník (2010). Evolution of the haem synthetic pathway in kinetoplastid flagellates: an essential pathway that is not essential after all? Int J Parasitol 40: 149-156.

L. Kořený, M. Oborník, and J. Lukeš (2013). Make it, take it, or leave it: heme metabolism of parasites. PLoS Pathog 9: e1003088.

T. S. Koskenkorva-Frank, G. Weiss, W. H. Koppenol, and S. Burckhardt (2013). The complex interplay of iron metabolism, reactive oxygen species, and reactive nitrogen species:

insights into the potential of various iron therapies to induce oxidative and nitrosative stress. Free Radic Biol Med 65: 1174-1194.

J. Kovárová, E. Horáková, P. Changmai, M. Vancová, and J. Lukeš (2013). Mitochondrial and nucleolar localization of cysteine desulfurase Nfs and the scaffold protein Isu in *Trypanosoma brucei*. Eukaryot Cell, 10.1128/EC.00235-13.

A. J. Kowaltowski, N. C. de Souza-Pinto, R. F. Castilho, and A. E. Vercesi (2009). Mitochondria and reactive oxygen species. Free Radic Biol Med 47: 333-343.

R. L. Krauth-Siegel, and M. A. Comini (2008). Redox control in trypanosomatids, parasitic protozoa with trypanothione-based thiol metabolism. Biochim Biophys Acta 1780: 1236-1248.

R. L. Krauth-Siegel, B. Enders, G. B. Henderson, A. H. Fairlamb, and R. H. Schirmer (1987). Trypanothione reductase from *Trypanosoma cruzi*. Purification and characterization of the crystalline enzyme. Eur J Biochem 164: 123-128.

R. L. Krauth-Siegel, and A. E. Leroux (2012). Low-molecular-mass antioxidants in parasites. Antioxid Redox Signal 17: 583-607.

S. Krieger, W. Schwarz, M. R. Ariyanayagam, A. H. Fairlamb, R. L. Krauth-Siegel, and C. Clayton (2000). Trypanosomes lacking trypanothione reductase are avirulent and show increased sensitivity to oxidative stress. Mol Microbiol 35: 542-552.

T. Kurz, J. W. Eaton, and U. T. Brunk (2011). The role of lysosomes in iron metabolism and recycling. Int J Biochem Cell Biol 43: 1686-1697.

T. Kurz, B. Gustafsson, and U. T. Brunk (2006). Intralysosomal iron chelation protects against oxidative stress-induced cellular damage. FEBS J 273: 3106-3117.

D. H. Lai, H. Hashimi, Z. R. Lun, F. J. Ayala, and J. Lukeš (2008). Adaptations of *Trypanosoma brucei* to gradual loss of kinetoplast DNA: *Trypanosoma equiperdum* and *Trypanosoma evansi* are petite mutants of *T. brucei*. Proc Natl Acad Sci U S A 105: 1999-2004.

D. J. Lane, A. M. Merlot, M. L. Huang, D. H. Bae, P. J. Jansson, S. Sahni, D. S. Kalinowski, and D. R. Richardson (2015). Cellular iron uptake, trafficking and metabolism: Key molecules and mechanisms and their roles in disease. Biochim Biophys Acta 1853: 1130-1144.

D. J. Lane, and D. R. Richardson (2014). The active role of vitamin C in mammalian iron metabolism: much more than just enhanced iron absorption! Free Radic Biol Med 75: 69-83.

N. Le Trant, S. R. Meshnick, K. Kitchener, J. W. Eaton, and A. Cerami (1983). Iron-containing superoxide dismutase from *Crithidia fasciculata*. Purification, characterization, and similarity to Leishmanial and trypanosomal enzymes. J Biol Chem 258: 125-130.

A. E. Leroux, D. A. Maugeri, F. R. Opperdoes, J. J. Cazzulo, and C. Nowicki (2011). Comparative studies on the biochemical properties of the malic enzymes from *Trypanosoma cruzi* and *Trypanosoma brucei*. FEMS Microbiol Lett 314: 25-33.

X. H. Liang, A. Haritan, S. Uliel, and S. Michaeli (2003). trans and cis splicing in trypanosomatids: mechanism, factors, and regulation. Eukaryot Cell 2: 830-840.

M. J. Ligtenberg, W. Bitter, R. Kieft, D. Steverding, H. Janssen, J. Calafat, and P. Borst (1994). Reconstitution of a surface transferrin binding complex in insect form *Trypanosoma brucei*. EMBO J 13: 2565-2573.

R. Lill (2009). Function and biogenesis of iron-sulphur proteins. Nature 460: 831-838.

S. I. Liochev, and I. Fridovich (1994). The role of $O_2^{\cdot -}$ in the production of $HO^{\cdot}$: *in vitro* and *in vivo*. Free Radic Biol Med 16: 29-33.

B. Liu, Y. Liu, S. A. Motyka, E. E. Agbo, and P. T. Englund (2005). Fellowship of the rings: the replication of kinetoplast DNA. Trends Parasitol 21: 363-369.

I. Liu (2015). Characterization of a novel glutathione peroxidase-type enzyme, Px IV, in African trypanosomes. MD thesis: Ruprecht-Karls-Universität Heidelberg.

F. López-Soto, N. León-Sicairos, M. Reyes-López, J. Serrano-Luna, C. Ordaz-Pichardo, C. Piña-Vázquez, G. Ortiz-Estrada, and M. de la Garza (2009). Use and endocytosis of iron-containing proteins by *Entamoeba histolytica* trophozoites. Infect Genet Evol 9: 1038-1050.

S. Lu, T. Suzuki, N. Iizuka, S. Ohshima, Y. Yabu, M. Suzuki, L. Wen, and N. Ohta (2007). *Trypanosoma brucei* vacuolar protein sorting 41 (VPS41) is required for intracellular iron utilization and maintenance of normal cellular morphology. Parasitology 134: 1639-1647.

H. Lüdemann, M. Dormeyer, C. Sticherling, D. Stallmann, H. Follmann, and R. L. Krauth-Siegel (1998). *Trypanosoma brucei* tryparedoxin, a thioredoxin-like protein in African trypanosomes. FEBS Lett 431: 381-385.

J. Lukeš, and S. Basu (2014). Fe/S protein biogenesis in trypanosomes - A review. Biochim Biophys Acta, 10.1016/j.bbamcr.2014.08.015.

J. Mach, J. Tachezy, and R. Sutak (2013). Efficient iron uptake via a reductive mechanism in procyclic *Trypanosoma brucei*. J Parasitol 99: 363-364.

K. R. Matthews (2005). The developmental cell biology of *Trypanosoma brucei*. J Cell Sci 118: 283-290.

P. Mauri, L. Benazzi, L. Flohé, M. Maiorino, P. G. Pietta, S. Pilawa, A. Roveri, and F. Ursini (2003). Versatility of selenium catalysis in PHGPx unraveled by LC/ESI-MS/MS. Biol Chem 384: 575-588.

P. A. Michels, F. Bringaud, M. Herman, and V. Hannaert (2006). Metabolic functions of glycosomes in trypanosomatids. Biochim Biophys Acta 1763: 1463-1477.

S. Mogk, A. Meiwes, C. M. Boßelmann, H. Wolburg, and M. Duszenko (2014). The lane to the brain: how African trypanosomes invade the CNS. Trends Parasitol 30: 470-477.

G. W. Morgan, C. L. Allen, T. R. Jeffries, M. Hollinshead, and M. C. Field (2001). Developmental and morphological regulation of clathrin-mediated endocytosis in *Trypanosoma brucei*. J Cell Sci 114: 2605-2615.

M. Moutiez, D. Meziane-Cherie, M. Aumercier, C. Sergheraert, and A. Tartar (1994). Compared reactivities of trypanothione and glutathione in conjugation reactions. Chem. Pharm. Bull. 42 2641–2644.

A. K. Mukherjee, S. K. Ghosal, and C. R. Maity (1997). Lysosomal membrane stabilization by alpha-tocopherol against the damaging action of *Vipera russelli* venom phospholipase A2. Cell Mol Life Sci 53: 152-155.

M. P. Murphy (2008). Targeting lipophilic cations to mitochondria. Biochim Biophys Acta 1777: 1028-1031.

M. P. Murphy, and R. A. Smith (2007). Targeting antioxidants to mitochondria by conjugation to lipophilic cations. Annu Rev Pharmacol Toxicol 47: 629-656.

E. Nagababu, and J. M. Rifkind (2000). Reaction of hydrogen peroxide with ferrylhemoglobin: superoxide production and heme degradation. Biochemistry 39: 12503-12511.

S. K. Natesan, L. Peacock, K. Matthews, W. Gibson, and M. C. Field (2007). Activation of endocytosis as an adaptation to the mammalian host by trypanosomes. Eukaryot Cell 6: 2029-2037.

D. J. Netz, C. M. Stith, M. Stümpfig, G. Köpf, D. Vogel, H. M. Genau, J. L. Stodola, R. Lill, P. M. Burgers, and A. J. Pierik (2012). Eukaryotic DNA polymerases require an iron-sulfur cluster for the formation of active complexes. Nat Chem Biol 8: 125-132.

V. D. Nguyen, M. J. Saaranen, A. R. Karala, A. K. Lappi, L. Wang, I. B. Raykhel, H. I. Alanen, K. E. Salo, C. C. Wang, and L. W. Ruddock (2011). Two endoplasmic reticulum PDI peroxidases increase the efficiency of the use of peroxide during disulfide bond formation. J Mol Biol 406: 503-515.

D. Nilsson, K. Gunasekera, J. Mani, M. Osteras, L. Farinelli, L. Baerlocher, I. Roditi, and T. Ochsenreiter (2010). Spliced leader trapping reveals widespread alternative splicing patterns in the highly dynamic transcriptome of *Trypanosoma brucei*. PLoS Pathog 6: e1001037.

A. Nißen (2014). The distinct roles of the tryparedoxin peroxidases Px I, Px II and Px III in African trypanosomes. MD thesis: Ruprecht-Karls-Universität Heidelberg.

F. Njiokou, C. Laveissière, G. Simo, S. Nkinin, P. Grébaut, G. Cuny, and S. Herder (2006). Wild fauna as a probable animal reservoir for *Trypanosoma brucei gambiense* in Cameroon. Infect Genet Evol 6: 147-153.

H. Nohl, and L. Gille (2005). Lysosomal ROS formation. Redox Rep 10: 199-205.

T. C. O'Brien, Z. B. Mackey, R. D. Fetter, Y. Choe, A. J. O'Donoghue, M. Zhou, C. S. Craik, C. R. Caffrey, and J. H. McKerrow (2008). A parasite cysteine protease is key to host protein degradation and iron acquisition. J. Biol. Chem. 283: 28934-28943.

R. S. Ohgami, D. R. Campagna, E. L. Greer, B. Antiochos, A. McDonald, J. Chen, J. J. Sharp, Y. Fujiwara, J. E. Barker, and M. D. Fleming (2005). Identification of a ferrireductase required for efficient transferrin-dependent iron uptake in erythroid cells. Nat Genet 37: 1264-1269.

F. R. Opperdoes, P. Baudhuin, I. Coppens, C. De Roe, S. W. Edwards, P. J. Weijers, and O. Misset (1984). Purification, morphometric analysis, and characterization of the glycosomes (microbodies) of the protozoan hemoflagellate *Trypanosoma brucei*. J Cell Biol 98: 1178-1184.

F. R. Opperdoes, and P. A. Michels (1993). The glycosomes of the Kinetoplastida. Biochimie 75: 231-234.

G. Ortíz-Estrada, S. Luna-Castro, C. Piña-Vázquez, L. Samaniego-Barrón, N. León-Sicairos, J. Serrano-Luna, and M. de la Garza (2012). Iron-saturated lactoferrin and pathogenic protozoa: could this protein be an iron source for their parasitic style of life? Future Microbiol 7: 149-164.

P. Overath, J. Czichos, and C. Haas (1986). The effect of citrate/cis-aconitate on oxidative metabolism during transformation of *Trypanosoma brucei*. Eur J Biochem 160: 175-182.

L. S. Paes, B. Suárez Mantilla, F. M. Zimbres, E. M. Pral, P. Diogo de Melo, E. B. Tahara, A. J. Kowaltowski, M. C. Elias, and A. M. Silber (2013). Proline dehydrogenase regulates redox state and respiratory metabolism in *Trypanosoma cruzi*. PLoS One 8: e69419.

P. N. Paradkar, K. B. Zumbrennen, B. H. Paw, D. M. Ward, and J. Kaplan (2009). Regulation of mitochondrial iron import through differential turnover of mitoferrin 1 and mitoferrin 2. Mol Cell Biol 29: 1007-1016.

E. Pays, B. Vanhollebeke, L. Vanhamme, F. Paturiaux-Hanocq, D. P. Nolan, and D. Pérez-Morga (2006). The trypanolytic factor of human serum. Nat Rev Microbiol 4: 477-486.

R. F. Peck, A. M. Shiflett, K. J. Schwartz, A. McCann, S. L. Hajduk, and J. D. Bangs (2008). The LAMP-like protein p67 plays an essential role in the lysosome of African trypanosomes. Mol. Microbiol. 68: 933-946.

J. Pépin, F. Milord, A. N. Khonde, T. Niyonsenga, L. Loko, B. Mpia, and P. De Wals (1995). Risk factors for encephalopathy and mortality during melarsoprol treatment of *Trypanosoma brucei gambiense* sleeping sickness. Trans R Soc Trop Med Hyg 89: 92-97.

D. Pérez-Morga, B. Vanhollebeke, F. Paturiaux-Hanocq, D. P. Nolan, L. Lins, F. Homblé, L. Vanhamme, P. Tebabi, A. Pays, P. Poelvoorde, A. Jacquet, R. Brasseur, and E. Pays (2005). Apolipoprotein L-I promotes trypanosome lysis by forming pores in lysosomal membranes. Science 309: 469-472.

H. L. Persson, Z. Yu, O. Tirosh, J. W. Eaton, and U. T. Brunk (2003). Prevention of oxidant-induced cell death by lysosomotropic iron chelators. Free Radic. Biol. Med. 34: 1295-1305.

F. Petrat, H. de Groot, and U. Rauen (2001). Subcellular distribution of chelatable iron: a laser scanning microscopic study in isolated hepatocytes and liver endothelial cells. Biochem J 356: 61-69.

R. L. Pisoni, T. L. Acker, K. M. Lisowski, R. M. Lemons, and J. G. Thoene (1990). A cysteine-specific lysosomal transport system provides a major route for the delivery of thiol to human fibroblast lysosomes: possible role in supporting lysosomal proteolysis. J Cell Biol 110: 327-335.

T. Pomorski, and A. K. Menon (2006). Lipid flippases and their biological functions. Cell Mol Life Sci 63: 2908-2921.

T. R. Pushpa-Rekha, A. L. Burdsall, L. M. Oleksa, G. M. Chisolm, and D. M. Driscoll (1995). Rat phospholipid-hydroperoxide glutathione peroxidase. cDNA cloning and identification of multiple transcription and translation start sites. J Biol Chem 270: 26993-26999.

T. Ramming, and C. Appenzeller-Herzog (2013). Destroy and exploit: catalyzed removal of hydroperoxides from the endoplasmic reticulum. Int J Cell Biol 2013: 180906.

B. Reuner, E. Vassella, B. Yutzy, and M. Boshart (1997). Cell density triggers slender to stumpy differentiation of *Trypanosoma brucei* bloodstream forms in culture. Mol Biochem Parasitol 90: 269-280.

L. Rivière, S. W. van Weelden, P. Glass, P. Vegh, V. Coustou, M. Biran, J. J. van Hellemond, F. Bringaud, A. G. Tielens, and M. Boshart (2004). Acetyl:succinate CoA-transferase in procyclic *Trypanosoma brucei*. Gene identification and role in carbohydrate metabolism. J Biol Chem 279: 45337-45346.

A. Roldán, M. A. Comini, M. Crispo, and R. L. Krauth-Siegel (2011). Lipoamide dehydrogenase is essential for both bloodstream and procyclic *Trypanosoma brucei*. Mol. Microbiol. 81: 623-639.

M. F. Ross, T. A. Prime, I. Abakumova, A. M. James, C. M. Porteous, R. A. Smith, and M. P. Murphy (2008). Rapid and extensive uptake and activation of hydrophobic triphenylphosphonium cations within cells. Biochem J 411: 633-645.

D. Salmon, F. Paturiaux-Hanocq, P. Poelvoorde, L. Vanhamme, and E. Pays (2005). *Trypanosoma brucei*: growth differences in different mammalian sera are not due to the species-specificity of transferrin. Exp Parasitol 109: 188-194.

D. Schell, N. K. Borowy, and P. Overath (1991). Transferrin is a growth factor for the bloodstream form of *Trypanosoma brucei*. Parasitol Res 77: 558-560.

T. Schlecker, M. A. Comini, J. Melchers, T. Ruppert, and R. L. Krauth-Siegel (2007). Catalytic mechanism of the glutathione peroxidase-type tryparedoxin peroxidase of *Trypanosoma brucei*. Biochem J 405: 445-454.

T. Schlecker, A. Schmidt, N. Dirdjaja, F. Voncken, C. Clayton, and R. L. Krauth-Siegel (2005). Substrate specificity, localization, and essential role of the glutathione peroxidase-type tryparedoxin peroxidases in *Trypanosoma brucei*. J. Biol. Chem. 280: 14385-14394.

A. Schneider, D. Bursać, and T. Lithgow (2008). The direct route: a simplified pathway for protein import into the mitochondrion of trypanosomes. Trends Cell Biol 18: 12-18.

M. Schneider, H. Förster, A. Boersma, A. Seiler, H. Wehnes, F. Sinowatz, C. Neumüller, M. J. Deutsch, A. Walch, M. Hrabé de Angelis, W. Wurst, F. Ursini, A. Roveri, M. Maleszewski, M. Maiorino, and M. Conrad (2009). Mitochondrial glutathione peroxidase 4 disruption causes male infertility. FASEB J 23: 3233-3242.

S. Scory, Y. D. Stierhof, C. R. Caffrey, and D. Steverding (2007). The cysteine proteinase inhibitor Z-Phe-Ala-CHN_2 alters cell morphology and cell division activity of *Trypanosoma brucei* bloodstream forms *in vivo*. Kinetoplastid Biol. Dis. 6: 2.

A. Seiler, M. Schneider, H. Förster, S. Roth, E. K. Wirth, C. Culmsee, N. Plesnila, E. Kremmer, O. Rådmark, W. Wurst, G. W. Bornkamm, U. Schweizer, and M. Conrad (2008). Glutathione peroxidase 4 senses and translates oxidative stress into 12/15-lipoxygenase dependent- and AIF-mediated cell death. Cell Metab. 8: 237-248.

A. D. Sheftel, and R. Lill (2009). The power plant of the cell is also a smithy: the emerging role of mitochondria in cellular iron homeostasis. Ann Med 41: 82-99.

A. D. Sheftel, A. S. Zhang, C. Brown, O. S. Shirihai, and P. Ponka (2007). Direct interorganellar transfer of iron from endosome to mitochondrion. Blood 110: 125-132.

A. Sheftel, O. Stehling, and R. Lill (2010). Iron-sulfur proteins in health and disease. Trends Endocrinol Metab 21: 302-314.

M. Shvartsman, R. Kikkeri, A. Shanzer, and Z. I. Cabantchik (2007). Non-transferrin-bound iron reaches mitochondria by a chelator-inaccessible mechanism: biological and clinical implications. Am J Physiol Cell Physiol 293: C1383-1394.

D. Steverding (1998). Bloodstream forms of *Trypanosoma brucei* require only small amounts of iron for growth. Parasitol. Res. 84: 59-62.

D. Steverding (2008). The history of African trypanosomiasis. Parasit Vectors 1: 3.

D. Steverding, D. W. Sexton, X. Wang, S. S. Gehrke, G. K. Wagner, and C. R. Caffrey (2012). *Trypanosoma brucei*: chemical evidence that cathepsin L is essential for survival and a relevant drug target. Int J Parasitol 42: 481-488.

D. Steverding, Y. D. Stierhof, M. Chaudhri, M. Ligtenberg, D. Schell, A. G. Beck-Sickinger, and P. Overath (1994). ESAG 6 and 7 products of *Trypanosoma brucei* form a transferrin binding protein complex. Eur J Cell Biol 64: 78-87.

D. Steverding, Y. D. Stierhof, H. Fuchs, R. Tauber, and P. Overath (1995). Transferrin-binding protein complex is the receptor for transferrin uptake in *Trypanosoma brucei*. J Cell Biol 131: 1173-1182.

S. J. Stone, M. C. Levin, P. Zhou, J. Han, T. C. Walther, and R. V. Farese, Jr. (2009). The endoplasmic reticulum enzyme DGAT2 is found in mitochondria-associated membranes and has a mitochondrial targeting signal that promotes its association with mitochondria. J Biol Chem 284: 5352-5361.

K. Stuart, R. Brun, S. Croft, A. Fairlamb, R. E. Gürtler, J. McKerrow, S. Reed, and R. Tarleton (2008). Kinetoplastids: related protozoan pathogens, different diseases. J Clin Invest 118: 1301-1310.

M. C. Taylor, and J. M. Kelly (2010). Iron metabolism in trypanosomatids, and its crucial role in infection. Parasitology 137: 899-917.

M. C. Taylor, A. P. McLatchie, and J. M. Kelly (2013). Evidence that transport of iron from the lysosome to the cytosol in African trypanosomes is mediated by a mucolipin orthologue. Mol. Microbiol. 89: 420-432.

A. Terman, and T. Kurz (2013). Lysosomal iron, iron chelation, and cell death. Antioxid Redox Signal 18: 888-898.

E. Tetaud, C. Giroud, A. R. Prescott, D. W. Parkin, D. Baltz, N. Biteau, T. Baltz, and A. H. Fairlamb (2001). Molecular characterisation of mitochondrial and cytosolic trypanothione-dependent tryparedoxin peroxidases in *Trypanosoma brucei*. Mol Biochem Parasitol 116: 171-183.

J. P. Thomas, P. G. Geiger, M. Maiorino, F. Ursini, and A. W. Girotti (1990). Enzymatic reduction of phospholipid and cholesterol hydroperoxides in artificial bilayers and lipoproteins. Biochim. Biophys. Acta 1045: 252-260.

A. G. Tielens, and J. J. Van Hellemond (1998). Differences in energy metabolism between Trypanosomatidae. Parasitol. Today 14: 265-272.

A. G. Tielens, and J. J. van Hellemond (2009). Surprising variety in energy metabolism within Trypanosomatidae. Trends Parasitol 25: 482-490.

A. M. Tomás, and H. Castro (2013). Redox metabolism in mitochondria of trypanosomatids. Antioxid Redox Signal 19: 696-707.

S. Toppo, L. Flohé, F. Ursini, S. Vanin, and M. Maiorino (2009). Catalytic mechanisms and specificities of glutathione peroxidases: variations of a basic scheme. Biochim Biophys Acta 1790: 1486-1500.

S. C. Tosatto, V. Bosello, F. Fogolari, P. Mauri, A. Roveri, S. Toppo, L. Flohé, F. Ursini, and M. Maiorino (2008). The catalytic site of glutathione peroxidases. Antioxid Redox Signal 10: 1515-1526.

K. E. Tripodi, S. M. Menendez Bravo, and J. A. Cricco (2011). Role of heme and heme-proteins in trypanosomatid essential metabolic pathways. Enzyme Res. 2011: 873230.

(2015).

J. F. Turrens (2003). Mitochondrial formation of reactive oxygen species. J. Physiol. 552: 335-344.

A. Uchiyama, J. S. Kim, K. Kon, H. Jaeschke, K. Ikejima, S. Watanabe, and J. J. Lemasters (2008). Translocation of iron from lysosomes into mitochondria is a key event during oxidative stress-induced hepatocellular injury. Hepatology 48: 1644-1654.

F. Ursini, S. Heim, M. Kiess, M. Maiorino, A. Roveri, J. Wissing, and L. Flohé (1999). Dual function of the selenoprotein PHGPx during sperm maturation. Science 285: 1393-1396.

F. Ursini, M. Maiorino, M. Valente, L. Ferri, and C. Gregolin (1982). Purification from pig liver of a protein which protects liposomes and biomembranes from peroxidative degradation and exhibits glutathione peroxidase activity on phosphatidylcholine hydroperoxides. Biochim Biophys Acta 710: 197-211.

P. Uzureau, S. Uzureau, L. Lecordier, F. Fontaine, P. Tebabi, F. Homblé, A. Grélard, V. Zhendre, D. P. Nolan, L. Lins, J. M. Crowet, A. Pays, C. Felu, P. Poelvoorde, B. Vanhollebeke, S. K. Moestrup, J. Lyngsø, J. S. Pedersen, J. C. Mottram, E. J. Dufourc, D. Pérez-Morga, and E. Pays (2013). Mechanism of *Trypanosoma brucei gambiense* resistance to human serum. Nature 501: 430-434.

M. Valko, D. Leibfritz, J. Moncol, M. T. Cronin, M. Mazur, and J. Telser (2007). Free radicals and antioxidants in normal physiological functions and human disease. Int J Biochem Cell Biol 39: 44-84.

J. Van Den Abbeele, Y. Claes, D. van Bockstaele, D. Le Ray, and M. Coosemans (1999). *Trypanosoma brucei* spp. development in the tsetse fly: characterization of the post-mesocyclic stages in the foregut and proboscis. Parasitology 118 (Pt 5): 469-478.

J. J. van Hellemond, F. R. Opperdoes, and A. G. Tielens (2005). The extraordinary mitochondrion and unusual citric acid cycle in *Trypanosoma brucei*. Biochem Soc Trans 33: 967-971.

H. G. van Luenen, R. Kieft, R. Mussmann, M. Engstler, B. ter Riet, and P. Borst (2005). Trypanosomes change their transferrin receptor expression to allow effective uptake of host transferrin. Mol. Microbiol. 58: 151-165.

L. Vanhamme, F. Paturiaux-Hanocq, P. Poelvoorde, D. P. Nolan, L. Lins, J. Van Den Abbeele, A. Pays, P. Tebabi, H. Van Xong, A. Jacquet, N. Moguilevsky, M. Dieu, J. P. Kane, P. De Baetselier, R. Brasseur, and E. Pays (2003). Apolipoprotein L-I is the trypanosome lytic factor of human serum. Nature 422: 83-87.

B. Vanhollebeke, G. De Muylder, M. J. Nielsen, A. Pays, P. Tebabi, M. Dieu, M. Raes, S. K. Moestrup, and E. Pays (2008). A haptoglobin-hemoglobin receptor conveys innate immunity to *Trypanosoma brucei* in humans. Science 320: 677-681.

B. Vanhollebeke, M. J. Nielsen, Y. Watanabe, P. Truc, L. Vanhamme, K. Nakajima, S. K. Moestrup, and E. Pays (2007). Distinct roles of haptoglobin-related protein and apolipoprotein L-I in trypanolysis by human serum. Proc. Natl. Acad. Sci. USA 104: 4118-4123.

B. Vanhollebeke, and E. Pays (2010). The trypanolytic factor of human serum: many ways to enter the parasite, a single way to kill. Mol Microbiol 76: 806-814.

J. Vasquez-Vivar, B. Kalyanaraman, and M. C. Kennedy (2000). Mitochondrial aconitase is a source of hydroxyl radical. An electron spin resonance investigation. J Biol Chem 275: 14064-14069.

L. Wang, L. Zhang, Y. Niu, R. Sitia, and C. C. Wang (2014). Glutathione peroxidase 7 utilizes hydrogen peroxide generated by Ero1α to promote oxidative protein folding. Antioxid Redox Signal 20: 545-556.

World Health Organization (2014) African trypanosomiasis (sleeping sickness) [World Health Organ Fact Sheet No 259]. http://www.who.int/mediacentre/factsheets/fs259/en/.

J. Widener, M. J. Nielsen, A. Shiflett, S. K. Moestrup, and S. Hajduk (2007). Hemoglobin is a co-factor of human trypanosome lytic factor. PLoS Pathog. 3: 1250-1261.

S. R. Wilkinson, D. Horn, S. R. Prathalingam, and J. M. Kelly (2003). RNA interference identifies two hydroperoxide metabolizing enzymes that are essential to the bloodstream form of the african trypanosome. J Biol Chem 278: 31640-31646.

S. R. Wilkinson, D. J. Meyer, M. C. Taylor, E. V. Bromley, M. A. Miles, and J. M. Kelly (2002a). The *Trypanosoma cruzi* enzyme TcGPXI is a glycosomal peroxidase and can be linked to trypanothione reduction by glutathione or tryparedoxin. J Biol Chem 277: 17062-17071.

S. R. Wilkinson, S. R. Prathalingam, M. C. Taylor, A. Ahmed, D. Horn, and J. M. Kelly (2006). Functional characterisation of the iron superoxide dismutase gene repertoire in *Trypanosoma brucei*. Free Radic Biol Med 40: 198-209.

S. R. Wilkinson, M. C. Taylor, S. Touitha, I. L. Mauricio, D. J. Meyer, and J. M. Kelly (2002b). TcGPXII, a glutathione-dependent Trypanosoma cruzi peroxidase with substrate specificity restricted to fatty acid and phospholipid hydroperoxides, is localized to the endoplasmic reticulum. Biochem J 364: 787-794.

C. C. Winterbourn (2008). Reconciling the chemistry and biology of reactive oxygen species. Nat Chem Biol 4: 278-286.

H. Wolburg, S. Mogk, S. Acker, C. Frey, M. Meinert, C. Schönfeld, M. Lazarus, Y. Urade, B. K. Kubata, and M. Duszenko (2012). Late stage infection in sleeping sickness. PLoS One 7: e34304.

H. V. Xong, L. Vanhamme, M. Chamekh, C. E. Chimfwembe, J. Van Den Abbeele, A. Pays, N. Van Meirvenne, R. Hamers, P. De Baetselier, and E. Pays (1998). A VSG expression site-associated gene confers resistance to human serum in *Trypanosoma rhodesiense*. Cell 95: 839-846.

L. J. Yant, Q. Ran, L. Rao, H. Van Remmen, T. Shibatani, J. G. Belter, L. Motta, A. Richardson, and T. A. Prolla (2003). The selenoprotein GPX4 is essential for mouse development and protects from radiation and oxidative damage insults. Free Radic Biol Med 34: 496-502.

M. H. Yoo, X. Gu, X. M. Xu, J. Y. Kim, B. A. Carlson, A. D. Patterson, H. Cai, V. N. Gladyshev, and D. L. Hatfield (2010). Delineating the role of glutathione peroxidase 4 in protecting cells against lipid hydroperoxide damage and in Alzheimer's disease. Antioxid Redox Signal 12: 819-827.

M. Yoshinari, and A. Taurog (1985). Lysosomal digestion of thyroglobulin: role of cathepsin D and thiol proteases. Endocrinology 117: 1621-1631.

X. Zhang, J. Cui, D. Nilsson, K. Gunasekera, A. Chanfon, X. Song, H. Wang, Y. Xu, and T. Ochsenreiter (2010). The *Trypanosoma brucei* MitoCarta and its regulation and splicing pattern during development. Nucleic Acids Res 38: 7378-7387.

X. Zhang, and J. J. Lemasters (2013). Translocation of iron from lysosomes to mitochondria during ischemia predisposes to injury after reperfusion in rat hepatocytes. Free Radic Biol Med 63: 243-253.

H. Zhao, Y. Cai, S. Santi, R. Lafrenie, and H. Lee (2005). Chloroquine-mediated radiosensitization is due to the destabilization of the lysosomal membrane and subsequent induction of cell death by necrosis. Radiat Res 164: 250-257.

N. Zhao, J. Gao, C. A. Enns, and M. D. Knutson (2010). ZRT/IRT-like protein 14 (ZIP14) promotes the cellular assimilation of iron from transferrin. J Biol Chem 285: 32141-32150.

R. Zimmermann, S. Eyrisch, M. Ahmad, and V. Helms (2011). Protein translocation across the ER membrane. Biochim Biophys Acta 1808: 912-924.

6 Appendix

6.1 BS px I-II$^{-/-}$: 5 mM ammonium chloride and 10 µM chloroquine

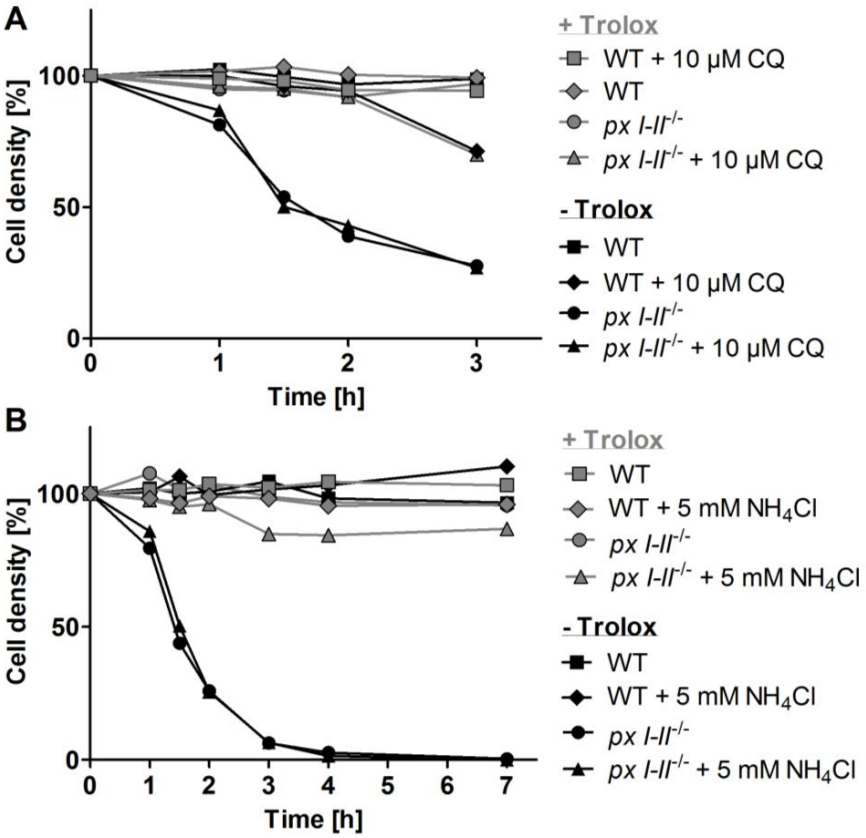

Figure 6.1: *Px I-II*$^{-/-}$ cell death is not attenuated in the presence of chloroquine and ammonium chloride. BS WT and *px I-II*$^{-/-}$ cells were **A.** pre-incubated with 10 µM chloroquine (CQ) at 37 °C for 30 min and transferred into standard medium ± 100 µM Trolox and 10 µM CQ and **B.** 5 mM ammonium chloride (NH_4Cl). After different times at **A.** 19 °C and **B.** 22 °C, cells were counted.

6.2 PC px I-III$^{-/-}$: 2nd antibody reaction (Alexa Fluor 488)

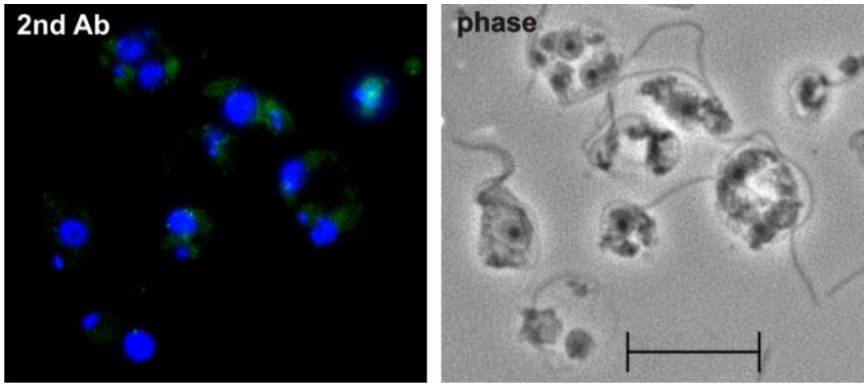

Figure 6.2: IF staining of PC *px I-III*$^{-/-}$ cells only with the 2nd Alexa Fluor 488 antibody. The parasites were kept at 27 °C in medium without Trolox for 4 h and subjected to immunofluorescence microscopy analysis. (*Left*) 2nd Ab, an overlay of the images taken from the staining using the 2nd Alexa Fluor 488 antibody (green) and the DAPI signal (blue); (*Right*) phase, phase contrast picture. The 2nd antibody alone displayed only a weak signal. (Scale bar: 10 µm)

6.3 PC WT and px I-III$^{-/-}$: Click-IT lipid peroxidation kit

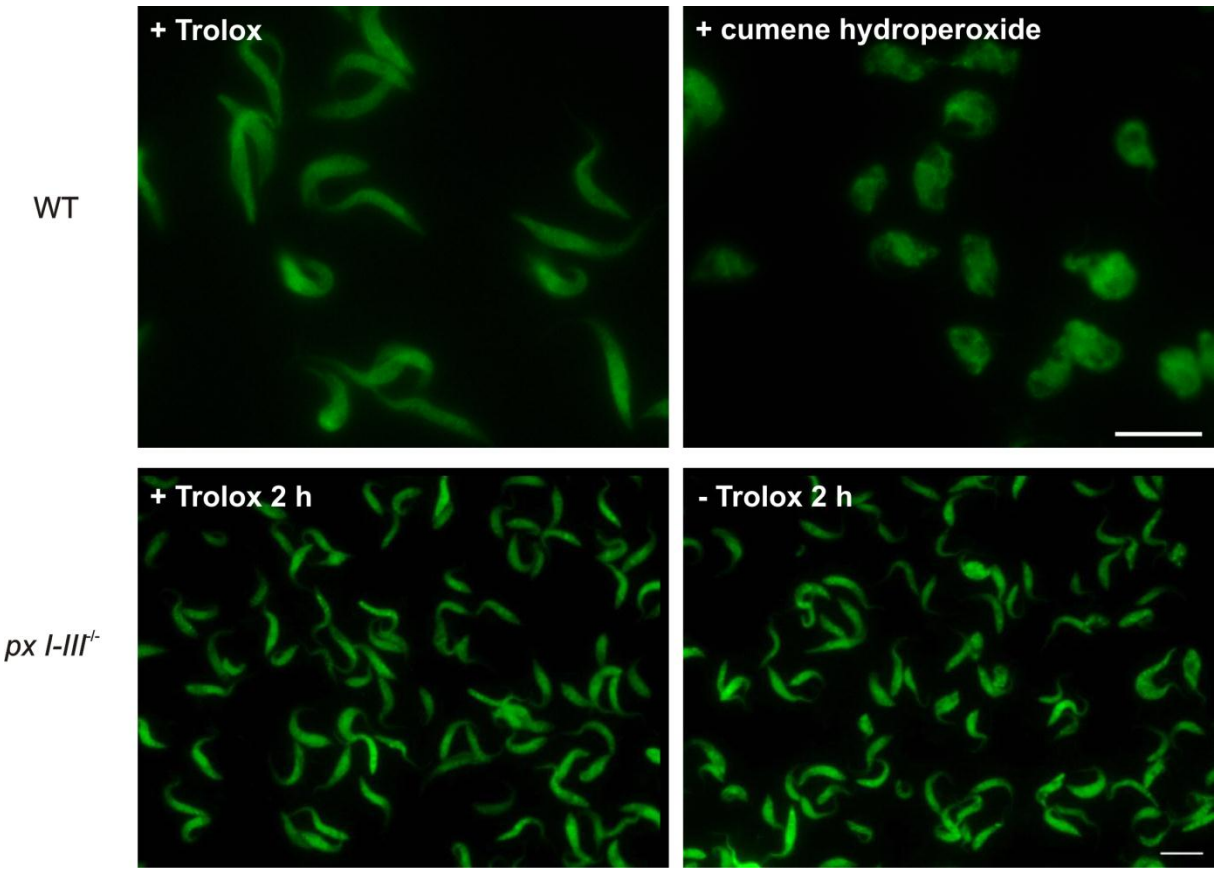

Figure 6.3: LAA treatment and stress induction does not enhance the signal intensity of putative lipid-peroxidation-derived protein modifications. (*Top*) WT PC parasites were cultivated at 27 °C for 2 h in MEM-Pros medium + 50 µM LAA in the presence of each 100 µM Trolox or cumene hydroperoxides and analyzed by immunofluorescence microscopy. LAA reaction signals (green). The LAA signal intensity did not change upon treatment with cumene hydroperoxide although the cells displayed a stressed phenotype. (*Bottom*) PC *px I-III*$^{-/-}$ cells were incubated at 27 °C for 2 h ± Trolox and + 50 µM LAA. The mutant cells revealed no enhanced LAA signal upon Trolox removal. (Scale bar: 10 µm)

6.4 PC WT cells: different concentrations of hemin and iron

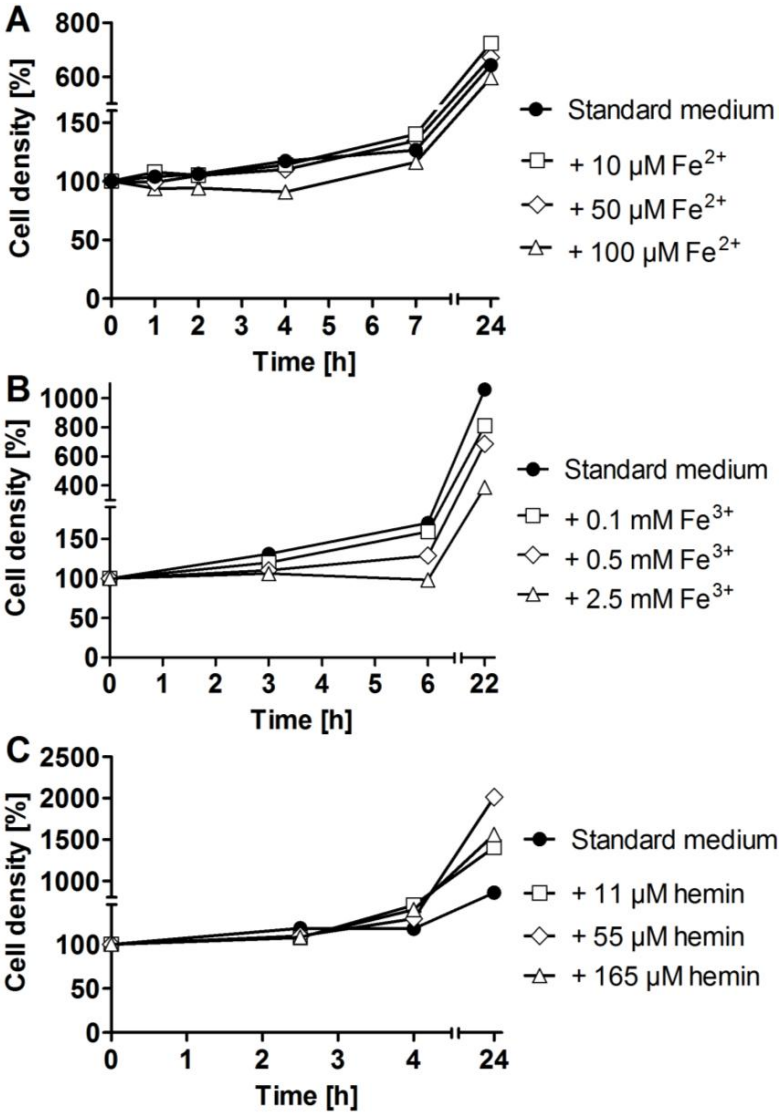

Figure 6.4: Different concentration of ferrous and ferric iron and hemin on PC WT cells. WT cells were incubated for 24 h at 27 °C in standard MEM-Pros medium supplemented with **A.** 10, 50, and 100 µM Fe^{2+}, **B.** 0.1, 0.5, and 2.5 mM Fe^{3+}, and **C.** 11, 55, and 165 µM hemin.

6.5 PC px I-III$^{-/-}$: hemin- and FCS-free medium ± Trolox

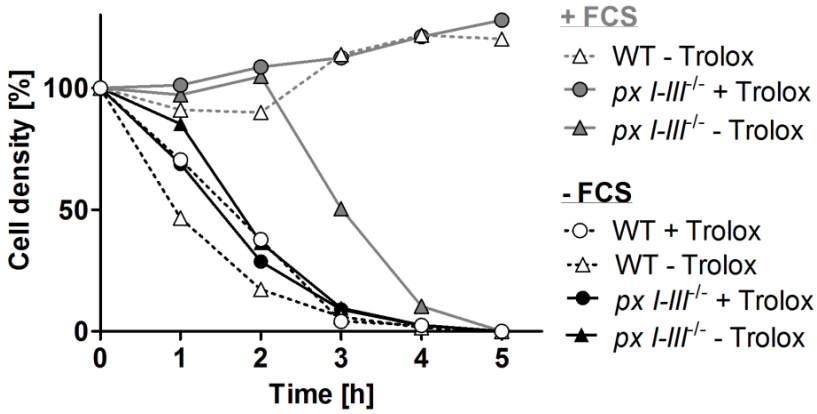

Figure 6.5: Lysis of PC *px I-III*$^{-/-}$ *T. brucei* is not attenuated in hemin-free medium. PC WT and *px I-III*$^{-/-}$ cells were kept for one week in hemin-free MEM-Pros medium. Cells were washed 3 times with 12 ml of 1x PBS and transferred to standard medium without exogenous added hemin and ± FCS. Cells were incubated at 27 °C and counted at the indicated times.

6.6 PC px I-III$^{-/-}$ *and BS px I-II*$^{-/-}$*: coenzyme Q10 supplementation*

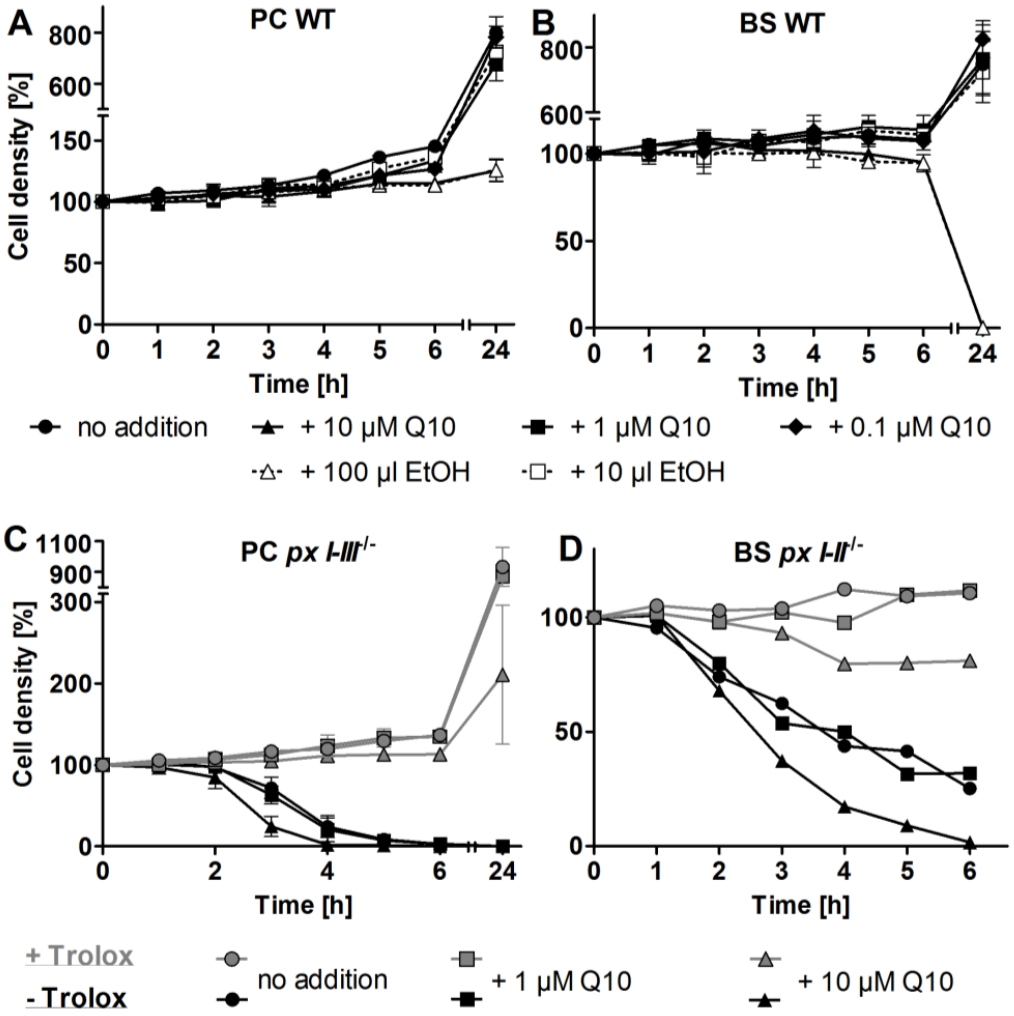

Figure 6.6: Supplementing medium with coenzyme Q10 does not affect the lysis of PC *px I-III*$^{-/-}$ and BS *px I-II*$^{-/-}$ parasites. A. and **B.** PC and BS WT cells were kept for 24 h in standard medium ± 10, 1, and 0.1 µM coenzyme Q10 (Q10) or 100 and 10 µl ethanol (EtOH). The amount of EtOH displays the solvent amount used for the Q10 supplementation (10 µM Q10 = 100 µl EtOH, 1 µM Q10 = 10 µl EtOH). **C.** and **D.** PC *px I-III*$^{-/-}$ and BS *px I-II*$^{-/-}$ parasites were incubated in standard medium ± Trolox ± 10 and 1 µM Q10. Slight growth defects were only seen in the presence of 10 µM Q10 but the solvent alone had already a toxic effect.

6.7 PC px III$^{-/-}$: PCR of the pac and bla resistance cassette

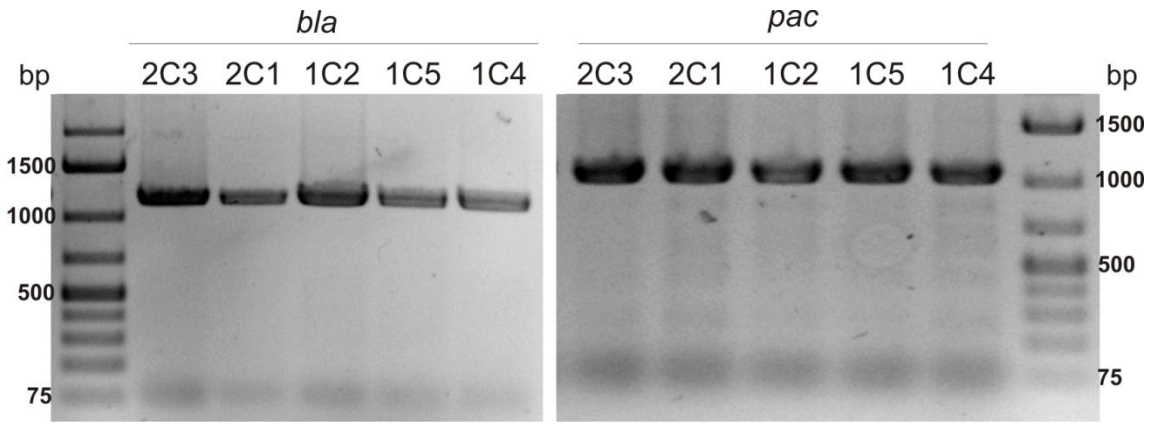

Figure 6.7: PC *px III*$^{-/-}$ parasites created by transfecting WT cells with the pHD1747/48_ KO*pxIII* plasmids display the resistance cassettes in the right locus. Genomic DNA of PC *px III*$^{-/-}$ clones 2C3, 2C1, 1C2, 1C5, and 1C4 generated by transfecting WT cells with pHD1747/48_KO*pxIII* vectors was isolated and analyzed by PCR. The primer pairs Bla-F and 3UTR_PxIII_R2 (*bla*) as well as PuroF_CH2 and 3UTR_PxIII_R2 (*pac*) were used for the detection of the blasticidin and puromycin resistance gene, respectively. The products were loaded on a 1% agarose gel (*bla*, 1164 bp; *pac*, 1043 bp).

6.8 Px IV triple Cys mutant: Test expression

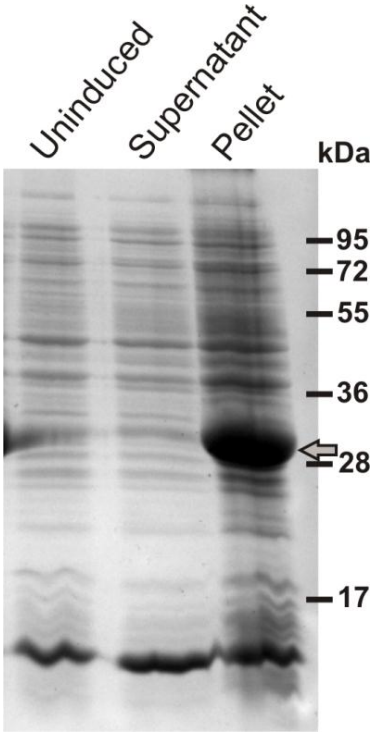

Figure 6.8: The triple Cys mutant of Px IV shows no increase in protein solubility. Test expression of the triple Cys mutant of Px IV (Cys26/81/134/Ser, grey arrow) linked to the Trx fusion protein was performed. Conditions were described in Table 3.1. The total lysate of the uninduced sample (prior to IPTG addition) as well as the supernatant and pellet fractions of the induced cultures were subjected to SDS-PAGE onto a 14% gel and stained with Coomassie. The Trx-Px IV fusion protein is marked by a grey arrow.

6.9 Px IV antibodies: Western blot analysis of cell lysate and recombinant Px IV

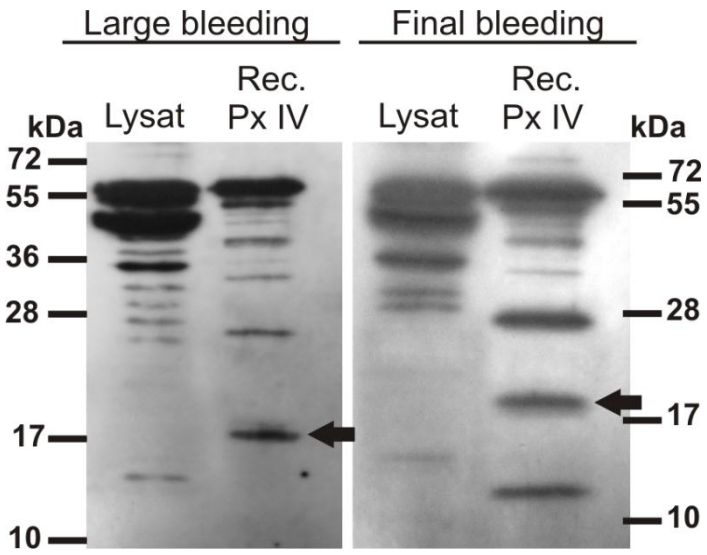

Figure 6.9: Antibodies against the authentic untagged Px IV hardly detect the recombinant protein and no band at the expected size was obtained in BS cell lysates. BS parasites (Lysat, 3 x 10^6 cells) and recombinant His_6-Px IV (Rec Px IV, 2400 ng large and 3388 ng final bleeding) were subjected to Western blot analysis using Px IV antiserum from the large and final bleeding (1:500). The samples were analyzed on a 14% SDS gel and the His_6-Px IV is marked by a black arrow.

6.10 Vector sequences

6.10.1 px IV into pETtrx-1b plasmid

tggcgaatgggacgcgccctgtagcggcgcattaagcgcggcgggtgtggtggttacgcgcagcgtgaccgctac
acttgccagcgccctagcgcccgctcctttcgctttcttcccttcctttctcgccacgttcgccggctttccccg
tcaagctctaaatcgggggctccctttagggttccgatttagtgctttacggcacctcgaccccaaaaaacttga
ttagggtgatggttcacgtagtgggccatcgccctgatagacggtttttcgccctttgacgttggagtccacgtt
ctttaatagtggactcttgttccaaactggaacaacactcaaccctatctcggtctattcttttgatttataagg
gattttgccgatttcggcctattggttaaaaaatgagctgatttaacaaaaatttaacgcgaattttaacaaaat
attaacgtttacaatttcaggtggcacttttcggggaaatgtgcgcggaacccctatttgtttatttttctaaat
acattcaaatatgtatccgctcatgaattaattcttagaaaaactcatcgagcatcaaatgaaactgcaatttat
tcatatcaggattatcaataccatatttttgaaaaagccgtttctgtaatgaaggagaaaactcaccgaggcagt
tccataggatggcaagatcctggtatcggtctgcgattccgactcgtccaacatcaatacaacctattaatttcc
cctcgtcaaaaataaggttatcaagtgagaaatcaccatgagtgacgactgaatccggtgagaatggcaaaagtt
tatgcatttctttccagacttgttcaacaggccagccattacgctcgtcatcaaaatcactcgcatcaaccaaac
cgttattcattcgtgattgcgcctgagcgagacgaaatacgcgatcgctgttaaaaggacaattacaaacaggaa
tcgaatgcaaccggcgcaggaacactgccagcgcatcaacaatattttcacctgaatcaggatattcttctaata
cctggaatgctgttttcccggggatcgcagtggtgagtaaccatgcatcatcaggagtacggataaaatgcttga
tggtcggaagaggcataaattccgtcagccagtttagtctgaccatctcatctgtaacatcattggcaacgctac
ctttgccatgtttcagaaacaactctggcgcatcgggcttcccatacaatcgatagattgtcgcacctgattgcc
cgacattatcgcgagcccatttatacccatataaatcagcatccatgttggaatttaatcgcggcctagagcaag
acgtttcccgttgaatatggctcataacacccttgtattactgtttatgtaagcagacagttttattgttcatg
accaaaatcccttaacgtgagttttcgttccactgagcgtcagaccccgtagaaaagatcaaaggatcttcttga
gatcctttttttctgcgcgtaatctgctgcttgcaaacaaaaaaaccaccgctaccagcggtggtttgtttgccg
gatcaagagctaccaactctttttccgaaggtaactggcttcagcagagcgcagataccaaatactgtccttcta
gtgtagccgtagttaggccaccacttcaagaactctgtagcaccgcctacatacctcgctctgctaatcctgtta
ccagtggctgctgccagtggcgataagtcgtgtcttaccgggttggactcaagacgatagttaccggataaggcg
cagcggtcgggctgaacgggggttcgtgcacacagcccagcttggagcgaacgacctacaccgaactgagatac
ctacagcgtgagctatgagaaagcgccacgcttcccgaagggagaaaggcggacaggtatccggtaagcggcagg
gtcggaacaggagagcgcacgagggagcttccagggggaaacgcctggtatctttatagtcctgtcgggtttcgc
cacctctgacttgagcgtcgatttttgtgatgctcgtcaggggggcggagcctatggaaaaacgccagcaacgcg
gccttttacggttcctggccttttgctggccttttgctcacatgttctttcctgcgttatcccctgattctgtg
gataaccgtattaccgcctttgagtgagctgataccgctcgccgcagccgaacgaccgagcgcagcgagtcagtg
agcgaggaagcggaagagcgcctgatgcggtattttctccttacgcatctgtgcggtatttcacaccgcatatat
ggtgcactctcagtacaatctgctctgatgccgcatagttaagccagtatacactccgctatcgctacgtgactg
ggtcatggctgcgccccgacacccgccaacacccgctgacgcgccctgacgggcttgtctgctcccggcatccgc
ttacagacaagctgtgaccgtctccgggagctgcatgtgtcagaggttttcaccgtcatcaccgaaacgcgcgag
gcagctgcggtaaagctcatcagcgtggtcgtgaagcgattcacagatgtctgcctgttcatccgcgtccagctc
gttgagtttctccagaagcgttaatgtctggcttctgataaagcgggccatgttaagggcggttttttcctgttt
ggtcactgatgcctccgtgtaagggggatttctgttcatgggggtaatgataccgatgaaacgagagaggatgct
cacgatacgggttactgatgatgaacatgcccggttactggaacgttgtgagggtaaacaactggcggtatggat
gcggcgggaccagagaaaaatcactcagggtcaatgccagcgcttcgttaatacagatgtaggtgttccacaggg
tagccagcagcatcctgcgatgcagatccggaacataatggtgcagggcgctgacttccgcgtttccagacttta
cgaaacacggaaaccgaagaccattcatgttgttgctcaggtcgcagacgttttgcagcagcagtcgcttcacgt
tcgctcgcgtatcggtgattcattctgctaaccagtaaggcaaccccgccagcctagccgggtcctcaacgacag
gagcacgatcatgcgcacccgtggggccgccatgccggcgataatggcctgcttctcgccgaaacgtttggtggc
gggaccagtgacgaaggcttgagcgagggcgtgcaagattccgaataccgcaagcgacaggccgatcatcgtcgc
gctccagcgaaagcggtcctcgccgaaaatgacccagagcgctgccggcacctgtcctacgagttgcatgataaa
gaagacagtcataagtgcggcgacgatagtcatgccccgcgcccaccggaaggagctgactgggttgaaggctct
caagggcatcggtcgagatcccggtgcctaatgagtgagctaacttacattaattgcgttgcgctcactgcccgc
tttccagtcgggaaacctgtcgtgccagctgcattaatgaatcggccaacgcgcggggagaggcggtttgcgtat
tgggcgccagggtggtttttcttttcaccagtgagacgggcaacagctgattgcccttcaccgcctggccctgag
agagttgcagcaagcggtccacgctggtttgccccagcaggcgaaaatcctgtttgatggtggttaacggcggga
tataacatgagctgtcttcggtatcgtcgtatcccactaccgagatatccgcaccaacgcgcagcccggactcgg
taatggcgcgcattgcgcccagcgccatctgatcgttggcaaccagcatcgcagtgggaacgatgccctcattca
gcatttgcatggtttgttgaaaaccggacatggcactccagtcgccttcccgttccgctatcggctgaatttgat
tgcgagtgagatatttatgccagccagccagacgcagacgcgccgagacagaacttaatgggcccgctaacagcg
cgatttgctggtgacccaatgcgaccagatgctccacgcccagtcgcgtaccgtcttcatgggagaaaataatac
tgttgatgggtgtctggtcagagacatcaagaaataacgccggaacattagtgcaggcagcttccacagcaatgg

catcctggtcatccagcggatagttaatgatcagcccactgacgcgttgcgcgagaagattgtgcaccgccgctt
tacaggcttcgacgccgcttcgttctaccatcgacaccaccacgctggcacccagttgatcggcgcgagatttaa
tcgccgcgacaatttgcgacggcgcgtgcagggccagactggaggtggcaacgccaatcagcaacgactgtttgc
ccgccagttgttgtgccacgcggttgggaatgtaattcagctccgccatcgccgcttccacttttcccgcgttt
tcgcagaaacgtggctggcctggttcaccacgcgggaaacggtctgataagagacaccggcatactctgcgacat
cgtataacgttactggtttcacattcaccaccctgaattgactctcttccgggcgctatcatgccataccgcgaa
aggttttgcgccattcgatggtgtccgggatctcgacgctctcccttatgcgactcctgcattaggaagcagccc
agtagtaggttgaggccgttgagcaccgccgccgcaaggaatggtgcatgcaaggagatggcgcccaacagtccc
ccggccacggggcctgccaccatacccacgccgaaacaagcgctcatgagcccgaagtggcgagcccgatcttcc
ccatcggtgatgtcggcgatataggcgccagcaaccgcacctgtggcgccggtgatgccggccacgatgcgtccg
gcgtagaggatcgagatctcgatcccgcgaaattaatacgactcactataggggaattgtgagcggataacaatt
cccctctagaaataattttgtttaactttaagaaggagatataccatgagcgataaaattattcacctgactgac
gacagttttgacacggatgtactcaaagcggacggggcgatcctcgtcgatttctgggcagagtggtgcggtccg
tgcaaaatgatcgccccgattctggatgaaatcgctgacgaatatcagggcaaactgaccgttgcaaaactgaac
atcgatcaaaaccctggcactgcgccgaaatatggcatccgtggtatcccgactctgctgctgttcaaaaacggt
gaagtggcggcaaccaaagtgggtgcactgtctaaaggtcagttgaaagagttcctcgacgctaacctggccgga
tctggcagtggttctggtCATCACCATCACCATCACtccgcgggtagcGAGAATCTTTATTTTCAGggcgCCatg
ggcaatggcggcgccatttttttctcactcggttctaatggacggtaacgcagtgatgctgtccaagtatgctggt
tgtgtaacggttcttgttaacactgcgtccctctgctcttttacatcttcaaacattcaacaccttatacacgtt
cagcaaaaatgggcctcacgaagtttcactgtcttagcctttccgtgctctcaatttggaaatcaagagccgaag
aagagggatgagatttgctgttgggtggctcgtaatggaattaactttcctgtgtttgataaagttaacctgaag
gggccgaatacacacccccctgtttcaaatgattcagtcgtcgcttggacctatacggtggaattacacgaaggtt
gtgtgcaatcgtgccggactcccatgcgtgaagcttcagccaggaagctcgctggaggagcttgagcgctatgtt
tcacagttgtgcgatgagtgaGGTACCggatccgaattcgagctccgtcgacaagcttgcggccgcactcgagca
ccaccaccaccaccactgagatccggctgctaacaaagcccgaaaggaagctgagttggctgctgccaccgctga
gcaataactagcataaccccttggggcctctaaacgggtcttgaggggtttttgctgaaaggaggaactatatc
cggat(6155 bp)

nnn = thioredoxin (*E. coli*); NNN = His-Tag; NNN = TEV cleavage site; NNN = *Nco*I site; **nnn** = ATG and GGC (inserted Gly) of *px IV* gene; nnn = *px IV* gene; NNN = *Acc*65I site

6.10.2 Truncated px IV into pETtrx-1b plasmid

…ataattttgtttaactttaagaaggagatataccatgagcgataaaattattcacctgactgacgacagttttg
acacggatgtactcaaagcggacggggcgatcctcgtcgatttctgggcagagtggtgcggtccgtgcaaaatga
tcgccccgattctggatgaaatcgctgacgaatatcagggcaaactgaccgttgcaaaactgaacatcgatcaaa
accctggcactgcgccgaaatatggcatccgtggtatcccgactctgctgctgttcaaaaacggtgaagtggcgg
caaccaaagtgggtgcactgtctaaaggtcagttgaaagagttcctcgacgctaacctggccggatctggcagtg
gttctggtCATCACCATCACCATCACtccgcgggtagcGAGAATCTTTATTTTCAGggcgCCatgggcctgtcca
agtatgctggttgtgtaacggttcttgttaacactgcgtccctctgctcttttacatcttcaaacattcaacacc
ttatacacgttcagcaaaaatgggcctcacgaagtttcactgtcttagcctttccgtgctctcaatttggaaatc
aagagccgaagaagagggatgagatttgctgttgggtggctcgtaatggaattaactttcctgtgtttgataaag
ttaacctgaaggggccgaatacacacccccctgtttcaaatgattcagtcgtcgcttggacctatacggtggaatt
acacgaaggttgtgtgcaatcgtgccggactcccatgcgtgaagcttcagccaggaagctcgctggaggagcttg
agcgctatgtttcacagttgtgcgatgagtgaGGTACCggatccgaattcg…(6101 bp)

The remaining vector sequence is shown in 6.10.1

nnn = thioredoxin (*E. coli*); NNN = His-Tag; NNN = TEV cleavage site; NNN = *Nco*I site; **nnn** = ATG and GGC (inserted Gly) of *px IV* gene; nnn = truncated *px IV* gene (Δ1-18); NNN = *Acc*65I site

6.10.3 px IV into pQE-30 plasmid

ctcgagaaatcataaaaaatttatttgctttgtgagcggataacaattataatagattcaattgtgagcggataa
caatttcacacagaattcattaaagaggagaaattaactatgagaggatcgCATCACCATCACCATCACGGATCC
atgaatggcggcgccatttttttctcactcggttctaatggacggtaacgcagtgatgctgtccaagtatgctggt
tgtgtaacggttcttgttaacactgcgtccctctgctcttttacatcttcaaacattcaacaccttatacacgtt

cagcaaaaatgggcctcacgaagtttcactgtcttagcctttccgtgctctcaatttggaaatcaagagccgaag
aagagggatgagatttgctgttgggtggctcgtaatggaattaactttcctgtgtttgataaagttaacctgaag
gggccgaatacacacccctgtttcaaatgattcagtcgtcgcttggacctatacggtggaattacacgaaggtt
gtgtgcaatcgtgccggactcccatgcgtgaagcttcagccaggaagctcgctggaggagcttgagcgctatgtt
tcacagttgtgcgatgagtgaCTGCAGccAAGCTTaattagctgagcttggactcctgttgatagatccagtaat
gacctcagaactccatctggatttgttcagaacgctcggttgccgccgggcgtttttttattggtgagaatccaag
ctagcttggcgagattttcaggagctaaggaagctaaaatggagaaaaaaatcactggatataccaccgttgata
tatcccaatggcatcgtaaagaacattttgaggcatttcagtcagttgctcaatgtacctataaccagaccgttc
agctggatattacggccttttaaagaccgtaaagaaaaataagcacaagttttatccggcctttattcacattc
ttgcccgcctgatgaatgctcatccggaatttcgtatggcaatgaaagacggtgagctggtgatatgggatagtg
ttcacccttgttacaccgttttccatgagcaaactgaaacgttttcatcgctctggagtgaataccacgacgatt
tccggcagtttctacacatatattcgcaagatgtggcgtgttacggtgaaaacctggcctatttccctaaagggt
ttattgagaatatgtttttcgtctcagccaatccctgggtgagtttcaccagttttgatttaaacgtggccaata
tggacaacttcttcgcccccgttttcaccatgggcaaatattatacgcaaggcgacaaggtgctgatgccgctgg
cgattcaggttcatcatgccgtttgtgatggcttccatgtcggcagaatgcttaatgaattacaacagtactgcg
atgagtggcagggcggggcgtaatttttttaaggcagttattggtgcccttaaacgcctggggtaatgactctct
agcttgaggcatcaaataaaacgaaaggctcagtcgaaagactgggcctttcgttttatctgttgtttgtcggtg
aacgctctcctgagtaggacaaatccgccctctagagctgcctcgcgcgtttcggtgatgacggtgaaaacctct
gacacatgcagctcccggagacggtcacagcttgtctgtaagcggatgccgggagcagacaagcccgtcagggcg
cgtcagcgggtgttggcgggtgtcggggcgcagccatgacccagtcacgtagcgatagcggagtgtatactggct
taactatgcggcatcagagcagattgtactgagagtgcaccatatgcggtgtgaaataccgcacagatgcgtaag
gagaaaataccgcatcaggcgctcttccgcttcctcgctcactgactcgctgcgctcggtcgttcggctgcggcg
agcggtatcagctcactcaaaggcggtaatacggttatccacagaatcaggggataacgcaggaaagaacatgtg
agcaaaaggccagcaaaaggccaggaaccgtaaaaaggccgcgttgctggcgtttttccataggctccgcccccc
tgacgagcatcacaaaaatcgacgctcaagtcagaggtggcgaaacccgacaggactataaagataccaggcgtt
tccccctggaagctccctcgtgcgctctcctgttccgaccctgccgcttaccggatacctgtccgcctttctccc
ttcgggaagcgtggcgctttctcatagctcacgctgtaggtatctcagttcggtgtaggtcgttcgctccaagct
gggctgtgtgcacgaaccccccgttcagcccgaccgctgcgccttatccggtaactatcgtcttgagtccaaccc
ggtaagacacgacttatcgccactggcagcagccactggtaacaggattagcagagcgaggtatgtaggcggtgc
tacagagttcttgaagtggtggcctaactacggctacactagaaggacagtatttggtatctgcgctctgctgaa
gccagttaccttcggaaaaagagttggtagctcttgatccggcaaacaaaccaccgctggtagcggtggttttt
tgtttgcaagcagcagattacgcgcagaaaaaaaggatctcaagaagatcctttgatcttttctacggggtctga
cgctcagtggaacgaaaactcacgttaagggattttggtcatgagattatcaaaaaggatcttcacctagatcct
tttaaattaaaaatgaagttttaaatcaatctaaagtatatatgagtaaacttggtctgacagttaccaatgctt
aatcagtgaggcacctatctcagcgatctgtctatttcgttcatccatagttgcctgactccccgtcgtgtagat
aactacgatacgggagggcttaccatctggccccagtgctgcaatgataccgcgagacccacgctcaccggctcc
agatttatcagcaataaaccagccagccggaagggccgagcgcagaagtggtcctgcaactttatccgcctccat
ccagtctattaattgttgccgggaagctagagtaagtagttcgccagttaatagtttgcgcaacgttgttgccat
tgctacaggcatcgtggtgtcacgctcgtcgtttggtatggcttcattcagctccggttcccaacgatcaaggcg
agttacatgatcccccatgttgtgcaaaaaagcggttagctccttcggtcctccgatcgttgtcagaagtaagtt
ggccgcagtgttatcactcatggttatggcagcactgcataattctcttactgtcatgccatccgtaagatgctt
ttctgtgactggtgagtactcaaccaagtcattctgagaatagtgtatgcggcgaccgagttgctcttgcccggc
gtcaatacgggataataccgcgccacatagcagaactttaaaagtgctcatcattggaaaacgttcttcggggcg
aaaactctcaaggatcttaccgctgttgagatccagttcgatgtaacccactcgtgcacccaactgatcttcagc
atcttttactttcaccagcgtttctgggtgagcaaaaacaggaaggcaaaatgccgcaaaaaagggaataagggc
gacacggaaatgttgaatactcatactcttcctttttcaatattattgaagcatttatcagggttattgtctcat
gagcggatacatatttgaatgtatttagaaaaataaacaaataggggttccgcgcacatttccccgaaaagtgcc
acctgacgtctaagaaaccattattatcatgacattaacctataaaaataggcgtatcacgaggccctttcgtct
tcac (3904 bp)

NNN = His-Tag; NNN = *Bam*HI site; nnn = *px IV* gene; NNN = *Pst*I site; NNN = *Hind*III site

6.10.4 px IV into pETGB-1a plasmid

tggcgaatgggacgcgccctgtagcggcgcattaagcgcggcgggtgtggtggttacgcgcagcgtgaccgctac
acttgccagcgccctagcgcccgctcctttcgctttcttcccttcctttctcgccacgttcgccggctttccccg
tcaagctctaaatcgggggctccctttagggttccgatttagtgctttacggcacctcgaccccaaaaaacttga
ttagggtgatggttcacgtagtgggccatcgccctgatagacggtttttcgccctttgacgttggagtccacgtt
ctttaatagtggactcttgttccaaactggaacaacactcaaccctatctcggtctattcttttgatttataagg
gattttgccgatttcggcctattggttaaaaaatgagctgatttaacaaaaatttaacgcgaattttaacaaaat

attaacgtttacaatttcaggtggcacttttcggggaaatgtgcgcggaacccctatttgtttatttttctaaat
acattcaaatatgtatccgctcatgaattaattcttagaaaaactcatcgagcatcaaatgaaactgcaatttat
tcatatcaggattatcaataccatatttttgaaaaagccgtttctgtaatgaaggagaaaactcaccgaggcagt
tccataggatggcaagatcctggtatcggtctgcgattccgactcgtccaacatcaatacaacctattaatttcc
cctcgtcaaaaataaggttatcaagtgagaaatcaccatgagtgacgactgaatccggtgagaatggcaaaagtt
tatgcatttctttccagacttgttcaacaggccagccattacgctcgtcatcaaaatcactcgcatcaaccaaac
cgttattcattcgtgattgcgcctgagcgagacgaaatacgcgatcgctgttaaaaggacaattacaaacaggaa
tcgaatgcaaccggcgcaggaacactgccagcgcatcaacaatattttcacctgaatcaggatattcttctaata
cctggaatgctgttttcccggggatcgcagtggtgagtaaccatgcatcatcaggagtacggataaaatgcttga
tggtcggaagaggcataaattccgtcagccagtttagtctgaccatctcatctgtaacatcattggcaacgctac
ctttgccatgtttcagaaacaactctggcgcatcgggcttcccatacaatcgatagattgtcgcacctgattgcc
cgacattatcgcgagcccatttatacccatataaatcagcatccatgttggaatttaatcgcggcctagagcaag
acgtttcccgttgaatatggctcataacacccttgtattactgtttatgtaagcagacagttttattgttcatg
accaaaatcccttaacgtgagttttcgttccactgagcgtcagaccccgtagaaaagatcaaaggatcttcttga
gatccttttttttctgcgcgtaatctgctgcttgcaaacaaaaaaaccaccgctaccagcggtggtttgtttgccg
gatcaagagctaccaactctttttccgaaggtaactggcttcagcagagcgcagataccaaatactgtccttcta
gtgtagccgtagttaggccaccacttcaagaactctgtagcaccgcctacatacctcgctctgctaatcctgtta
ccagtggctgctgccagtggcgataagtcgtgtcttaccgggttggactcaagacgatagttaccggataaggcg
cagcggtcgggctgaacgggggttcgtgcacacagcccagcttggagcgaacgacctacaccgaactgagatac
ctacagcgtgagctatgagaaagcgccacgcttcccgaagggagaaaggcggacaggtatccggtaagcggcagg
gtcggaacaggagagcgcacgagggagcttccagggggaaacgcctggtatctttatagtcctgtcgggtttcgc
cacctctgacttgagcgtcgatttttgtgatgctcgtcaggggggcggagcctatggaaaaacgccagcaacgcg
gccttttacggttcctggccttttgctggccttttgctcacatgttctttcctgcgttatcccctgattctgtg
gataaccgtattaccgcctttgagtgagctgataccgctcgccgcagccgaacgaccgagcgcagcgagtcagtg
agcgaggaagcggaagagcgcctgatgcggtattttctccttacgcatctgtgcggtatttcacaccgcatatat
ggtgcactctcagtacaatctgctctgatgccgcatagttaagccagtatacactccgctatcgctacgtgactg
ggtcatggctgcgccccgacacccgccaacacccgctgacgcgccctgacgggcttgtctgctcccggcatccgc
ttacagacaagctgtgaccgtctccgggagctgcatgtgtcagaggttttcaccgtcatcaccgaaacgcgcgag
gcagctgcggtaaagctcatcagcgtggtcgtgaagcgattcacagatgtctgcctgttcatccgcgtccagctc
gttgagtttctccagaagcgttaatgtctggcttctgataaagcgggccatgttaagggcggttttttcctgttt
ggtcactgatgcctccgtgtaagggggatttctgttcatgggggtaatgataccgatgaaacgagagaggatgct
cacgatacgggttactgatgatgaacatgcccggttactggaacgttgtgagggtaaacaactggcggtatggat
gcggcgggaccagagaaaaatcactcagggtcaatgccagcgcttcgttaatacagatgtaggtgttccacaggg
tagccagcagcatcctgcgatgcagatccggaacataatggtgcagggcgctgacttccgcgtttccagacttta
cgaaacacggaaaccgaagaccattcatgttgttgctcaggtcgcagacgttttgcagcagcagtcgcttcacgt
tcgctcgcgtatcggtgattcattctgctaaccagtaaggcaaccccgccagcctagccgggtcctcaacgacag
gagcacgatcatgcgcacccgtggggccgccatgccggcgataatggcctgcttctcgccgaaacgtttggtggc
gggaccagtgacgaaggcttgagcgagggcgtgcaagattccgaataccgcaagcgacaggccgatcatcgtcgc
gctccagcgaaagcggtcctcgccgaaaatgacccagagcgctgccggcacctgtcctacgagttgcatgataaa
gaagacagtcataagtgcggcgacgatagtcatgccccgcgcccaccggaaggagctgactgggttgaaggctct
caagggcatcggtcgagatcccggtgcctaatgagtgagctaacttacattaattgcgttgcgctcactgcccgc
tttccagtcgggaaacctgtcgtgccagctgcattaatgaatcggccaacgcgcggggagaggcggtttgcgtat
tgggcgccagggtggtttttctttcaccagtgagacgggcaacagctgattgcccttcaccgcctggccctgag
agagttgcagcaagcggtccacgctggtttgccccagcaggcgaaaatcctgtttgatggtggttaacggcggga
tataacatgagctgtcttcggtatcgtcgtatcccactaccgagatatccgcaccaacgcgcagcccggactcgg
taatggcgcgcattgcgcccagcgccatctgatcgttggcaaccagcatcgcagtgggaacgatgccctcattca
gcatttgcatggtttgttgaaaaccggacatggcactccagtcgccttcccgttccgctatcggctgaatttgat
tgcgagtgagatatttatgccagccagccagacgcagacgcgccgagacagaacttaatgggcccgctaacagcg
cgatttgctggtgacccaatgcgaccagatgctccacgcccagtcgcgtaccgtcttcatgggagaaaataatac
tgttgatgggtgtctggtcagagacatcaagaaataacgccggaacattagtgcaggcagcttccacagcaatgg
catcctggtcatccagcggatagttaatgatcagcccactgacgcgttgcgcgagaagattgtgcaccgccgctt
tacaggcttcgacgccgcttcgttctaccatcgacaccaccacgctggcacccagttgatcggcgcgagatttaa
tcgccgcgacaatttgcgacggcgcgtgcagggccagactggaggtggcaacgccaatcagcaacgactgtttgc
ccgccagttgttgtgccacgcggttgggaatgtaattcagctccgccatcgccgcttccacttttcccgcgttt
tcgcagaaacgtggctggcctggttcaccacgcgggaaacggtctgataagagacaccggcatactctgcgacat
cgtataacgttactggtttcacattcaccaccctgaattgactctcttccgggcgctatcatgccataccgcgaa
aggttttgcgccattcgatggtgtccgggatctcgacgctctcccttatgcgactcctgcattaggaagcagccc
agtagtaggttgaggccgttgagcaccgccgccgcaaggaatggtgcatgcaaggagatggcgcccaacagtccc
ccggccacggggcctgccaccatacccacgccgaaacaagcgctcatgagcccgaagtggcgagcccgatcttcc
ccatcggtgatgtcggcgatataggcgccagcaaccgcacctgtggcgccggtgatgccggccacgatgcgtccg
gcgtagaggatcgagatctcgatcccgcgaaattaatacgactcactataggggaattgtgagcggataacaatt

ccccctctagaaataattttgtttaactttaagaaggagatataccatgaaaCATCACCATCACCATCACcccatg
aaacagtacaagcttatcctgaacggtaaaaccctgaaaggtgaaaccaccaccgaagctgttgacgctgctacc
gcggaaaaagttttcaaacagtacgctaacgacaacggtgttgacggtgaatggacctacgacgacgctaccaaa
accttcacggtaaccgaaggatctggcagtggttctGAGAATCTTTATTTTCAGggcgCCatgggcaatggcggc
gccatttttttctcactcggttctaatggacggtaacgcagtgatgctgtccaagtatgctggttgtgtaacggtt
cttgttaacactgcgtccctctgctcttttacatcttcaaacattcaacaccttatacacgttcagcaaaaatgg
gcctcacgaagtttcactgtcttagcctttccgtgctctcaatttggaaatcaagagccgaagaagagggatgag
atttgctgttgggtggctcgtaatggaattaactttcctgtgtttgataaagttaacctgaaggggccgaataca
caccccctgtttcaaatgattcagtcgtcgcttggacctatacggtggaattacacgaaggttgtgtgcaatcgt
gccggactcccatgcgtgaagcttcagccaggaagctcgctggaggagcttgagcgctatgtttcacagttgtgc
gatgagtgaGGTACCggatccgaattcgagctccgtcgacaagcttgcggccgcactcgagcaccaccaccacca
ccactgagatccggctgctaacaaagcccgaaaggaagctgagttggctgctgccaccgctgagcaataactagc
ataaccccttggggcctctaaacgggtcttgaggggtttttgctgaaaggaggaactatatccggat (6245
bp)

NNN = His-Tag; nnn = GB; NNN = TEV cleavage site; NNN = *Nco*I site; **nnn** = ATG and GGC (inserted Gly) of *px IV* gene; nnn = *px IV* gene; NNN = *Acc*65I site

6.10.5 px IV into pETZZ-1a plasmid

…taagaaggagatataccatgaaaCATCACCATCACCATCACcccatgaaacaacacgatgaagccgtagacaac
aaattcaacaaagaacaacaaaacgcgttctatgagatcttacatttacctaacttaaacgaagaacaacgaaac
gccttcatccaaagtttaaaagatgacccaagccaaagcgctaacctttagcagaagctaaaaagctaaatgat
gctcaggcgccgaaagtcgacaacaaattcaacaaagaacaacaaaacgcgttctatgagatcttacatttacct
aacttaaacgaagaacaacgaaacgccttcatccaaagtttaaaagatgacccaagccaaagcgctaacctttta
gcagaagctaaaaagctaaatgatgctcaggcgccgaaagtagacgcggatctggcagtggttctGAGAATCTT
TATTTTCAGggcgCCatgggcaatggcggcgccatttttttctcactcggttctaatggacggtaacgcagtgatg
ctgtccaagtatgctggttgtgtaacggttcttgttaacactgcgtccctctgctcttttacatcttcaaacatt
caacaccttatacacgttcagcaaaaatgggcctcacgaagtttcactgtcttagcctttccgtgctctcaatttt
ggaaatcaagagccgaagaagagggatgagatttgctgttgggtggctcgtaatggaattaactttcctgtgttt
gataaagttaacctgaaggggccgaatacacacccccctgtttcaaatgattcagtcgtcgcttggacctatacgg
tggaattacacgaaggttgtgtgcaatcgtgccggactcccatgcgtgaagcttcagccaggaagctcgctggag
gagcttgagcgctatgtttcacagttgtgcgatgagtgaGGTACC… (6206 bp)

The remaining vector sequence is shown in 6.10.4

NNN = His-Tag; nnn = ZZ; NNN = TEV cleavage site; NNN = *Nco*I site; **nnn** = ATG and GGC (inserted Gly) of *px IV* gene; nnn = *px IV* gene; NNN = *Acc*65I site

6.10.6 px IV into pETMBP-1a plasmid

…aataattttgtttaactttaagaaggagatataccatgaaaCATCACCATCACCATCACcccatgaaaatcgaa
gaaggtaaactggtaatctggattaacggcgataaaggctataacggtctcgctgaagtcggtaagaaattcgag
aaagataccggaattaaagtcaccgttgagcatccggataaactggaagagaaattcccacaggttgcggcaact
ggcgatggccctgacattatcttctgggcacacgaccgctttggtggctacgctcaatctggcctgttggctgaa
atcaccccggacaaagcgttccaggacaagctgtatccgtttacctgggatgccgtacgttacaacggcaagctg
attgcttacccgatcgctgttgaagcgttatcgctgatttataacaaagatctgctgccgaacccgccaaaaacc
tgggaagagatcccggcgctggataaagaactgaaagcgaaaggtaagagcgcgctgatgttcaacctgcaagaa
ccgtacttcacctggccgctgattgctgctgacgggggttatgcgttcaagtatgaaaacggcaagtacgacatt
aaagacgtgggcgtggataacgctggcgcgaaagcgggtctgaccttcctggttgacctgattaaaaacaaacac
atgaatgcagacaccgattactccatcgcagaagctgcctttaataaaggcgaaacagcgatgaccatcaacggc
ccgtgggcatggtccaacatcgacaccagcaaagtgaattatggtgtaacggtactgccgaccttcaagggtcaa
ccatccaaaccgttcgttggcgtgctgagcgcaggtattaacgccgccagtccgaacaaagagctggcaaaagag
ttcctcgaaaactatctgctgactgatgaaggtctggaagcggttaataaagacaaaccgctgggtgccgtagcg
ctgaagtcttacgaggaagagttggcgaaagatccacgtattgccgccactatggaaaacgcccagaaaggtgaa
atcatgccgaacatcccgcagatgtccgctttctggtatgccgtgcgtactgcggtgatcaacgccgccagcggt
cgtcagactgtcgatgaagccctgaaagacgcgcagactaattcggatctggcagtggttctGAGAATCTTTAT

TTTCAGggcgCCatgggcaatggcggcgccatttttttctcactcggttctaatggacggtaacgcagtgatgctg
tccaagtatgctggttgtgtaacggttcttgttaacactgcgtccctctgctcttttacatcttcaaacattcaa
caccttatacacgttcagcaaaaatgggcctcacgaagtttcactgtcttagcctttccgtgctctcaatttgga
aatcaagagccgaagaagagggatgagatttgctgttgggtggctcgtaatggaattaactttcctgtgtttgat
aaagttaacctgaaggggccgaatacacacccccctgtttcaaatgattcagtcgtcgcttggacctatacggtgg
aattacacgaaggttgtgtgcaatcgtgccggactcccatgcgtgaagcttcagccaggaagctcgctggaggag
cttgagcgctatgtttcacagttgtgcgatgagtgaGGTACC…(6929 bp)

The remaining vector sequence is shown in 6.10.4

NNN = His-Tag; nnn = MBP; NNN = TEV cleavage site; NNN = *Nco*I site; **nnn** = ATG and GGC (inserted Gly) of *px IV* gene; nnn = *px IV* gene; NNN = *Acc*65I site

6.10.7 px IV into pETNusA-1a plasmid

…tttgtttaactttaagaaggagatataccatgaaaCATCACCATCACCATCACcccatgaaagaaattttggct
gtagttgaagccgtatccaatgaaaaggcgctacctcgcgagaagattttcgaagcattggaaagcgcgctggcg
acagcaacaaagaaaaaatatgaacaagagatcgacgtccgcgtacagatcgatcgcaaaagcggtgattttgac
actttccgtcgctggttagttgttgatgaagtcacccagccgaccaaggaaatcacccttgaagccgcacgttat
gaagatgaaagcctgaacctgggcgattacgttgaagatcagattgagtctgttacctttgaccgtatcactacc
cagacggcaaaacaggttatcgtgcagaaagtgcgtgaagccgaacgtgcgatggtggttgatcagttccgtgaa
cacgaaggtgaaatcatcaccggcgtggtgaaaaaagtaaaccgcgacaacatctctctggatctgggcaacaac
gctgaagccgtgatcctgcgcgaagatatgctgccgcgtgaaaacttccgccctggcgaccgcgttcgtggcgtg
ctctattccgttcgcccggaagcgcgtggcgcgcaactgttcgtcactcgttccaagccggaaatgctgatcgaa
ctgttccgtattgaagtgccagaaatcggcgaagaagtgattgaaattaaagcagcggctcgcgatccgggttct
cgtgcgaaaatcgcggtgaaaaccaacgataaacgtatcgatccggtaggtgcttgcgtaggtatgcgtggcgcg
cgtgttcaggcggtgtctactgaactgggtggcgagcgtatcgatatcgtcctgtgggatgataacccggcgcag
ttcgtgattaacgcaatggcaccggcagacgttgcttctatcgtggtggatgaagataaacacactatggacatc
gccgttgaagccggtaatctggcgcaggcgattggccgtaacggtcagaacgtgcgtctggcttcgcaactgagc
ggttgggaactcaacgtgatgaccgttgacgacctgcaagctaagcatcaggcggaagcgcacgcagcgatcgac
accttcaccaaatatctcgacatcgacgaagacttcgcgactgttctggtagaagaaggcttctcgacgctggaa
gaattggcctatgtgccgatgaaagagctgttggaaatcgaaggccttgatgagccgaccgttgaagcactgcgc
gagcgtgctaaaaatgcactggccaccattgcacaggcccaggaagaaagcctcggtgataacaaaccggctgac
gatctgctgaaccttgaaggggtagatcgtgatttggcattcaaactggccgcccgtggcgtttgtacgctggaa
gatctcgccgaacagggcattgatgatctggctgatatcgaagggttgaccgacgaaaaagccggagcactgatt
atggctgcccgtaatatttgctggttcggtgacgaagcgactggatctggcagtggttctGAGAATCTTTATTTT
CAGGGCGCCatgggcaatggcggcgccatttttttctcactcggttctaatggacggtaacgcagtgatgctgtcc
aagtatgctggttgtgtaacggttcttgttaacactgcgtccctctgctcttttacatcttcaaacattcaacac
cttatacacgttcagcaaaaatgggcctcacgaagtttcactgtcttagcctttccgtgctctcaatttggaaat
caagagccgaagaagagggatgagatttgctgttgggtggctcgtaatggaattaactttcctgtgtttgataaa
gttaacctgaaggggccgaatacacacccccctgtttcaaatgattcagtcgtcgcttggacctatacggtggaat
tacacgaaggttgtgtgcaatcgtgccggactcccatgcgtgaagcttcagccaggaagctcgctggaggagctt
gagcgctatgtttcacagttgtgcgatgagtgaGGTACCggatccgaattcgagctccgtcga… (7307 bp)

The remaining vector sequence is shown in 6.10.4

NNN = His-Tag; nnn = NusA; NNN = TEV cleavage site; NNN = *Nco*I site; **nnn** = ATG and GGC (inserted Gly) of *px IV* gene; nnn = *px IV* gene; NNN = *Acc*65I site

6.10.8 px I-III KO into pHD1747 plasmid

ctaaattgtaagcgttaatattttgttaaaattcgcgttaaattttgttaaatcagctcatttttaaccaata
ggccgaaatcggcaaaatcccttataaatcaaaagaatagaccgagatagggttgagtgttgttccagtttggaa
caagagtccactattaaagaacgtggactccaacgtcaaagggcgaaaaaccgtctatcagggcgatggcccact
acgtgaaccatcaccctaatcaagtttttttggggtcgaggtgccgtaaagcactaaatcggaaccctaaagggag
cccccgatttagagcttgacggggaaagccggcgaacgtggcgagaaaggaagggaagaaagcgaaaggagcggg
cgctagggcgctggcaagtgtagcggtcacgctgcgcgtaaccaccacacccgccgcgcttaatgcgccgctaca

gggcgcgtcccattcgccattcaggctgcgcaactgttgggaagggcgatcggtgcgggcctcttcgctattacg
ccagctggcgaaaggggatgtgctgcaaggcgattaagttgggtaacgccagggttttcccagtcacgacgttg
taaaacgacggccagtgagcgcgcgTAATACGACTCACTATAGGGcgaattgggtaccgggccccccCTCGAGgg
taacgaaattgcgttagaaggtaaaaggatgggggctgcacttgtttgtctcatgaaacttttaatatcccttc
gtaagcgcatgcgttaactaagaagggtgccaagccctgccactcagtttgtgaccggctttgtgccaggtaatg
ctgagagccccaataatctacactcgacacaatattgagtgaaccagagacccgtgtgtgtgtgcgtgtggaggg
cgggattacatgtaatgaatttgtggtgcctgcatgtgtttggaccgctcatttgacgaaaaagaaaaagttctc
ttttggcatcaaccataacatctcgtaaaagggaaggttggtaggtttacgcgcgaacgagtaggttggaggagg
cgcctacAAGCTTgatagcttaccatgaccgagtacaagcccacggtgcgcctcgccacccgcgacgacgtcccc
agggccgtacgcaccctcgccgccgcgttcgccgactaccccgccacgcgccacaccgtcgatccagaccgccac
atcgagcgggtcaccgagctgcaagaactcttcctcacgcgcgtcgggctcgacatcggcaaggtgtgggtcgcg
gacgacggcgcagcagtggcggtctggaccacgccggagagcgtcgaagcgggggcggtgttcgccgagatcggc
ccgcgcatggccgagttgagcggttcccggctggccgcgcagcaacagatggaaggcctcctggcgccgcaccgg
cccaaggagcccgcgtggttcctggccaccgtcggtgtctcgcccgaccaccagggcaagggtctgggcagcgcc
gtcgtgctccccggagtggaggcggccgagcgcgccggggtgcccgccttcctggagacctccgcgccccgcaac
ctcccttctacgagcggctcggcttcaccgtcaccgccgacgtcgaggtgcccgaaggaccgcgcacctggtgc
atgacccgcaagcccggtgcctgaatcGAATTCCTGCAGaagaagaatacgtctctggaccgcgacaacgcaaga
cgcgggaggggggtgttttggtgtgctttgctgcgctgttaagttttcattgtgtctgtgtttttcattgtttct
atttttaccgagtactcagcactggcttgaggcaatcagtggagttgaggttgaaagggagggccgcggaagctg
ctcagagagatgcaagaaccgaatttgcgatcccttgcgggggtgcattgtctctccccttttggtgcaagttcc
acacgtatcgtacccgccgtttatcttggacgtggaagcaaatccaacgtctgccacggacgggcactcgtacta
tccgcgaaccctgttgtcgcggcctccagttgcataatgagcgaagaagtgtggtgtagagggtttttcttctca
agaaaccgaagcacctctcagatagttggttaaatagtgtggtttactgtcttcgtagtctccacaaatgacgtt
attgcagtagattcagtttgcttcattcctttggGCGGCCGCcaccgcggtggagctccagcttttgttcccttt
agtgagggttaattgcgcgcttggcgtaatcatggtcatagctgtttcctgtgtgaaattgttatccgctcacaa
ttccacacaacatacgagccggaagcataaagtgtaaagcctggggtgcctaatgagtgagctaactcacattaa
ttgcgttgcgctcactgcccgctttccagtcgggaaacctgtcgtgccagctgcattaatgaatcggccaacgcg
cggggagaggcggtttgcgtattgggcgctcttccgcttcctcgctcactgactcgctgcgctcggtcgttcggc
tgcggcgagcggtatcagctcactcaaaggcggtaatacggttatccacagaatcaggggataacgcaggaaaga
acatgtgagcaaaaggccagcaaaaggccaggaaccgtaaaaaggccgcgttgctggcgtttttccataggctcc
gccccccctgacgagcatcacaaaaatcgacgctcaagtcagaggtggcgaaacccgacaggactataaagatacc
aggcgtttccccctggaagctccctcgtgcgctctcctgttccgaccctgccgcttaccggatacctgtccgcct
ttctcccttcgggaagcgtggcgctttctcatagctcacgctgtaggtatctcagttcggtgtaggtcgttcgct
ccaagctgggctgtgtgcacgaaccccccgttcagcccgaccgctgcgccttatccggtaactatcgtcttgagt
ccaacccggtaagacacgacttatcgccactggcagcagccactggtaacaggattagcagagcgaggtatgtag
gcggtgctacagagttcttgaagtggtggcctaactacggctacactagaaggacagtatttggtatctgcgctc
tgctgaagccagttaccttcggaaaaagagttggtagctcttgatccggcaaacaaaccaccgctggtagcggtg
gtttttttgtttgcaagcagcagattacgcgcagaaaaaaggatctcaagaagatcctttgatcttttctacgg
ggtctgacgctcagtggaacgaaaactcacgttaagggattttggtcatgagattatcaaaaggatcttcacct
agatccttttaaattaaaaatgaagttttaaatcaatctaaagtatatatgagtaaacttggtctgacagttacc
aatgcttaatcagtgaggcacctatctcagcgatctgtctatttcgttcatccatagttgcctgactccccgtcg
tgtagataactacgatacgggagggcttaccatctggccccagtgctgcaatgataccgcgagacccacgctcac
cggctccagatttatcagcaataaaccagccagccggaagggccgagcgcagaagtggtcctgcaactttatccg
cctccatccagtctattaattgttgccgggaagctagagtaagtagttcgccagttaatagtttgcgcaacgttg
ttgccattgctacaggcatcgtggtgtcacgctcgtcgtttggtatggcttcattcagctccggttcccaacgat
caaggcgagttacatgatcccccatgttgtgcaaaaaagcggttagctccttcggtcctccgatcgttgtcagaa
gtaagttggccgcagtgttatcactcatggttatggcagcactgcataattctcttactgtcatgccatccgtaa
gatgcttttctgtgactggtgagtactcaaccaagtcattctgagaatagtgtatgcggcgaccgagttgctctt
gcccggcgtcaatacgggataataccgcgccacatagcagaactttaaaagtgctcatcattggaaaacgttctt
cggggcgaaaactctcaaggatcttaccgctgttgagatccagttcgatgtaacccactcgtgcacccaactgat
cttcagcatcttttactttcaccagcgtttctgggtgagcaaaaacaggaaggcaaaatgccgcaaaaaagggaa
taagggcgacacggaaatgttgaatactcatactcttcctttttcaatattattgaagcatttatcagggttatt
gtctcatgagcggatacatatttgaatgtatttagaaaaataaacaaatagggggttccgcgcacatttccccgaa
aagtgccac (4434 bp)

NNN = T7 promoter; NNN = *Xho*I site; nnn = 5'UTR of *px I*; NNN = *Hind*III site; nnn = *pac*; NNN = *Eco*RI site; NNN = *Pst*I site; nnn = 3'UTR of *px III*; NNN = *Not*I site

6.10.9 px I-III KO into pHD1748 plasmid

ctaaattgtaagcgttaatattttgttaaaattcgcgttaaattttgttaaatcagctcatttttttaaccaata
ggccgaaatcggcaaaatcccttataaatcaaaagaatagaccgagatagggttgagtgttgttccagtttggaa
caagagtccactattaaagaacgtggactccaacgtcaaagggcgaaaaaccgtctatcagggcgatggcccact
acgtgaaccatcaccctaatcaagtttttttggggtcgaggtgccgtaaagcactaaatcggaaccctaaagggag
cccccgatttagagcttgacggggaaagccggcgaacgtggcgagaaaggaagggaagaaagcgaaaggagcggg
cgctagggcgctggcaagtgtagcggtcacgctgcgcgtaaccaccacacccgccgcgcttaatgcgccgctaca
gggcgcgtcccattcgccattcaggctgcgcaactgttgggaagggcgatcggtgcgggcctcttcgctattacg
ccagctggcgaaaggggatgtgctgcaaggcgattaagttgggtaacgccagggttttcccagtcacgacgttg
taaaacgacggccagtgagcgcgcg**TAATACGACTCACTATAGGG**cgaattgggtaccgggccccccctt**CTCGA**
Gggtaacgaaattgcgttagaaggtaaaaggatgggggctgcacttgtttgtctcatgaaacttttaatatccc
ttcgtaagcgcatgcgttaactaagaagggtgccaagccctgccactcagtttgtgaccggctttgtgccaggta
atgctgagagccccaataatctacactcgacacaatattgagtgaaccagagacccgtgtgtgtgtgcgtgtgga
gggcgggattacatgtaatgaatttgtggtgcctgcatgtgtttggaccgctcatttgacgaaaaagaaaaagtt
ctcttttggcatcaaccataacatctcgtaaaagggaaggttggtaggtttacgcgcgaacgagtaggttggagg
aggcgcctac**AAGCTT**gatcatggccaagcctttgtctcaagaagaatccaccctcattgaaagagcaacggcta
caatcaacagcatccccatctctgaagactacagcgtcgccagcgcagctctctctagcgacggccgcatcttca
ctggtgtcaatgtatatcattttactgggggaccttgtgcagaactcgtggtgctgggcactgctgctgctgcgg
cagctggcaacctgacttgtatcgtcgcgatcggaaatgagaacaggggcatcttgagcccctgcggacggtgcc
gacaggtgcttctcgatctgcatcctgggatcaaagccatagtgaaggacagtgatggacagccgacggcagttg
ggattcgtgaattgctgccctctggttatgtgtgggagggctaagcacatc**GAATTC**CTGCAGaagaagaatacg
tctctggaccgcgacaacgcaagacgcgggaggggggtgttttggtgtgctttgctgcgctgttaagttttcatt
gtgtctgtgtttttcattgtttctatttttaccgagtactcagcactggcttgaggcaatcagtggagttgaggt
tgaaagggagggccgcggaagctgctcagagagatgcaagaaccgaatttgcgatcccttgcgggggtgcattgt
ctctccccttttggtgcaagttccacacgtatcgtacccgccgtttatcttggacgtggaagcaaatccaacgtc
tgccacggacgggcactcgtactatccgcgaaccctgttgtcgcggcctccagttgcataatgagcgaagaagtg
tggtgtagagggtttttcttctcaagaaaccgaagcacctctcagatagttggttaaatagtgtggtttactgtc
ttcgtagtctccacaaatgacgttattgcagtagattcagtttgcttcattcctttgg**GCGGCCGC**caccgcggt
ggagctccagcttttgttccctttagtgagggttaattgcgcgcttggcgtaatcatggtcatagctgtttcctg
tgtgaaattgttatccgctcacaattccacacaacatacgagccggaagcataaagtgtaaagcctggggtgcct
aatgagtgagctaactcacattaattgcgttgcgctcactgcccgctttccagtcgggaaacctgtcgtgccagc
tgcattaatgaatcggccaacgcgcggggagaggcggtttgcgtattgggcgctcttccgcttcctcgctcactg
actcgctgcgctcggtcgttcggctgcggcgagcggtatcagctcactcaaaggccgtaatacggttatccacag
aatcaggggataacgcaggaaagaacatgtgagcaaaaggccagcaaaaggccaggaaccgtaaaaaggccgcgt
tgctggcgtttttccataggctccgccccctgacgagcatcacaaaaatcgacgctcaagtcagaggtggcgaa
acccgacaggactataaagataccaggcgtttccccctggaagctccctcgtgcgctctcctgttccgaccctgc
cgcttaccggatacctgtccgcctttctcccttcgggaagcgtggcgctttctcatagctcacgctgtaggtatc
tcagttcggtgtaggtcgttcgctccaagctgggctgtgtgcacgaacccccgttcagcccgaccgctgcgcct
tatccggtaactatcgtcttgagtccaacccggtaagacacgacttatcgccactggcagcagccactggtaaca
ggattagcagagcgaggtatgtaggcggtgctacagagttcttgaagtggtggcctaactacggctacactagaa
ggacagtatttggtatctgcgctctgctgaagccagttaccttcggaaaaagagttggtagctcttgatccggca
aacaaaccaccgctggtagcggtggtttttttgtttgcaagcagcagattacgcgcagaaaaaaggatctcaag
aagatcctttgatcttttctacggggtctgacgctcagtggaacgaaaactcacgttaagggattttggtcatga
gattatcaaaaaggatcttcacctagatccttttaaattaaaaatgaagttttaaatcaatctaaagtatatatg
agtaaacttggtctgacagttaccaatgcttaatcagtgaggcacctatctcagcgatctgtctatttcgttcat
ccatagttgcctgactccccgtcgtgtagataactacgatacgggagggcttaccatctggccccagtgctgcaa
tgataccgcgagacccacgctcaccggctccagatttatcagcaataaaccagccagccggaagggccgagcgca
gaagtggtcctgcaactttatccgcctccatccagtctattaattgttgccgggaagctagagtaagtagttcgc
cagttaatagtttgcgcaacgttgttgccattgctacaggcatcgtggtgtcacgctcgtcgtttggtatggctt
cattcagctccggttcccaacgatcaaggcgagttacatgatcccccatgttgtgcaaaaaagcggttagctcct
tcggtcctccgatcgttgtcagaagtaagttggccgcagtgttatcactcatggttatggcagcactgcataatt
ctcttactgtcatgccatccgtaagatgcttttctgtgactggtgagtactcaaccaagtcattctgagaatagt
gtatgcggcgaccgagttgctcttgcccggcgtcaatacgggataataccgcgccacatagcagaactttaaaag
tgctcatcattggaaaacgttcttcggggcgaaaactctcaaggatcttaccgctgttgagatccagttcgatgt
aacccactcgtgcacccaactgatcttcagcatcttttactttcaccagcgtttctgggtgagcaaaaacaggaa
ggcaaaatgccgcaaaaaagggaataagggcgacacggaaatgttgaatactcatactcttcctttttcaatatt
attgaagcatttatcagggttattgtctcatgagcggatacatatttgaatgtatttagaaaaataaacaaatag
gggttccgcgcacatttccccgaaaagtgccac (4233 bp)

NNN = T7 promoter; NNN = *Xho*I site; nnn = 5'UTR of *px I*; NNN = *Hind*III site; nnn = *bla*; NNN = *Eco*RI site; NNN = *Pst*I site; nnn = 3'UTR of *px III*; NNN = *Not*I site

6.10.10 3'UTR of px II + MTS into pHD1747 plasmid

…CTCGAGgtaattaagtcagaagggaagtggttaaggggcaagattctgtttttgtgaacgaggtagtgcatcaa
ctaatattgtacagattagtcgccttcagttcctatttcgctttgtttttgtccttgcgtcgttgggaagcaaca
caaacaagactaccaactcgtgctgcgttcatctcggaaaaagAAGCTTgat… (4236 bp)

The remaining vector sequence is shown in 6.10.8

NNN = *Xho*I site; nnn = 3'UTR of *px II*; nnn = inserted mutations (*Hind*III site and ATG); nnn = MTS of *px III*; NNN = *Hind*III site

6.10.11 3'UTR of px II + MTS into pHD1748 plasmid

…CTCGAGgtaattaagtcagaagggaagtggttaaggggcaagattctgtttttgtgaacgaggtagtgcatcaa
ctaatattgtacagattagtcgccttcagttcctatttcgctttgtttttgtccttgcgtcgttgggaagcaaca
caaacaagactaccaactcgtgctgcgttcatctcggaaaaagAAGCTTgat… (4035 bp)

The remaining vector sequence is shown in 6.10.9

NNN = *Xho*I site; nnn = 3'UTR of *px II*; nnn = inserted mutations (*Hind*III site and ATG); nnn = MTS of *px III*; NNN = *Hind*III site

6.10.12 px I-II re-insertion into pHD1748-Neo plasmid

…gcctacAAGCTTACGCGTatgtctacaatctttgactttgaggtgcttgacgccgaccataagccatataatct
cgtgcaacacaagggctctccgctactgatatacaatgtggcatgcaaagccggttacacaaagggtggttatga
aacggcgacaacactctacaacaagtacaagtcacagggcttcactgttttggtgtttccctgcaatgagtttgg
tggtcaggaagccggaaacgaggaggaaatcaaggagtttgtatgcaccaagttcaaggctgagtttccaattat
ggcgaaaattaacgtaaatggtgaaaacgcacacccattgtatgagtacatgaaaaaaactaaacctggtattct
tgcaacgaaggctatcaaatggaactttacatccttcctcattgatcgagatggcgtacccgtggagcgcttctc
acctggtgcctctgtgaaggatattgaggagaaactcattccactgctcgaaagcacgcagagcgcgtgatggat
ttgtcgctgaaacggagtgcgcggctggtgatgtgaagtgctaccgatgatcgaggacagtgaagttgtaaatga
taatatgaaaaacgcgntaatgaagggaccgtaagtttgcccgcttatggtgattatggcacccaggtgtaacgc
cagcggaggtcatttgtttttctccattataatttttttgttttgaaagggcgttgtgtcgtgtgtcactcagtg
aatgttgctgtaattaagtcagaagggaagtggttaaggggcaagcttctgtttttgtgaacgaggtagtgcatc
aactaatattgtacagattagtcgccttcagttcctatttcgctttgtttttgtccttgcgtcgttgggaagcaa
cacaaacaagactaccaactccttcggcactcattcggataaaaagatgtcagctgcttcgtcaatctttgactt
tgaggtgcttgacgccgaccataagccatataatctcgtgcaacacaagggctctccgctactgatatacaatgt
ggcaagtaaatgcggttacacaaagggtggttatgaaacggcgacaacactctacaacaagtacaagtcacaggg
cttcactgttctggcgttcccgtgtaaccaatttggtggtcaggaacccggaaacgaggaggaaatcaaggagtt
tgtatgcaccaagttcaaggctgagtttccaattatggcgaaaattaacgtaaatggtgaaaacgcacacccatt
gtatgagtacatgaaaaaaactaaacctggtatcctcaaaacgaaggctatcaaatggaactttacatccttcct
cattgatcgagatggcgtacccgtggagcgcttctcacctggtgcctctgtgaaggatattgagaaaaaactcat
tccactgctcgaaagcacgcagagcgcgtgatggatttgtcgctgaaacggagtgcgcggctggtgatgtgaagt
gctaccgatgatcgaggacagtgaagttgtaaatgataatatgaaaaacgcgntaatgaagggaccgtaagtttg
cccgcttatggtgattatggcacccaggtgtaacgccagcggaggtcatttgtttttctccattataatttttt
gttttgaaagggcgttgtgtcgtgtgtcactcagtgaatgttgctgtaattaagtcagaagggaagtggttaagg
ggcaagcttctgtttttgtgaacgaggtagtgcatcaactaatattgtacagattagtcgccttcagttcctatt
tcgctttgtttttgtccttgcgtcgttgggaagcaacacaaacaagactaccaactcTCTAGAatggtggaacaa
gatggattgcacgcaggttctccggccgcttgggtggagaggctattcggctatgactgggcacaacagacaatc
ggctgctctgatgccgccgtgttccggctgtcagcgcaggggcgcccggttcttttttgtcaagaccgacctgtcc
ggtgccctgaatgaactgcaggacgaggcagcgcggctatcgtggctggccacgacgggcgttccttgcgcagct

gtgctcgacgttgtcactgaagcgggaagggactggctgctattgggcgaagtgccggggcaggatctcctgtca
tctcaccttgctcctgccgagaaagtatccatcatggctgatgcaatgcggcggctgcatacgcttgatccggct
acctgcccattcgaccaccaagcgaaacatcgcatcgagcgagcacgtactcggatggaagccggtcttgtcgat
caggatgatctggacgaagagcatcaggggctcgcgccagccgaactgttcgccaggctcaaggcgcgcatgccc
gacggcgaggatctcgtcgtgacccatggcgatgcctgcttgccgaatatcatggtggaaaatggccgcttttct
ggattcatcgactgtggccggctgggtgtggcggaccgctatcaggacatagcgttggctacccgtgatattgct
gaagagcttggcggcgaatgggctgaccgcttcctcgtgctttacggtatcgccgctcccgattcgcagcgcatc
gccttctatcgccttcttgacgagttcttctgaGAATTCCTGCAGaagaag… (6468 bp)

The remaining vector sequence is shown in 6.10.9

nnn = 5'UTR of *px I*; NNN = *Hind*III site; NNN = *Mlu*I site; nnn = *px I*; nnn = 3'UTR of *px I*; nnn = *px II*; nnn = 3'UTR of *px II*; NNN = *Xba*I site; nnn = *neo*; NNN = *Eco*RI site; NNN = *Pst*I site; nnn = 3'UTR of *px III*

6.10.13 px I-II re-insertion into pHD1748-Pac plasmid

…TCTAGAatgaccgagtacaagcccacggtgcgcctcgccacccgcgacgacgtccccagggccgtacgcaccct
cgccgccgcgttcgccgactaccccgccacgcgccacaccgtcgatccagaccgccacatcgagcgggtcaccga
gctgcaagaactcttcctcacgcgcgtcgggctcgacatcggcaaggtgtgggtcgcggacgacggcgcagcagt
ggcggtctggaccacgccggagagcgtcgaagcgggggcggtgttcgccgagatcggcccgcgcatggccgagtt
gagcggttcccggctggccgcgcagcaacagatggaaggcctcctggcgccgcaccggcccaaggagcccgcgtg
gttcctggccaccgtcggtgtctcgcccgaccaccagggcaagggtctgggcagcgccgtcgtgctccccggagt
ggaggcggccgagcgcgccggggtgcccgccttcctggagacctccgcgccccgcaacctccccttctacgagcg
gctcggcttcaccgtcaccgccgacgtcgaggtgcccgaaggaccgcgcacctggtgcatgacccgcaagcccgg
tgcctgagaattcCTGCAG… (6273 bp)

The remaining vector sequence is shown in 6.10.12

NNN = *Xba*I site; nnn = *neo*; NNN = *Eco*RI site; NNN = *Pst*I site

6.10.14 px II re-insertion into pHD1748-Neo plasmid

…agtcacgacgttgtaaaacgacggccagtgagcgcgcgTAATACGACTCACTATAGGGcgaattgggtaccggg
ccccccttCTCGAGggtaacgaaattgcgttagaaggtaaaaggatgggggctgcacttgtttgtctcatgaaa
ctttttaatatcccttcgtaagcgcatgcgttaactaagaagggtgccaagccctgccactcagtttgtgaccgg
ctttgtgccaggtaatgctgagagccccaataatctacactcgacacaatattgagtgaaccagagacccgtgtg
tgtgtgcgtgtggagggcgggattacatgtaatgaatttgtggtgcctgcatgtgtttggaccgctcatttgacg
aaaaagaaaaagttctcttttggcatcaaccataacatctcgtaaaagggaaggttggtaggtttacgcgcgaac
gagtaggttggaggaggcgcctacAAGCTTACGCGTatgtcagctgcttcgtcaatctttgactttgaggtgctt
gacgccgaccataagccatataatctcgtgcaacacaagggctctccgctactgatatacaatgtggcaagtaaa
tgcggttacacaaagggtggttatgaaacggcgacaacactctacaacaagtacaagtcacagggcttcactgtt
ctggcgttcccgtgtaaccaatttggtggtcaggaacccggaaacgaggaggaaatcaaggagtttgtatgcacc
aagttcaaggctgagtttccaattatggcgaaaattaacgtaaatggtgaaaacgcacacccattgtatgagtac
atgaaaaaaactaaacctggtatcctcaaaacgaaggctatcaaatggaactttacatccttcctcattgatcga
gatggcgtacccgtggagcgcttctcacctggtgcctctgtgaaggatattgagaaaaaactcattccactgctc
gaaagcacgcagagcgcgtgatggatttgtcgctgaaacggagtgcgcggctggtgatgtgaagtgctaccgatg
atcgaggacagtgaagttgtaaatgataatatgaaaaacgcgntaatgaagggaccgtaagtttgcccgcttatg
gtgattatggcacccaggtgtaacgccagcggaggtcatttgtttttctccattataatttttttgttttgaaag
ggcgttgtgtcgtgtgtcactcagtgaatgttgctgtaattaagtcagaagggaagtggttaaggggcaagcttc
tgtttttgtgaacgaggtagtgcatcaactaatattgtacagattagtcgccttcagttcctatttcgctttgtt
tttgtccttgcgtcgttgggaagcaacacaaacaagactaccaactcTCTAGAatggtggaacaagatggattgc
acgcaggttctcCGGCCGCTTGGGTGGAGAGGCTATTCGGCTATGACTGGGCACAACAGACAATCGGCTGCTCTG
ATGCCGCCGTGTTCCGGCTGTCAGCGCAGGGGCGCCCGGTTCTTTTTGTCAAGACCGACCTGTCCGGTGCCCTGA
ATGAACTGCAGGACGAGGCAGCGCGGCTATCGTGGCTGGCCACGACGGGCGTTCCTTGCGCAGCTGTGCTCGACG
TTGTCACTGAAGCGGGAAGGGACTGGCTGCTATTGGGCGAAGTGCCGGGGCAGGATCTCCTGTCATCTCACCTTG
CTCCTGCCGAGAAAGTATCCATCATGGCTGATGCAATGCGGCGGCTGCATACGCTTGATCCGGCTACCTGCCCAT

TCGACCACCAAGCGAAACATCGCATCGAGCGAGCACGTACTCGGATGGAAGCCGGTCTTGTCGATCAGGATGATC
TGGACGAAGAGCATCAGGGGCTCGCGCCAGCCGAACTGTTCGCCAGGCTCAAGGCGCGCATGCCCGACGGCGAGG
ATCTCGTCGTGACCCATGGCGATGCCTGCTTGCCGAATATCATGGTGGAAAATGGCCGCTTTTCTGGATTCATCG
ACTGTGGCCGGCTGGGTGTGGCGGACCGCTATCAGGACATAGCGTTGGCTACCCGTGATATTGCTGAAGAGCTTG
GCGGCGAATGGGCTGACCGCTTCCTCGTGCTTTACGGTATCGCCGCTCCCGATTCGCAGCGCATCGCCTTCTATC
GCCTTCTTGACGAGTTCTTCTGAGAATTCCTGCAGaagaagaatacgtctctggaccgcgacaacgcaagacgcg
ggaggggggtgttttggtgtgctttgctgcgctgttaagttttcattgtgtctgtgtttttcattgtttctattt
ttaccgagtactcagcactggcttgaggcaatcagtggagttgaggttgaaagggagggccgcggaagctgctca
gagagatgcaagaaccgaatttgcgatcccttgcgggggtgcattgtctctccccttttggtgcaagttccacac
gtatcgtacccgccgtttatcttggacgtggaagcaaatccaacgtctgccacggacgggcactcgtactatccg
cgaaccctgttgtcgcggcctccagttgcataatgagcgaagaagtgtggtgtagagggtttttcttctcaagaa
accgaagcacctctcagatagttggttaaatagtgtggtttactgtcttcgtagtctccacaaatgacgttattg
cagtagattcagtttgcttcattcctttggGCGGCCGCcaccgcggt… (5541 bp)

The remaining vector sequence is shown in 6.10.9

NNN = T7 promoter; NNN = *Xho*I site; nnn = 5'UTR of *px I*; NNN = *Hind*III site; NNN = *Mlu*I site; nnn = *px II*; nnn = 3'UTR of *px II*; NNN = *Xba*I site; nnn = *neo*; NNN = *Eco*RI site; NNN = *Pst*I site; nnn = 3'UTR of *px III*; NNN = *Not*I site

6.10.15 px II re-insertion into pHD1748-Pac plasmid

…cacaaacaagactaccaactcTCTAGAatgaccgagtacaagcccacggtgcgcctcgccacccgcgacgacgt
ccccagggccgtacgcaccctcgccgccgcgttcgccgactaccccgccacgcgccacaccgtcgatccagaccg
ccacatcgagcgggtcaccgagctgcaagaactcttcctcacgcgcgtcgggctcgacatcggcaaggtgtgggt
cgcggacgacggcgcagcagtggcggtctggaccacgccggagagcgtcgaagcgggggcggtgttcgccgagat
cggcccgcgcatggccgagttgagcggttcccggctggccgcgcagcaacagatggaaggcctcctggcgccgca
ccggcccaaggagcccgcgtggttcctggccaccgtcggtgtctcgcccgaccaccagggcaagggtctgggcag
cgccgtcgtgctccccggagtggaggcggccgagcgcgccggggtgcccgccttcctggagacctccgcgccccg
caacctccccttctacgagcggctcggcttcaccgtcaccgccgacgtcgaggtgcccgaaggaccgcgcacctg
gtgcatgacccgcaagcccggtgcctgaGAATTCCTGCAGaagaag… (5346 bp)

The remaining vector sequence is shown in 6.10.14

NNN = *Xba*I site; nnn = *pac*; NNN = *Eco*RI site; NNN = *Pst*I site; nnn = 3'UTR of *px III*

6.10.16 px III-ARL re-insertion into pHD1748-Neo plasmid

…AAGCTTACGCGTatggtggaacaagatggattgcacgcaggttctccggccgcttgggtggagaggctattcgg
ctatgactgggcacaacagacaatcggctgctctgatgccgccgtgttccggctgtcagcgcaggggcgcccggt
tctttttgtcaagaccgacctgtccggtgccctgaatgaactgcaggacgaggcagcgcggctatcgtggctggc
cacgacgggcgttccttgcgcagctgtgctcgacgttgtcactgaagcgggaagggactggctgctattgggcga
agtgccggggcaggatctcctgtcatctcaccttgctcctgccgagaaagtatccatcatggctgatgcaatgcg
gcggctgcatacgcttgatccggctacctgcccattcgaccaccaagcgaaacatcgcatcgagcgagcacgtac
tcggatggaagccggtcttgtcgatcaggatgatctggacgaagagcatcaggggctcgcgccagccgaactgtt
cgccaggctcaaggcgcgcatgcccgacggcgaggatctcgtcgtgacccatggcgatgcctgcttgccgaatat
catggtggaaaatggccgcttttctggattcatcgactgtggccggctgggtgtggcggaccgctatcaggacat
agcgttggctacccgtgatattgctgaagagcttggcggcgaatgggctgaccgcttcctcgtgctttacggtat
cgccgctcccgattcgcagcgcatcgccttctatcgccttcttgacgagttcttctgaTCTAGAtggatttgtcg
ctgaaacggagtgcgcggctggtgatgtgaagtgctaccgatgatcgaggacagtgaagttgtaaatgataatat
gaaaaacgcgntaatgaagggaccgtaagtttgcccgcttatggtgattatggcacccaggtgtaacgccagcgg
aggtcatttgtttttctccattataatttttttgttttgaaagggcgttgtgtcgtgtgtcactcagtgaatgtt
gctgtaattaagtcagaagggaagtggttaaggggcaagcttctgtttttgtgaacgaggtagtgcatcaactaa
tattgtacagattagtcgccttcagttcctatttcgctttgtttttgtccttgcgtcgttgggaagcaacacaaa
caagactaccaactcatgctgcgttcatctcggaaaaagatgtcagctgcttcgtcaatctttgactttgaggtg
cttgacgccgaccataagccatataatctcgtgcaacacaagggctctccgctactgatatacaatgtggcaagt
aaatgcggttacacaaagggtggttatgaaacggcgacaacactctacaacaagtacaagtcacagggcttcact

gttctggcgttcccgtgtaaccaatttggtggtcaggaacccggaaacgaggaggaaatcaaggagtttgtatgc
accaagttcaaggctgagtttccaattatggcgaaaattaacgtaaatggtgaaaacgcacacccattgtatgag
tacatgaaaaaaactaaacctggtatccttgcaacgaaggctatcaaatggaactttacatccttcctcattgat
cgagatggcgtacccgtggagcgcttctcacctggtgcctctgtgaaggatattgaggaaaaactcattccgctg
ctcgggagttgaGAATTCCTGCAGaagaa… (5553 bp)

The remaining vector sequence is shown in 6.10.14

NNN = *Hind*III site; NNN = *Mlu*I site; nnn = *neo*; NNN = *Eco*RI site; NNN = *Xba*I site; nnn = 3'UTR of *px II*; nnn = *px III*-ARL; NNN = *Eco*RI site; NNN = *Pst*I site; nnn = 3'UTR of *px III*

6.10.17 px III-ARL re-insertion into pHD1748-Pac plasmid (theoretical)

…AAGCTTACGCGTatgaccgagtacaagcccacggtgcgcctcgccacccgcgacgacgtccccagggccgtacg
caccctcgccgccgcgttcgccgactaccccgccacgcgccacaccgtcgatccagaccgccacatcgagcgggt
caccgagctgcaagaactcttcctcacgcgcgtcgggctcgacatcggcaaggtgtgggtcgcggacgacggcgc
agcagtggcggtctggaccacgccggagagcgtcgaagcgggggcggtgttcgccgagatcggcccgcgcatggc
cgagttgagcggttcccggctggccgcgcagcaacagatggaaggcctcctggcgccgcaccggcccaaggagcc
cgcgtggttcctggccaccgtcggtgtctcgcccgaccaccagggcaagggtctgggcagcgccgtcgtgctccc
cggagtggaggcggccgagcgcgccggggtgcccgccttcctggagacctccgcgccccgcaacctccccttcta
cgagcggctcggcttcaccgtcaccgccgacgtcgaggtgcccgaaggaccgcgcacctggtgcatgacccgcaa
gcccggtgcctgaTCTAGA… (5358 bp)

The remaining vector sequence is shown in 6.10.16

NNN = *Hind*III site; NNN = *Mlu*I site; nnn = *neo*; NNN = *Eco*RI site; NNN = *Xba*I site

6.10.18 px IV KO into pHD1747-Neo plasmid

…ggccagtgagcgcgcgTAATACGACTCACTATAGGGcgaattgggtaccgggcccccccCTCGAGtgcaaggtca
atcacatttttttcgcttctggtggaggttttaccgcgatgggatgagccaaatgtctccatctctgaagaagtt
ccgcatgctgtcgtgagttttgctgcttttgtttccttcagctgactttccaagtgatgaggaaaaagacagga
agaacaacaaagcagtagccgattgtttgcttatttcttgaatccaggactcccgcatccgttcgtgtgttttca
agtgtaaaggtttagcctgctgttgcatttcaccttcaatgcgacgcttttaacttcaatctcatatgactatca
gttgaattagtaacggtgacccgactgctttcttttccctcttcttctttgtcacgtaaagtacttttaaacgag
tcgtgccctAAGCTTatggtggaacaagatggattgcacgcaggttctccggccgcttgggtggagaggctattc
ggctatgactgggcacaacagacaatcggctgctctgatgccgccgtgttccggctgtcagcgcaggggcgcccg
gttcttttttgtcaagaccgacctgtccggtgccctgaatgaactgcaggacgaggcagcgcggctatcgtggctg
gccacgacgggcgttccttgcgcagctgtgctcgacgttgtcactgaagcgggaagggactggctgctattgggc
gaagtgccggggcaggatctcctgtcatctcaccttgctcctgccgagaaagtatccatcatggctgatgcaatg
cggcggctgcatacgcttgatccggctacctgcccattcgaccaccaagcgaaacatcgcatcgagcgagcacgt
actcggatggaagccggtcttgtcgatcaggatgatctggacgaagagcatcaggggctcgcgccagccgaactg
ttcgccaggctcaaggcgcgcatgcccgacggcgaggatctcgtcgtgacccatggcgatgcctgcttgccgaat
atcatggtggaaaatggccgcttttctggattcatcgactgtggccggctgggtgtggcggaccgctatcaggac
atagcgttggctacccgtgatattgctgaagagcttggcggcgaatgggctgaccgcttcctcgtgctttacggt
atcgccgctcccgattcgcagcgcatcgccttctatcgccttcttgacgagttcttctgaGAATTCCTGCAGcgg
gtgtacattcagcgtataatttgtagcgtacgggcgtatgtaggggcatggtatgttttataccctcatgtttag
tatacctcatcttagtgagagcaggtgtctgaccctaggtggttggcattttgcttgtcatgtaagttgaacggt
tccaactactctttcgattaaactgcgcgtcattcagttttggcacaactccttctttttgtttctcactctatcc
ccatatgttgcaggtggaatacgacctcaaagtgaaataggaagcaaagacaattcttttaaggtagtattagtg
ttgagtgttagcaaagaggagtcacacctgaataccggaaagtacttatctggaaaattgattgacagaggctga
caaaacaaggcagaggacaccccgttttcttgacgctaGCGGCCGCcaccg… (4521 bp)

The remaining vector sequence is shown in 6.10.8

NNN = T7 promoter; NNN = *Xho*I site; nnn = 5'UTR of *px IV*; NNN = *Hind*III site; nnn = *neo*; NNN = *Eco*RI site; NNN = *Pst*I site; nnn = 3'UTR of *px VI*; NNN = *Not*I site

6.10.19 px IV in pHD1700 plasmid (theoretical)

gaattcgagctcatatagttggtatgtattctaattccagactactggcgtgggataaacatgtccccctgatta
aaaggaaagattccatagcccattagtgcaaagataattggtacaccgtcaaaaacacatgggagaccacacgat
acgacactgtgaccgtagcatcaattccgcactcgatataactctatcgaagaacttccatggtacaaactggtc
gccacggtctgctccacacggagatcatcgtatcatttttatcgatagcggccgctatcgatgtatgccttggcc
ctgatggcatgccaatttcactacaacggactatgtggaccccgttatcatggaaatgcgctagttggaggaagt
tagaccgcgccggaaaagagaggggtagagaaaatgacaacttggaagatatccacacacgcacggtgaaacgtt
agcaacaattattagggaagcacgcttgccctagtcccacgagtaaccaagactccaaaagcctttctggcacag
agagcgagccgaaatggaaaagagaaacaatgcctgcactaacactactgagcgattcgcctcgccgcggaggac
cgaatactaataacgacacttgcggtcaaaaagtagaagaacaaatgctcaacgatgagtgaatcaggttagggt
agttggaaaattatacagaatgtctttggcaacacaccggtaccgtcattggggttaagcggaaaggtgtgtgtc
agtaggttgtgaggtgaaagcgttttcagatgcatagtgagcttaatgtccttttcacagtatatcgtgtctgat
aggtatctcttattagtatagtcgaatactagtcaatagtgcgttttgtgcaaaatgtccattttgtggcagtga
tggggttgttttatgctattccgtgtctctgggtgggcgtgcattgaaaataggggttatcgggtagggatctcc
ctatcagtgatagagatctccctatcagtgatagagatccctgagtactgagtttaacatgttctcgtcccgggc
tgcacgcgccttcgagtttttttccttttccccatttttttcaacttgaagacttcaattacaccaaaaagtaa
aattcacaagcttcgcggggcccACGCGTatgaatggcggcgccatttttttctcactcggttctaatggacggta
acgcagtgatgctgtccaagtatgctggttgtgtaacggttcttgttaacactgcgtccctctgctcttttacat
cttcaaacattcaacaccttatacacgttcagcaaaaatgggcctcacgaagtttcactgtcttagcctttccgt
gctctcaatttggaaatcaagagccgaagaagagggatgagatttgctgttgggtggctcgtaatggaattaact
ttcctgtgtttgataaagttaacctgaaggggccgaatacacacccccctgtttcaaatgattcagtcgtcgcttg
gacctatacggtggaattacacgaaggttgtgtgcaatcgtgccggactcccatgcgtgaagcttcagccaggaa
gctcgctggaggagcttgagcgctatgtttcacagttgtgcgatgagtgaGGATCCaacgagcaaaagctcattt
ctgaagaggacttgttaattaacgagcaaaagctcatttctgaagaggacttgtaacaccgggttgtgtggccaa
aattgttctgtagtcgctgtgagttgacacggctagtgcttatgattttcctcgcgtgtggtgcctgtactcagc
cctatgccttatttgcaacacatttacgtacagcgcacaagagaagagaagatcacttgaagataataaatatag
ggttgtaggcatcttgtttaactcaaattttctcgtcttggtgtgtcgacatgattgaaatagtgccaccagttg
tgtttgatgcgtttgttatctatgcagtattctgcagtttaatttgttggatgagctatttcattaattttttg
ccttctcttctttttgggttcgctcgagtttccacccagcgcgggtgcattctggctcttatatatacttattgtc
atgacagagtatattgtactgtgttgataagggacgggtaactgtattgaagagccgatgcttttgacatgttag
atataatatgttttattgtaaagtcaatacaacacacaataggataataatgataaagttaaaaaagtatatata
gtaatagaaatatatcttatataggaaagattaagcagtaaaagtagcgcttacggcgtacggagcaggagagca
actgaccgctctcagagcccgggcacagcaaggtcttctgaaattcatgttttttttttttttactctgcattgc
agtctccgctcttatttagttttgctttacgtaaggtctcgttgctgccataaaataagctctagaactagtgat
gaaaaagcctgaactcaccgcgacgtctgtcgagaagtttctgatcgaaaagttcgacagcgtctccgacctgat
gcagctctcggagggcgaagaatctcgtgctttcagcttcgatgtaggagggcgtggatatgtcctgcgggtaaa
tagctgcgccgatggtttctacaaagatcgttatgtttatcggcactttgcatcggccgcgctcccgattccgga
agtgcttgacattggggaattcagcgagagcctgacctattgcatctcccgccgtgcacagggtgtcacgttgca
agacctgcctgaaaccgaactgcccgctgttctgcagccggtcgcggaggccatggatgcgatcgctgcggccga
tcttagccagacgagcgggttcggcccattcggaccgcaaggaatcggtcaatacactacatggcgtgatttcat
atgcgcgattgctatccccatgtgtatcactggcaaactgtgatggacgacaccgtcagtgcgtccgtcgcgcag
gctctcgatgagctgatgctttgggccgaggactgccccgaagtccggcacctcgtgcacgcggatttcggctcc
aacaatgtcctgacggacaatggccgcataacagcggtcattgactggagcgaggcgatgttcggggattcccaa
tacgaggtcgccaacatcttcttctggaggccgtggttggcttgtatggagcagcagacgcgctacttcgagcgg
aggcatccggagcttgcaggatcgccgcggctccgggcgtatatgctccgcattggtcttgaccaactctatcag
agcttggttgacggcaatttcgatgatgcagcttgggcgcagggtcgatgcgacgcaatcgtccgatccggagcc
gggactgtcgggcgtacacaaatcgcccgcagaagcgcggccgtctggaccgatggctgtgtagaagtactcgcc
gatagtggaaaccgacgccccagcactcgtccgagggcaaaggaatagagtagatgccgaccgggatcgatcccc
cgatcctaacaccgggttgtgtggccaaaattgttctgtagtcgctgtgagttgacacggctagtgcttatgatt
ttcctcgcgtgtggtgcctgtactcagccctatgccttatttgcaacacatttacgtacagcgcacaagagaaga
gaagatcacttgaagataataaatatagggttgtaggcatcttgtttaactcaaattttctcgtcttggtgtgtc
gacatgattgaaatagtgccaccagttgtgtttgatgcgtttgttatctatgcagtattctgcaaggccttgcaa
ggccttgcaggcatgcaagctagcttgtattctatagtgtcacctaaatcgtatgtgtatgatacataaggttat
gtattaattgtagccgcgttctaacgacaatatgtacaagcctaattgtgtagcatctggcttactgaagcagac
cctatcatctctctcgtaaactgccgtcagagtcggtttggttggacgaaccttctgagtttctggtaacgccgt
tccgcaccccggaaatggtcagcgaaccaatcagcagggtcatcgctagccagatcctctacgccggacgcatcg
tggccggcatcaccggcgccacaggtgcggttgctggcgcctatatcgccgacatcaccgatggggaagatcggg
ctcgccacttcgggctcatgagcgcttgtttcggcgtgggtatggtggcaggccccgtggccgggggactgttgg
gcgccatctccttgcaccattccttgcggcggcggtgctcaacggcctcaacctactactgggctgcttcctaat
gcaggagtcgcataagggagagcgtcgatatggtgcactctcagtacaatctgctctgatgccgcatagttaagc

cagccccgacacccgccaacacccgctgacgcgccctgacgggcttgtctgctcccggcatccgcttacagacaa
gctgtgaccgtctccgggagctgcatgtgtcagaggttttcaccgtcatcaccgaaacgcgcgagacgaaagggc
ctcgtgatacgcctatttttataggttaatgtcatgataataatggtttcttagacgtcaggtggcacttttcgg
ggaaatgtgcgcggaacccctatttgtttatttttctaaatacattcaaatatgtatccgctcatgagacaataa
ccctgataaatgcttcaataatattgaaaaaggaagagtatgagtattcaacatttccgtgtcgcccttattccc
ttttttgcggcattttgccttcctgtttttgctcacccagaaacgctggtgaaagtaaaagatgctgaagatcag
ttgggtgcacgagtgggttacatcgaactggatctcaacagcggtaagatccttgagagttttcgccccgaagaa
cgttttccaatgatgagcacttttaaagttctgctatgtggcgcggtattatcccgtattgacgccgggcaagag
caactcggtcgccgcatacactattctcagaatgacttggttgagtactcaccagtcacagaaaagcatcttacg
gatggcatgacagtaagagaattatgcagtgctgccataaccatgagtgataacactgcggccaacttacttctg
acaacgatcggaggaccgaaggagctaaccgcttttttgcacaacatgggggatcatgtaactcgccttgatcgt
tgggaaccggagctgaatgaagccataccaaacgacgagcgtgacaccacgatgcctgtagcaatggcaacaacg
ttgcgcaaactattaactggcgaactacttactctagcttcccggcaacaattaatagactggatggaggcggat
aaagttgcaggaccacttctgcgctcggcccttccggctggctggtttattgctgataaatctggagccggtgag
cgtgggtctcgcggtatcattgcagcactggggccagatggtaagccctcccgtatcgtagttatctacacgacg
gggagtcaggcaactatggatgaacgaaatagacagatcgctgagataggtgcctcactgattaagcattggtaa
ctgtcagaccaagtttactcatatatactttagattgatttaaaacttcatttttaatttaaaaggatctaggtg
aagatccttttgataatctcatgaccaaaatcccttaacgtgagttttcgttccactgagcgtcagaccccgta
gaaaagatcaaaggatcttcttgagatccttttttttctgcgcgtaatctgctgcttgcaaacaaaaaaaccaccg
ctaccagcggtggtttgtttgccggatcaagagctaccaactctttttccgaaggtaactggcttcagcagagcg
cagataccaaatactgtccttctagtgtagccgtagttaggccaccacttcaagaactctgtagcaccgcctaca
tacctcgctctgctaatcctgttaccagtggctgctgccagtggcgataagtcgtgtcttaccgggttggactca
agacgatagttaccggataaggcgcagcggtcgggctgaacgggggttcgtgcacacagcccagcttggagcga
acgacctacaccgaactgagatacctacagcgtgagctatgagaaagcgccacgcttcccgaagggagaaaggcg
gacaggtatccggtaagcggcagggtcggaacaggagagcgcacgagggagcttccagggggaaacgcctggtat
ctttatagtcctgtcgggtttcgccacctctgacttgagcgtcgatttttgtgatgctcgtcaggggggcggagc
ctatggaaaaacgccagcaacgcggccttttacggttcctggccttttgctggccttttgctcacatgttcttt
cctgcgttatcccctgattctgtggataaccgtattaccgcctttgagtgagctgataccgctcgccgcagccga
acgaccgagcgcagcgagtcagtgagcgaggaagcggaagagcgcccaatacgcaaaccgcctctccccgcgcgt
tggccgattcattaatgcagctggcttatcgaaattaatacgactcactatagggagaccg (6661 bp)

nnn = GPEET promoter; nnn = Tet operator; NNN = *Mlu*I site; nnn = *px VI* gene; NNN = *Bam*HI site; nnn = myc-tag